Titre: Title:	Using NIRS to Capture and Investigate Brain Pulsatility and Its Association with Aging and Cardiovascular Diseases
Auteur: Author:	Hanieh Mohammadi
Date:	2020
Type:	Mémoire ou thèse / Dissertation or Thesis
Référence: Citation:	Mohammadi, H. (2020). Using NIRS to Capture and Investigate Brain Pulsatility and Its Association with Aging and Cardiovascular Diseases [Thèse de doctorat, Polytechnique Montréal]. PolyPublie. https://publications.polymtl.ca/5261/

URL de PolyPublie: PolyPublie URL:	https://publications.polymtl.ca/5261/
Directeurs de recherche: Advisors:	Frédéric Lesage, & Yves Joanette
Programme: Program:	Génie biomédical

POLYTECHNIQUE MONTRÉAL

affiliée à l'Université de Montréal

Using NIRS to Capture and Investigate Brain Pulsatility and Its Association with Aging and Cardiovascular Diseases

HANIEH MOHAMMADI

Institut de génie biomédical

Thèse présentée en vue de l'obtention du diplôme de *Philosophiæ Doctor*

Génie biomédical

Avril 2020

POLYTECHNIQUE MONTRÉAL

affiliée à l'Université de Montréal

Cette thèse intitulée :

Using NIRS to Capture and Investigate Brain Pulsatility and Its Association with Aging and Cardiovascular Diseases

présentée par **Hanieh MOHAMMADI**

en vue de l'obtention du diplôme de *Philosophiæ Doctor*

a été dûment acceptée par le jury d'examen constitué de :

Frédéric LEBLOND, président

Frédéric LESAGE, membre et directeur de recherche

Yves JOANETTE, membre et codirecteur de recherche

Hélène GIROUARD, membre

Mamadou DIOP, membre externe

DEDICATION

To my beloved father, Naser
my ambitious grandpa, Ayatali
who was very much ahead of his time (1916-1998)
and my dear Paul

ACKNOWLEDGEMENTS

I have a great deal of gratitude for both my advisors Professor Lesage and Professor Joanette for their perfect mentoring and supporting me during my studies. Thank you to both of you that apart from your academic excellence always had great patience with me and provided me even-tempered management of the research team. Thank you to both of you for supporting the ideas proactively. I am grateful for your forthcoming advice and positive attitude throughout the project.

I would like to thank Professor Louis Bherer who instructed me from time to time and sharing the data of his team with me. Special thanks to Professor Pierre Jolicoeur for giving me the resources in his lab to help me to progress on the project.

Given the complexity of the project involving humans I appreciate skillful people who helped me to progress in the project; Mrs. Karima Bekhiti, Mrs. Carollyn Hurst, Mr. Andre Cyr, Mrs. Nadia Jaffer, Dr. Thomas Vincent, Dr. Catherine-alexandra Gregoire and Mrs. Ana-Maria Voinescu.

Special thanks to Dr. Ali Kassab who thought me how to collect data with the most detailed knowledge that he had and helped me to ensure acquiring good data. Special thanks to Dr. Ke Peng for his great support on data analysis in the last few years even during the time that he was at Harvard Medical School.

Thanks to all my amazing colleagues at Polytechnique Montreal, Samuel Bélanger, Mahnoush Amiri, Maxim Abran, Joël Lefebvre, Leila Abrishami Shokoh, Cong Zhang, Mehran Sharafi, Parikshat Sirpal and Yuankang Lu. Thanks to all my amazing colleagues at CRIUGM. I thank all my friends who without them it was impossible to finish my PhD. Dr. Saeed Mirsoheil and Dr. Farhad Ghazvinian. Special thanks to my friends who stayed so close while they were beyond the borders: Fariba Adineh, Hossein Taheri and Sarah Irannejad. I sincerely thank to my teachers Mr. Abbas Farzam and Mr. Bahram Jamasbi.

I sincerely thank to taxpayers in Canada and Quebec who contributed to funding of this project. I appreciate them and I see myself responsible for providing the best what I can for the Canadian nation.

Last but not the least, I sincerely thank to my parents who always encouraged me to follow my dreams. Special thanks to sunshine of my life Paul who boundlessly supported me with everything that he had to ensure I am on track to reach my goals.

RÉSUMÉ

Alors que la longévité des humains augmente en raison des progrès de la recherche en santé, le vieillissement apparaît comme un facteur de risque critique pour un large éventail de pathologies humaines. « Un homme à l'âge de ses artères » est un dicton qui met l'accent sur l'importance des parois vasculaires en santé pour soutenir un vieillissement en santé. Chez un individu jeune et en bonne santé, lorsque le sang est pompé vers le cerveau, l'élasticité des artères atténue les fluctuations pulsatiles du sang, en particulier au niveau des grandes artères. Ainsi, malgré la nature pulsatile du sang dans les artères majeures, un écoulement continu est finalement atteint dans les capillaires cérébraux durant la systole et la diastole. Un métabolisme cérébral sain et une intégrité microvasculaire dépendent fortement d'un flux sanguin cérébral continu, même durant la diastole. Au cours du vieillissement, les parois artérielles des vaisseaux se modifient, devenant plus rigides et plus épaisses, diminuant ainsi leur capacité à amortir les fluctuations pulsatiles. Le résultat est qu'une pression d'impulsion plus élevée est transmise vers la microcirculation cérébrale. Une telle altération de l'interaction cœur-cerveau médiée par la fonction vasculaire est fondamentale pour une hypothèse biomécanique qui relie une pulsatilité artérielle plus élevée aux lésions cérébrales. Il est en effet supposé qu'une pulsatilité cérébrale plus élevée chez les personnes âgées contribue à la présence de dommages à la microcirculation cérébrale, à l'amincissement cortical et conséquemment au déclin cognitif. Il est connu que la présence de facteurs de risque cardiovasculaires tels que l'hypertension, le diabète et la dyslipidémie pourrait entraîner des dommages accumulés aux parois artérielles. Par conséquent, l'issue défavorable du vieillissement artériel sur le système vasculaire cérébral en aval peut être plus profonde en présence de facteurs de risque cardiovasculaire. L'autre facteur qui influence l'interaction cœur-cerveau est la performance du cœur car celui-ci est la source de la pulsatilité. Dans les maladies cardiaques, telles que la maladie coronarienne, l'une des maladies cardiaques liées à l'âge chez les personnes âgées, le flux sanguin cérébral du cerveau peut être réduit.

Afin d'étudier la pulsatilité cérébrale et son association aux modifications cérébrales structurelles et hémodynamiques, trois études ont été ici menées. L'impact du vieillissement en bonne santé sur la pulsatilité cérébrale et son association à l'épaisseur corticale a été étudié en examinant des individus jeunes et plus âgés en bonne santé. Un protocole d'imagerie cérébral multimodal a été utilisé pour étudier la pulsatilité cérébrale. La pulsatilité intracrânienne a été indexée par imagerie

par résonnance magnétique par contraste de phases (CP-IRM) dans les artères carotides et vertébrales internes et le canal du liquide céphalorachidien au niveau de l'espace sous-arachnoïdien cervical. La pulsatilité cérébrale régionale à travers le cortex a été quantifiée par une mesure de spectroscopie dans l'infrarouge proche (NIRS) fonctionnelle. L'association entre la pulsatilité et la performance cognitive a ensuite été explorée à l'aide de la tâche de Stroop. Les données NIRS fonctionnelles ont été utilisées pour indexer la pulsatilité chez les personnes âgées présentant des conditions de facteur de risque cardiovasculaire et une maladie coronarienne. Là, le NIRS fonctionnel a permis l'étude de l'hémodynamique cérébrale même dans une expérience basée sur la mobilité et a donc été utilisé pour étudier l'impact de la marche de faible intensité sur la dynamique de la pulsatilité cérébrale.

Les résultats montrent le potentiel de contribution du NIRS fonctionnel pour étudier la pulsatilité cérébrale. Plus particulièrement, ils indiquent que la pulsatilité cérébrale évolue à la fois dans un contexte de vieillissement en santé et en présence de pathologies du vieillissement. Cette recherche suggère des pistes prometteuses pour de futures recherches sur la pulsatilité cérébrale en tant qu'indice potentiel de la santé cérébrovasculaire, soit un paramètre qui pourrait à terme devenir un nouvel indicateur de santé cérébrale dans le vieillissement en santé comme dans les cas de maladies cardio-vasculaires lors du vieillissement.

ABSTRACT

As longevity increases due to advancements in science and medical technology, aging is emerging as a critical risk factor for a wide range of human pathologies. “A man is as old as his arteries” is a famous saying that emphasizes the importance of ensuring healthy vessel wall to sustain health in aging. In young and healthy individuals, as blood travels towards the brain, the elasticity of the arteries’ wall attenuates the pulsatile fluctuations of blood, especially the large central arteries. Accordingly, despite the pulsatile nature of the blood circulation in the central arteries, a almost steady flow is achieved in the brain capillaries during both systole and diastole, a condition which is required in order not to impact on the integrity of the neurons. Healthy brain metabolism and microvascular integrity are highly dependent upon steady cerebral blood flow, even during diastole. However, in the course of aging, the vessels evolve towards stiffer and thicker arterial walls and the ability of the arteries to damp the pulsatile fluctuations diminishes. The result is a higher pulse pressure traveling to the brain microcirculation. Such alteration in heart-brain interaction mediated by vascular function is fundamental to a biomechanical hypothesis that relates the higher arterial pulsatility to damage in the brain. Higher cerebral pulsatility is hypothesized to contribute to the damage to the brain microcirculation and to cortical thinning that can result in cognitive decline in older adults. It is known that the presence of classic cardiovascular risk factors such as hypertension, diabetes, and dyslipidemia could lead to accumulated damage to the arterial walls. Hence, the adverse outcome of arterial aging on the downstream brain vasculature may be more profound in the presence of cardiovascular risk factors. The other factor that influences heart-brain interaction is the performance of the heart, as it is the source of pulsatility. In heart diseases, such as coronary artery disease, which is one of the prevalent age-related heart diseases among older adults, the cerebral blood flow could reduce.

In order to better understand the relationship between brain pulsatility and its association with brain structural and hemodynamic modifications, three studies were conducted. The impact of healthy aging on cerebral pulsatility and its association with cortical thickness was explored by examining healthy young and older individuals. A multi-modal brain imaging protocol was used to study cerebral pulsatility. Intracranial pulsatility was indexed with PC-MRI in the internal carotid and vertebral arteries and cerebrospinal fluid canal at the cervical subarachnoid space. The regional cerebral pulsatility across the cortex was quantified through a measure from functional

NIRS data. The association of pulsatility and cognitive performance was then explored using the Stroop test. Functional NIRS data was used to index pulsatility in older adults with cardiovascular risk factor continuum conditions and coronary artery disease. There, functional NIRS enabled the study of cerebral hemodynamics even in a mobility-based experiment and so was employed to study the impact of low-intensity walking on the dynamics of cerebral pulsatility.

The results showed the potential of using functional NIRS to study brain pulsatility and indicated that cerebral pulsatility evolves in both healthy and in the presence of cardiovascular pathology. This research suggests promising avenues for future investigations on cerebral pulsatility as a potential index of cerebrovascular health and this parameter may become a new parameter in patients' clinical profiles.

TABLE OF CONTENTS

LIST OF TABLES

LIST OF FIGURES

LIST OF SYMBOLS AND ABBREVIATIONS

ASL	Arterial spin labeling
ACE	Angiotensin converting enzyme
ARA	Angiotensin antagonist receptor
AW	After walking
BBB	Blood brain barrier
BDI	Beck depression inventory
BMI	Body mass index
BW	Before walking
CAD	Coronary artery disease
CBF	Cerebral blood flow
CABG	Coronary artery bypass graft
CHD	Coronary heart disease
CSF	Cerebrospinal fluid
CO_2	Dioxide carbon
CPA	Cerebral pulse amplitude
CRF	Cardiorespiratory fitness
CVRF	Cardiovascular risk factors
DCS	Diffuse correlation spectroscopy
DDST	Digital symbol substitution test
DBP	Diastolic blood pressure;
ECG	Electrocardiogram
FDR	False discovery rate
FOV	Field of view
eTIV	Total intracranial volume
GDS	Geriatrics depression scale
HCVRF	High cardiovascular risk factors
HDL	High-density lipoprotein
HIV	Human immunodeficiency virus
ICA(s)	Internal carotid artery (ies)

ICP	Intracranial pressure
LCVRF	Low cardiovascular risk factors
LDL	Low-density lipoprotein
LED	Light emitting diode
Lp_{ArtCSF}	Latency between arterial inflow and CSF outflow systolic peak
RPA	Right pre-auricular
PC-MRI	Phase contrast MRI
PI	Pulsatility index
PPG	Pulse plethysmography
PRF	Pulse relaxation function
PTTp	Pulse transit time to the peak of the pulse
PWV	Pulse wave velocity
RAVLT	Ray auditory, verbal learning test
SatO2	Blood oxygen saturation
SBP	Systolic blood pressure
SI	Stroop color word interference
TE	Echo time
TMT A/B	Trail making A and B
TOF-MRA	Time-of-flight magnetic resonance angiography
TR	Repetition time
LPA	Left pre-auricular
mBLL	Modified Beer-Lambert law
MCA	Middle cerebral artery
METs	Metabolic equivalents
MIP	Maximum intensity projection
MPRAGE	Magnetization prepared rapid gradient echo
MoCA	Montreal cognitive assessment
NIRS	Near-infrared spectroscopy
NU	Neutral
OSPAN	Operation word span
VA(s)	Vertebral artery(ies)

V_{enc}	Velocity encoding
WAIS	Wechsler adult intelligence scale
2D	Two dimensional
3D	Three dimensional
4D	Four dimensional

CHAPTER 1 INTRODUCTION

In this chapter, cerebral pulsatility and the methods used for its measure are briefly explained. The general and detailed context of the problem is discussed in terms of cerebral pulsatility and its alteration in healthy aging, in the presence of cardiovascular risk factors (CVRF) and coronary artery disease (CAD). The association of healthy aging to brain structural changes and hemodynamic changes is explored. Finally, the objectives, hypotheses and roadmap of implementing the methodology are laid out.

1.1 General context

From 1971 to 2011, the number of seniors above 65 years old doubled in the province of Quebec, Canada (Institut de la Statistique du Québec, 2015). Official reports in the statistics database of Quebec anticipate that the percent of older adults to younger will double from 14% to 28% by the year 2056 (Institut de la Statistique du Québec, 2015). Occurring not only in Quebec, demographic aging of the Canadian population is also projected to double in number of elderly individuals aged 65 or over by the year 2061, in comparison to the year 2009 (Canada, S 2015). This significant increase in the number of senior individuals is not only specific to Quebec and Canada but is a worldwide trend, tripling the number of seniors by the year 2050 (Lutz & Kc, 2010). These statistics highlight the necessity of several economic plans for providing social support and advanced health care services for the upcoming epidemic of age-related diseases created by this growing proportion of seniors in the population.

Increasing longevity is concomitant with the emergence of age-related diseases including “cardiovascular” and “cerebrovascular” diseases. As their names suggest vascular function is a prime contributor to these two categories of disease. All the vessels in the body are affected by the aging process. Arterial stiffening is a signature of vascular aging and alters the structure and function of the arterial walls (Kohn, Lampi, & Reinhart-King, 2015). While arteries are aging, the elastin fibers fragment and are gradually replaced by stiffer collagen, especially in the large elastic arteries. In the stiffer arteries, pulse pressure (or pulsatility, *i.e.,* the difference between systolic peak and diastolic minimum) enhances with a higher vascular impedance to blood flow in the

downstream cerebral arteries (Mitchell et al., 2011). These vascular modifications can lead to impairment in the cognitive functions (Scuteri et al., 2007). Earlier studies on age-related cognitive decline and vascular impairment were found to be two different categories of age-related disease (Mitchell 2015). Thanks to advancements in non-invasive imaging in recent decades (an example of such Figure 1A, 1B) that provided non-invasive and in-vivo assessment of vascular structure. The advancements in non-invasive imaging in recent decades have shown greater clarity into the interrelation of these categories in light of the growing research indicating that the normal function of the brain may deteriorate if the delicate link between blood flow and the brain is upset by vascular dysfunction. The term "vascular dementia" is a concept that has linked cognitive deficits to vascular impairments (Caisberger & Vališ, 2018).

A large body of literature reported vascular correlates of age-related modifications in several domains. For instance, vascular risk factors and microcirculation damage in the brain are reported as important contributors to emerging dementia (Stone, Johnstone, Mitrofanis, & O'Rourke, 2015). Thus, vascular wall treatments were selected as the target for general prevention and treatment (Nguyen, Dominguez, Nguyen, & Gullapalli, 2010; Shabir, Berwick, & Francis, 2018). Higher pulsatility is associated with cerebral microvascular and structural modifications and lower cognitive performance in several domains (Mitchell, 2015). Indeed, long-term higher cerebral pulsatility could modify neurovascular architecture and brain metabolism (Attwell et al., 2010). Reports on healthy individuals link age-related decreased perfusion (Mitchell et al., 2004, 2011), cortical thinning (Pasha et al., 2015) and cognitive decline (Li, Lyu, Ren, An, & Dong, 2017), with arterial stiffness as a significant mediator to this association (Raz, Ghisletta, Rodrigue, Kennedy, & Lindenberger, 2010; Raz & Rodrigue, 2006). As the result of such modifications, seniors may experience changes in sensory processing and motor performance and decline in cognitive processes with poorer performance in tasks of higher complexity (Qiu, Kivipelto, & Von Strauss, 2009). Indeed, higher prevalence of mild-cognitive impairment and dementia is one of the most reported aspect of an aging population (Salthouse, 2010).

Several authors have reported the undeniable impact of vascular aging not only on the neurophysiology (Deary et al., 2009) but also on neuroanatomy of the brain (Abdelkarim et al., 2019). In the larger picture, previous reports assess that in the course of aging the brain shrinks at

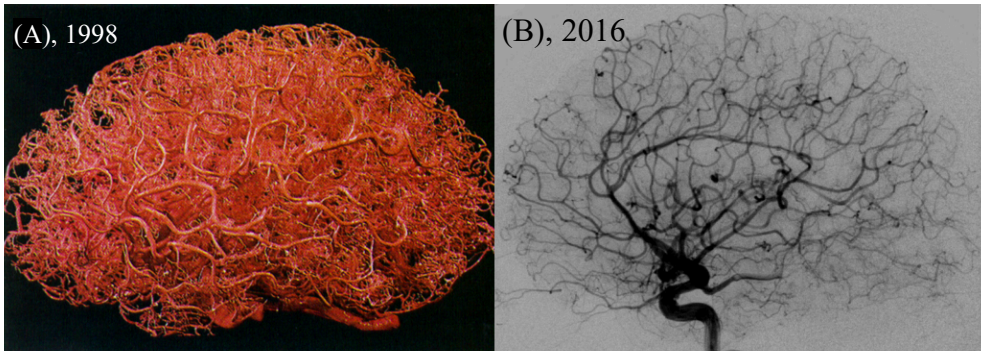

Figure 1-1 Dense network of cerebral blood vessels in the human head. In this image, brain parenchymal tissue was dissolved after plastic emulsion was injected into the cerebral vessels. Image source: (Zlokovic & Apuzzo, 1998). (B) Digital subtraction angiographic arterial phase of the human brain. The image was produced using a contrast medium and subtracting pre-contrast image from the original images. This imaging technique was under development from 1996. Image source (Wang, Kim, Normoyle, & Llano, 2016).

distinct rate across the cortex (Fjell et al., 2009; Lemaitre et al., 2012; Mitchell et al., 2011; Peters, 2006; Salat et al., 2004) with expansion of cerebrospinal fluid (CSF) (Lemaitre et al., 2012; Matsumae et al., 1996). Hence, identifying mechanisms of age-related brain structural changes and cognitive impairments yields substantial advantages by providing earlier detection, increasing the chance of successful prevention or treatment. Identifying these mechanisms are important as despite substantial progress towards understanding the pathogenesis of age-related dementia (Jellinger, 2008; Kalaria, 2016, 2018), available treatment options are not significantly effective (Benetos et al., 2002; Casey, Antimisiaris, & O'Brien, 2010). Scientific enquiries to reverse the dementia process have met very limited success (Day, 2019), making prevention even more important at this time (Rakesh, Szabo, Alexopoulos, & Zannas, 2017). In this thesis, pulsatility in the dense network of cerebral circulation (Figure 1A) was explored as a mechanism that may contribute to age-related alterations in the brain and cognitive outcomes.

1.2 General problem statement

Several studies have linked central arterial stiffness to decreased cognitive abilities (Benetos et al., 2012; Hughes et al., 2018; Jefferson et al., 2018; Waldstein et al., 2008; Watson et al., 2011) and

cortical atrophy (Maillard et al., 2016; Palta et al., 2019; Pasha et al., 2015; Zhai et al., 2018). In several studies, pulse wave velocity (PWV) is used as the gold standard for indexing arterial stiffness in the central arteries. Doppler ultrasound (Figueras et al., 2006) and phase contrast magnetic resonance imaging (PC-MRI) are the modalities used to assess the pulsatility in the large arteries (Wåhlin, Ambarki, Birgander, Malm, & Eklund, 2014). Peripheral assessment of the pulsatility is determined using a pulse plethysmograph (Uangpairoj & Shibata, 2013). However, these techniques are limited to probing larger vessels and produce a single, global measure of pulsatility. Given the dense arterial network of the brain (Figure 1A and 1B), depending on the regional stiffness and damage of the underlying vasculature, the vulnerability of brain tissue supplied with this vasculature could be different. Hence, one could raise the hypothesis that the spatial distribution of pulsatility could provide complementary information about selective vulnerability of brain regions. In this thesis, functional NIRS is used to quantify pulsatility indices across the cortex. With this hemodynamic imaging technique, the measurements are indirect and are the result of interactions of elements of neurovascular coupling, electrical, metabolic and vascular phenomena generating the signals. In this thesis, we hypothesized that pulsatility measured with functional NIRS is related to regional cerebral arterial stiffness. We tested this hypothesis by exploring the association between PC-MRI data (index of vascular stiffness) and pulsatility indexed with functional NIRS data. Further, the impact of healthy aging and the cardiovascular degradation continuum from healthy to cardiovascular disease and CAD on cerebral pulsatility is explored.

1.2.1 Cerebral pulsatility and its elements

In light of studying the pressure and flow in the arteries, the most obvious feature of the arterial blood circulation that until recently has often been neglected, needs to be considered which is its pulsatile nature. The heart is a pulsatile pump and generates pulsatile pressure and flow. This pulse oscillates close to its mean between systole and diastole. The morphology of this oscillating pulse is highly dependent upon biomechanical properties of the vessel wall. In a young and healthy individual, the arteries, especially the aorta, are highly compliant, and hence there is an optimal impedance mismatch with the first branches of central arteries (due to their difference in arterial wall properties and diameter). When the left ventricle contracts, it generates a forward travelling wave with a high energy. When this pulse encounters impedance discontinuity between aorta and

its branches, a portion of the pulse reflects to the aorta and therefore is not transmitted to the brain with full magnitude (Mitchell, 2008). The elastic and compliant arteries accommodate the blood with a moderate increase in their walls pressure[1] and thus the pulse wave travels along the conduit arteries at a relatively low velocity (Mitchell, 2015). The aggregate of all the reflected pulse waves from the entire arterial tree produces a total reflected wave that typically returns to the aorta in early diastole (Mitchell, 2008). These mechanisms not only contribute to enhancing coronary perfusion (Mitchell et al., 2011) but also function as a protective mechanism that restricts transmission of the higher-energy pulse into the cerebral microcirculatory system (Mitchell, 2008). This coordinated action buffers the energy of the pulse as required releases the remaining potential energy of the arterial wall and conducts the blood through the artery (McDonald, 1955). The wave thus reflected from the periphery returns to the heart in diastole, augments diastolic pressure and further minimizes systolic pulse pressure (Mitchell, 2015). In the elastic artery, such mechanisms cause that the diastolic period is optimally delayed, which has an important effect on tissue oxygenation (McDonald, 2011). Naturally, the physiology of the organs in the body has evolved to benefit from this pulsatile nature. This is seen in the vascular signaling pathways that are particularly responsive to the cyclic circumferential stretch, sensing strain on the arterial wall. For instance, aortic and carotid baroreceptors sense the pressure of the pulse and through signaling pathways regulate the pulse that is traveling to the brain (McDonald, 2011). The end sites where the significant damping of the pulsatility occurs in the microcirculation are the cerebral arterioles, which by vasodilation and vasoconstriction adjust and regulate blood flow as it travels to the cerebral capillaries (Mitchell, 2015; Mitchell et al., 2011). Thereby, despite the pulsatile nature of the flow in the central arteries, there is a mostly steady flow during both systole and diastole in brain capillaries (O'Rourke & Hashimoto, 2007; O'Rourke & Safar, 2005). Healthy brain metabolism and microvascular integrity are highly dependent on maintaining cerebral blood flow even during diastole (Willie, Tzeng, Fisher, & Ainslie, 2014).

In an aging arterial tree, the proportion of elastin in the arterial wall components decreases

[1] Referring to the pressure-volume curve (Marmarou, Shulman, & LaMorgese, 1975) and the concept of compliance. In the highly compliant medium, the increase in the volume leads to a small increase in the pressure.

(O'Rourke & Hashimoto, 2007; Vlachopoulos, Charalambos, Michael O'Rourke, 2011) and thus the ability of the artery to act as an elastic reservoir and damp the pressure fluctuation decreases (Hashimoto & Ito, 2009). In conjunction with this effect, a disproportionate increase in the stiffness of the aorta compared to its branches leads to progressive impedance matching between the aorta and first-generation central arteries (Mitchell, 2008, 2015). These two alteration reduce damping of the pulsatility and hence the amount of wave reflection at the boundary between aorta and central arteries. A reduction in wave reflection at this important interface leads to transmission of a forward wave with higher energy and its dissipation in the end organs including the brain. The brain, as high-resting-flow organ, has low terminal impedance, facilitating the penetration of a greater percentage of the pulsatility deeply into the cerebral microcirculation. Cerebral arterioles respond to this abnormal pulse by constricting and eventually remodeling, which is a protective mechanism to increase the resistance and limits local blood flow to the tissue (Mitchell, 2015). Due to this adaptive mechanism, even though the tissue may experience hypoperfusion (Vlachopoulos, Charalambos, Michael O'Rourke, 2011), the capillaries initially remain protected from pulsatile flow and may at least partially maintain their steady flow (Mitchell, 2008). Nevertheless, over time, barotrauma and the damage induced on the arterial wall compromise the reactivity of arterioles and thereby brain capillaries may be exposed to pulsatile flow (Mitchell, 2008, 2015). The endothelial function of the cerebral arteries can also be distressed by higher pulsatility. This microcirculatory dysfunction may lead to cumulative tissue damage, blood brain barrier (BBB) impairment (Garcia-Polite et al., 2017) and microvascular hemorrhage (Stone et al., 2015). Eventually, CBF may become uncoupled with the metabolic needs of the underlying tissue (Toth, Tarantini, Csiszar, & Ungvari, 2017).

In recent years, a growing body of literature has prompted interest in relations between pulsatile hemodynamics and damage to cerebral microcirculation (McDonald, 2011). Not only cortical regions have been investigated but also deep brain structure such as subcortical brain regions; white matter (Tan et al., 2019) and basal ganglia (Geurts, Zwanenburg, Klijn, Luijten, & Biessels, 2019) are not exempt from rigors of higher pulsatility. These deeper brain structures are perfused from arteries at the base of the brain (circle of Willis) where being closer to the central arteries exposes the tissue to a higher level of pulsatility that may even be higher than what cortical regions experience. This abnormal pulsatility can lead to various manifestations of cerebral small vessel diseases. Indeed, a chronic increase in pulsatility is reported to be associated with the presence of

white matter hyper-intensities (Zwanenburg, 2018) and white matter signal abnormalities (Tan et al., 2019) on MRI images. Taken together, these reports suggest that arterial stiffness, rather than being a '*normal*' feature of aging lead to pathologies in aging which may cause substantial brain damage.

Healthy aging lead to modification of CBF (Diaz-Otero, Garver, Fink, Jackson, & Dorrance, 2016) also CVRF such as hypertension (Blanco, Müller, & Spence, 2017), diabetes mellitus (Liu et al., 2018) and dyslipidemia (Warsch et al., 2010) are associated with cerebral small vessel disease. Even though the mechanisms of this association are not entirely clear, a possible pathway is through enforcing some degree of modification to the arterial walls and higher pulse pressure to the vasculature (which apart from stiffening of the arteries adds some cumulative damage). Studies have linked vascular risk factors to hypoperfusion, flow misregulation, BBB modifications and cognitive decline (Iadecola & Davisson, 2008). To treat this situation, the arterial wall is considered as a target for therapy (Mancia et al., 2013).

As part of age-related increased central pulse pressure, coronary artery perfusion pressure may become impaired (as a consequence of the premature arrival of the aggregated reflected waves in the late systole instead of early diastole). Age-related arterial stiffness and CVRF are shared risk factors for CAD. Previous research linked CAD to alterations of the blood flow supplying the brain. Such studies suggest that CAD may promote cerebral small vessel disease, which is a major contributor to dementia in older adults (Ng, Turek, & Hakim, 2013). Furthermore, age-related arterial stiffness, CVRF and CAD are associated with cortical brain atrophy and cognitive decline (Bateman, Levi, Schofield, Wang, & Lovett, 2008; Henry Feugeas et al., 2005; Vlachopoulos, Charalambos, Michael O'Rourke, 2011). Damage to the arterial walls and transfer of greater pulsations to the brain's microvasculature could lead to microvascular rupture and subsequent micro-hemorrhages, and impairment in the endothelial functions (O'Rourke & Hashimoto, 2007). Studies reported a higher CBF during physical activity. While increased metabolism is the most well-known reason for the increasing the CBF, vascular factors are strongly modulating this effect. One mechanism is the increase in carbon dioxide as a result of physical activity, which is reported strongly to regulate CBF by inducing dilation in the cerebral vessel diameter. Moreover, in the CAD patients, as a result of physical activity and the demands of working muscles, cardiac output could change and therefore alter the perfusion. Hence, it was of interest to explore the impact of walking on alterations of cerebral pulsatility.

Cerebral blood flow and pulsatility in the human brain not solely depends on the arterial pulse. As the human brain is in the cranium space including blood, CSF and brain, the total mechanical interaction between these components will define the pulsatility imposed on the brain (Wåhlin et al., 2010). Inside the cranium, the CSF encompasses the brain tissue. In each cardiac cycle, the volume of oxygenated blood enters the cranium and the intracranial pressure rises. To alleviate this pressure, CSF fluid shifts to the spinal canal and the venous system drains the blood (Alperin, Lee, Loth, Raksin, & Lichtor, 2000; Enzmann, Pelc, & McComb, 1993; O'connell, 1943; Stoquart-ElSankari et al., 2007; Wagshul, Eide, & Madsen, 2011). Together, while the effect of pulsatility in the brain is explored the role of other intracranial components in such interaction needs to be considered in the analysis.

1.3 Methods of assessing cerebral pulsatility

There are several non-invasive methods for quantitative assessment of pulsatility (Figure 1-2). For instance, PC-MRI is often used to measure the pulsatility index in the cerebral arteries supplying the brain tissue, such as carotids and vertebral arteries (Holmgren, Wåhlin, Dunås, Malm, & Eklund, 2019; Vikner et al., 2019; Wåhlin et al., 2014) and down to MCA (Zarrinkoob et al., 2016). Doppler ultrasound (Terzi, Arslanoğlu, Demiray, Eren, & Cancuri, 2014) is used to index pulsatility in ICAs. Transcranial doppler is used to assess pulsatility in MCA from temporal window (De Riva et al., 2012). Another simple and inexpensive peripheral index of arterial pulsatility is determined based upon the difference between systole and diastole in the pulse cycle using a pulse plethysmograph (Uangpairoj & Shibata, 2013). Using a sphygmomanometer, brachial pulsatility can be calculated from the difference between systolic and diastolic arterial pressures (Wåhlin et al., 2010, 2014). All these techniques introduce a single, global index of pulsatility and do not reflect the spatial distribution of pulsatility across the cortical regions where damage occurs. Cerebral pulsatility is dependent upon the distribution of stiffness in the underlying arterial network in the brain and thus varies in each segment of the cerebral vascular tree (Fabiani et al., 2014; Tan et al., 2017). Recently, Ruesch et al., (2020) non-invasively assessed the intracranial pressure by the use of microvascular CBF acquired from diffuse correlation spectroscopy (DCS) data in non-human subjects.

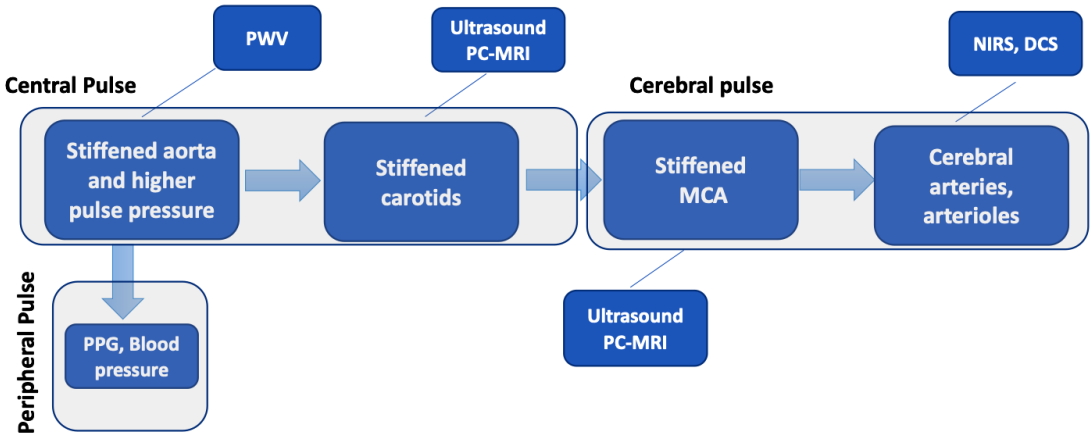

Figure 1-2 The chart of pathways of propagating pulse pressure from heart to periphery and examples of most commonly used imaging modalities in the literature for the measurement of pulsatility.

In this thesis, the focus is on a new approach for the measurement of pulsatility across the cortex using functional NIRS data. The NIRS technique, with its higher temporal resolution, can assess regional cerebral pulsatility across the cortex non-invasively and in a more natural setting even in mobility-based tasks. The morphology of the cerebral arterial pulse is in some ways similar to pulse plethysmograph data, a strong and identifiable component in the functional NIRS data. This signal can be measured in each recording location, with appropriate sensor contact to the head. The pulsatile motion of blood expands the walls of cerebral arteries and arterioles. The new volume of blood entering the vascular bed in each cardiac cycle induces periodic alterations to the concentration of oxy-hemoglobin, which attenuates near-infrared light absorption. Near-infrared source and detector pairs can measure this attenuation in the probed region. In the last few years, functional NIRS was used to study pulsatility in the regional microcirculation with parameters extracted from the characteristics of the cerebral pulse in the data (Chiarelli et al., 2017; Fabiani et al., 2014; Tan et al., 2017). Among cerebral pulsatility parameters quantified by functional NIRS data that were shown to vary with aging are the cerebral pulse amplitude and the cerebral pulse relaxation function (PRF, Chiarelli et al., 2017; Tan et al., 2019, 2017; Fabiani et al., 2014). We used the same parameters to study cardiovascular degradation continuum in the older adults. For the study of the healthy aging, we introduce the use of pulse-transit-time-to-the-peak-of-the-pulse (PTTp) as a pulsatility parameter. The PTTp is the time it takes for the pulse to travel from the

heart to the downstream measurement point. The PTTp is associated with arterial path length and the integration of arterial stiffness along the path traveled by that blood. Hypothetically, if we control for the length of the artery, a shorter PTTp is an indication of higher arterial stiffness (Likitlersuang, Teachavorasinskun, Surarak, Oh, & Balasubramaniam, 2013). This parameter is used before in several studies with PGG where the aim was to assess the arterial stiffness (Smith, Argod, Pépin, & Lévy, 1999). In this thesis, we used functional NIRS data to study cerebral pulsatility in the microcirculation in the healthy aging, cardiovascular disease continuum and in the presence of CAD. For healthy aging, the association between cerebral pulsatility and brain structure such as cortical thickness is explored.

1.4 Main contributions

In the study of healthy aging, cerebral pulsatility and its association with cortical thickness is explored. I took care of the ethics applications for three different ethics committees: the Centre de recherche de l'Institut universitaire de gériatrie de Montréal (CRIUGM), Polytechnique Montreal and the Montreal Heart Institute (MHI). For the first two ethics committees, I was responsible for all forms of correspondence. The MHI ethics committee requires French documents, so I did everything except translation to French. After the study was approved by these three ethics committees, I collected the data as a multi-session study from 79 participants. Neuropsychology test was performed by one of our native French speaker colleagues at CRIUGM. Participants completed three visits each, each visit at most two hours in duration. The first visit included a blood draw after overnight fasting and a neuropsychology test following a light breakfast. Neuropsychology test was performed by a French speaking college in our team at CRIUGM. The first session of the study was concluded with familiarizing the participant with functional NIRS and MRI. In the second visit, resting MRI data and the weight and height of each participant were collected. In the third visit, resting-state NIRS data were collected simultaneously with electrocardiogram (ECG) and PPG. Following resting-state data collection, our participants performed Stroop test while functional NIRS was capturing their brain activation data. Blood pressure was measured at the beginning and end of the third session. For participants, the blood

pressure values were reported as an average[2]. Furthermore, for this study I've analyzed the data and wrote article 1 and the draft for article 3 (in preparation, presented as a chapter with some results).

In the study of pathologies in aging, the impact of cardiovascular degradation from low cardiovascular risk factors (LCVRF) to high cardiovascular risk factors (HCVRF) and CAD on pulsatility in the cerebral microcirculation is explored. The data were collected by another team at Montreal Heart Institute, Montreal, Canada, in advance and provided to me as the first part of a longitudinal study. Given the difficulties of the data collection phase, especially for human studies, my gratitude is owed to Dr. Louis Bherer for sharing the data with our team at Polytechnique Montreal. In this study, I analyzed the data and wrote the publication as the main contributions.

1.5 Link between studies and current limitations

The three studies in this thesis aim to assess alterations of cerebral pulsatility as cardiovascular system degrades (from young to old, LCVRF, HCVRF and CAD in the older adults).

In the study of healthy aging the aim was to study the impact of healthy aging on alteration of cerebral and peripheral pulsatility and its association with structural and functional changes to the brain. These objectives were addressed in objectives AIM1 and AIM3, respectively. Due to time constraints, the article for AIM3 is still in preparation and presented as a normal short chapter.

We further continued to study cerebral pulsatility associated with cardiovascular degradation in the most prevalent conditions in older adults, which are CVRF and CAD disease. As functional NIRS provide the possibility to study hemodynamic response in mobility-based task, the impact of short-duration walking on changes of cerebral pulsatility was explored. For the study on individuals with CVRF and CAD patients, structural MRI and PC-MRI (or ultrasound data) were not available. Therefore, to have a more complete picture about CAD and its impact on cerebral pulsatility, we planned to continue to study this group of participants in the near future with a similar procedure as in study 1 (healthy aging).

[2] There was no statistically significant difference between the first (at the beginning of the session) and second (end of the session) blood pressure measurements.

1.6 Objectives and aims

AIM1: To determine the impact of healthy aging on the spatial distribution of pulsatility across the cortex and to assess whether this distribution is reflected in the cortical thinning and cognitive performance.

Hypothesis 1.1: In the course of aging from young to older, the optical measure of cerebral pulsatility increases (or PTTp indexed with NIRS decreases). There is an association between regional cortical thickness and regional PTTp across the cortex.

Hypothesis 1.2: Cerebral pulsatility measured with PTTp is associated with performance of the MoCA task in older adults.

Hypothesis 1.3: In the flow parameters measured with PC-MRI in the cervical subarachnoid space, the latency between the cerebral arterial inflow systolic peak and the CSF outflow systolic peak was negatively associated with global cortical thickness.

Article 1 : Hanieh Mohammadi, Ke Peng, Ali Kassab, Louis Bherer, Anil Nigam, Frédéric Lesage and Yves Joanette. Cortical Thinning is Associated with Brain Pulsatility In the Older Adults: An MRI and NIRS Study. Submitted to Neurobiology of aging (March 2020)

AIM2: To determine the impact of LCVRF, HCVRF and CAD on cerebral pulsatility measured with cerebral pulse amplitude and PRF and to evaluate how short-duration walking could impact cerebral pulsatility across the cortex differently in these clinical groups.

Hypothesis 2.1 The cerebral pulse amplitude increases and PRF decreases as cardiovascular degradation progresses from LCVRF to HCVRF and CAD.

Hypothesis 2.2 Short-duration walking decreases cerebral pulse amplitude and increases PRF.

Article 2: Hanieh Mohammadi, Thomas Vincent, Ke Peng, Anil Nigam, Mathieu Gayda, Sarah Fraser, Yves Joanette, Frédéric Lesage, and Louis Bherer. Coronary Artery Disease and Its Impact on the Pulsatile Brain: A Functional NIRS Study. Submitted to Human Brain Mapping (Dec 2019).

AIM3: To determine the link between cerebral pulsatility and reaction time in the Stroop color-word interference test and to determine spatial correlation between age-related functional reorganization and regional cerebral pulsatility in older adults.

Hypothesis 3.1 As cerebral pulsatility increases (PTTp decreases), reaction time to the color-word interference test increases.

Hypothesis 3.2 Functional reorganization in the color-word interference test have spatial correlation with regions with lower regional pulsatility as measured with PTTp.

Chapter 6 (or article 3 in preparation): Age-related functional reorganization in the brain is correlates with brain regions with lower pulsatile stress.

CHAPTER 2 LITERATURE REVIEW

This chapter presents an overview of the pertinent literature on cerebral pulsatility and its relevance to brain structure and function. It is complementary to the articles in chapter 4, 5 and the results in chapter 6. This brief review focuses on human studies, with selected related animal studies superficially discussed.

Large-scale longitudinal and cross-sectional studies on older adults have linked age-related higher central arterial stiffness to brain atrophy and cognitive decline. In recent years, some authors have reported that cognitive decline is correlated to the pulsatile component of blood flow in the large arteries supplying the brain. This literature suggests that age-related higher arterial stiffness is causing a chronically increased pulse pressure. Higher pulse pressure likely contributes to the emergence of several spectrums of brain microvascular dysfunctions, cerebral small vessel diseases, cortical thinning, and cognitive decline. Based on these reports, it is pertinent to evaluate whether regionally higher pulsatility in some regions of the brain contribute to brain aging and perhaps advances cognitive decline in older individuals. Nevertheless, it is crucial to note that these reports and the research in this thesis could not prove causality. They indicate association if any region of brain in particular is more strongly linked and vulnerable to higher pulsatility.

2.1 Aging and alterations in the arterial structure and function

The arterial tree has the two major utilities of conducting the blood from the heart to the end organs and buffering the pulsatile blood fluctuations (O'Rourke & Hashimoto, 2007). The conduit and cushion outcomes together exploit wave reflection for enhanced coronary flow (Mitchell, 2008). The cushioning function depends upon, among others, the interplay between the generated flow, the elasticity (or compliance)[3] of the arterial tree and the viscosity of the blood (O'Rourke & Hashimoto, 2007). The arterial walls are comprised of three layers that are positioned concentrically: the inner, the middle and the outer. The inner layer has an internal elastic lamina and endothelial cells formed a layer within the confines of blood and vessel wall. The middle layer mostly comprised of smooth muscle and collagen fibers and the outer layer mainly include elastin

[3]In this thesis, we followed the approach of Fabiani et al. (2014) and did not attempt to distinguish between elasticity and compliance.

and collagen fibers (Baker, Tortora, & Nostakos, 1976). The collagen, elastin, and smooth muscle are load-bearing media of the vascular wall (McDonald, 2011). The abundant elastin and collagen in the large central arteries provide them an exceptional competence on damping the pulse pressure. In arterial walls at lower pressure, elastin fibers have a major contribution to the mechanical strength of the vessel. Collagen fibers bear the load for higher pressures (Mitchell, 2018; Mitchell et al., 2004; Vlachopoulos, Charalambos, Michael O'Rourke, 2011). The impact of aging on each layer of arterial walls is heterogeneous. Aging effects on the central arteries could be simply described as dilating (as the result of extending of the central pulse pressure) (Farasat et al., 2008), thickening of the wall and stiffening (O'Rourke, 2007). The latter impact manifests by a replacement of elastic elastin with stiffer collagen fibers (Faury, 2001; Hodis & Zamir, 2009). This age-related change has a profound impact on the aorta and the carotid arteries as they are highly compliant, and their walls consist of an abundant amount of elastin in their compounds. This is seen in the post-mortem studies reported that even in healthy individuals, the intimal layer of the aortic and carotid wall became thicker (Finn, Kolodgie, & Virmani, 2010).

The modification on the arterial wall has been associated with elastin fatigue as a result of the long-term bearing of cycles with higher stress. Eventually, elastin becomes thinner and fragmented thus transferring the load from elastin to considerably stiffer collagen. Collagen fibers are stiffer hence are less efficient in damping the pulsatility, leading to the diminishing of the damping of the energy of the traveling pulse which could be seen as an increased PWV (McDonald, 2011). Literature describes aging of the vascular wall as an outcome of long term heartbeat mechanical stresses that are imposed on the arterial wall (Stone, Johnstone, Mitrofanis, & O'Rourke, 2015). Therefore, depending on the damage on vascular and the vascular territory the damage on the vasculature and on the end-organ may vary (Chiarelli et al., 2017). These literature motivates assessment of pulsatility in the cerebral microcirculation and explore its association with cortical thickness.

2.2 Association between pressure and flow pulsatility

In each cardiac cycle, the heartbeat produces the pressure and flow that propagates in the arterial tree. This pulse oscillates around its mean and is composed of the steady and pulsatile components. The steady component (is often approximated by diastolic blood pressure+1/3 (systolic blood

pressure- diastolic blood pressure) is associated with cardiac output and resistance of the vasculature in the entire arterial tree. The pulsatile component is greatly linked to ventricular ejection fraction, the compliance of the aorta and reflected wave returning to central aorta. The blood flows in the arteries because of the pressure gradient generated by heart (Darne, Girerd, Safar, Cambien, & Guize, 1989). If there is a complete obstruction in the artery (such as a large blood clot), despite pressure gradient there could be no flow (McDonald, 1974). The pressure and flow are related physical phenomena; however, the differences between them are important. As mentioned above, pulse pressure is propagated through the arterial tree. However, the blood requires displacement in the vascular bed. The link between pressure and flow is strongly modulated by wave reflection as the result of impedance mismatch between branching arteries (Mitchell, 2014; Mitchell et al., 2011a; Stone, Johnstone, Mitrofanis, & O'Rourke, 2015). Stiffening of the aorta leads to higher impedance ($Z_c = P_F/Q_F$). In this equation, P_F is the amplitude of the forward pressure wave that comes from the left ventricle and Q_F is the forward flow wave. Flow pulsations across the brain are highly dependent on the biomechanical properties of the vasculature and the location of the measurement (Wagshul, Eide, & Madsen, 2011). As aging and diseases could change the blood flow pulsatility, this subject has gained the attention of researchers for use as a diagnostic tool. For instance, in individuals with chronic hypertension, systolic blood pressure is higher and some studies relate this to the stiffening of central arteries (Iadecola & Davisson, 2008), most importantly in the aorta as it is the most compliant artery in the human body. A large body of literature has linked higher systolic pressure to cerebrovascular damage such as gray matter and white matter lesions, cognitive decline and kidney diseases (Mitchell et al., 2011; O'Rourke, Safar, & Dzau, 2010; Tarumi et al., 2014). Higher PWV is associated with congestive heart failure through cardiac afterload (Desai, Mitchell, Fang, & Creager, 2009). This raises the question: is the increased higher mean pressure and/or higher pulse pressure associated with this damage? Marmarou et al. (1975) reported that as mean pressure rises, the magnitude of the pressure change rises exponentially (as the result of changes of volume), such as occurs in systolic inflow (pressure-volume relationship). The exponential association that relates pressure and volume indicates that with a higher mean pressure, pulse pressure also increases, even if the volume of blood has not changed. Marmarou and colleagues discussed the compliance curve presented in Figure 2-1, based on observed data. Compliance is defined as $\Delta V/\Delta P$, where ΔV describes changes in volume and ΔP changes in pressure. In a highly compliant

system, the increase in volume, even when large, corresponds to a small increase in pressure. The non-linear exponential association between pressure and volume in the brain shows that as mean pressure increases, the compliance of the system decreases (Marmarou et al., 1975). In another experiment, O'Rourke (1987), reported that higher mean pressure is linked to higher pulsatility which in turn lead to higher degree of destruction in the vessel wall. Ündar et al., (2002) suggested that flow pulsatility is associated with energy gradient that is getting delivered to the organs. In a simulation, where the mean pressure was kept constant, Shepard et al, (1966) reported that under pulsatile flow compared to steady flow, about 2.4 times greater energy were delivered to the tissue. Taken together, these literatures highlighting the importance of quantifying the burden of pulsatility and considering it as a component of age-related alterations.

2.3 Higher arterial stiffness and higher pulse pressure in the brain

In a compliant artery, the pressure pulse generated from the left ventricle travels with adequately slow pulse wave velocity (about 5–7 $m.s^{-1}$) to the peripheral arteries. As this pulse pressure is traveling towards the brain, it is damped by the arterial tree, leading ultimately to continuous blood flow in the capillary microcirculation (O'Rourke & Hashimoto, 2007; Stone et al., 2015). The efficiency of the transformation from pulsatile flow to the ultimately steady flow (the Windkessel effect) is greatly modulated by the compliance of larger arteries, which damp and smooth the pulsatility as the pulse travels to cerebral microcirculation (Watson et al., 2011). Cerebral arterioles hamper the pulsatility by the pressure-dependent myogenic response (Vrselja, Brkic, Mrdenovic, Radic, & Curic, 2014). The myogenic tone is a significant mechanism that protects the capillaries from receiving higher pulse pressure (Mitchell, 2018). With age-related arterial stiffness (or lower compliance), a higher-speed pulse wave velocity (about 8-15 $m.s^{-1}$) travels towards the brain (Hirata, Yaginuma, O'Rourke, & Kawakami, 2006). The systolic peak increases and reduces the diastolic minimum of the pulse (thereby increasing the pulse pressure) and exposes distal brain arteries to a pulse with a higher stress (Mitchell et al., 2004). In the process of aging, with diminishing myogenic tone, part of the protective mechanism of cerebral microcirculation is lost and the higher pulse pressure travels to capillaries (McDonald, 2011).

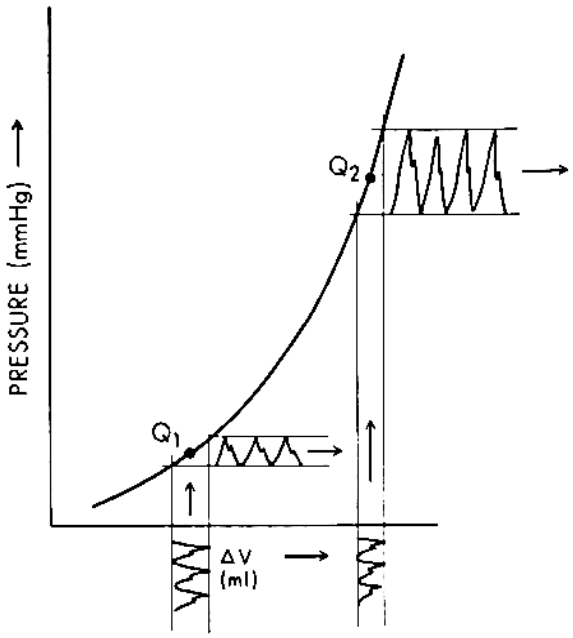

Figure 2-1 the exponential relationship between pressure and volume for brain tissue. Image source: Mamarou et al. (1975). The increase in the pressure pulsatility with a higher mean pressure even if the volume stays constant can be exponential.

The interaction of pulse pressure and microcirculation in the literature is formulated as a biomechanical hypothesis for the human brain (because of several obstacles involved in studying human brain microcirculation in vivo). However, in ex-vivo, from experiments on aged mice, Springo et al., (2015) reported a higher pulse pressure in the brain arteries leading to impairment in the myogenic response of cerebral arteries. Ex-vivo studies on mice Raignault et al. (2018) reported that on isolated arteries, which imposed pulsed conditions, reported that pulse pressure was sensed by the endothelium (Raignault, Bolduc, Lesage, & Thorin, 2017). The endothelium modulated the endothelial nitric oxide synthase activity and controlled myogenic tone in the cerebral arteries. Other in-vitro evidences suggest that increased matrix stiffness may impair flow-induced dilation by reducing the ability of the endothelium to response into higher shear stress (Donato, Machin, & Lesniewski, 2018). Taken together, these literature suggest that higher pulsatility could damage cerebral microcirculation.

2.4 Relationship between higher pulsatility and cognitive decline

Increased stiffness of the arteries and elevation of the central pulse pressure is linked to a faster rate of emerging cognitive decline (Tsao et al., 2016). Despite dynamic alterations of perfusion pressure between systolic maximum and diastolic minimum, cerebral autoregulation mechanisms maintain relatively constant blood flow in the capillaries (Jefferson et al., 2018). Given the essential needs of neurons for a constant supply of oxygen and glucose, this role of the arterial tree is important. Healthy neural function and cerebral microvascular integrity are highly dependent upon maintaining optimal blood flow during diastole when the driving force of the heart to supply the end organs is absent (Willie, Tzeng, Fisher, & Ainslie, 2014).

There is a large body of literature reporting that chronic higher pulsatility is linked to cognitive deficits (Hughes et al., 2018; Mitchell et al., 2011; Nation et al., 2016; Obisesan et al., 2008; Pase, Herbert, Grima, Pipingas, & O'Rourke, 2012; Pase et al., 2010). Cognitive decline as the adverse impact of age-related arterial stiffness was also extensively addressed in previous studies with PWV (Fujiwara et al., 2005; Hazzouri et al., 2013; Singer et al., 2013). As mentioned, cerebral arterioles respond to higher pulsatility by constricting, limiting blood flow to tissue and impairing the metabolism of the tissue. Over time and with diminishing arterioles shielding mechanisms, capillaries receive higher pulsatile load (McDonald, 2011; Mitchell, 2008), and this effect by itself could damage the metabolism of neurons (Scioli, Bielli, Arcuri, Ferlosio, & Orlandi, 2014). With a disruption in regulation of local CBF, neurovascular coupling impairment emerges which is seen in several studies on human. In the Baltimore longitudinal study, Waldstein et al. (2008) reported that individuals with a higher baseline PWV whom brachial pulse pressure elevated faster were associated with lowered cognitive performance. In the Reykjavik study, exploiting a large numbers of older adults, a significant link between higher PWV and reduced cognitive performance was reported (Mitchell et al., 2011). In the Rotterdam study, cerebral microbleeds were correlated to decline in several domains of cognition (Poels et al., 2012). A large-scale analysis on more than 6000 individuals showed a strong link between age-related arterial stiffness and cognitive impairment (Rabkin, 2012). Studies with transcranial Doppler also reported that an increased pulsatility in ICAs is a predictor of cognitive decline in older adults (Wardlaw et al., 2017). Similar results were reported in the studies on the MCA (which is spatially closer to gray matter) (Harris,

Reyhan, Ramli, Prihartono, & Kurniawan, 2018). Based on animal studies, Sadekova and colleagues proposed a mechanism by which arterial stiffness lead to cognitive impairment. They proposed that age-related arterial stiffness leads to increased pulsatile flow in the large and medium-sized cerebral blood vessels. The higher pulsatility and its stresses on the cerebral tissue are associated with the production of reactive oxygen species and cerebral gliosis. A higher oxidative stress and inflammatory damage can impair endothelial cell function and increase BBB permeability. The consequence of this hemodynamic modification is reduced cerebral blood flow and neurovascular uncoupling. Moreover, with an impaired cerebral perfusion, the delivery of nutrients and the clearance of toxic products is compromised, which in turn could contribute to neurodegeneration and cognitive decline (Sadekova et al. 2017). Their proposed mechanism was in line with mechanism proposed by other studies that link higher pulsatility to cognitive decline. For instance, Montgolfier and colleagues proposed that higher pulsatile CBF could shear the endothelium, leading to cognitive decline (Montgolfier, et al., 2020). Some ex-vivo studies proposed that higher pulsatility lead to damages on the microcirculation. For instance, ex-vivo studies on the human BBB Garcia-Polite et al. (2017) suggested that higher circumferential shearing and abnormally higher flow pulsatility in microvasculature provokes functional impairment in endothelial cells. This impairment could disrupt BBB transportation and downregulate the metabolic needs of neurons in neurovascular unit. They explored this effect by defining two markers to evaluate capillary function: junctional tightness and the transportation limit in the capillary-like circulation. They reported that higher shear stress and pulsatility, altered the junctional morphology, restricted the permeability and limited transport of nutrient and other solutes. Interestingly, they showed that this effect could be reverted if blood flow is restored to its regular form. Such results are not directly discuss how higher pulsatility in the brain lead to cognitive decline, but they at least partially may explain that as higher pulsatility penetrates to microcirculation, it may disrupt metabolic needs of the neurons by which the cognitive decline emerges. Together, these studies highlight the hypothesis by Stone et al., (2015) that the brain is damaged by the pulse of aging, causing neuronal loss, which, over time, leads to poor brain aging and dementia.

2.5 The link between cerebral pulsatility and cortical thinning

Age-related arterial stiffness is linked to cortical thinning (Pasha et al., 2015; Priyanka A. Abhang, 2016). Yet, the mechanisms of this association are not entirely clear. One mechanism could be through brain tissue damage following transmission of higher pulsatility into the cerebral microvasculature (O'Rourke & Safar, 2005). In the literature, age-related higher central arterial pulsatility is associated with microhemorrhages (O'Rourke, 2007) and a higher level of brain amyloid plaques even in the healthy aging (Rodrigue et al., 2012). Moreover, cerebral small vessel diseases, a higher prevalence of microinfarcts are reported as cascade of events that have vascular and hemodynamic correlates to atrophy of brain parenchyma (Hughes et al., 2013; Mitchell et al., 2011; McDonald 2011; De Montgolfier et al., 2020). Acutely, age-related higher intracranial pressure and emergence of mechanically injured vessels lead to compression of surrounding blood vessels and brain tissue (Xi, Keep, & Hoff, 2006). These alterations promote higher resistance to flow and lead to ischemic pathology (Yang, Betz, Chenevert, Brunberg, & Hoff, 1994). Lowered synthesis of parenchymal and endothelial vasoactive agents also reported to contribute to cortical thinning (Del Zoppo and Mabuchi, 2003). Studies suggested that cortical atrophy is a manifestation of hypoperfusion and poorly oxygenated tissue that ultimately begins to shrink (Knopman, 2006; Raz et al., 2010). In-vivo, an animal study on single brain vessels of rodents showed that increased pulse pressure damages small cerebral vessels and increases silent microbleeds (Baraghis et al., 2011). Together, these literatures suggest that arterial stiffness could alter the metabolism of the tissue which could induce reduction of cortical thickness. However, other factors than pulsatility, including CBF also play a role in cortical thinning. For instance reduced CBF is linked with impairment in the integrity of the cerebral structure, including reduced cortical thickness (Alosco et al., 2014, 2013; Waldstein et al., 2008). Asllani et al. (2016) and Marshall et al. (2017) report that the altered hemodynamics in the larger cerebral arteries is a factor contributing to downstream cortical thinning. In a similar experiment Alosco et al. (2014) also reported a coexisting lower cerebral blood flow and loss of cortical thickness without explicit cerebral infarction. Further studies are needed to further clear the underlying mechanisms linking cerebral pulsatility, CBF, cortical thinning and the progression of dementia.

2.6 The interplay between intracranial compartments: arterial, CSF and vein pulsatility

The magnitude of the pulsatility imposed on the cerebral tissue is not only depends on pulsations of the arteries supplying the brain. As the cerebral tissue is encased in the rigid cranium, the pressure exerted on the brain depends on an optimal mechanical and temporal coupling between intracranial components; blood, CSF and the brain.

The higher diameter in the aorta in comparison with arterioles and capillaries diameter causes a lower resistance to flow in the aorta compared to arterioles. Hence, there is a higher inflow for the aorta and a slower inflow for the arterioles. The arteries expand to accommodate the extra volume of the blood. Blood and CSF are incompressible fluids; thus, the increased volume causes intracranial pressure to rise (Wagshul et al., 2011; Whedon & Glassey, 2009). A fraction of this raised pressure gradient is negated by displacement of the CSF to the spinal canal (Alperin, Lee, Loth, Raksin, & Lichtor, 2000; Balédent, Henry-Feugeas, & Idy-Peretti, 2001; Wåhlin et al., 2010). Subsequently, flushing of the fluid occurs in the cerebral venous and aqueduct CSF compartments. The interplay between arterial inflow and CSF outflow are closely coupled and demands an optimum elasticity between the cerebrovascular and craniospinal compartments. The spinal canal higher resistance to CSF flow as the result of aging can impair the temporal coordination between these compartments and delay CSF flushing, which may appear as smoother CSF peaks in older adults (Stoquart-ElSankari et al., 2007). Hence, elevates the intracranial pressure. This higher pressure in the cranium may cause a tendency to push the brain down in the direction of the foramen magnum (Uftring, Chu, Alperin, & Levin, 2000) and which in turn compress the cerebral vasculature (Bragin, Bush, & Nemoto, 2013). In conjunction with this effect, resistance to flow as the result of arterial stiffness in a positive loop could amplify the resistance of cerebral vasculature to blood flow (Chiarelli et al., 2017). Bateman and colleagues suggested that the time lag between the arterial inflow systolic peak and the CSF systolic peak is a measure of the compliance of the intracerebral compartments (Bateman et al., 2008). Although arterial and CSF pulsatility has been the subject of extensive research, less is known about age-related modification of veins. Schaller (2004) suggested that the veins pulsate passively due to arterial pulsations in healthy older adults. Similar results were reported by Stoquart-ElSankari et al. (2007) where venous waveform of young and older adults closely resemble arterial waveform. However,

they suggested that pulsatile flow in the capillaries could push the extra interstitial fluid to venules. Bateman and colleagues discussed that with diminishing of the Windkessel mechanisms as a result of aging, a higher arterial pulsatility may penetrate the compressible cerebral veins. The major difference between compensating the arterial pulsatility through CSF outflow with the damping the pulsatility through venous compression is in the latter, the energy of the pulse is lost in the venous system. Thereby, may affect venous return and increases the preload in the heart (Bateman et al., 2008). In summary, these studies are emphasizing on the interplay between intracranial and craniospinal compartment to maintain the optimal cerebral pulsatility.

2.7 Cardiovascular risk factors and cerebral pulsatility

Age-related vascular stiffness is known to contribute to emerging cardiovascular disease (Cecelja & Chowienczyk, 2012). Here, it is discussed that CVRF induce cerebrovascular damage that may lead to increased pulsatility in the brain. Hypertension, diabetes type 2, dyslipidemia, high BMI, smoking are some of the classical CVRF that may change the mechanical properties of vessels, over time accumulating the damage and accelerating the aging of the vessel walls (Lee & Joo, 2019) where damages on the vascular wall may manifest themselves in a greater PWV seen in the individuals with several CVRF (Cecelja & Chowienczyk, 2012). Indeed, studies show that in the presence of CVRF, the association of age and PWV is stronger (Baldo et al., 2018). It is to be noted that not all the CVRF have the same burden on the vasculature, some CVRF such as blood pressure to a greater extent and other such as dyslipidemia in some studies to a lesser extent is associated to changes in PWV. Indeed, some studies reported that hypertension and diabetes are CVRF that have a stronger association with a higher PWV compared to dyslipidemia (Taquet et al., 1993; Benetos et al., 2002). Although diabetes mellitus and hypertension are reported to be independently link to cognitive deficits, coexisting of both conditions was concomitant to a lower cognitive performance (Elias et al., 1997; Knopman et al., 2001). The link between hypertension and cognitive decline was escalated in carriers of apolipoprotein (Nishtala et al., 2014).

Studies exploring the link between dyslipidemia and cognition reported that both high and low total cholesterol concentration have an association with cognitive decline (Elias, Elias, D'Agostino, Sullivan, & Wolf, 2005; van Vliet, van de Water, de Craen, & Westendorp, 2009). To account for the collective influence of CVRF in an individual, some studies used the Framingham score to quantify the cumulative effect of CVRF for each individual in their

experiments (Wilson et al., 1998). A greater Framingham score is a result of the higher collective effect of classical CVRF and perhaps greater damage to the arterial walls. Even if CVRF are medically treated, their negative impact is still seen by means of a higher PWV compared to controls (Amar, Ruidavets, Chamontin, Drouet, & Ferrières, 2001; Mitchell, 2008). Pase and colleagues reported that higher Framingham CVRF scores are related to a lower mean blood velocity and a higher blood velocity pulsatility in the MCA (Pase, Grima, Stough, Scholey, & Pipingas, 2012). They proposed that CVRF might be associated with cerebrovascular damage and lowered cognitive performance as a consequence of reduced cerebral perfusion and a higher CBF pulsatility. A large-scale study named Whitehall II on about 4800 individuals reported that the higher Framingham CVRF score has a negative association with cognitive performance (Kaffashian et al., 2011). Similarly, Pase et al., proposed that age-related modification in arterioles may impair the autoregulation mechanism and hence the microcirculation (Pase et al., 2012). Over time, hypertension can modify the limits of autoregulation to a higher pressure (Paulson, Strandgaard, & Edvinsson, 1990). Because of this modification, the brain gets protected from some degree of higher pressure but becomes more susceptible to cerebral hypoperfusion, especially in older adults under treatment with antihypertensive medications (Qiu, Winblad, & Fratiglioni, 2005). It is conceivable that lowering blood pressure with these medications does not lead to cerebral dysfunction since cerebral autoregulation mechanisms and compensatory mechanisms discourage hypoperfusion (O'Rourke & Safar, 2005). However, studies on older adults indicated that administration of antihypertensive medication should be carefully considered as an improper treatment could cause cerebral hypoperfusion (through lowing the blood pressure, low cardiac output and may leads to CBF insufficiency) and contribute to emerging dementia (Qiu, Winblad, & Fratiglioni, 2005).

2.8 Coronary artery disease and cerebral pulsatility

One consequence of age-related arterial stiffness is impairing cardiac-arterial coupling which in turn impairs coronary artery perfusion (Mitchell, 2008). In a healthy individual, the reflected wave returns to central arteries in the late systole which is supporting the coronary arteries perfusion. However, hemodynamic modification in the stiffer arterial tree lead to faster return of the reflected wave to the central aorta in the late systole which increases the central pressure during systole and impair the coronary perfusion (Mitchell, 2008). In addition, cardiac afterload is also increasing

which over time could lead to ventricular hypertrophy. These modifications on the heart in addition to ischemia in the coronary arteries increase the risk of CAD. The question of to which extent CAD affects cerebral pulsatility and its association to brain structure, function and regulating CBF is important as a large population of people across the world are suffering from CAD. CAD disease could alter cardiac output, and this is a substantial modification as the brain receives a significant proportion of this output. Studies on older adults reported that cerebral hypoperfusion is a consequence of reduced cardiac output as a result of reduced stroke volume caused by left ventricular dysfunction (Haeusler, Laufs, & Endres, 2011), which is often seen in individuals with CAD. Studies related lower cardiac output to cerebral hypoperfusion and metabolism impairment as the downstream impact of cardiovascular deficits (De La Torre, 2012).

The CVRF are the shared risk factors for CAD and cerebrovascular disease. Both CAD (Deckers et al., 2017; Lane, 1991) and cerebrovascular disease (Leritz et al., 2011) are reported to impair cognitive functions. The concept of "cardiogenic dementia" relates the lower cardiac output to cognitive decline (Lane, 1991). Jefferson and colleagues reported an association between hypoperfusion measured by lower resting cardiac output and cognitive performance in older adults with stable cardiovascular disease (Jefferson et al., 2018). In a cross-sectional and longitudinal study on the European and Chinese population, age-related arterial stiffness was reported to have a strong relationship with higher systolic blood pressure and cardiovascular complications. In this regard, Chantler, Lakatta, & Najjar, (2008) indexed the coupling between the left ventricle and the arterial system. They reported that although age-related arterial stiffness has significant relevance to cardiovascular outcomes, age-related modification has significant implications for the heart and vascular system in a bidirectional relationship.

2.9 Frontiers of science on pulsatility: Functional NIRS as a promising technique

In the year 2007, Themelis and collogues, used NIRS data to extract pulsatile components of blood flow from the brain of newborn piglets (Themelis et al., 2007). Themelis used laser doppler ultrasound to confirm that the heartbeat oscillation in the NIRS data is assessing the local changes of CBF. In the year 2014, Fabiani et al. reported that heartbeat oscillation in the functional NIRS data could be used to quantify pulsatility parameters that are associated with brain structure and function (Fabiani et al., 2014). Among the cerebral pulsatility parameters measured with functional

NIRS that were shown to vary with age are the cerebral pulse amplitude and the cerebral PRF (Chiarelli et al., 2017; Tan et al., 2019, 2017; Fabiani et al., 2014). Both of these two parameters were associated with aging; however, cerebral pulse amplitude had a greater association with aging compared to PRF (Tan et al., 2017). Tan *et al.* (2017) used functional NIRS data to extract cerebral pulse amplitude and delineated the map of pulsatility across the cortex. Their findings demonstrated that optically indexed cerebral pulse parameters are associated with the cognitive load of the Sternberg memory task (Tan et al., 2016). They reported that in the task-related areas the local cerebral amplitude is reduced. They suggested that this observation in the data is the impact of vasodilation. In another study Tan *et al*. (2017) reported that PRF is associated with cardiorespiratory fitness but this link was not found for cerebral pulse amplitude. The regional PRF was related to individual differences in regional cortical volume (Chiarelli et al., 2017). Their finding was a significant result as it was linking an estimate of regional arterial elasticity to preserving or losing of the cortical volume.

Table 2-1 is a summary of selected studies on cerebral pulsatility on humans, with an emphasis on the imaging modalities as well as the pulsatility parameters used to analyze the data. A high arterial pulsatility measured with transcranial doppler was accompanied by brain tissue damage (Mok et al., 2012). Abnormal pulsating in the arteries and veins measured with PC-MRI was also associated with dysfunction of the Windkessel mechanism in elderly individuals with dementia (Bateman, Levi, Schofield, Wang, & Lovett, 2008). In a recent pre-clinical study, ICP was quantified using CBF from diffuse correlation spectroscopy (Ruesch et al., 2020). They showed that over 90% of the variance of invasively measured ICP could be explained by the estimate of ICP from diffuse correlation spectroscopy. Crucially, despite these several methods and parameters to quantify pulsatility in the brain; pulsatility parameters may or may not be directly compared across modalities as they do not always have the same interpretation. However, pulsatility parameters may be related, as they measure different aspects of pulsatility.[4]

[4] For instance, Themelis et al., (2007) discussed that pulsatility measured with NIRS (which is changes in near-infrared light attenuation) is related to flow through blood volume changes. The ICP monitoring provides the pressure-based measure of pulsatility in an invasive procedure. Transcranial Doppler and PC-MRI measure vascular velocity pulsations non-invasively. These measures are related to each other, but the relationship is not necessarily linear.

2.10 Functional NIRS and mobility-based experiments

Functional NIRS is one of leading imaging techniques that is available as a portable device. It enables the study of cerebral hemodynamic in walking-based experiments (Watanabe, Mavanagi, Ito, & Koizumi, 1995). Most of the studies that used functional NIRS to study cortical activity during walking used oxyhemoglobin concentration as the main measurand and compared this parameter during walking versus rest (Eggenberger, Wolf, Schumann, & de Bruin, 2016; Fraser, Dupuy, Pouliot, Lesage, & Bherer, 2016; Holtzer et al., 2017; Pelicioni, Tijsma, Lord, & Menant, 2019).

Some studies assessed changes in cerebral hemodynamics associated with walking on treadmills (Eggenberger et al., 2016) and some others with walking over ground (Verghese, Wang, Ayers, Izzetoglu, & Holtzer, 2017). Clark *et al*. (2014) reported that for seniors, prefrontal cortex activity was increased because a higher somatosensation was stimulated by walking on the treadmill compared to over ground walking (Clark, Christou, Ring, Williamson, & Doty, 2014).

Studies that tested the impact of speed of walking on cortical activity reported a higher prefrontal activation in the fast-speed walking compared to slow walking (Metzger et al., 2017). In another study comparing the prefrontal activity in the usual walking compared to standing, no statistically significant difference was reported (Mirelman et al., 2014). Some studies reported that energy cost of walking is highly associated to older adults functional performance (Wert, Brach, Perera, & VanSwearingen, 2013). Therefore, in some experiments the participants were instructed to self-select their walking speed. Such studies reported that this instruction minimizes the energy consumption (Wert, Brach, Perera, & VanSwearingen, 2013). Walking with self-selected pace influences the performance of the seniors, especially in dual tasks (Mirelman et al., 2014).

Motor control automaticity literature reported that standing alone could increase cerebral oxygenation to motor cortex and prefrontal cortex areas in comparison to the condition in which the person is performing an external task (dual task). This literature suggested that when the individuals are focused on standing, they perform the usual automatic control of posture. However, when the individuals are standing and are given to the task that requires external focus (*i.e.,* a cognitive task) they tend to focus less on posture and allow automatic control (which is expected to diminish the role of prefrontal cortex in postural control) (Clark, 2015).

In another study, Osofundiya *et al*. (2016) reported that there is a higher prefrontal activation for dual task (walking and cognitive task) compared to standing or usual walking. Together, the studies assessing the impact of physical activity on cerebral hemodynamics used several protocols with different experimental details which require caution when the results are compared between studies.

Table 2-1 Selected articles on cerebral pulsatility, method and main results. CPA: cerebral pulse amplitude, OSPAN task: operation span task. ASL: arterial spin labeling

Study	Participants	Imaging modalities	Pulsatility parameter	Main results
Shi et al., 2020	n=60, 52-83	PC-MRI	Difference between systole and diastolic flow divided by mean flow	Increased pulsatility is associated with cerebrovascular pulsatility and not CBF
Tan et al., 2019	n=93; 18-87 years old	NIRS, structural MRI	PRF	Lower PRF associated with white matter lesions
Holmgren et al., 2019	n=35, 79-91 years old	4D flow MRI, 2D PC-MRI, structural MRI	Difference between systole and diastolic flow, cerebral arterial pulsatility volume load, cerebral Gosling's pulsatility index	Validation of method: 4D flow MRI can be used for cerebral arterial pulsatility, compliance and cerebrovascular resistance can be calculated
Vikner et al., 2019	n=38; 70-91 years old	4D flow MRI, 2D PC-MRI, structural MRI	Cerebral arterial pulsatility and resistivity index	Validation of method: cerebral pulsatility index increases with age
Veraar et al., 2019	n=32, mean:57-73	Transcranial Doppler	Flow mode (pulsatile flow versus non-pulsatile flow)	Non-pulsatile flow linked to increased cerebrovascular reactivity
Unnerbäck et al., 2019	n=13, 22-75 years old	ICP monitoring, PC-MRI	Pulsatile amplitude in ICP	Intracranial pressure is associated to pulsatile component of CBF
Nakamura & Muraoka, 2018	n=31, mean: 19-23	Brightness-mode ultrasound	β- stiffness index and arterial compliance	Central arterial stiffness and arterial compliance were associated with pulsatility index
Chiarelli et al., 2017	n=48; 18-75 years old	NIRS, structural MRI	PRF	Regional cortical volume associated with regional PRF
Tan et al., 2017	n=48; 18-75 years old	NIRS, structural MRI	CPA, PRF	CPA and PRF associated with age. CPA associated with brachial pulse pressure. PRF associated with OSPAN task

Study	Participants	Imaging modalities	Pulsatility parameter	Main results
Tan et al., 2016	Experiment 1: n=51 Experiment 2: n=52 55-87 years old	NIRS, structural MRI	Experiment1: Breath-holding index (changes in CPA after holding breath) Experiment2: CPA	Experiment 1: Breath-holding index associated to CPA variation. Experiment 2: CPA decreased as Sternberg memory task load increased.
Zarrinkoob et al., 2016	n=94, 20-30 years old and 64-80 years old	Aortic PWV, PC-MRI	Cerebral arterial pulsatility index and damping factor (proximal to distal pulsatility index)	Damping pulsatility index was significantly higher in younger compared to older. PWV was not associated to cerebral arterial pulsatility index
Fabiani et al., 2014	n=53; 55-87 years old	NIRS, structural MRI, ASL	CPA, PRF, pulse transit time (from neck to location of measurement on the head)	CPA was correlated with age and brachial pulsatility index. PRF was associated with ASL
Harris et al., 2018	n=66, 28-65 years old	Transcranial Doppler	Difference between systole and diastolic peak velocity cerebral divided by mean velocity	MCA pulsatility index was significantly different between cognitively normal and cognitive impairment (assessed by MoCA)
Viola et al., 2013	n=31; 62-77 years old	NIRS, transcranial Doppler	Difference between systole and diastolic peak velocity cerebral divided by mean velocity	Higher pulsatility index in MCA is associated with cognitive impairment
Schubert et al., 2015	n=21; 23-40 years old	Structural MRI, PC-MRI	Difference between systole and diastolic peak velocity cerebral divided by mean velocity, resistance index (the same nominator divided by maximum velocity)	Pulsatility index and resistance index both decreased significantly as blood traveled from C6 to V4 (intra-dural)
Takahashi et al., 2011	n=50; 18-50 years old	NIRS, lase Doppler	Magnitude of pulsatile component in Doppler signal	Changes in oxyhemoglobin in far channels were associated to amplitude of doppler blood flow signal

CHAPTER 3 ELEMENTS OF METHODOLOGY

This chapter discusses some elements of materials and methods to complement the articles presented in chapters 4 (article 1) and 5 (article 2) and the results in chapter 6.

This chapter is divided by experiments: experiment I and experiment II. Experiment I has two parts: part I.I and part I.II. Part I.I provides thesis methodology used to study the cerebral pulsatility in healthy aging and its association to cortical thickness, considering both young and older adults. Part I.II describes the methodology used to explore the association between cerebral pulsatility and cognition. Part I.II is preliminary in nature, is ongoing and will be published as a research paper if the results, once complete, achieve statistical significance. Experiment II describes the methodological approach to explore the impact of the cardiovascular risk factor continuum and of CAD on cerebral pulsatility. As mentioned in the introduction (chapter 1), although experiment II is integral to this thesis, the data collection for experiment II is not a contribution of this thesis. Hence, data collection and analysis for experiment II are predominantly discussed in article 2 (chapter 5). In both experiments, functional NIRS data used to extract pulsatility parameters across the cortex.

3.1 Diffuse optical imaging

Diffuse optical imaging is a non-invasive imaging technique that benefits from relatively low attenuation of light in the near-infrared range to probe the optical properties of biological or nonbiological tissues (Jue & Masuda, 2013). The use of near-infrared light for measuring blood oxygenation dates back to 1860 when German scientist Felix Hoppe-Seylet reported that adding units of oxygen into the blood alters the optical absorption of the illuminated tissue (Miescher, 1866). In 1949, Hill and Keynes showed small changes in the opacity of the nerve trunk following stimulation in the nerve (Hill, 1949). After almost three decades, Frans Jöbsis discovered that near-infrared light in the optical window can be used to measure changes in intravascular oxy- and deoxyhemoglobin concentration in anesthetized cats (Jobsis, 1977). Over the following decades, several optical imaging techniques with different spatial and temporal resolutions were established and functional NIRS has broadly extended its applications for the

study of human brain tissue, in no small part due to its capacity to measure changes in cerebral oxygenation during rest and activation (Jue & Masuda, 2013).

The near-infrared optical window is located in the 650 to 1350 nm range, where the light has greater penetration in tissue (Smith, Mancini, & Nie, 2009). Near-infrared light with a wavelength above 900 nm is almost entirely absorbed by intracellular and extracellular water. Likewise, near-infrared light below 650 nm is greatly absorbed by hemoglobin. However, within the range of 680 to 900 nm, the skull bone, cerebral white matter, and the skin dermis are relatively transparent to near-infrared light (Figure 3-1, left). The main chromophores are oxy- and deoxyhemoglobin, the concentrations of which change in the activation state in comparison with resting (Shi, Sordillo, Rodríguez-Contreras, & Alfano, 2016). This led to the development of instruments to measure hemoglobin changes. NIRS is a medium-sized, portable device that inexpensively supports non-invasive study of brain activity with a higher temporal resolution in a more natural setting than does functional MRI (Amiri et al., 2014). In studies with NIRS, a near-infrared light source optically injects light into the scalp. This light penetrates cerebral tissue and a fraction is absorbed by oxy- and deoxyhemoglobin and cytochrome c-oxidase while another fraction of the photons returns to the surface of the head (Fabiani et al., 2014). These detected photons pursue banana-shaped paths from source to detector, which are a few centimeters apart. A near-infrared detector collects the backscattered photons that have interacted with the tissue (Figure 3-1, right). The attenuation of the near-infrared light is due to the different optical properties of absorption and scattering of the underlying tissue. In continuous wave NIRS by assuming that the scattering and water concentration do not change, the changes in light attenuation are linked to the variation of the light absorption due to the changing concentrations of oxy- and deoxy hemoglobin (Jue & Masuda, 2013). The functional state of the brain determines the changes in chromophores and defines the amount of the near-infrared light absorbed. The spectral absorption of hemoglobin depends upon whether it is oxygenated or deoxygenated and hence these may be differentiated.[5] In the near-infrared optical window (650 to 900 nm), two or more wavelengths are selected, with one wavelength above and one below the isosbestic point at 805 nm, which is the point at which deoxy- and oxy-hemoglobin have identical absorption coefficients. Using the modified Beer-Lambert law (mBLL), relative

[5] The absorption of cytochrome c-oxidase is 10 times smaller than oxy- and deoxyhemoglobin.

concentration changes can be calculated as a function of total photon path length enabling the study of cerebral function (Yang, Yuan, Feng, & Wang, 2019). There are other elements in cerebral tissue that have some absorption capacity, such as melanin, although in the near-infrared range their absorption capacity compared to oxy- and deoxyhemoglobin is often neglected (Matas, Sowa, Taylor, & Mantsch, 2002).

3.2 Functional NIRS and neurovascular coupling

Neurons demand a constant supply of nutrients and oxygen for generating action potentials. Blood perfusion provides oxygen, glucose, and other substances through capillaries for the active neurons. The firing of neurons leads to vasodilation and an increase in the regional cerebral blood flow and oxygenation. While neurons are functionally active, oxygen metabolism increases significantly. This increased oxygen consumption reduces tissue oxygenation, which is overcompensated by the increase in the regional CBF which translates into an increase in oxygenated hemoglobin, a mechanism known as “neurovascular coupling”. Accordingly, a brain region is considered active when regional cerebral flow increases, generating an increase in the oxyhemoglobin and a decrease in deoxyhemoglobin. In other words, in the active brain area, there is an oversupply ofoxyhemoglobin (Huneau, Benali, & Chabriat, 2015).

3.3 Functional NIRS and cerebral pulsatility

Themelis and colleagues (2007) used NIRS to measure the pulsatile component of CBF from heartbeat fluctuations captured in the NIRS data (Themelis et al., 2007). The functional NIRS data measured on the scalp often contain systemic oscillations that originate from heartbeat pulse pressure, which is in many of the previous studies was treated as noise and was removed from the data in the preprocessing steps.

The pulsatile motion of blood expands the elastic arteries and arterioles (Figure 3-2). It also induces periodic alterations in the concentration of oxy-hemoglobin, which attenuates near-infrared light absorption. This attenuation can be measured by a near-infrared source and detector pair that probes the underlying tissue (Themelis et al., 2007). It has been suggested that the

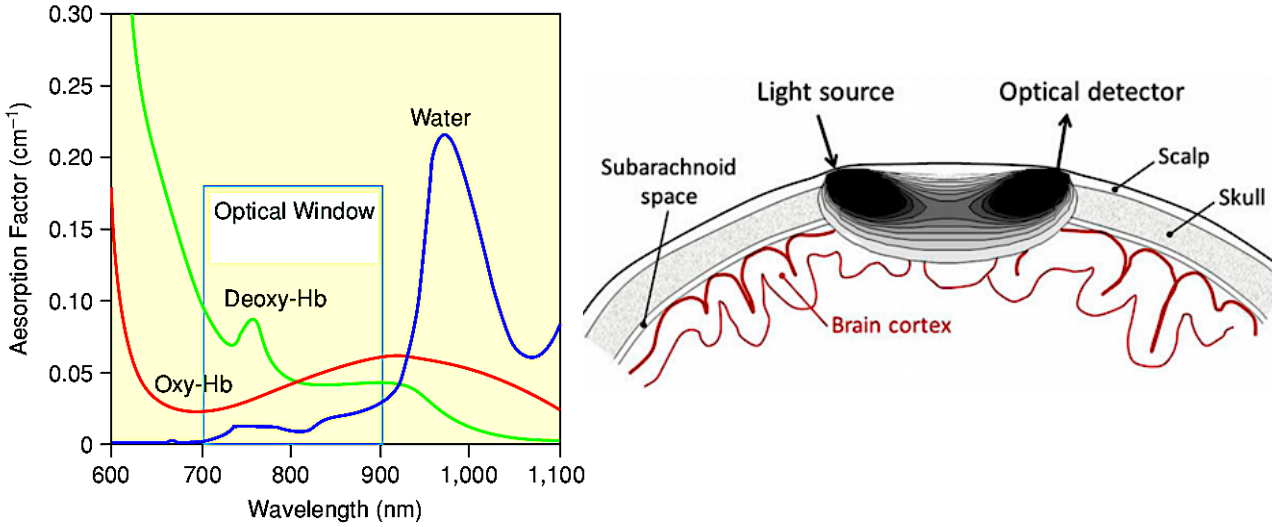

Figure 3-1 Left: absorption spectrum for oxy- and deoxy hemoglobin and the optical window of the near-infrared light. Above 900 nm, most of the photons are absorbed by the water (Image source: Izzetoglu, Bunce, Izzetoglu, Onaral, & Pourrezaei, 2007). Right: the near-infrared light from the light source is optically injected into the scalp from a near-infrared source. A few centimeters away from the source, a detector will collect the light returning from the scalp. In the 2D view photons follow a banana-shaped path from light source to detector, image source (Quaresima & Ferrari, 2019).

attenuation of the related to blood flow (Themelis et al., 2007; Tong & Frederick, 2010). In recent years, these systemic oscillations were used to extract physiological information about the underlying tissues (Chiarelli et al., 2017; Fabiani et al., 2014; Tan et al., 2017). As blood in the arteries is saturated with oxyhemoglobin, the intensity of the functional NIRS data at 830 nm is more sensitive to absorption of oxyhemoglobin (Chiarelli et al., 2017; Kirlilna et al., 2013; Themelis et al., 2007) compared to 695 nm and hence in recent years 830 nm was used for the study of arterial pulsatility. Our analysis showed that heartbeat data extracted from the deoxyhemoglobin wavelength has lower stability compared to oxyhemoglobin (Figure 3-2). When using the modified Beer-lambert law, both oxy- and deoxy hemoglobin intensity changes are generally used to calculate concertation changes. The instability of peaks in deoxyhemoglobin could impact the location of peaks in oxyhemoglobin. Therefore, we followed the approach of literature (Fabiani et al., 2014; Themelis et al., 2007) and solely considered oxyhemoglobin for extracting pulsatility index.

In study 1 (cerebral pulsatility and cortical thinning), the parameter to study cerebral pulsatility was PTTp and for the study 2 (cerebral pulsatility and cardiovascular disease) the cerebral pulsatility parameters were cerebral pulse amplitude and PRF. The latter two pulsatility parameters were suggested by Tan *et al.* (2019), Chiarelli *et al*. (2017) and Fabiani *et al*. (2014). However, both cerebral pulse amplitude and PRF rely on the values of the y-axis in the NIRS signals which could cause contamination by partial volume effect and may lead to under- or overestimation of parameters (Huppert et al., 2009). We addressed this problem in the pulsatility parameters selected for study 1 and we chose a parameter relying on the time axis (PTTp as pulsatility parameter). The PTTp is the time from ECG R-peak to subsequent systolic peak in the NIRS data. Unfortunately, we could not calculate PTTp for study 2 and compare it with the results of study 1, because we did not have ECG data (synchronized with NIRS) with which to extract PTTp.

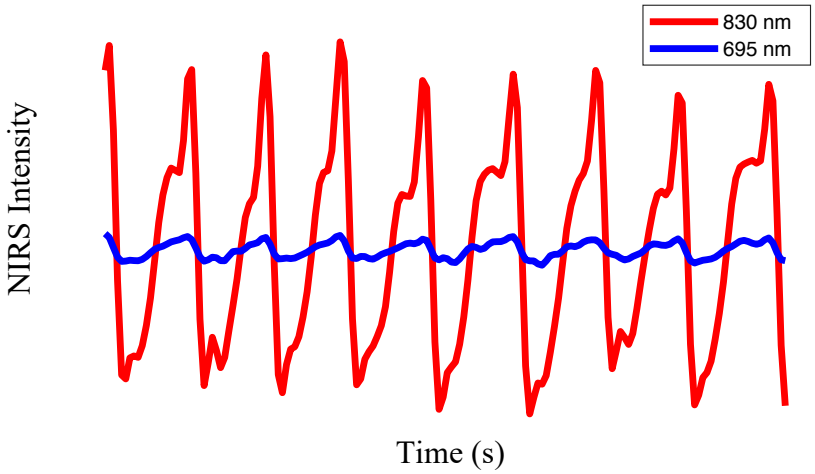

Figure 3-2 , Example of heartbeat oscillations extracted from functional NIRS data for two wavelengths, 695 nm and 830 nm. As illustrated, 830 nm is more sensitive to 830 nm (absorption of oxyhemoglobin) compared to 695 nm (absorption of deoxy hemoglobin).

3.3.1 Experiment I

In experiment I.I, the impact of healthy aging on changes of pulsatility in the brain and its association to regional cortical thickness was explored in the framework of a cross-sectional study. Healthy aging was defined as the absence of classic CVRF: high blood pressure, dyslipidemia, smoking (tobacco or any other substances) and obesity and possessing general cardiovascular and cerebrovascular health (as defined in chapter 4-article 1).

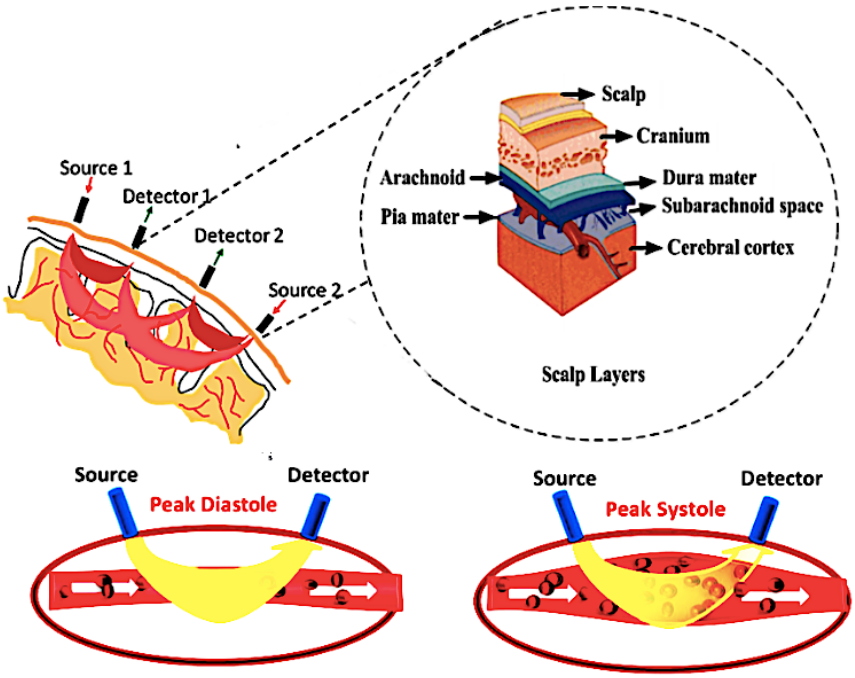

Figure 3-3 Optical measure of cerebral pulse waveform using a near-infrared source and detector pair. During systole, a new volume of oxygenated blood is pulsated into the arterial bed, which attenuates the intensity of the NIRS signal (Image source: merged from three references[6]).

In this experiment, both older and younger individuals were matched for sex in their respective groups. The age range of younger adults was 19-31 years as research indicates CBF declines appreciably starting in the early 30s (Stoquart-El Sankari et al., 2007). Geriatric studies tracking cognition from middle age (55 years old) to older ages (95 years old) reported the emergence of cognitive aging between 65 and 75 years old (Small, Dixon, & McArdle, 2011). As one of the aims of the first experiment was to explore the modulating impact of pulsatility on cognition, the age range of older adults was defined to be 65 to 75 years old. Peng et al (2014) reported that the metabolic rate of oxygen is higher at noon than in the early morning. Considering this research, more than 90% of the participants were scheduled between 8:30 to 11:30 AM (for all the three sessions), within which the effect of time was counterbalanced across the participants. All the participants were asked to avoid using caffeine beverages for the day of the experiment for all

[6] Image sources : https://nirx.net/fnirs-and-nirx, Fabiani et al, 2014. The image source for scalp and pial matter is unknown.

three sessions (McLellan, Caldwell, & Lieberman, 2016). Participants were asked to respect 12 to 14 hours of fasting overnight and the blood draw was scheduled as the first task in the morning (participants were instructed to avoid exercise or walking long distances while they were fasting). After the blood draw, the blood was centrifuged in CRIUGM for 15 minutes and within 2 hours was transported to a hospital where the blood was analyzed. The methodology for this experiment was developed based on two major non-invasive brain imaging techniques, MRI and functional NIRS. We used PC-MRI to measure flow pulsatility in the cervical subarachnoid space at the level of the C2-C3 vertebrae. The functional NIRS was used to measure pulsatility across the cortex. Optical intensity was measured in 8 resting state blocks, each 1 minute long. The resting state paradigm in this study was similar to Chiarelli et al., (2017); Tan et al., (2017), related to non-evoked cerebral responses. Prior to the experiment, each participant was instructed to avoid high-level brain activity such as planning the day or a future activity or counting numbers. During the measurement, participants were instructed to stay immobile, to let their minds wander and to concentrate on their breathing. The functional NIRS data were collected with a Brainsight NIRS machine (Rogue-Research Inc.) with four bays, each with 8-channel modules. Each module consisted of eight high-sensitivity detectors. In addition, in each module there were four proximity detectors assigned as short channels (a total of 143 oxyhemoglobin channels) in the continuous wave NIRS instrument with a sampling rate of 20 Hz. The functional NIRS device used in this study had monochromatic laser diodes with low laser power (20 mW) that emit two continuous frequency modulated wavelengths, 695 nm and 830 nm, where deoxyhemoglobin and oxyhemoglobin are respectively dominant chromophores. Near-infrared sources and detectors were mounted on a flexible elastomer stripe (Brainsight, Rogue-Research Inc.). The helmet accounts for various head contours between participants and facilitates manually moving hair aside to ensure a suitable contact between optodes and scalp. The helmet was fixed on the head with two black, stretchable fabric wraps. One of the stretchable wraps covered frontal and temporal areas and the other one motor areas. This helped boost light-coupling efficiency while maintaining an

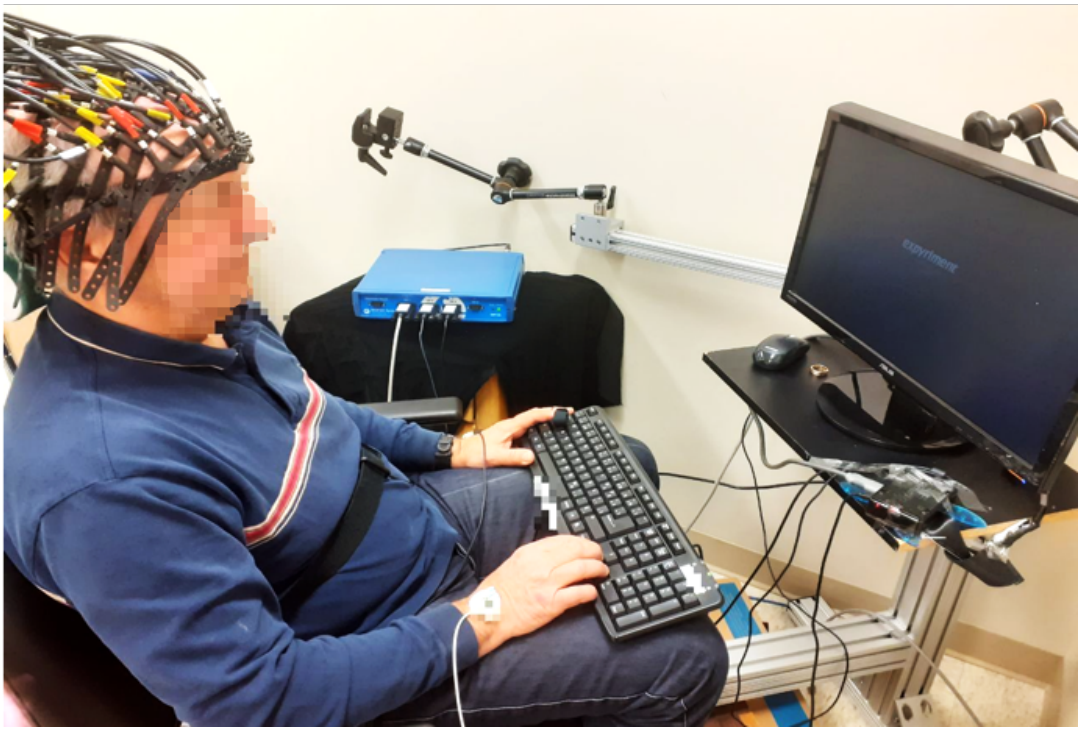

Figure 3-4, Experimental setup for the first experiment. Near-infrared sources and detectors were mounted on flexible elastomer stripes (Brainsight, Rouge Research). The ECG, PPG and respiratory belt modules were synchronized with functional NIRS and measured the data concurrently.

orthogonal orientation on the participant's head. Moreover, a telescopic arm in the Brainsight compartment provided a stable support for the weight of the optical fibers. A comfortable chair, neck rest and footrest were provided to the participants to help them remain immobile during the experiment. Experiments took place in a dark room with a regulated temperature of 22 degrees (according to the Brainsight manual, room temperature above 26 degrees could reduce near-infrared penetration depth). A lightweight black fabric covered the helmet and the optode compartments to mitigate pollution by ambient light. Experimental setup is shown in Figure 3-3.

3.3.1.1 Anatomical MRI

Parameter details and the analysis of structural MRI are explained in chapter 4 (article 1).

3.3.1.2 3D time-of-flight MR angiography

A three-dimensional (3D) time-of-flight (TOF) magnetic resonance angiography (MRA) or 3D-TOF-MRA sequence provided a clear assessment of vascular anatomy in the cervical subarachnoid space and was used to select the best anatomical planes for flow quantification. After collecting the 3D-TOF-MRA data, a maximum intensity projection (MIP) implemented on Siemens software was used to display the cervical vessels (Figure 3-4). Measurement planes were selected perpendicular to arteries between the C2 and C3 vertebrae, above the bifurcation of the internal and external carotid artery (where round VAs and ICAs cross-sections are completely clear in the transverse planes). Figure 3-4A, B illustrates the straight arteries of younger adults. Selecting a perpendicular plane for younger adults was time-efficient and required shorter scan times as one plane could be used to measure the velocity in all four cervical arteries. It was challenging to select optimal transverse planes for tortuously shaped arteries, which are common in elderly participants (Figure 3-4C, E, D and F). Such cases required an independent scan sequence for each artery. Acquisition times for this sequence depended on the heart rate of the participant and varied from 5 to 7 minutes.

3.3.1.3 Phase contrast MRI

PC-MRI is an MRI sequence in which blood flow velocity is encoded in the phase images in several time frames. Since its development, this technique is widely used to quantify arterial, venous and CSF flow and flow direction (Enzmann et al., 1993). This technique exploits the phase effect in the flow. When two spins, one stationary and one moving, are exposed to a pair of bipolar gradients, the moving spin experiences a phase shift proportional to its velocity and the stationary spin does not. Moreover, an opposite phase shift would be produced by two spins that are flowing at the same speed but in the opposite direction. Hence, by measuring the phase shift, the velocity and then flow are computed (Wymer, Patel, Burke, & Bhatia, 2020). With the imaging technique

employed, stationary spins appear as gray and moving spin appears as bright or dark, depending upon the direction of the flow (Figure 3-5).

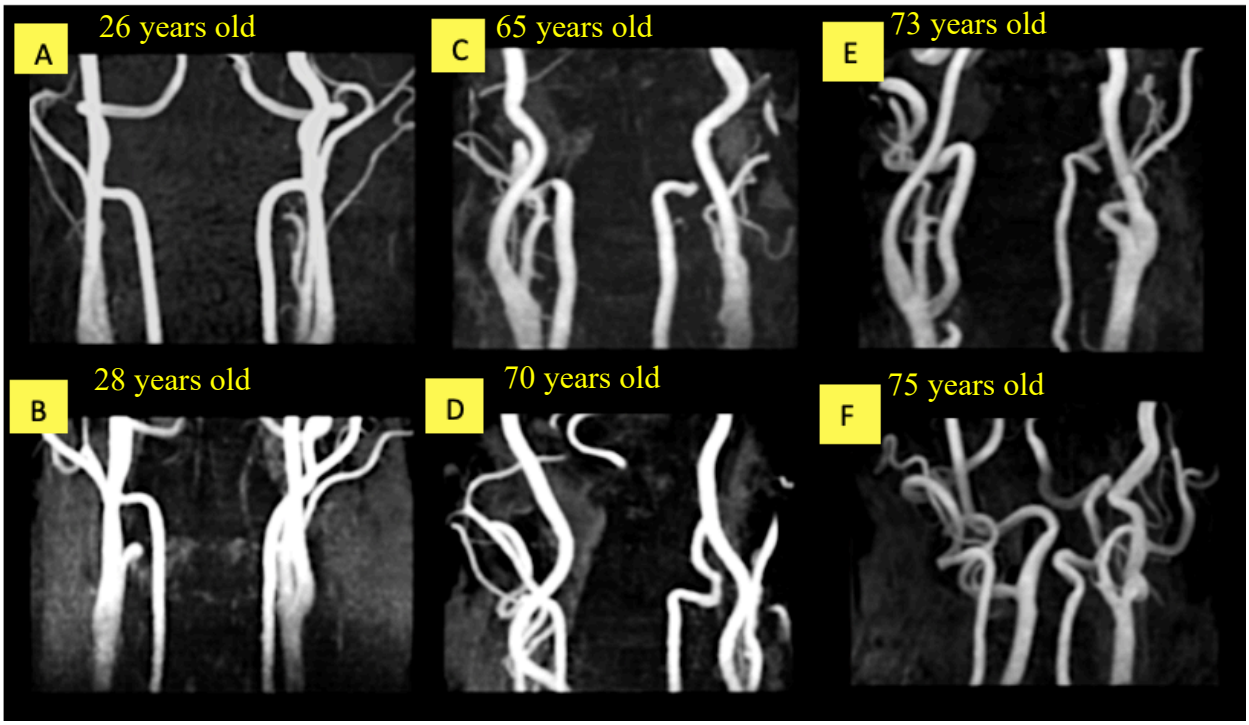

Figure 3-5 Examples of acquired TOF-MRA images; Coronal view of 3D-TOF-MRA for a healthy young participants and older participants reconstructed with a MIP algorithm. Participants did not have classical cardiovascular risk factors. The tortuously shaped arteries in some older participants required an independent scan with a perpendicular plane for each artery. The transverse plane for measuring arterial pulsatility was selected using 3D-TOF-MRA at the cervical subarachnoid space between C2 and C3 vertebrae, above the bifurcations.

Degree of sensitivity of the bipolar gradient needs to be adjusted on the speed of the blood flow in the vessel, which is controlled by an operator-set parameter called velocity encoding (V_{enc}). This parameter is set in cm. s^{-1} and is tuned to reflect the highest velocity expected in the vessel of interest. The V_{enc} parameter defines the duration and amplitude of the bipolar gradient that will be used during data acquisition. Values of V_{enc}, if too high reduce the quality of the measurement (Figure 3-5D). Values of $V_{enc,}$ below the peak velocity cause aliasing (Figure 3-5A). The closer the V_{enc} is to the maximum flow, the more accurate and clear the acquired velocity image will be (Figure 3-5C). In order to optimize the value of V_{enc} to produce quality phase images with clear

systole and diastole, the velocity-encoded phase contrast scout sequence is used to acquire images with multiple V_{enc} values, all specified by the operator. Scout images were used to determine the person-specific velocity sensitization or V_{enc} value with clear systole and diastole phase images

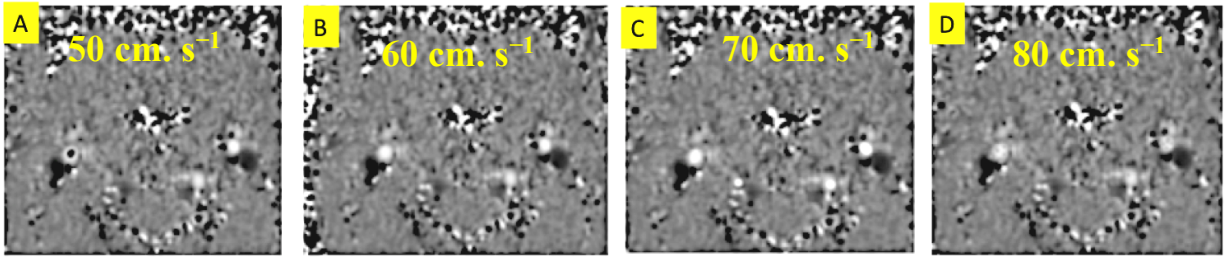

Figure 3-6 The velocity-encoded phase contrast scout sequence is used to acquire images with multiple V_{enc} (as specified by the operator) to choose the optimum V_{enc}.

that do not produce aliasing. For instance, in Figure 3-5, four V_{enc} values were selected: 50, 60, 70, and 80 cm. s^{-1}. As seen in Figure 3-5A, V_{enc} set to 50 cm. s^{-1} produced aliasing. For V_{enc}=60 cm. s^{-1}, the left VA is not fully clear and bright (Figure 3-5B). With V_{enc}= 70 cm. s^{-1}, both ICAs and VAs are bright and clear without aliasing (Figure 3-5C). With V_{enc}=80 cm. s^{-1}, the quality of the signal was diminished, being blurrier compared to V_{enc} 70 cm. s^{-1} (Figure 3-5D). Hence, V_{enc}=70 cm.s^{-1} was selected for the PC-MRI arterial flow measurement. Examples of V_{enc} for arteries and CSF are presented in Table 3-1.

PC-MRI images were acquired in 25 time frames. For example, in the Figure 3-6 (A-F) some selected CSF phase images are shown where systolic peak and diastolic peak are clearly identifiable. In addition, selected phase images for ICAs and VAs are also presented in Figure 3-6 (K-N).

To analyze the PC-MRI data as explained in article 1, manual segmentation of the ICAs, VAs lumen was carried out on the transverse slice of the phase image using MATLAB 2018 (MathWorks, Natick, MA, USA). The manual segmentation on the phase image was delineated by the largest boundaries of the lumen (often at the end of the systolic peak) to track the movement of arterial lumen during systole and diastole (Wåhlin et al., 2010). The points describing the segmented area were copied on the phase image and were constant between cardiac phases. In the pixel of the segmented area on the phase image, phase shift is proportional to $\pm V_{enc}$. Background velocity was calculated from a static region on phase data close enough to the vessel lumen to detect local phase errors and was subtracted from the velocity. This region was selected far enough

not to include vessel wall or air. Velocity waveforms were calculated from the mean velocity of the region of interest for each time frame. The CSF canal segmentation and analysis were performed in a procedure analogous to that of cervical arteries. An example of the result of the analysis is presented in Figure 3-7.

Table 3-1 Velocity encoding values that was chosen to acquire PC-MRI data

Age	V_{enc} (Artery, cm/sec)	V_{enc} (CSF, cm/sec)	Location of transverse plane
19	50	6	C2-C3
22	60	6	C2-C3
24	60	8	C2-C3
26	60	8	On C2
28	65	8	On C2
65	70	8	On C2
69	75	9	On C2
72	60	8	C2-C3
75	70	8	C2-C3

Velocity encoding values that was chosen to acquire PC-MRI data on the cervical arterial vessels (ICAs and VAs), CSF spinal canal. The location of the selected transverse plane for younger and older adults is also presented.

It could be seen in this figure where there is a clear wave reflection for younger adults compared to older adults (Figure 3-7A, B). In Figure 3-7C, the CSF velocity waveform for older compared to younger adults lost the sharpness and CSF waveforms are sharper for young adults the systolic peak arrives earlier (similar pattern was observed when CSF data of younger and older adults were compared qualitatively across the participants).

3.3.2 Near-channels and far channels

Study 2 (pulsatility and CAD) was performed on the pre-collected data and short distance source and detector was not part of their design, likely because of (1) a limited number of sources and detectors in the prototype (2) large-head near-infrared LEDs (larger radius) used in the design of prototype. With the large-head LEDs, the closest distance between source and detectors that are tightly attached would be about 1.5 cm. This distance is twice what is recommend in the literature

(0.8 cm). For study 1 (cerebral pulsatility and cortical thinning), we had short channel data. Our analysis showed that if we regress short channels from far channels, we regress the heartbeat epochs from NIRS data. In another attempt, we regressed heartbeat epochs of short channels from heartbeat epochs of far channels. As there was a time delay between the systolic peaks of the short channels and far channels, regressing these two signals created a new, artefactual peak location in the regressed data (our analysis was strictly related to location of systolic peak). Eventually, we used PC-MRI data and extracted external (ECA) and internal carotid artery (ICA) velocity waveforms (Figure 3-7). Our data showed that short channel PTTp (source-detector distance (SD) < 2 cm) was highly correlated with external carotid artery PTTp. Likewise, far channel PTTp (2 <SD< 6.6 cm) was highly correlated with internal carotid artery PTTp (Figure 3-8). Therefore, in our data analysis we used solely far channel data between 2 <SD< 6.6 cm.

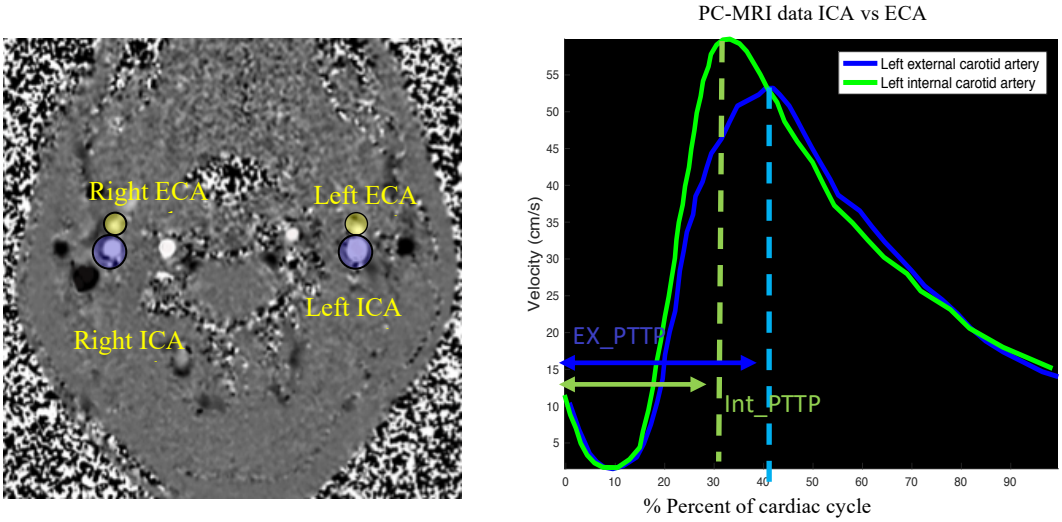

Figure 3-7 , Left: Example of a transverse slice extracted from PC-MRI data showing left ICA, right ICA, left ECA, right ECA. Right: Velocity waveforms for left ECA and left ICA for one participant. As we can see there is a time delay between the peaks in ICA versus ECA.

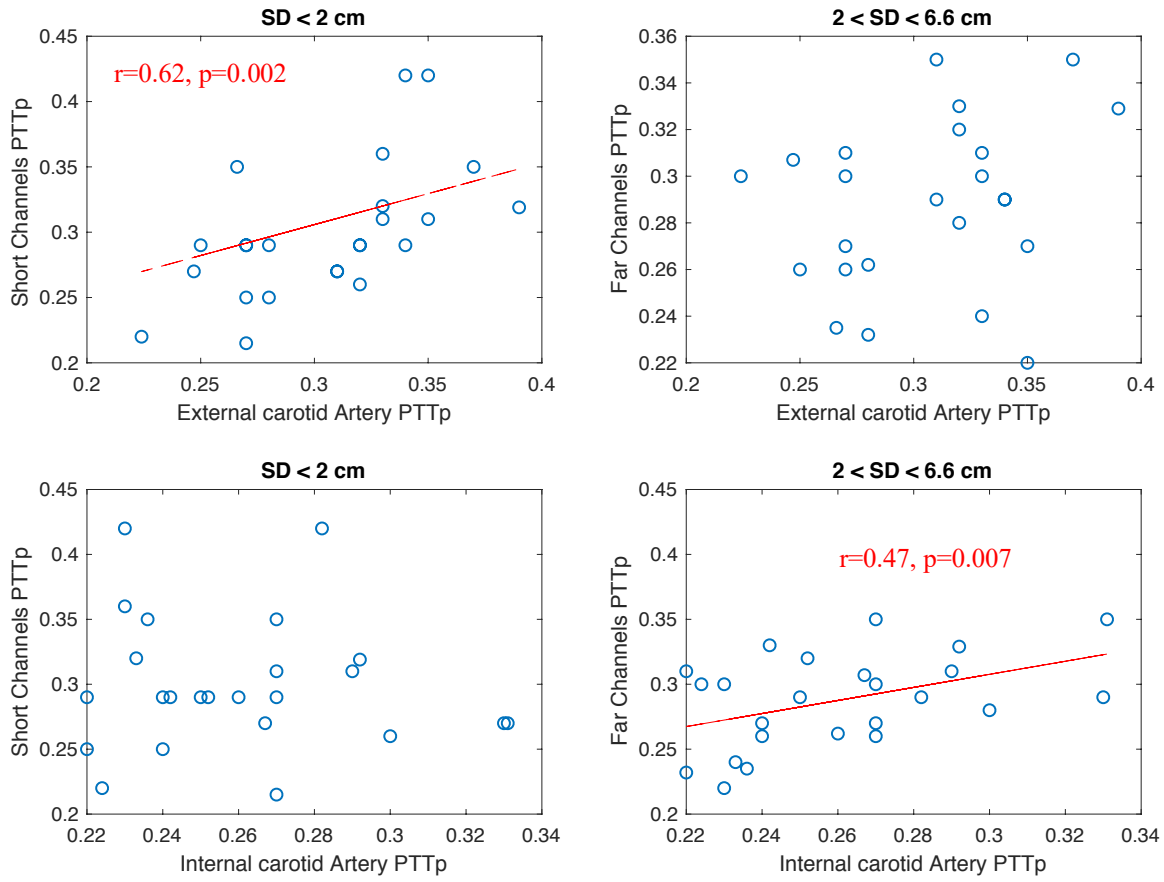

Figure 3-8, Correlation between short/far channels PTTp *vs* ECA_{PTTp}/ ICA_{PTTp} for 2 different source-detector distances (SD). As we can see short channels PTTp (SD < 2 cm) were highly correlated to ECA_{PTTp} and far channel PTTP (2<SD<6.6 cm) was highly correlated to ICA_{PTTp}

3.3.3 Experiment I.II

Experiment I.II was performed following the resting state NIRS acquisition with the same participants. Participants were trained for the Stroop color-word interference task before starting the session. The 8 minutes of resting-state (Experiment I.I), was followed by a Stroop color-word interference task designed in 8 blocks for a total time of 500 s. Each block consists of 20 s rest and 34 s activation period (total time of 54 sec for a block). In each activation period in each block, 9 trials were displayed on the screen (Figure 3-8). For each trial, 3.278 s response time (based on

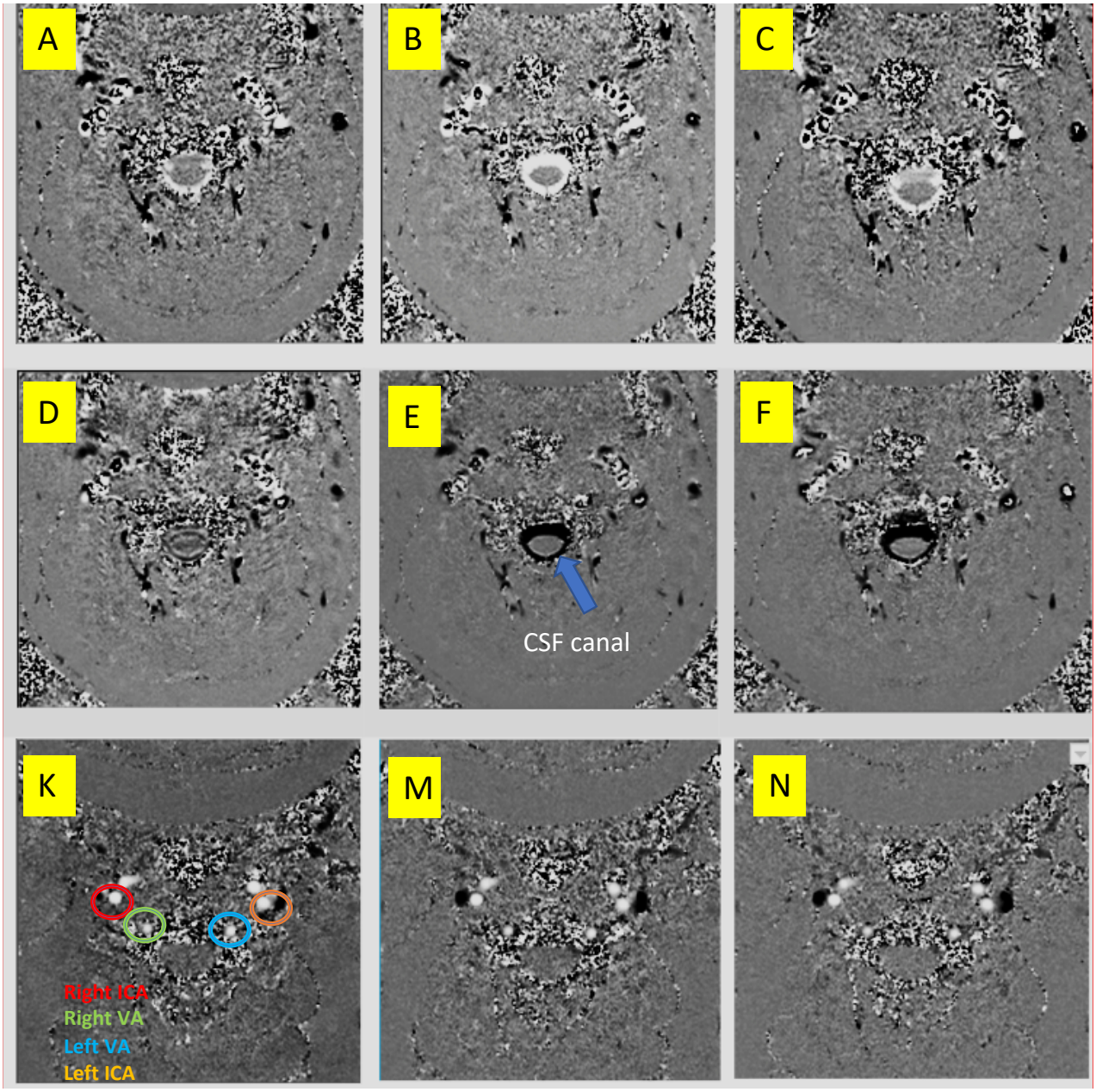

Figure 3-9 , PC-MRI images at systolic, intermediate and diastolic phases of the cardiac cycle. The images from A to F are the selected phase images for CSF in the spinal canal. The images from K to N are selected phase images for arterial blood flow. The transverse plane was perpendicular to the arteries and was located at the C2-C3 cervical subarachnoid space. White pixels represent inflow and black pixels represent outflow. Gray pixels indicate a static region. To detect local phase error, a static region on phase data was selected that was close enough to vessel lumen while also far enough not to include vessel wall or air.

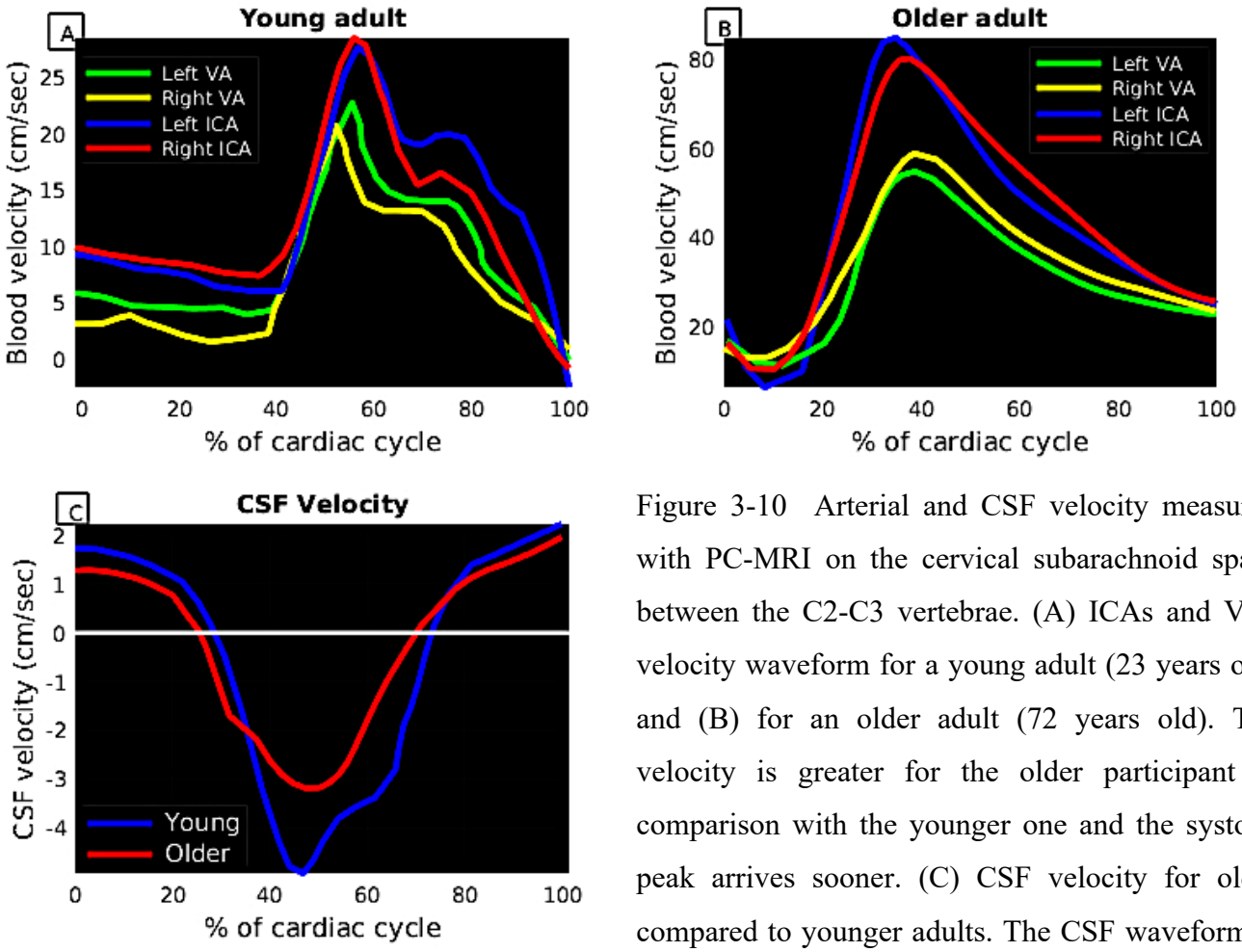

Figure 3-10 Arterial and CSF velocity measured with PC-MRI on the cervical subarachnoid space between the C2-C3 vertebrae. (A) ICAs and VAs velocity waveform for a young adult (23 years old) and (B) for an older adult (72 years old). The velocity is greater for the older participant in comparison with the younger one and the systolic peak arrives sooner. (C) CSF velocity for older compared to younger adults. The CSF waveform is sharper for young adults than for young adults.

our pilot study data), were considered. Before appearing each trial on the screen, a white cross "+" was displayed for 0.5 s to bring the participant to attention that the trial is coming (Amiri et al., 2014). Duration of each block, rest time and response time was not changed across the task blocks. In each trial, on the monitor on the top row, one of the colors of (green, blue, yellow, red) was printed where the participant instructed to choose the color of the word from the tree choices on the bottom row, on the arrows of the keyboard. From a total of 8 blocks of the task, 4 blocks were Stroop color-word interference (SI) and the other 4 blocks were control or neutral (NU) blocks. The sequence of the blocks was (NU-SI-NU-SI-NU-SI-NU-SI). In the neutral blocks, the participant had to choose the color of the letters on the top row (XXXX, WWWW) on the color

choices on the bottom row (Figure 3-8). Participants were instructed to validate their response in case that they answered the trial faster and they are waiting for the next trial. The blocks were counterbalanced across the participants. During rest block participants were instructed to focus on their breathing and avoid heavy brain activity. ECG, PPG, and functional NIRS were recording data concurrently (Figure 3-3).

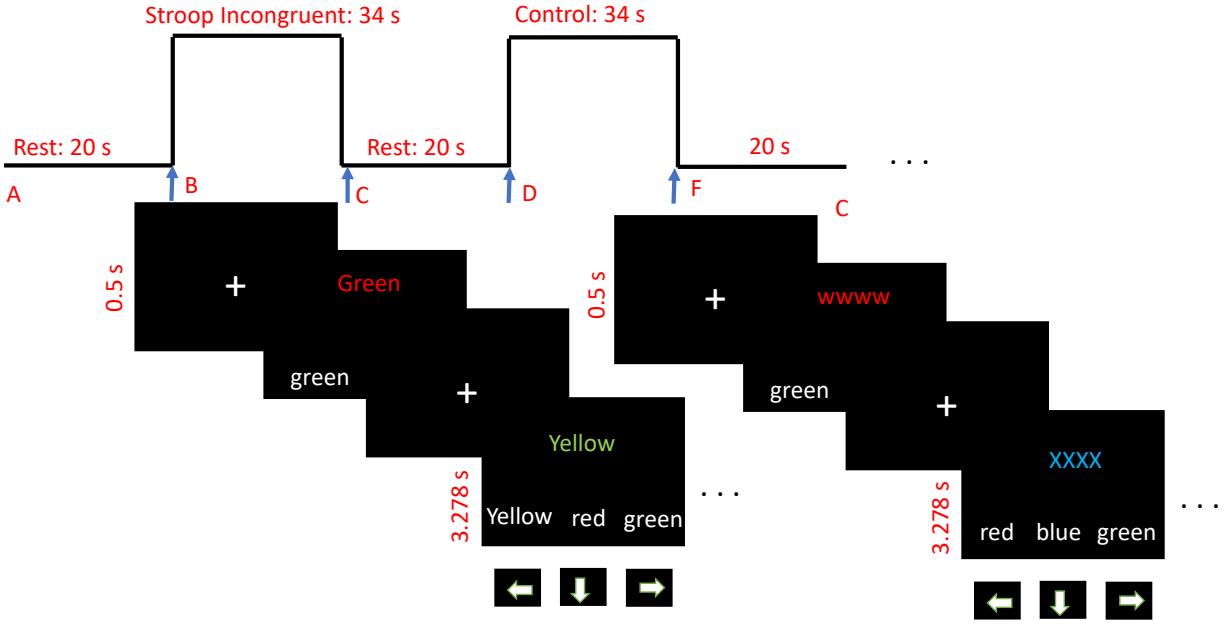

Figure 3-11 Schema of the task diagram for Stroop color-word interference (the arrows shows time duration from A to C) and control blocks (neutral, C to F). Arrows B and C shows beginning and end of the activation block. The same is true for the arrows showing D and F.

3.4 Experiment II:

We refer to chapter 5 (article 2), materials and methods.

CHAPTER 4 ARTICLE 1: CORTICAL THINNING IS ASSOCIATED WITH BRAIN PULSATILITY IN OLDER ADULTS: AN MRI AND NIRS STUDY

The following article is the culmination of our work towards answering objective 1. Chronologically, the chapter 4 article was written after the Chapter 5 article. The articles in this thesis are ordered to mimic human aging: young adult, older adult, and then pathologies in aging (CVRF and CAD). This article is submitted to Neurobiology of Aging.

Hanieh Mohammadi[1,2], Ke Peng[3,4], Ali Kassab[4], Anil Nigam[5], Louis Bherer[2,5], Frédéric Lesage[1,5] and Yves Joanette[2,6]

[1] Laboratory of Optical and Molecular Imaging, Biomedical Engineering Institute, Polytechnique Montreal, Montreal, Quebec, Canada

[2] Research Center, University Institute of Geriatrics of Montreal, Montreal, Quebec, Canada

[3] Center for Pain and the Brain, Boston Children's Hospital and Harvard Medical School, Boston, Massachusetts, USA

[4] Research Center, University of Montreal Health Centre, Montreal, Quebec, Canada

[5] Research Center, Montreal Heart Institute, Montreal, Quebec, Canada

[6] Faculty of Medicine, University of Montreal, Montreal, Quebec, Canada

4.1 Abstract

Aging is accompanied by global brain atrophy occurring unequally distributed across the brain. Cortical thickness has been shown to decrease over the course of aging with a larger loss in the frontal and temporal subregions. In this work, we explored the association between regional cortical thickness and regional brain pulsatility among healthy individuals. Sixty healthy non-demented individuals were enrolled in the study, and were divided into two age groups, young (aged 19-31) and older (aged 65-75) adults. Each individual underwent a series of different scans

for data collection including a near-infrared spectroscopy (NIRS) scan to quantify regional cerebral pulsatility from cerebral pulse transit time to the peak of the pulse (PTTp), a magnetic resonance imaging (MRI) anatomical scan to measure cortical thickness, phase contrast MRI (PC-MRI) to measure arterial and cerebrospinal fluid (CSF) pulsatility in the cervical subarachnoid space, and pulse plethysmography to quantify pulsatility in peripheral arteries (PPG_{PTTp}). Using correlation analysis, we observed a significant association between regional cerebral pulsatility and regional cortical thickness in older adults. The greatest association was found in the superior and middle temporal areas and superior, middle and inferior frontal lobe, which are the regions perfused first by the internal carotid arteries (ICAs). This association dropped in the postcentral and superior parietal regions. Moreover, our data did not show a statistically significant association between PPG_{PPTp} and $NIRS_{PTTp}$, highlighting the importance of measuring pulsatility in the brain. These findings suggest higher brain pulsatility as a potential risk factor that plays a role in the emergence of age-related cognitive decline for some cognitive domain more than others.

Keywords: Near-infrared spectroscopy, cerebral pulsatility, cortical thinning, aging, cognitive decline

4.2 Introduction

Normal brain aging is concomitant with a universal but nonuniform atrophy in cerebral tissue (McGinnis et al., 2011; Thambisetty et al., 2010). Age-related atrophy has been the subject of scientific inquiry, but to date, the mechanisms contributing to this nonuniformity are not entirely clear.

Several previous studies linked age-related brain atrophy to the stiffer arterial system. In particular, a body of research described an association between damaged microcirculation (of the arterioles, capillaries and venules) and regional cerebral atrophy and white matter hyperintensities (Bateman et al., 2008; Feugeas et al., 2009; Feugeas et al., 2005). Bateman and colleagues, suggested that as a component of normal aging, a stiffer arterial tree promotes dysfunction of the Windkessel mechanisms especially in the large central arteries (Bateman et al., 2008). In the stiffer arterial tree, the higher speed of the pulse leads to the premature arrival of the reflected pulse wave during late systole instead of during early diastole. Thus, systolic pressure is elevated whilst diastolic pressure is reduced resulting in a higher pulse pressure. This evolved pulse has higher energy

(Mitchell, 2015) and while traveling, imposes higher circumferential and shearing stress on the arterial walls (Vlachopoulos, Charalambos, Michael O'Rourke, 2011). At each cardiac cycle, this pulse, is transmitted to the brain via the carotid and vertebral arteries, leading to mechanical stress onto the brain vasculature (McDonald, 2011) eventually dissipating in the brain tissue (Mitchell, 2015). Cerebral arterioles respond to higher pulsatility by constricting, aiming to increase the resistance to protect cerebral capillaries and hence limit the regional cerebral blood flow (Mitchell, 2018). With an average of seventy-five heartbeats per minute, every year, the cerebrovascular system is subjected to about forty million cycles with higher mechanical stress. Over time, this large number of cycles with higher pulsatility promotes mechanical fatigue in cerebral arteries and arterioles, which remodels the arteries and compromises the reactivity of arterial walls (McDonald, 2011). Not only the characteristics of the pulse, but also the architecture of brain vasculature as a low-resistance and high-resting-flow organ exceptionally facilitates its susceptibility to the penetration of the pulse into the cerebral microvasculature (Mitchell, 2008).

The magnitude of the pulsatility exerted on brain tissue is not solely dependent on arterial pulse (Stoquart-ElSankari et al., 2007; Wagshul et al., 2011; Wåhlin et al., 2014). As the human brain is enclosed in a rigid cranium, optimum intracranial pressure depends on mechanical coupling between volume of blood, CSF and the brain. During systole, incoming blood causes a cerebrovascular distention in the intracranial compartment to accommodate the increased volume. Blood and CSF are incompressible fluids and the augmented volume thus increases cerebral spinal fluid (CSF) pressure (Wagshul et al., 2011). This pressure gradient is then partially compensated by pushing the CSF to the spinal canal (Alperin et al., 2000; Balédent et al., 2001; Wåhlin et al., 2010). Therefore, temporal coupling between arterial and CSF pulsatility may provide additional information about the age-related modification in the dynamic of intracranial pulsatility.

The spatially nonuniform atrophy in the human brain is characterized by a reduction in gray matter which is particularly present in both the frontal and the temporal subregions (Bartzokis et al., 2001). MRI studies on healthy individuals indeed point to the largest reduction in cortical thickness belongs to the prefrontal (Fjell et al., 2009; Good et al., 2001; Lemaitre et al., 2012) and temporal subregions (Fjell et al., 2009; Lemaitre et al., 2012; Storsve et al., 2014). Functional data support this finding by showing lower performance on cognitive tasks that require an intact prefrontal cortex structure and function fidelity (Wilson et al., 2010). Bigler et al. (2002) and Du et al. (2006) also reported the presence of atrophy in the temporal lobe in normal aging. An amplification of

this phenomenon has been documented for individuals with Alzheimer's disease where atrophy in temporal lobe subregions was correlated to performance in the episodic memory (Gallagher and Koh, 2011).

It has been proposed that the decrease in the frontal and temporal cortical thickness with aging could have a vascular nature (Leritz et al., 2011). More specifically, large portions of the frontal and temporal lobes are located upstream of ICA territories where an age-related morphologic change in these arteries are often concomitant with a chronic decrease in the mean blood flow and an increased pulsatile component. Indeed, in a study in middle-aged adults, lower mean blood flow and higher pulsatility were reported in the middle cerebral artery (MCA) (Pase et al., 2012). These alterations may result in an enhanced preferential vulnerability of the structures of the brain located in the watershed of these arteries, thus impacting cognitive abilities for which these areas are important. If such a mechanism would be confirmed, it would support the hypothesis by Stone et al. (2015) suggesting that the brain is being degraded by the cardiac pulse (Stone et al., 2015), and that brain regions with higher pulsatility will undergo larger changes in cortical thickness.

Previous studies have linked age-related vascular damage to modifications of the anatomical integrity of the brain and its impact on cognitive function. Elevated central arterial stiffness was linked with cortical thinning of the frontal regions (Pasha et al., 2015). In other studies, global gray matter atrophy was shown to occur in conjunction with high blood pressure (Jochemsen et al., 2013; Kern et al., 2017; Van Dijk et al., 2004). High arterial pulsatility was shown to be accompanied by brain damage (Mok et al., 2012) and cognitive decline (Mitchell et al., 2011; Obisesan et al., 2008). Abnormal flow pulsatility in arteries and veins was also reported in older adults with dementia (Bateman et al., 2008). Finally, a 28-year longitudinal study showed a relationship between midlife hypertension with late-life frontal and temporal cortical thinning (Vuorinen et al., 2013). Yet, despite these correlative studies between pulsatility in the large central arteries and the degradation of brain regions, no direct comparison between the regional distribution of pulsatility on the brain and cortical thickness was done to describe selective regional cortical thinning.

The overall goal of this study is to explore the association between cortical thickness and cerebral pulsatility and to explore its link to the temporal coupling between CSF and arterial pulsatility. In order to do so, we used phase-contrast MRI (PC-MRI) to measure the input arterial pulse into the brain from the ICAs and vertebral arteries (VAs). Next, we quantified the pulsatility across the

brain using near-infrared spectroscopy (NIRS) imaging. The NIRS technique with its high temporal resolution enabled studying cerebral pulsatility in a more natural setting (Chiarelli et al., 2017; Fabiani et al., 2014; Tan et al., 2017). Every heartbeat exerts a pressure gradient in the dense cerebral arterial network and leads to local alterations in the volume of oxygenated blood in the arteriolar vascular bed. This leads to alterations of oxyhemoglobin concentration and thus the amount of absorbed near-infrared light (Chiarelli et al., 2017; Fabiani et al., 2014; Tan et al., 2017; Themelis et al., 2007). Using NIRS to measure the pulsatile component of arterial oscillations on the cortex was first conducted by Themelis et al. (2007) in a newborn pig. Fabiani et al. (2014) developed and applied the technique on the human brain to measure the spatial distribution of pulsatility across the cortex. Their work correlated cerebral optical pulse parameters with local cerebrovascular health (Tan et al., 2017), hemodynamic changes associated to voluntary breath holding (Chiarelli et al., 2017), cardiorespiratory fitness (Tan et al., 2017), individual differences in the cortical volume (Chiarelli et al., 2017) as well as white matter signal abnormalities (Tan et al., 2019). Using pulse transit to peak of the pulse extracted from NIRS data, we explored the relationship between age-related local modification of cortical thickness and the pulse. We further explored the association between cerebral arterial pulsatility measured with NIRS and peripheral arterial pulsatility using a pulse plethysmograph (PPG) on the index finger (Uangpairoj and Shibata, 2013). More specifically, the aims of the present study were two-fold: (1) To assess the relationship between regional cerebral pulsatility and cortical thickness. We hypothesize that higher regional pulsatility is associated with greater regional cortical thinning. (2) To assess the relationship between temporal coupling of arterial and CSF pulsatility on cortical thickness. It was expected that higher delay between arterial inflow and CSF outflow systolic peak is associated with lower global cortical thickness.

4.3 Material and method

4.3.1 Study population

A total of 71 individuals were recruited for the study. A medical doctor reviewed blood test results and participants whose clinical profile precluded eligibility were excluded from the study. Likewise, those participants for whom data quality were not good were excluded from the analysis (total of 11 participants). The data for the remaining 60 healthy individuals was grouped into

healthy elderly (aged 65 to 75) and healthy young (aged 19-31) controls. Table 4-1 summarizes demographic characteristics of the participants whose data were used for the analysis.

Table 4-1 Characteristics of study population

Characteristics	Healthy young (n=30)	Healthy older (n=30)
Female/male (n)	16/14	15/15
Age (years)	25.41 (2.97)	69.12(2.92)
Height (cm)	171.92 (8.47)	167.28 (26.53)
Weight (kg)	68.67 (7.46)	68.30(14.05)
BMI ($kg.m^{-2}$)	24.13 (4.78)	24.85 (2.56)
Head circumference (cm)	57.11 (7.53)	58.16 (5.44)
Total year of education (years)	18.07 (2.86)	15.31 (2.77)
Resting SBP (mmHg)	122.60 (4.09)	122.93 (4.67)
Resting DBP (mmHg)	80.96 (7.16)	79.93 (7.86)
Pulse pressure (mmHg)	39.11 (5.06)	42.07 (6.16)
Heart rate (beat/min)	70.17 (6.83)	71.59 (6.75)
Blood sample parameters		
Total cholesterol (mmol. L^{-1})	5.12 (0.34)	4.67 (0.48)
Cholesterol-LDL (mmol. L^{-1})	1.97 (0.66)	2.17(0.66)
Cholesterol-HDL (mmol. L^{-1})	1.56 (0.28)	1.42 (0.58)
Cholesterol Non-HDL (mmol. L^{-1})	2.41 (0.77)	3.64 (1.09)
Triglycerides (mmol. L^{-1})	0.93 (0.57)	1.37 (0.47)
Sodium (mmol. L^{-1})	139.53 (1.57)	140.63 (1.83)
Potassium (mmol. L^{-1})	4.09 (0.18)	4.27 (0.25)
Chloride (mmol. L^{-1})	104.80 (1.71)	104.73 (2.42)
C-reactive protein (mg. L^{-1})	1.42 (1.81)	2.78 (2.99)
Medication therapy		
Aspirin, n (%)	0 (0)	2 (0.06)

Continuous variables are mean (standard deviation), n: number of participants, BMI: body mass index; LPA left pre-auricular, RPA: right pre-auricular, SBP: systolic blood pressure; DBP: diastolic blood pressure; LDL: low-density lipoprotein; HDL: high-density lipoprotein. Pulse pressure is difference between systolic and diastolic pressure measured on the arm.

4.3.2 Screening procedure

Inclusion criteria were healthy, MRI compatible and right-handed (Edinburgh handedness inventory, Oldfield, 1971). All participants were native French speakers. Exclusion criteria were claustrophobia and presence of classical cardiovascular risk factors. The cut off values for clinical parameters were hypertension: blood pressure > 139/89 mm Hg, high low-density lipoprotein (LDL > 3.36 mmol. L^{-1}), low high-density lipoprotein (HDL < 1.3 mmol. L^{-1}), total cholesterol > 5.2 mmol. L^{-1}, cholesterol non-HDL > 3.37 mmol. L^{-1}, high triglycerides > 1.7 mmol. L^{-1}, C-

reactive protein > 5 mg. L^{-1} and being out of range for 133 < sodium < 145 mmol. L^{-1} and 3.5 < potassium < 5 mmol. L^{-1} and 100 < chloride < 109 mmol. L^{-1}. Other exclusion criteria included the presence of any of the following self-reported conditions: diabetes, history of infarction, cardiovascular or cerebrovascular disease, history of epilepsy, history of respiratory disease (asthma and allergy), medication affecting the nervous system (benzodiazepine or antidepressants), vasoactive medication such as blood pressure control medication (beta-blockers, calcium-antagonists, angiotensin-converting-enzyme inhibitors, angiotensin-antagonist inhibitors), anticoagulant medication (such as warfarin or heparin, Xarelto), alcoholism (for women more than 2 glasses of wine and for men more than 3 glasses of wine per day), body mass index (BMI) 30 kg/m2, involuntary movement, uncorrected hearing or vision, history of cancer, human immunodeficiency virus (HIV), exercise training (more than 2 hours per week), smoking, daltonism, and psychiatric or neurological illness. The study was approved by three ethics committees of the CRIUGM (*Centre de Recherche de l'Institut Universitaire de Gériatrie de Montréal*), Polytechnique Montréal and the Montreal Heart Institute. All participants provided written consent prior to their participation with the option to drop out at any time.

4.3.3 Recording sessions

Data were collected as a multi-session study. Participants completed three visits, each of which lasted at most two hours long. The first visit included a 7 ml blood draw after overnight fasting (12 to 14 hours) and a neuropsychology test following a light breakfast. The first session concluded with familiarizing the participant with NIRS and MRI. In the second visit, resting MRI data and the weight and height of each participant were collected (Table 4-1). In the third visit, resting state NIRS data were collected simultaneously with electrocardiography (ECG), and pulse oximetry data (PPG). Blood pressure was measured at the beginning and end of the third session. The blood pressure values are reported as an average.

4.3.4 Assessment of cognitive function

All participants were administered a battery of neuropsychological tests as follow: the subsections of the Wechsler adult intelligence scale (WAIS-III, Wechsler, 1997) for vocabulary, similarities, matrix reasoning, direct and inverse digit span, and the digital symbol substitution test (DSST);

the Ray auditory verbal learning test (Rey 1964) and the four sessions of the Stroop test (Jensen and Rohwer, 1966). Finally, the Montreal cognitive assessment (MoCA; Nasreddine et al., 2005) and geriatric depression scale (GDS; Yesavage et al., 1982) were used for older participants. The Beck depression inventory-II (BDI, Beck et al., 1961) were used to assess young participants. Table 4-2 summarizes the cognitive measures and two sample t-test p-values between groups. Older adults cognitive measures were within the average range of their age implying normal cognitive functioning (according to psychometric standard data).

Table 4-2 Cognitive characteristics and depression scale for the study population

Name of test	Variable	Younger (n=30)	Older (n=30)	t-test
MoCA		-	27.06 (2.54)	-
	TMT-A	19.92 (4.76)	34.33 (11.44)	<0.001
TMT	TMT-B	50.55 (13.64)	79.17(34.33)	<0.001
	Vocabulary	41.29 (8.16)	42.09 (11.06)	0.13
	Similarities	22.43 (6.78)	20.38 (6.05)	0.003
	Matrix reasoning	23.19 (2.91)	17.12 (7.55)	<0.001
WAIS	Direct digit span	9.67 (5.28)	8.16 (4.28)	0.03
	Inverse digit span	7.8 (2.11)	7.50 (2.27)	0.7
	DDST	87.47 (12.55)	62.69 (15.37)	<0.001
	Color of the block	27.42 (5.62), 0.43 (0.2), 0 (0)	29.16 (4.14), 0.13 (0.34), 0.33 (0.18)	0.20
Stroop	Read the word	20.027 (4.04), 0 (0), 0.08 (0.1)	21.59 (3.89), 0 (0), 0 (0)	0.16
	Color-word interference	48.60 (6.51), 0.86 (0.82), 0.54 (0.52)	57.96 (11.95), 0.42 (0.92), 0.42 (0.19)	0.00
	Color-word Switching	49.54 (8.13), 0.82 (1.30), 0.60 (0.98)	60.85 (17.39), 0.78(1.6), 0.75 (1.43)	0.006
RAVLT	Immediate recall	11.39 (2.46)	9.16 (2.51)	0.002
	20-min delayed recall	10.40 (3.27)	8.51 (3.28)	0.043
GDS		-	3.38 (2.09)	-
BDI		7.11 (4.11)	-	-

MoCA: Montreal cognitive assessment; TMT A/B: Trail making test A / trail making B (time); WAIS: Wechsler adult intelligence scale; DDST: digital symbol substitution test; RAVLT: Ray auditory, verbal learning test (number of the recalled words and standard deviation); GDS: geriatrics depression scale; BDI: Beck depression inventory-II. For each subsection of Stroop test, the results divided into three parts: the first part is time in sec, second part is corrected errors and third part is non-corrected errors. Results are presented as mean (standard deviation). The t-test are between older adults and younger controls.

4.3.5 MRI imaging and analysis

Three different MRI sequences were acquired on a 3 Tesla MRI Scanner Prisma Fit, Siemens Medical Solutions, Erlangen, Germany) located at the functional neuroimaging unit at CRIUGM, Montreal, Canada with a 32-channel head/neck coil.

4.3.5.1 Anatomical MRI imaging

A volumetric magnetization prepared rapid gradient echo (MPRAGE) was used to obtain high-resolution, 3D, T1-weighted sagittal anatomical MR images with a good gray/white matter contrast with the following parameters: TR/TE=2400/2.17 ms, TI=1000 ms, flip angle = 8 degrees, filed of view (FOV) read 224 mm, FOV phase 100%, voxel size = 1 × 1 × 1 mm^3, slice thickness 1 mm, slice and phase resolution 100%, and echo spacing 6.6 ms. Participants were instructed to relax and stay immobile during the scan.

4.3.5.2 Phase-contrast MRI

2D PC-MRI was used to measure velocity and flow in the cervical subarachnoid space in ICAs and VAs. Two MRI sequences, a 3D time-of-flight magnetic resonance angiography (3D-TOF-MRA) and velocity encoding scouts (PC scouts), were employed to plan the PC-MRI. A 3D-TOF-MRA sequence with TR/TE=20/3.11 ms, flip angle 10-15 degrees, FOV read 220 mm, FOV phase 75%, slice thickness 0.7 mm, and voxel size 0.6x0.6x0.7 mm^3, provided a clear assessment of vascular anatomy in the cervical subarachnoid space and were used to select the best anatomical planes for flow quantification (Figure 4-1A, 1B, 1C). After collecting the 3D-TOF-MRA data, a maximum intensity projection (MIP), implemented on Siemens software was used to display the cervical vessels on the plane. Next, a transverse plane was chosen perpendicular to the vessels, between the C2 and C3 vertebra, above the bifurcation of the internal and external carotid artery, where VA and ICA cross-sections are completely clear in the transverse plane (Figure 4-1K). It was challenging to select one optimal transverse plane for tortuously-shaped arteries common in some of the older adults for use with PC-MRI. Such cases (Figure 4-1C) required an independent scan sequence for each artery. Straight arteries in the young

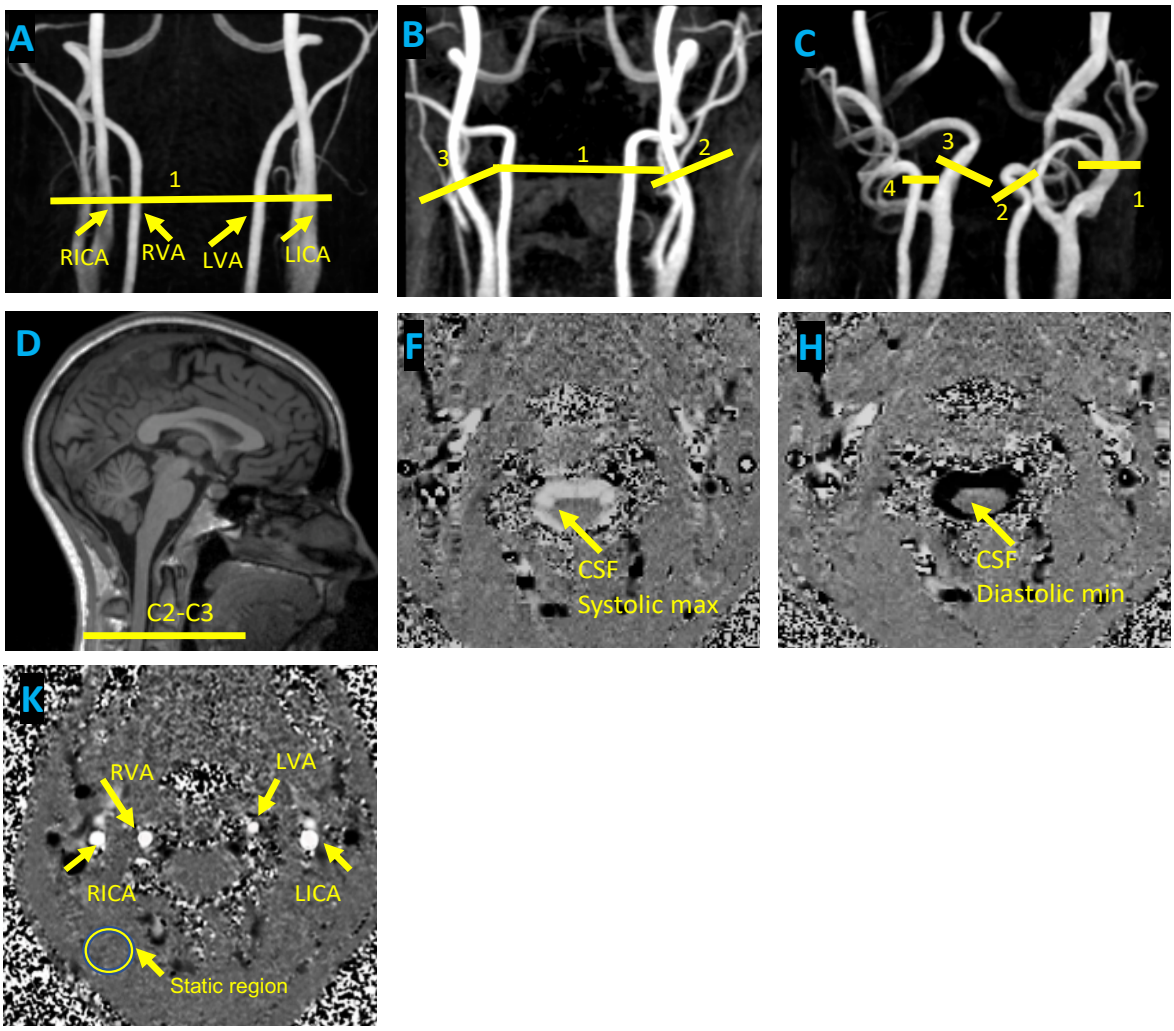

Figure 4-1, Examples of acquired MRI images; (A) Coronal view of 3D-TOF-MRA for a healthy young (26 years old) participant reconstructed with MIP algorithm. A transverse plane marked with yellow color was chosen to acquire arterial flow pulsatility from cervical arteries (B) healthy older adult 65 years old and, (C) healthy older adults 75 years. Both participants did not have known classical risk factors, no previous trauma or surgery in the neck. The tortuously shaped arteries in some of the older participants required an independent scan with a perpendicular plane for each artery (D) MPRAGE image showing the chosen transverse slice between C2 and C3 vertebrae. CSF measurement plane was selected from axial reconstruction of MPRAGE where the spinal canal is between C2 and C3 vertebrae (F) CSF spinal canal at systolic peak (H) CSF spinal canal in diastolic peak (K) Transverse slice showing Left ICA (LICA), right ICA (RICA), left VA (LVA), right VA (RVA). Transverse plane for measuring arterial pulsatility was selected using 3D-TOF-MRA at cervical subarachnoid space between C2 and C3 vertebrae above bifurcation.

White pixels represent inflow and black pixels represent outflow. Gray pixels indicate static region. A static region on phase data close enough to vessel lumen far enough not to include vessel wall or air was chosen to detect local phase error.

participants facilitated the selection of an optimal transverse plane (Figure 4-1A). Acquisition time for this sequence depended on the heart rate of the participant and varied between 5-7 minutes. That sequence was followed by a velocity-encoded phase contrast scout sequence with parameters TR/TE=127.35/6.20 ms, flip angle 15-20 deg, slice thickness 6 mm, voxel size 1x1x6 mm3, FOV read 256 mm, and FOV phase 100% to acquire images with multiple velocity encoding (V_{ENCs}) as specified by the operator, which in this study was often 60, 70, 80, or 90 cm.s^{-1}. Scout images were used to determine the person-specific velocity sensitization or V_{ENC} value with a clear systole and diastole phase image that does not produce aliasing. Acquisition times for the PC scout were between 45 and 60 s. The V_{ENCs} were used to obtain the final velocities and flow curve in the PC-MRI sequence with the following acquisition parameters: TR/TE=27.36/8.16 ms, flip angle 15, FOV read 135 mm, FOV phase 100%, echo spacing 13.7 ms, slice thickness 5 mm, and voxel size 1x1x5 mm3. Acquisition times for this sequence were between 6-8 minutes. For CSF velocity measurement, axial reconstruction of structural images was employed to select an axial measurement plane between the C2 and C3 cervical arteries far enough from the cerebral aqueduct to avoid turbulence, where the CSF spinal canal is nicely shaped (Figure 4-1F and 4-1H).

Similar to arteries, velocity-encoded phase contrast scouts were used to find the optimum V_{ENC} for CSF (often 8, 9, 10, 11 cm.s^{-1}). The PC-MRI sequence for measuring CSF velocity and flow parameters were TR/TE= 28.36/8.51 ms, flip angle 10 to 15 degrees, FOV read 135 mm, FOV phase 100%, echo spacing 13.7 ms, slice thickness 5 mm, and voxel size 0.5x0.5x5 mm^3. Over sixty percent of participants had arterial V_{ENC} of 60 cm.s^{-1} and CSF VENC of 8 cm.s^{-1}. Data were collected for 25 cardiac cycles. During the PC-MRI session, participants were instructed to look at the screen with an image of a white cross in the center on a black background and to concentrate on their breathing.

Manual segmentation of the ICAs, VAs and lumen was carried out on a transverse slice of the magnitude images using MATLAB 2018a (MathWorks, Natick, MA, USA). The manual segmentation on the magnitude image was delineated by the largest boundaries of the lumen (often

at the end of the systolic peak) to track the movement of arterial lumen during systole and diastole. The points describing the segmented area were on the phase image and were copied on entire cardiac phase frames. In the PC-MRI phase image, maximum phase shift in each direction is proportional to $\pm V_{ENC}$. Background velocity was calculated from a static region on phase data close enough to the vessel lumen to detect local phase errors and far enough not to include vessel wall or air (Figure 4-1K). Blood flow waveform in each cervical artery were calculated from the spatial mean of pixel velocity multiply to area of pixel within each time frame subtracted from background flow (Wåhlin et al., 2014, 2012). Flow waveform for ICAs and VAs were interpolated to the same length and averaged. CSF canal segmentation and analysis were performed in a procedure analogous to that of cervical arteries.

4.3.5.3 Cortical thickness analysis

Freesurfer 6.0 was used to segment cortical brain regions (Dale et al., 1999; Fischl et al., 2002) of the T1-weighted anatomical 3D MRI. The Desikan-Killiany atlas was used to define the cortical regions (Desikan et al., 2006). In short, Freesurfer was corrected the MRI images for intensity nonuniformity using an intensity normalization algorithm in several steps (see Dale et al., 1999). The skull was then automatically stripped from the intensity-normalized image. Resulting MRI images were co-registered to the Montreal Neurological Institute (MNI) using affine transformations. For each individual, the quality of each slice of the surface-based segmentation was visually reviewed and inaccuracies in segmentation were corrected using guidelines proposed by the Martinos Center for Biomedical Imaging[7], where applicable. For instance, pial surface errors were fixed by "Gcut" option or voxel editing. Extra- and infra-skull stripping was corrected using watershed parameters. If in any slice, white matter was incorrectly labeled as gray matter or vice versa (which is an intensity normalization error, often occurring for temporal lobes or frontal subregions), intensity normalization control points were employed to boost the intensity in the surrounding voxels. It is to be noted that as the NIRS optodes did not cover all the cortical regions on the head, the cortical thickness data were used for data analysis were from the cortical surfaces covered by NIRS or "NIRS-covered cortical areas". The "Cortical thickness of a volume-defined

[7] https://surfer.nmr.mgh.harvard.edu/fswiki/FsTutorial/TroubleshootingDataV6.0

ROI" in the Freesurfer was used to accomplish this goal where the FSL tool (Smith et al., 2004) and an in-house developed scripts is used to create the mask for the analysis of region of interest.

4.3.6 Physiological data acquisition and analysis

NIRS was synchronized a PPG and an electrocardiogram (ECG) with a BIOPAC BSL PRO MP36U-W (Groningen, Netherlands) module with four channels. A trigger was sent from the MP36 to the NIRS device using the SSL58L module upon starting the physiological data recording.

4.3.6.1 ECG

The first channel (CH1) was assigned to lead *I* of the ECG (SS2L ECG electrodes Lead Set, BIOPAC) where the left wrist was referenced to the right wrist using BIOPAC Disposable Electrodes (EL503). ECG signals were acquired with a sampling rate of 200 Hz. Electrical noise and interference from the ECG signal were filtered with a 0.5 Hz–100 Hz band-pass filter. With the aim of improving the quality of the signal, the location of the ECG electrode was mildly abraded with an abrasive pad after the skin was disinfected with alcohol. During analysis of the ECG data, R-wave peaks were identified by searching for local maxima exceeding a voltage threshold (the voltage thresholds chosen were specific to each participant). R-wave peaks outside of the range of mean$\pm$2(SD) of inter-beat intervals were identified as artefacts and were discarded. Visual inspection was performed to verify there is no misidentification or no detection error is presented in the ECG R-wave peaks had been corrected or discarded from data.

4.3.6.2 PPG

The second channel (CH2) was assigned to PPG using an SS4L finger transducer working in reflectance mode, which was placed on the index finger of the left hand. Participants were instructed to avoid using nail polish on the index finger, especially red as it may interfere with PPG measurement. Dynamic pulsatile waveforms were recorded at a sampling rate of 100 Hz. The PPG signals were evaluated for quality using the signal-to-noise ratio (SNR, Venema et al., 2012):

$$SNR = 20.\log\left(\frac{\sum_{0.15Hz}^{3Hz} PSD(f)}{\sum_{30Hz}^{\infty} PSD(f)}\right) dB$$

The area under the curve of the AC component of the power spectral density (PSD, 0.15–3 Hz) was considered as signal whereas frequencies higher than 30 Hz were defined as noise (Venema et al., 2012). Signal with SNR >12 dB was used for statistical analyses (Saritas et al., 2019). PPG data for each block were analysed separately. The baseline shift in each resting state block was eliminated by piecewise cubic spline interpolation. The area under the curve for each PPG heartbeat epoch was calculated and epochs with area under the curve within the range of mean$\pm$2(standard deviation) were kept. PPG heartbeats were then interpolated to the same length and averaged. A correlation between each heartbeat epoch and the average heartbeat were calculated. Heartbeat epochs with a correlation$\geq$0.7 were considered for further analysis.

4.3.7 NIRS data recording and analysis

Optical intensity was measured for 8 minutes consisting of 8 blocks of 60 seconds resting state. A resting state paradigm similar to (Eggebrecht et al., 2014; Tan et al., 2017) was followed. Participants were instructed to stay immobile and concentrate on breathing. NIRS data were collected at 20Hz using four bays (Brainsight, Rogue Research Inc.). Each module consisted of eight high-sensitivity detectors and four proximity detectors assigned as short channels. Monochromatic laser diodes emitting at two continuous wavelengths, 695 nm and 830 nm, were used. As arterial blood is saturated with oxyhemoglobin, the channels with 830 nm wavelength have higher sensitivity to arterial pulsatility concentration changes (Chiarelli et al., 2017; Themelis et al., 2007), hence, only the data for this wavelength is used to study pulsatility with NIRS. Near-infrared sources and detectors were placed and fixed on a flexible elastomer stripe (Brainsight, Rogue Research Inc.) that could be adjusted according to head size.

A telescopic arm in the Brainsight compartment provided a stable support for the weight of the optical fibers. Experiments took place in a dark room with a regulated temperature of 21 degrees. A lightweight black fabric covered the helmet to mitigate detection of ambient light. A comfortable chair, footrest and neck rest were provided to facilitate

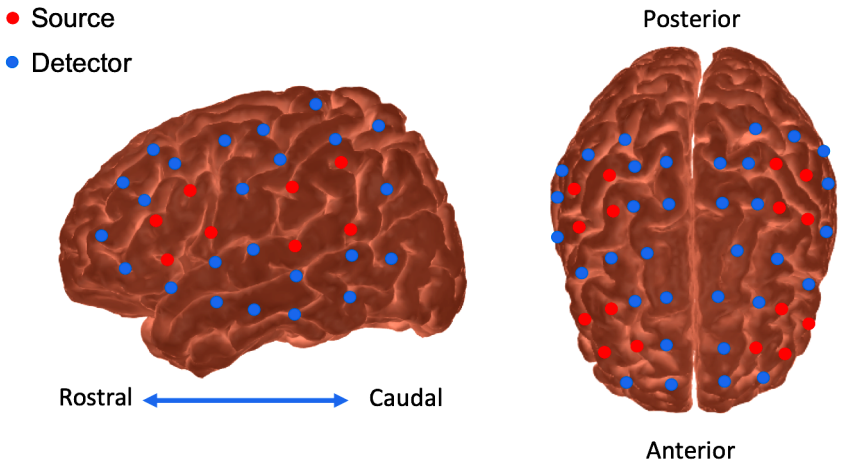

Figure 4-2 From left to right; NIRS source and detector montage plotted on the sagittal and horizontal view. The montage has symmetry for the right and left hemisphere. Red circles indicate sources and blue circles indicate detectors. A total of 48 detectors and 16 sources were located on the head.

staying immobile during the experiment. In order to increase signal to noise ratio of the pulse coming from brain, data from source-detector separation of 2 to 6.6 cm were used.

Trigger management at the starts and ends of each block was performed with Expyriment 0.9.0 (Krause and Lindemann, 2014) on Python 2.7. Data analysis was performed using MATLAB 2018a (MathWorks, Natick, MA, USA). The saturated channels were discarded from further analysis. The intensity NIRS data for all the channels were normalized to their temporal mean. The data were then filtered with a bandpass filter with a cut-off frequency of 0.5-5 Hz to eliminate unwanted high- and low-frequency noise (Tan et al., 2017). This frequency interval is associated with physiology data originating from the frequency of the heartbeat. Motion artefacts were identified using Homer2 toolbox, (motion artifact function, Huppert et al., 2009) and the output vectors were visually checked and often removed from the analysis. In order to check the quality of heartbeats in each channel, we employed a metric called scalp coupling index (SCI) introduced by Pollonini et al. (2014) which was defined as cross-correlation of the two wavelengths data from a same NIRS channel. A higher SCI is normally an indication of a better quality for the measurement of heartbeat epochs for a particular channel. In our study, only channels with SCI >= 0.7, were considered for further analysis. The heartbeat epochs were extracted from each

channel of NIRS data and were time-locked to the onset of the ECG R-wave peak to the R-wave peak of the next cycle (which is itself synchronized with NIRS). The baseline shift of every individual heartbeat epoch was corrected by piecewise cubic spline interpolation. After this step, NIRS pulsatility index were extracted.

4.3.8 Tracing NIRS optodes and MRI co-registration

Following the NIRS acquisition, the location of the three fiducial points, namely the left and right pre-auricular points (LPA and RPA) and the nasion, and source as well as each source and detector were digitized with a Polaris Vicra (Northern Digital Inc.) optical tracking system mounted on the Brainsight system (Figure 4-2). The 3D sources and detectors coordinates were then saved in MNI space. Optode coordinates and anatomical MRI were co-registered on the surface of the cortex and anatomical labels of each channel was extracted using the MATLAB toolbox, AtlasViewer (Aasted et al., 2015).

4.3.9 Pulsatility parameter

4.3.9.1 NIRS and PPG pulsatility index value

In this study we used cerebral pulse-transit-time-to-the-peak-of-the-pulse (PTTp, Allen, 2007) measured with NIRS as the pulsatility parameter. The $NIRS_{PTTp}$ is the time it takes for the pulse to transit from the heart left ventricle to the downstream measurement point and is related to arterial path length, and the rigidity of arterial walls integrated along the travel path. In the literature this parameter is often extracted from PPG and is related to arterial elasticity (PTTp, Allen, 2007). The distention of the arterial wall accommodates the blood transiently rising in the vascular wall. The impedance of the artery to the flow of blood is related to downstream resistance in the peripherally and also the elasticity of the vessel wall, therefore associated with aging and vascular impairment (Gómez García et al., 2014). Thereby, a shorter PPG_{PTTp} indicates a shorter artery (Smith et al., 1999), or is related to higher arterial rigidity (Allen, 2007; Allen and Murray, 2003). Furthermore, PPG_{PTTp} is shown to be nearly linearly proportional to blood pressure (Smith et al., 1999) and is inversely proportional to pulse wave velocity (PWV, Gizdulich, 1984). Smith and colleagues reported that (PPG_{PTTp}) is related to arterial elasticity and a higher blood pressure shorten the pulse transit time. Conversely, reducing of the blood pressure increases the pulse transit time (Smith et al., 1999).

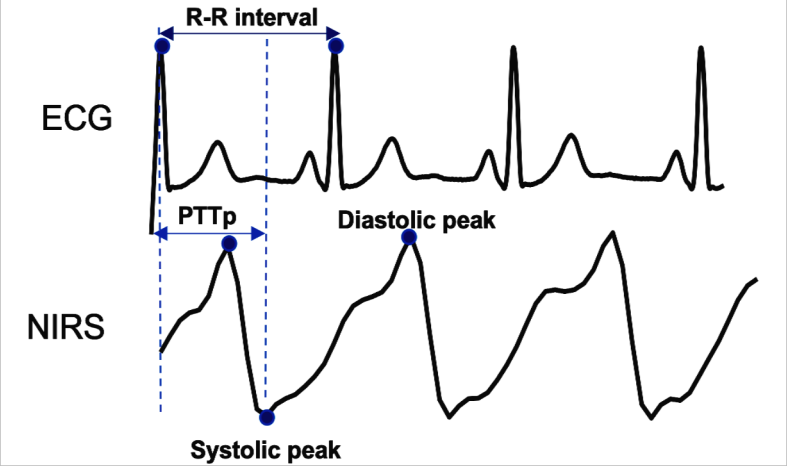

Figure 4-3 Characterization of cerebral pulse measured with NIRS synchronized with ECG. The PTTp is the time from ECG R-peak to subsequent systolic peak in the NIRS data. In the ECG data, the R-wave reflects depolarization of the ventricular myocardium and signals the beginning of systole (Allen, 2007). The systolic upstroke in the does not occur immediately following the R-wave. The systolic upstroke appears after a short delay. The reason for this delay is the time it takes for the depolarization wave to propagate across the ventricles (Allen and Murray, 2003). The pressure then builds up following an isovolumetric contraction. Subsequently, the aortic valve opens and blood flows to the aorta and travels across the body (Allen, 2007).

After the R peak in the ECG data, the first local maximum in the NIRS data is a diastolic peak and the first local maximum in the opposite direction is the cerebral systolic peak (Figure 4-3). The PTTp for each heartbeat epoch was then divided to the duration of the cardiac cycle (the corresponding ECG R-R interval in NIRS data). As the median is more robust to outliers than the mean, we report the pulsatility index as median value. During the analysis of the data we observed that a noisy pulsatility index is often found in the first quantile and fourth quantile of the data. Therefore, in each channel, the PTTp data were split into four quantiles and solely the second and third quantile pulsatility indices (median PTTp) were averaged. This value was then reported as pulsatility index for the channel. Typically, the systolic peak took place between 218 and 433 ms after the onset of the R-wave.

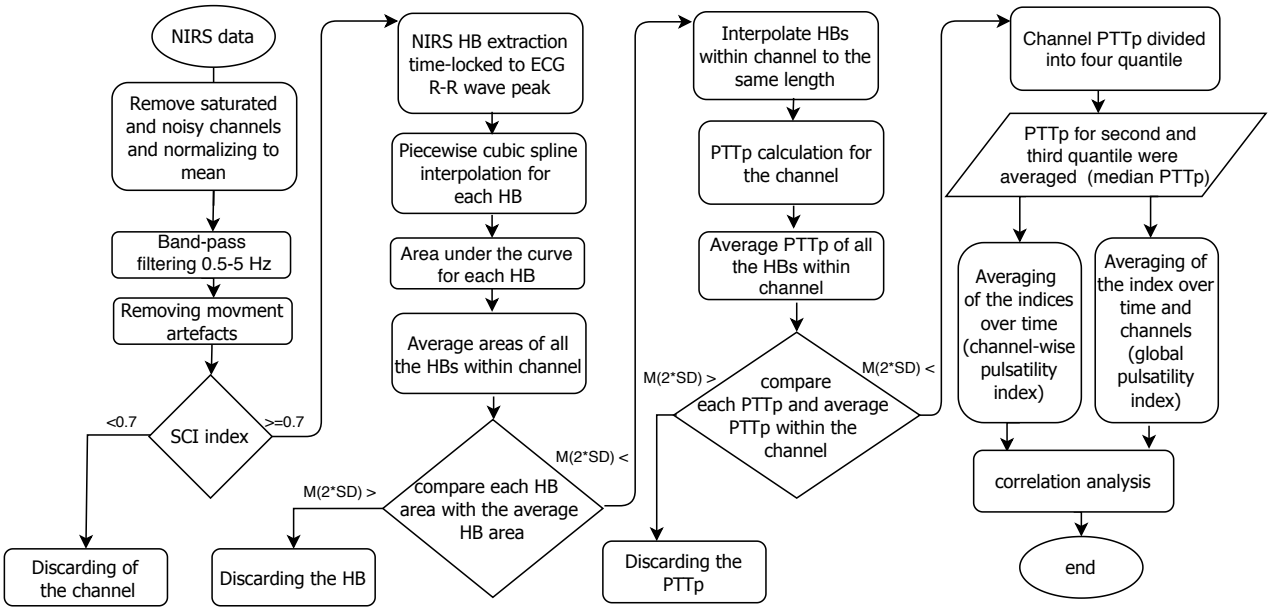

Figure 4-4 Schematic diagram of NIRS data processing to extract pulsatility parameter index ($NIRS_{PTTp)}$ and analysis. HB is a notation for NIRS heartbeat epoch. M(SD) is a notation for mean and standard deviation.

The average of the PTTp across all the channels was used to summarize the pulsatility index of an individual. We defined this NIRS-covered average PTTp across all the channels as global PTTp. A schematic diagram of processing of the NIRS data to extract pulsatility index used in this study is summarized in Figure 4-4.

4.3.9.2 Cervical arterial pulsatility index

Total cerebral blood flow was determined as the sum of the flow waveform of both ICAs and both VAs. This curve was used to extract a value of the cervical arterial pulsatility index (caPI, Wåhlin, Ambarki, Birgander, Malm, & Eklund, 2014):

$$caPI = \frac{[Systolic\ Maximum\ Flow] - [Diastolic\ Minimum\ Flow]}{[Time\ Averaged\ Mean\ Flow]}$$

caPI is a dimensionless parameter that reflects the dynamic alteration of flow between systolic peak and diastolic minimum. It was often reported to reflect the resistance of downstream vasculature to the blood flow (Bude and Rubin, 1999; Wåhlin et al., 2014) and the degree of arterial wall elasticity and compliance (C.S. and R.W., 1984). In a stiffer artery, the average mean flow decreases and the difference between systolic maximum and diastolic minimum blood flow

increases. This yields a higher caPI number in older adults (Wåhlin et al., 2014; Zarrinkoob et al., 2016).

PC-MRI provides the measure of absolute flow pulsatility and is sensitive to the size of vessel. To overcome this sensitivity, we calculated the caPI as presented in the formula. Since caPI is normalized to mean flow, it is a measure that indicates relative vascular pulsatility. Unlike NIRS that measures the arterial oscillations in real time in each cardiac cycle, PC-MRI provides pulsatility as the average collected over many cardiac cycles. We need to note that in the analysis we also normalized the NIRS signal to mean and averaged NIRS pulsatility over time and then explored the correlation between NIRS pulsatility and MRI pulsatility.

It is also to be noted that we did not use the same pulsatility index formula for NIRS heartbeat epochs as is used for caPI. While it is possible to rely on the values of the y-axis of the flow pulsatility waveform (measured with PC-MRI), relying on the amplitude change in the NIRS signals could cause contamination by partial volume effect, which leads to under- or overestimation of parameters (Huppert et al., 2009).

4.3.9.3 Latency between systolic arterial peak and CSF flushing peak

The CSF flow pulsatility curve was calculated from the PC-MRI CSF velocity images using a procedure similar to the calculation of the arterial flow pulsatility (Stoquart-ElSankari et al., 2007; Wåhlin et al., 2014). CSF and arterial flow pulsatility curves were then interpolated and the latency between the arterial systolic peak and the CSF flushing peak (Lp_{ArtCSF}) was calculated. Lp_{ArtCSF} indicates the temporal coupling between arterial and CSF flow pulsatility and is a measure of intracranial compliance (Stoquart-ElSankari et al., 2007). In older adults, Lp_{ArtCSF} increases which is an indication an indication of lower cerebrovascular compliance (Uftring et al., 2000).

4.3.9.4 Brachial pulsatility index

Brachial pulsatility index was calculated as the difference between systolic maximum and diastolic minimum of blood pressure measured on the arm (Wåhlin et al., 2014).

4.3.10 Data and statistical Analysis

We used linear regression to control for the effect of sex, height in $NIRS_{PTTp}$, caPI and Lp_{ArtCSF} data. For cortical thickness, we controlled for the mentioned parameters plus total intracranial volume (eTIV). Outliers were removed from analysis using a generalized extreme studentized deviate test (or 'gesd') implemented in MATLAB 2018a. We used correlation to explore the relationship between variables regional cortical thickness and regional pulsatility. Correlation between pulsatility and cortical thickness in each cortical region was based on bootstrap test 2000 Bootstrap samples, (Efron and Tibshirani, 1986; Wåhlin et al., 2014) to test the stability of p-values with 95% confidence interval. The p-values were corrected with false discovery rate (FDR) using Benjamini and Hochberg method (Benjamini and Hochberg, 1995).

4.4 Results

Linear regression indicated sex and height impact for global $NIRS_{PTTp}$ in both older adults $F(2,27) = 5.75$, $p=0.028$ and younger controls $F(2,27)=4.16$, $p=0.042$. In order to ensure these variables are not confounding $NIRS_{PTTp}$ results, we used linear regression to subtract the effect of these variables. As mentioned, for cortical thickness and Lp_{ArtCSF} data, linear regression was used to adjust for the eTIV and the mean arterial net flow, respectively. Variables were then normalized between 0 and 1. This procedure was performed separately for older adults and younger controls.

For both study groups, we assessed the reliability of the $NIRS_{PTTp}$ across eight blocks of rest by a correlation matrix. Correlation coefficients were higher than 0.969, $p<0.001$. Thus, for the rest of the analysis, the $NIRS_{PTTp}$ in each region were averaged across all the blocks. A student t-test indicated that there was a statistically significant difference between global $NIRS_{PTTp}$ between young 0.81±0.16 and old adults 0.58±0.21 ($p<0.001$).

4.4.1 Relationship between global NIRS pulsatility, cervical arterial pulsatility and age

The correlation analysis showed there was a statistically significant association between the measure of MRI arterial pulsatility (caPI) and global NIRS pulsatility ($NIRS_{PTTp}$) both in older ($r=-0.62$, $p <0.001$) and in younger adults ($r= -0.32$, $p<0.039$). There was a statistically significant

correlation between global $NIRS_{PTTp}$ and age in the older adults (r=-0.581, p=0.003) but not for younger controls (p>0.1).

4.4.2 Spatial relationship between cortical thickness and NIRS pulsatility

We divided cortical regions to 18 subregions based on Desikan-Killiany atlas (Desikan et al., 2006). Figure 4-5 on the top row shows the average of $NIRS_{PTTp}$ (and middle row for NIRS-covered cortical thickness) in each 18 anatomical regions across all the participants within each group projected on the cortex. Correlation analysis indicated that there is a statically significant association between global $NIRS_{PTTp}$ and global NIRS-covered cortical thickness in older adults (r=0.4311, p<0.001), but not in younger controls (r=0.12, p>0.1).

Table 4-3 lists a correlation analysis in each of 18 cortical regions between regional cortical thickness and corresponding regional $NIRS_{PTTp}$. The p-values are FDR-corrected and are based on 2000 Bootstrap samples with 95% confidence interval. The largest correlations were evident in the left and right superior temporal, middle temporal, superior frontal and inferior frontal regions in the older adults.

4.4.3 Comparing regional correlations between older and younger adults

In each anatomical region of Table 4-3, we compared the correlation coefficients between regional $NIRS_{PTTp}$ and cortical thickness of older to younger adults. To do so, we transformed the correlation coefficients into z-scores (Fisher's-r-to-z transformation) and z-scores were compared and analysed for statistical significance. The region-based z-scores that after FDR-correction had one-tailed significance level of p<0.05 are projected on the cortex (Figure 4-5).

The z-statistics shows a difference between older adults and younger controls in superior and middle temporal and superior and middle frontal in both hemispheres.

4.4.4 Relationship between global cortical thickness and latency between arterial and CSF systolic peak

A Student t-test on the PC-MRI data indicated that there is a statistically significant difference in Lp_{ArtCSF} between the older and younger adults (p<0.001). The mean normalized Lp_{ArtCSF} was 0.575 ±1.92 in older adults and 0.30±0.08 value of the younger participants.

Table 4-3 Values in the table represents correlation coefficients between regional NIRS-covered cortical thickness and regional $NIRS_{PTTp}$ in young and older adults.

	Young		Older	
	Left Hemisphere	Right Hemisphere	Left Hemisphere	Right Hemisphere
Superior frontal	0.11, (-0.12, 0. 23)	0.12, (-0.11,0.34)	**0.59*, (0.34, 0.72)**	**0.58*, (0.41, 0.78)**
Middle frontal	0.10, (-0.19, 0.71)	0.10, (-0.13, 0.26)	**0.58**, (0.33, 0.61)**	**0.59**, (0.20, 0.75)**
Inferior frontal	0.13, (0.11, 0.37)	0.13, (-0.13, 0.42)	**0.52***, (0.28, 0.86)**	**0.47***, (0.28, 0.74)**
Superior temporal	0.15, (0.06, 0.61)	0.15, (0.01, 0.56)	**0.63***, (0.43, 0.86)**	**0.61***, (0.43, 0.86)**
Middle temporal	0.14, (0.05, 0.77)	0.13, (0.05, 0.65)	**0.61***, (0.38, 0.83)**	**0.61***, (0.28, 0.85)**
Precentral	0.13, (-0.41, 0.62)	0.15, (-0.33, 0.59)	**0.34**, (0.15, 0.74)**	0.31, (-0.006 0.73)
Postcentral	0.13, (-0.21, 0.62)	0.14, (-0.22,0.77)	0.21, (-0.36, 0.74)	0.25, (-0.26, 0.62)
Superior parietal	0.11, (-0.20,0.54)	0.13, (-0.15, 0.24)	0.28, (-0.17, 0.46)	0.21, (-0.14, 0.65)
Inferior parietal	0.12, (-0.11, 0.63)	0.14, (-0.81, 0.66)	**0.23*, (0.06, 0.72)**	**0.32*, (0.02, 0.76)**

Boldface indicates significance. Data is controlled for sex, height, years of education and eTIV. The p-values are FDR-corrected and are based on 2000 Bootstrap samples with 95% confidence interval. *p<0.05, **p<0.01, ***p<0.001.›

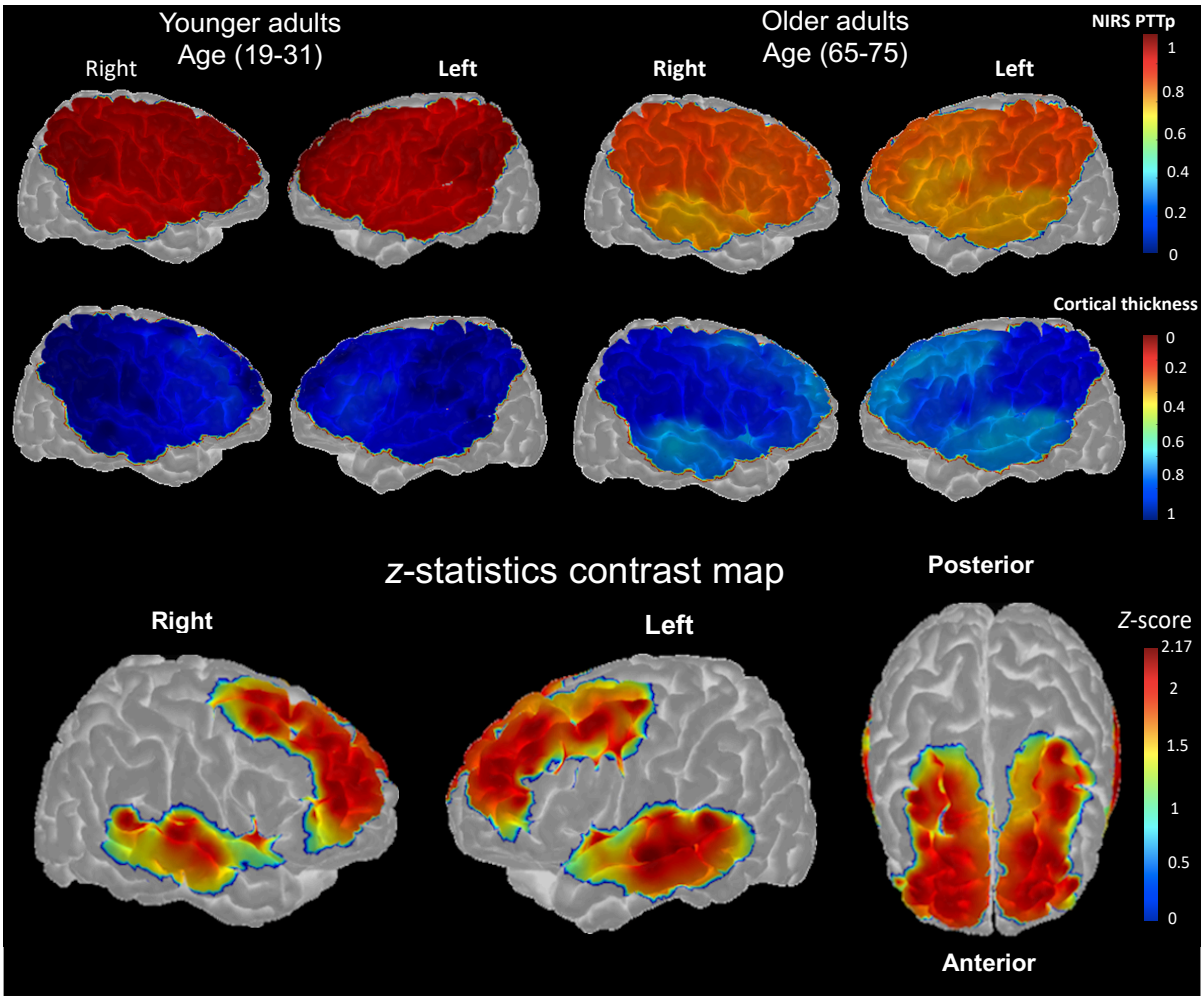

Figure 4-5 (Top) Spatial distribution of normalized cerebral pulsatility and normalized cortical thickness (averaged within each region across all the participants) within each group is projected on the cortex. The lower $NIRS_{PTTp}$ is related to higher pulsatility. For cortical thickness higher values indicated higher cortical thickness. (Bottom) The z-score contrast map of the differences in the correlation coefficients of $NIRS_{PTTP}$ *vs*. cortical thickness between the older adults and the younger controls, $p<0.05$, FDR-corrected.

Our data indicated that there is a statistically significant positive association between age and Lp_{ArtCSF} for older participants ($r= 0.585$, $p=0.0013$) but not for younger participants ($p>0.1$). Moreover, there was a significant negative association between global cortical thickness and Lp_{ArtCSF} in older ($r=-0.507$, $p=0.0081$) but not in younger participants ($p>0.1$). Mechanical coupling between arterial and CSF flow at the level of C2-C3 vertebrae is shown in Figure 4-6. The shape of the flow waveform indicated that in the older participants, the arterial flow arrives to its systolic peaks more sharply and faster. In our data set, older adult data often showed a loss of sharpness in the CSF systolic peak compared to younger adults.

4.4.5 Relationship between NIRS Pulsatility and cognitive score

Across older participants, the average $NIRS_{PTTp}$ for superior, middle and inferior frontal and superior and middle temporal areas were correlated to MoCA score ($r=0.38$, $p=0.012$).

4.4.6 Relationship between brachial pulsatility index and other variables

Brachial pulsatility index did not have statistically significant association with caPI nor with global $NIRS_{PTTp}$ for both older and younger adults ($p>0.1$). The example different spatial distribution of cerebral pulsatility in two older adults with identical blood pressure is presented in Figure 4-7. Supplementary data.

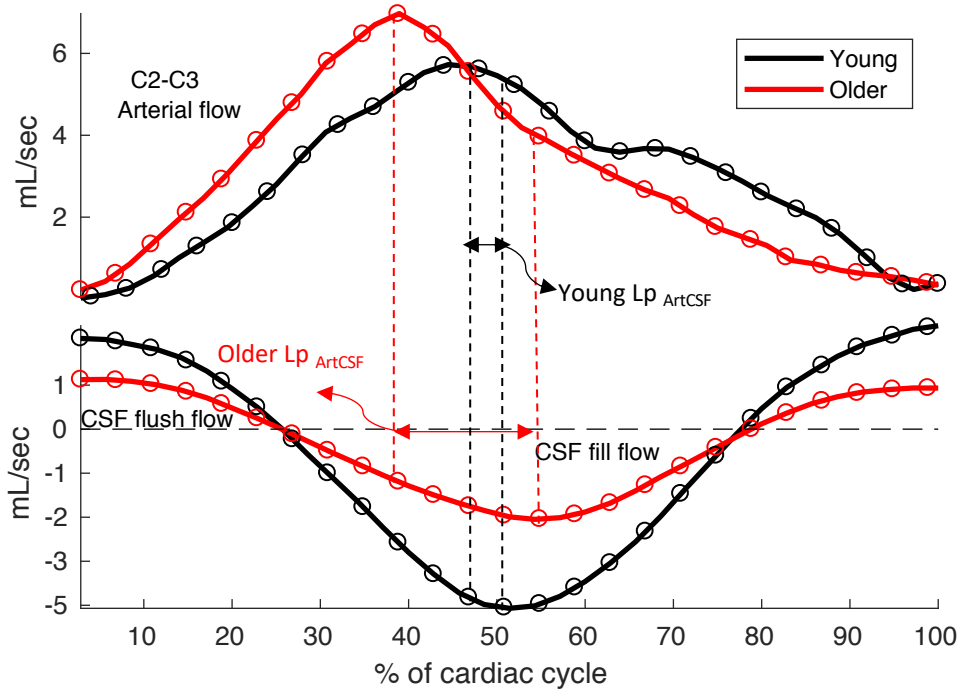

Figure 4-6 Temporal coordination between the cerebral blood and CSF flow as measured with PC-MRI at the level of the C2-C3 cervical subarachnoid space. Shown are results from for a young (21 years old) and an older (75 years old) participant. During systole, arterial inflow increases the cerebral blood volume in the cranial cavity. This higher pressure is partly compensated by flushing the CSF into the spinal canal. In the older individual, as is typical in our older group, there is a higher latency between the arterial systolic peak and the CSF flushing peak compared to the younger. The signals are shown as a function of percent of cardiac cycle in order to compare the older and younger participants. Additionally, the baseline flow is removed to have the same starting points. Negative sign in the CSF flow pulsatility is indication of direction of the flow towards spinal canal. Circles on each graph indicates twenty-five-time frames of PC-MRI.

4.5 Discussion

This study noninvasively assessed the association between regional cerebral pulsatility and regional cortical thickness in younger and older adults. By using regional pulsatility quantified from functional NIRS data, and the regional cortical thickness measured from structural MRI, the main results shows an statistically significant association between regional cortical thickness and

regional pulsatility in the frontal and temporal subregions in the older adults but not for younger adults.

4.5.1 Aging and higher cerebral pulsatility

Our data first support a statistically significant higher global cerebral pulsatility (as expressed by shorter $NIRS_{PTTp)}$ in older compared to younger adults. This results are in line with other studies reporting a higher pulsatility in the course of aging (Fabiani et al., 2014; Mitchell, 2008; Tan et al., 2017; Vlachopoulos, Charalambos, O'Rourke, 2011). Previously, Fabiani and colleagues used optical pulse measured with NIRS to index the arterial elasticity and cerebral pulse pressure in several region across the cortex (Fabiani et al., 2014). Here, we followed similar principles and used heartbeat epochs produced from oxyhemoglobin concentration oscillations in cerebral arteries and arterioles to quantify cerebral pulsatility. However, the pulsatility parameter that we used in this study was PTTp or the time it takes for the pulse wave to travel from the heart to the downstream measurement point. This time is associated to the arterial wall properties (especially cumulative rigidity of all the arteries wall along the travel path) and the length of the artery. In literature it is reported that the stiffer artery speed of propagation of the pulse for both forward and backward waves increases (Giannattasio, 2004; Weber et al., 2008, 2004) which is seen as a higher PWV (about 15%) in healthy older adults (Hughes and Parker, 2009). Here, we hypothesized that (by controlling for height of participants and also by comparing the results between young and older adults) shorter PTTp measured with NIRS is related to higher arterial stiffness. Previously, the PTTp was extracted peripherally and used as an indirect indicator of arterial stiffness (Stamatakis et al., 2013; Tang et al., 2017), sympathetic activity (Pitson et al., 1995) and endothelial function (Maltz and Budinger, 2005). It was also used as an indicator of arterial blood pressure (Bilo et al., 2015; Geddes et al., 1981).

4.5.2 Relationship between NIRS pulsatility and MRI arterial pulsatility index

In this study we explored the association between cerebral pulsatility across two modalities of NIRS and PC-MRI where a shorter PTTp (measured with NIRS) had a significant negative association with caPI (measured with PC-MRI). This association is expected since PC-MRI

provides flow pulsatility (Wåhlin et al., 2014; Zarrinkoob et al., 2016) and arterial oscillations in the NIRS signal are related to pulsatile flow by blood volume changes (Themelis et al., 2007). Themelis and colleagues discussed that in each cardiac cycle, local expansion of the arterial bed occur to accommodate a new volume of oxygenated blood changing the near-infrared light intensity (Themelis et al., 2007). Based on the hemodynamic model suggested by (Cook, 2001; Wisely and Cook, 2001), this cyclic change in the blood volume is related to pulsatile component of blood flow in the underlying vascular network where the source and detector are located.

A flow pulsatility measured with MRI is a parameter related to arterial stiffness and previously used in the literature (Peper et al., 2018). PC-MRI is shown to be highly correlated to PWV (see review article: Wentland et al., 2014). This is of interest as many epidemiological studies have reported strong association between higher PWV and arterial stiffness (O'Rourke, 2007) and microvascular damage (Poels et al., 2012; Scuteri et al., 2007; Tsao et al., 2013). Some validation studies used PC-MRI to measure PWV and compared the results to PWV measured with tonometry and reported no significant differences between two methods even in patients (Rogers et al., 2001; Suever et al., 2012). The same was true for of intravascular pressure measurements and the arterial stiffness with PC-MRI where an agreement between two methods was reported.

4.5.3 Relationship between regional NIRS pulsatility and cortical thickness

Our data indicates that in older adults the regional $NIRS_{PTTp}$ is correlated with regional cortical thickness (see Table 4-3). In the younger adults, there was a weak association between regional pulsatility and regional cortical thickness. For older adults, this association varied spatially and was lower for brain regions further from the pulse sources at the ICAs and VAs. In other words, the association between $NIRS_{PTTp}$ and cortical thickness across several regions of the brain followed a gradient, with the greatest association occurring in the regions first perfused such as; the superior and middle temporal and superior areas and the middle and inferior frontal areas (territories of ICAs, and also MCAs and its branches). Likewise, the association decreased in more downstream regions such as the postcentral and superior parietal cortex. This result is in line with other MRI studies having reported greater cortical thinning in the prefrontal (Lemaitre et al., 2012; Salat et al., 2004; Storsve et al., 2014; Thambisetty et al., 2010) and temporal (Fjell et al., 2009; McGinnis et al., 2011; Salat et al., 2004) areas than in the postcentral (Lemaitre et al., 2012; Salat et al., 2004) and supramarginal regions (Salat et al., 2004). Hypothetically, as these regions are

spatially closer to ICAs, the higher pulsatility in the ICAs as a result of aging may contribute to their selective susceptibility. It is likely that as pulse travels along the cerebral arteries further away from ICAs, the autoregulation mechanism further dampens and regulates the pulse. Hence, potentially preserving the cortical thickness in brain regions such as the postcentral and superior frontal cortices. Schubert et al. (2015) reported that arterial flow pulsatility is reduced as the blood travels from the distal to proximal segment of the vessels (Schubert et al., 2015). In another study using PC-MRI, Zarrinkoob and collogues discussed the "pulsatility damping factor" and reported that the ratio between arterial pulsatility from proximal arteries (ICAs and VAs) to distal cerebral arteries (distal segment of anterior cerebral artery) is lower for older adults compared to the younger controls (Zarrinkoob et al., 2016). They suggested that this result could be an indication of higher flow pulsatility, as a consequence of age-related arterial stiffness. Spence, (2019), reminds that the brain is perfused by cerebral large arteries and their distal branches is where the gradient of blood pressure significantly drops. He suggested that cerebral small vessel disease need to be interpreted considering these blood pressure gradients. McDonald, discussed that a high PWV (where speed of pulse transmission both forward and backward wave is higher), apart from impairing coronary perfusion, could influence endothelium in the arterioles, damage regulation of the local blood flow, leading to decline of the capillary bed and contributing to cortical thinning (McDonald, 2011). Consequently, the interpretation we provide to account for our results is not incompatible with many of the previously proposed dynamic effect of age, vascular stiffness, pulsatility and the anatomical vascular characteristics of different brain regions.

Previous studies do suggest that the penetration of the higher pulse pressure within the microcirculation could induce microvascular damage. Ex-vivo studies on human blood-brain-barrier (BBB) suggested that abnormally higher shear stress and flow pulsatility in microvasculature induces functional impairment in the endothelial cells. Such a mechanism could explain why we found an association between higher cerebral pulsatility (measured by lower $NIRS_{PTTp}$) and lower cognitive abilities in older adults as measured by the MoCA.

Much less is known about the impact of higher pulsatilty on the cerebral vasculature in healthy young individuals. Our data suggest that, in young adults, the spatial distribution of pulsatility across the cortex does not significantly change, most likely due to the higher elasticity in the cerebral arteries. For older adults, our results indicate a higher correlation between cortical thickness and $NIRS_{PTTp}$ in the temporal and frontal subregions when compared to young

individuals. It is likely that this difference between young and older adults in our data is related to the higher pulsatile stress in the aging vasculature. This result is consistent with previous research reporting that frontal and temporal subregions are more vulnerable to aging (Gordon et al., 2008). Studies on cerebral blood flow indicate that reduced cerebral blood flow is associated with impairment in the integrity of the cerebral structure, including reduced cortical thickness in frontal and temporal lobes (Alosco et al., 2014, 2013; Waldstein et al., 2008). Zimmerman and colleagues (2014), reported that regional CBF measured with MRI is associated with atrophy in the frontal and parietal subregions. Asllani et al. (2016) and Marshall et al. (2017) report a greater regional cortical thinning ipsilateral to the territories supplied by the lower carotid flow as the result of occlusion in the absence of any asymmetry in the regions unaffected by the occluded circulation. Their research suggested that the altered hemodynamics in the larger cerebral arteries is a factor contributing to downstream cortical thinning. In a similar experiment Alosco *et al*. (2014) also reported a coexisting lower cerebral blood flow and loss of cortical thickness without explicit cerebral infarction. Not only aging studies but also studies on the carriers of Alzheimer's disease genes concluded that a reduced prefrontal cortical thickness is exacerbated in those older adults (Austin et al., 2011). These literature reports suggest that a decreased CBF may be a mediator of the effect of high pulsatility on reduced cortical thickness.

4.5.4 Relationship between global cortical thickness and the latency between arterial and CSF systolic peak

In the course of aging the brain experiences global structural changes. It is plausible that these structural changes are associated with abnormalities in the mechanical properties of the cranial compartment. These abnormalities tend to alter mechanical coupling of the arterial pulsations and resulting pulsation of CSF at the skull base (Uftring et al., 2000; Wåhlin et al., 2014). Temporal coordination between the entering of the blood volume into the cerebral compartment during systole and the shifting of CSF to the spinal canal contributes to optimum intracranial pressure (Whedon and Glassey, 2009). In older adults, the increased resistance of the spinal canal could delay the compensatory shift of CSF, which temporarily amplifies the pressure in the cranium (Uftring et al., 2000). Such an explanation would be compatible with our results indicating a qualitative decrease in cervical CSF flush peak amplitude and the loss of sharpness in the peaks in the older adults. As the brain is contained within the rigid cranium, this higher intracranial pressure

tends to push the brain down towards the foramen magnum (Uftring et al., 2000) which also tends to compress the cerebral vasculature (Bragin et al., 2013), and in a feedback loop increases the resistance of cerebral vasculature to blood flow (Chiarelli et al., 2017). The decrease of global cortical thickness might be a long-term consequence of higher intracranial pressure which in turn increases arterial resistance. Such an explanation is in line with part of our results which show: (1) a higher Lp_{ArtCSF} in older adults compared to younger and (2) a statistically significant correlation between global cortical thickness and the Lp_{ArtCSF} in the older individuals.

4.5.5 The necessity of measuring cerebral pulsatility at the cortical level

Our data did not show a statistically significant association between PPG_{PTTp} and global $NIRS_{PTTp}$. This result suggests that cerebral pulsatility cannot be reliably be ascertained from current peripheral pulsatility measurements. In our study, the cerebral arterial pulsatility measured with functional NIRS depends on the location of the oxyhemoglobin wavelength systolic peak, whereas for peripheral measure of arterial pulsatility we used a commercial PPG device. In the current technology used in PPG devices, the signal is oxygen saturation (SaO_2) or relative concentration of oxyhemoglobin to total hemoglobin (sum of oxy- and deoxyhemoglobin) which alters the locations of systolic peak in the PPG data (Elgendi, 2012). Further research is needed to determine experimentally whether data on the oxyhemoglobin wavelength of PPG could have some association with cerebral pulsatility measured with oxyhemoglobin sensitive wavelength.

Our data did not show a significant association between global $NIRS_{PTTp}$ and brachial pulsatility index. This result is in accordance with Wåhlin et al. (2014), who concluded that in comparison with brachial pulsatility index, pulsatility measured from blood flow that is entering to cranial compartment is a better representative of the pulse that is transmitted to the brain. A possible explanation for such results could be a number of the unique features in the cerebral circulation compared to peripherally measured pulsatility. Moreover, the cerebral cortex is perfused from the arteries located on the surface of the cortex and penetrate via branches of the pial network. These arteries could damp pulses with cerebral arteriolar myogenic tone (Mitchell, 2008) and offer some degree of protection to the brain (O'Rourke and Hashimoto, 2007). Also arterial stiffness is not homogeneous in the body and stiffness distribution may vary from one inidvidual to another. Consequently, this study suggest that it is important to have access to measures of pulsatility

directly at the brain level rather than to extrapolate from measures of pulsatility at the peripheral level, such as brachial pulsatility.

4.5.6 Limitations

Although NIRS provides the possibility of quantifying optical measure of the spatial distribution of cerebral pulsatility on the cortex, the technology is limited by optical penetration depth, which precludes measuring pulsatility in subcortical regions. Moreover, the NIRS device used in this study was limited by the number of sources and detectors which was not sufficient to cover the entire cortex. For instance, part of superior frontal, lateral orbitofrontal, inferior temporal and occipital lobe were not fully covered by the optical array. Finally, the results presented in this paper do not conclude on causality but rather showed an association between an index related to vasculature stiffness and cortical thickness. Further studies focused on the possible causality links will be needed.

4.6 Conclusion

In summary, the data in the present study support a significant association between regional cortical thickness and cerebral pulsatility extracted from NIRS signals in the older adults. Cerebral pulsatility was quantified by PTTp which is extracted from heartbeat epochs and was correlated to caPI measured with PC-MRI. Spatially, shorter PTTp were seen in the brain regions located upstream of the major cerebral arteries; including subregions of the; temporal and frontal lobes which were concomitant with cortical thinning in those regions in the older adults compared to younger adults. Moreover, the higher Lp_{ArtCSF} or a higher delay between arterial inflow and CSF outflow systolic peak was associated with lower global cortical thickness. Our data indicated that cerebral pulsatility could not be evident from current PPG data. Our findings suggest that cerebral pulsatility indexed with functional NIRS might have the potential to provide complementary information about age-related cerebrovascular impairments.

Disclosure statement

The authors declare no actual or potential conflicts of interest.

4.7 Acknowledgment

This work was supported by an operating grant (YJ, FL, LB) from the Canadian Institute of Health Research (MOP-191272 & IOP-271115). FL is supported by the Canadian Research Chair in Optical and Vascular Imaging, LB is supported by the Mirella and Lino Saputo research chair on cardiovascular health and the prevention of cognitive decline. KP is supported by the TransMedTech Excellent Scholarship from the Montreal TransMedTech Institute.

4.8 Supplementary data

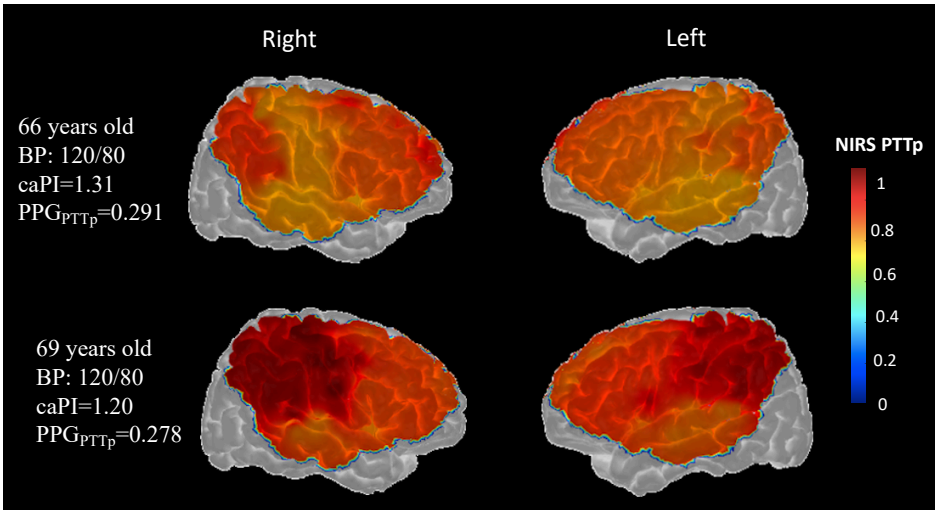

Figure 4-7 Spatial distribution of normalized cerebral pulsatility for 2 different older adults projected on the cortex. As we can see in this figure, even though the blood pressure is identical for these two individuals, the cervical blood flow pulsatility (caPI; measured with PC-MRI) and the spatial distribution of NIRS$_{PTTp}$ are different. Interestingly, 69 years old individual shows lower pulsatile stress, especially in the parietal subregions compared to 66 years old participant. Our results show that cerebral pulsatility is not always evident from measure of blood pressure in peripherally and needs to measure in the brain.

4.9 References

Aasted, C.M., Yücel, M.A., Cooper, R.J., Dubb, J., Tsuzuki, D., Becerra, L., Petkov, M.P., Borsook, D., Dan, I., Boas, D.A., 2015. Anatomical guidance for functional near-infrared spectroscopy: AtlasViewer tutorial. Neurophotonics 2, 020801. https://doi.org/10.1117/1.nph.2.2.020801

Allen, J., 2007. Photoplethysmography and its application in clinical physiological measurement. Physiol. Meas. https://doi.org/10.1088/0967-3334/28/3/R01

Allen, J., Murray, A., 2003. Age-related changes in the characteristics of the photoplethysmographic pulse shape at various body sites, in: Physiological Measurement. pp. 297–307. https://doi.org/10.1088/0967-3334/24/2/306

Alosco, M.L., Gunstad, J., Jerskey, B.A., Xu, X., Clark, U.S., Hassenstab, J., Cote, D.M., Walsh, E.G., Labbe, D.R., Hoge, R., Cohen, R.A., Sweet, L.H., 2013. The adverse effects of reduced cerebral perfusion on cognition and brain structure in older adults with cardiovascular disease. Brain Behav. 3, 626–636. https://doi.org/10.1002/brb3.171

Alosco, M.L., Gunstad, J., Xu, X., Clark, U.S., Labbe, D.R., Riskin-Jones, H.H., Terrero, G., Schwarz, N.F., Walsh, E.G., Poppas, A., Cohen, R.A., Sweet, L.H., 2014. The impact of hypertension on cerebral perfusion and cortical thickness in older adults. J. Am. Soc. Hypertens. 8, 561–570. https://doi.org/10.1016/j.jash.2014.04.002

Alperin, N.J., Lee, S.H., Loth, F., Raksin, P.B., Lichtor, T., 2000. MR-intracranial pressure (ICP): A method to measure intracranial elastance and pressure noninvasively by means of MR imaging: Baboon and human study. Radiology 217, 877–885. https://doi.org/10.1148/radiology.217.3.r00dc42877

Asllani, I., Slattery, P., Fafard, A., Pavol, M., Lazar, R.M., Marshall, R.S., 2016. Measurement of cortical thickness asymmetry in carotid occlusive disease. NeuroImage Clin. 12, 640–644. https://doi.org/10.1016/j.nicl.2016.09.013

Austin, B.P., Nair, V.A., Meier, T.B., Xu, G., Rowley, H.A., Carlsson, C.M., Johnson, S.C., Prabhakaran, V., 2011. Effects of hypoperfusion in Alzheimer's disease. Adv. Alzheimer's Dis. 2, 253–263. https://doi.org/10.3233/978-1-60750-793-2-253

Balédent, O., Henry-Feugeas, M.C.C., Idy-Peretti, I., 2001. Cerebrospinal fluid dynamics and relation with blood flow: A magnetic resonance study with semiautomated cerebrospinal fluid

segmentation. Invest. Radiol. 36, 368–377. https://doi.org/10.1097/00004424-200107000-00003

Bartzokis, G., Beckson, M., Lu, P.H., Nuechterlein, K.H., Edwards, N., Mintz, J., 2001. Age-related changes in frontal and temporal lobe volumes in men: A magnetic resonance imaging study. Arch. Gen. Psychiatry 58, 461–465. https://doi.org/10.1001/archpsyc.58.5.461

Bateman, G.A., Levi, C.R., Schofield, P., Wang, Y., Lovett, E.C., 2008. The venous manifestations of pulse wave encephalopathy: Windkessel dysfunction in normal aging and senile dementia. Neuroradiology 50, 491–497. https://doi.org/10.1007/s00234-008-0374-x

Beck, A.T., Ward, C.H., Mendelson, M., Mock, J., Erbaugh, J., 1961. An Inventory for Measuring Depression. Arch. Gen. Psychiatry 4, 561–571. https://doi.org/10.1001/archpsyc.1961.01710120031004

Benjamini, Y., Hochberg, Y., 1995. Controlling the False Discovery Rate: A Practical and Powerful Approach to Multiple Testing. J. R. Stat. Soc. Ser. B 57, 289–300. https://doi.org/10.1111/j.2517-6161.1995.tb02031.x

Bigler, E.D., Anderson, C. V, Blatter, D.D., Andersob, C. V, 2002. Temporal lobe morphology in normal aging and traumatic brain injury. AJNR. Am. J. Neuroradiol. 23, 255–66.

Bilo, G., Zorzi, C., Ochoa Munera, J.E., Torlasco, C., Giuli, V., Parati, G., 2015. Validation of the Somnotouch-NIBP noninvasive continuous blood pressure monitor according to the European Society of Hypertension International Protocol revision 2010. Blood Press. Monit. 20, 291–294. https://doi.org/10.1097/MBP.0000000000000124

Bragin, D.E., Bush, R.C., Nemoto, E.M., 2013. Effect of cerebral perfusion pressure on cerebral cortical microvascular shunting at high intracranial pressure in rats. Stroke 44, 177–181. https://doi.org/10.1161/STROKEAHA.112.668293

Bude, R.O., Rubin, J.M., 1999. Relationship between the resistive index and vascular compliance and resistance. Radiology 211, 411–417. https://doi.org/10.1148/radiology.211.2.r99ma48411

C.S., N., R.W., B., 1984. Renal artery flow velocity analysis: A sensitive measure of experimental and clinical renovascular resistance. J. Surg. Res.

Chiarelli, A.M., Fletcher, M.A., Tan, C.H., Low, K.A., Maclin, E.L., Zimmerman, B., Kong, T., Gorsuch, A., Gratton, G., Fabiani, M., 2017. Individual differences in regional cortical volumes across the life span are associated with regional optical measures of arterial

elasticity. Neuroimage 162, 199–213. https://doi.org/10.1016/j.neuroimage.2017.08.064

Cook, L.B., 2001. Extracting arterial flow waveforms from pulse oximeter waveforms apparatus. Anaesthesia 56, 551–5. https://doi.org/10.1046/j.1365-2044.2001.01986.x

Dale, A.M., Fischl, B., Sereno, M.I., 1999. Cortical surface-based analysis: I. Segmentation and surface reconstruction. Neuroimage 9, 179–194. https://doi.org/10.1006/nimg.1998.0395

Del Zoppo, G.J., Mabuchi, T., 2003. Cerebral microvessel responses to focal ischemia. J. Cereb. Blood Flow Metab. https://doi.org/10.1097/01.WCB.0000078322.96027.78

DePaola, N., Phelps, J.E., Florez, L., Keese, C.R., Minnear, F.L., Giaever, I., Vincent, P., 2001. Electrical impedance of cultured endothelium under fluid flow. Ann. Biomed. Eng. 29, 648–656. https://doi.org/10.1114/1.1385811

Desikan, R.S., Ségonne, F., Fischl, B., Quinn, B.T., Dickerson, B.C., Blacker, D., Buckner, R.L., Dale, A.M., Maguire, R.P., Hyman, B.T., Albert, M.S., Killiany, R.J., 2006. An automated labeling system for subdividing the human cerebral cortex on MRI scans into gyral based regions of interest. Neuroimage 31, 968–980. https://doi.org/10.1016/j.neuroimage.2006.01.021

Du, A.T., Schuff, N., Chao, L.L., Kornak, J., Jagust, W.J., Kramer, J.H., Reed, B.R., Miller, B.L., Norman, D., Chui, H.C., Weiner, M.W., 2006. Age effects on atrophy rates of entorhinal cortex and hippocampus. Neurobiol. Aging 27, 733–740. https://doi.org/10.1016/j.neurobiolaging.2005.03.021

Efron, B., Tibshirani, R., 1986. Bootstrap methods for standard errors, confidence intervals, and other measures of statistical accuracy. Stat. Sci. 1, 54–75. https://doi.org/10.1214/ss/1177013815

Eggebrecht, A.T., Ferradal, S.L., Robichaux-Viehoever, A., Hassanpour, M.S., Dehghani, H., Snyder, A.Z., Hershey, T., Culver, J.P., 2014. Mapping distributed brain function and networks with diffuse optical tomography. Nat. Photonics 8, 448–454. https://doi.org/10.1038/nphoton.2014.107

Elgendi, M., 2012. On the Analysis of Fingertip Photoplethysmogram Signals. Curr. Cardiol. Rev. 8, 14–25. https://doi.org/10.2174/157340312801215782

Fabiani, M., Low, K.A., Tan, C.H., Zimmerman, B., Fletcher, M.A., Schneider-Garces, N., Maclin, E.L., Chiarelli, A.M., Sutton, B.P., Gratton, G., 2014. Taking the pulse of aging: Mapping pulse pressure and elasticity in cerebral arteries with optical methods.

Psychophysiology 51, 1072–1088. https://doi.org/10.1111/psyp.12288

Fischl, B., Salat, D.H., Busa, E., Albert, M., Dieterich, M., Haselgrove, C., Van Der Kouwe, A., Killiany, R., Kennedy, D., Klaveness, S., Montillo, A., Makris, N., Rosen, B., Dale, A.M., 2002. Whole brain segmentation: Automated labeling of neuroanatomical structures in the human brain. Neuron 33, 341–355. https://doi.org/10.1016/S0896-6273(02)00569-X

Fjell, A.M., Westlye, L.T., Amlien, I., Espeseth, T., Reinvang, I., Raz, N., Agartz, I., Salat, D.H., Greve, D.N., Fischl, B., Dale, A.M., Walhovd, K.B., 2009. High consistency of regional cortical thinning in aging across multiple samples. Cereb. Cortex 19, 2001–2012. https://doi.org/10.1093/cercor/bhn232

Gallagher, M., Koh, M.T., 2011. Episodic memory on the path to Alzheimer's disease. Curr. Opin. Neurobiol. https://doi.org/10.1016/j.conb.2011.10.021

Garcia-Polite, F., Martorell, J., Del Rey-Puech, P., Melgar-Lesmes, P., O'Brien, C.C., Roquer, J., Ois, A., Principe, A., Edelman, E.R., Balcells, M., 2017. Pulsatility and high shear stress deteriorate barrier phenotype in brain microvascular endothelium. J. Cereb. Blood Flow Metab. 37, 2614–2625. https://doi.org/10.1177/0271678X16672482

Geddes, L.A., Voelz, M.H., Babbs, C.F., Bourland, J.D., Tacker, W.A., 1981. Pulse Transit Time as an Indicator of Arterial Blood Pressure. Psychophysiology 18, 71–74. https://doi.org/10.1111/j.1469-8986.1981.tb01545.x

Giannattasio, C., 2004. Arterial stiffness. Curr. Hypertens. Rep. https://doi.org/10.1007/s11906-004-0047-z

Gizdulich, P., 1984. On a non-invasive evaluation of pulse wave velocity in human peripheral arteries. Clin. Phys. Physiol. Meas. 5, 33–6.

Gómez García, M.T., Troncoso Acevedo, M.F., Rodriguez Guzmán, M., Alegre de Montaner, R., Fernández Fernández, B., Del Río Camacho, G., González-Mangado, N., 2014. Can pulse transit time be useful for detecting hypertension in patients in a sleep unit? Arch. Bronconeumol. 50, 278–284. https://doi.org/10.1016/j.arbr.2014.05.001

Good, C.D., Johnsrude, I.S., Ashburner, J., Henson, R.N.A., Friston, K.J., Frackowiak, R.S.J., 2001. A voxel-based morphometric study of ageing in 465 normal adult human brains. Neuroimage 14, 21–36. https://doi.org/10.1006/nimg.2001.0786

Gordon, B.A., Rykhlevskaia, E.I., Brumback, C.R., Lee, Y., Elavsky, S., Konopack, J.F., McAuley, E., Kramer, A.F., Colcombe, S., Gratton, G., Fabiani, M., 2008. Neuroanatomical

correlates of aging, cardiopulmonary fitness level, and education. Psychophysiology 45, 825–838. https://doi.org/10.1111/j.1469-8986.2008.00676.x

Havlik, R.J., Foley, D.J., Sayer, B., Masaki, K., White, L., Launer, L.J., 2002. Variability in midlife systolic blood pressure is related to late-life brain white matter lesions: The Honolulu-Asia aging study. Stroke 33, 26–30. https://doi.org/10.1161/hs0102.101890

Henry-Feugeas, M.C., Roy, C., Baron, G., Schouman-Claeys, E., 2009. Leukoaraiosis and pulse-wave encephalopathy: Observations with phase-contrast MRI in mild cognitive impairment. J. Neuroradiol. 36, 212–218. https://doi.org/10.1016/j.neurad.2009.01.003

Henry Feugeas, M.C., De Marco, G., Peretti, I.I., Godon-Hardy, S., Fredy, D., Claeys, E.S., 2005. Age-related cerebral white matter changes and pulse-wave encephalopathy: Observations with three-dimensional MRI. Magn. Reson. Imaging 23, 929–937. https://doi.org/10.1016/j.mri.2005.09.002

Hughes, A.D., Parker, K.H., 2009. Forward and backward waves in the arterial system: Impedance or wave intensity analysis? Med. Biol. Eng. Comput. 47, 207–210. https://doi.org/10.1007/s11517-009-0444-1

Huppert, T.J., Diamond, S.G., Franceschini, M.A., Boas, D.A., 2009. HomER: A review of time-series analysis methods for near-infrared spectroscopy of the brain. Appl. Opt. 48. https://doi.org/10.1364/AO.48.00D280

Itoh, Y., Suzuki, N., 2012. Control of brain capillary blood flow. J. Cereb. Blood Flow Metab. https://doi.org/10.1038/jcbfm.2012.5

Jefferson, A.L., Cambronero, F.E., Liu, D., Moore, E.E., Neal, J.E., Terry, J.G., Nair, S., Pechman, K.R., Rane, S., Davis, L.T., Gifford, K.A., Hohman, T.J., Bell, S.P., Wang, T.J., Beckman, J.A., Carr, J.J., 2018. Higher aortic stiffness is related to lower cerebral blood flow and preserved cerebrovascular reactivity in older adults. Circulation 138, 1951–1962. https://doi.org/10.1161/CIRCULATIONAHA.118.032410

Jensen, A.R., Rohwer, W.D., 1966. Not to be reproduc:d by photoprht or microfilm without written permission from the publiskt T'I-IE STRCOP COLOR-WORD TEST: A REVIEW 1 was later, Acta Psychologica. North-Holland Publishing Co.

Jochemsen, H.M., Muller, M., Visseren, F.L., Scheltens, P., Vincken, K.L., Mali, W.P., Van Der Graaf, Y., Geerlings, M.I., 2013. Blood pressure and progression of brain atrophy the SMART-MR study. JAMA Neurol. 70, 1046–1053.

https://doi.org/10.1001/jamaneurol.2013.217

Kern, K.C., Wright, C.B., Bergfield, K.L., Fitzhugh, M.C., Chen, K., Moeller, J.R., Nabizadeh, N., Elkind, M.S.V., Sacco, R.L., Stern, Y., DeCarli, C.S., Alexander, G.E., 2017. Blood pressure control in aging predicts cerebral atrophy related to small-vessel white matter lesions. Front. Aging Neurosci. 9. https://doi.org/10.3389/fnagi.2017.00132

Knopman, D.S., 2006. Dementia and cerebrovascular disease. Mayo Clin. Proc. https://doi.org/10.4065/81.2.223

Krause, F., Lindemann, O., 2014. Expyriment: A Python library for cognitive and neuroscientific experiments. Behav. Res. Methods 46, 416–428. https://doi.org/10.3758/s13428-013-0390-6

Lemaitre, H., Goldman, A.L., Sambataro, F., Verchinski, B.A., Meyer-Lindenberg, A., Weinberger, D.R., Mattay, V.S., 2012. Normal age-related brain morphometric changes: Nonuniformity across cortical thickness, surface area and gray matter volume? Neurobiol. Aging 33, 617.e1-617.e9. https://doi.org/10.1016/j.neurobiolaging.2010.07.013

Leritz, E.C., Salat, D.H., Williams, V.J., Schnyer, D.M., Rudolph, J.L., Lipsitz, L., Fischl, B., McGlinchey, R.E., Milberg, W.P., 2011. Thickness of the human cerebral cortex is associated with metrics of cerebrovascular health in a normative sample of community dwelling older adults. Neuroimage 54, 2659–2671. https://doi.org/10.1016/j.neuroimage.2010.10.050

Maltz, J.S., Budinger, T.F., 2005. Evaluation of arterial endothelial function using transit times of artificially induced pulses. Physiol. Meas. 26, 293–307. https://doi.org/10.1088/0967-3334/26/3/013

Marshall, R.S., Asllani, I., Pavol, M.A., Cheung, Y.-K., Lazar, R.M., 2017. Altered cerebral hemodyamics and cortical thinning in asymptomatic carotid artery stenosis. https://doi.org/10.1371/journal.pone.0189727

McDonald, D.A., 2011. Blood flow in arteries. EDWARD ARNOLD PUBL. https://doi.org/10.1146/annurev.fluid.29.1.399

McGinnis, S.M., Brickhouse, M., Pascual, B., Dickerson, B.C., 2011. Age-Related changes in the thickness of cortical zones in humans. Brain Topogr. 24, 279–291. https://doi.org/10.1007/s10548-011-0198-6

Mitchell, G.F., 2018. Aortic stiffness, pressure and flow pulsatility, and target organ damage. J. Appl. Physiol. https://doi.org/10.1152/japplphysiol.00108.2018

Mitchell, G.F., 2015. Cerebral small vessel disease: Role of aortic stiffness and pulsatile

hemodynamics. J. Hypertens. https://doi.org/10.1097/HJH.0000000000000717

Mitchell, Gary F, 2008. Effects of central arterial aging on the structure and function of the peripheral vasculature: Implications for end-organ damage. J. Appl. Physiol. https://doi.org/10.1152/japplphysiol.90549.2008

Mitchell, Gary F., 2008. Effects of central arterial aging on the structure and function of the peripheral vasculature: Implications for end-organ damage. J. Appl. Physiol. https://doi.org/10.1152/japplphysiol.90549.2008

Mitchell, G.F., Van Buchem, M.A., Sigurdsson, S., Gotal, J.D., Jonsdottir, M.K., Kjartansson, Ó., Garcia, M., Aspelund, T., Harris, T.B., Gudnason, V., Launer, L.J., 2011. Arterial stiffness, pressure and flow pulsatility and brain structure and function: The Age, Gene/Environment Susceptibility-Reykjavik Study. Brain 134, 3398–3407. https://doi.org/10.1093/brain/awr253

Mok, V., Ding, D., Fu, J., Xiong, Y., Chu, W.W.C., Wang, D., Abrigo, J.M., Yang, J., Wong, A., Zhao, Q., Guo, Q., Hong, Z., Wong, K.S., 2012. Transcranial Doppler ultrasound for screening cerebral small vessel disease: a community study. Stroke 43, 2791–3. https://doi.org/10.1161/STROKEAHA.112.665711

Nasreddine, Z.S., Phillips, N.A., Bédirian, V., Charbonneau, S., Whitehead, V., Collin, I., Cummings, J.L., Chertkow, H., 2005. The Montreal Cognitive Assessment, MoCA: A brief screening tool for mild cognitive impairment. J. Am. Geriatr. Soc. 53, 695–699. https://doi.org/10.1111/j.1532-5415.2005.53221.x

O'connell, J.E.A., 1943. The vascular factor tn intracranial pressure and the maintenance of the cerebrospinal fluid circulation. Brain 66, 204–228. https://doi.org/10.1093/brain/66.3.204

O'Rourke, M.F., 2007. Arterial aging: Pathophysiological principles. Vasc. Med. https://doi.org/10.1177/1358863X07083392

O'Rourke, M.F., Hashimoto, J., 2007. Mechanical factors in arterial aging: a clinical perspective. J. Am. Coll. Cardiol. 50, 1–13. https://doi.org/10.1016/j.jacc.2006.12.050

Obisesan, T.O., Obisesan, O.A., Martins, S., Alamgir, L., Bond, V., Maxwell, C., Gillum, R.F., 2008. High blood pressure, hypertension, and high pulse pressure are associated with poorer cognitive function in persons aged 60 and older: The Third National Health and Nutrition Examination Survey. J. Am. Geriatr. Soc. 56, 501–509. https://doi.org/10.1111/j.1532-5415.2007.01592.x

Ohtake, M., Morino, S., Kaidoh, T., Inoué, T., 2004. Three-dimensional structural changes in

cerebral microvessels after transient focal cerebral ischemia in rats: Scanning electron microscopic study of corrosion casts. Neuropathology 24, 219–227. https://doi.org/10.1111/j.1440-1789.2004.00560.x

Oldfield, R.C., 1971. The assessment and analysis of handedness: The Edinburgh inventory. Neuropsychologia 9, 97–113. https://doi.org/10.1016/0028-3932(71)90067-4

Pasha, E.P., Kaur, S.S., Gonzales, M.M., Machin, D.R., Kasischke, K., Tanaka, H., Haley, A.P., 2015. Vascular function, cerebral cortical thickness, and cognitive performance in middle-aged hispanic and non-hispanic caucasian adults. J. Clin. Hypertens. 17, 306–312. https://doi.org/10.1111/jch.12512

Peper, E.S., Strijkers, G.J., Gazzola, K., Potters, W. V., Motaal, A.G., Luirink, I.K., Hutten, B.A., Wiegman, A., Van Ooij, P., Van Den Born, B.J.H., Nederveen, A.J., Coolen, B.F., 2018. Regional assessment of carotid artery pulse wave velocity using compressed sensing accelerated high temporal resolution 2D CINE phase contrast cardiovascular magnetic resonance. J. Cardiovasc. Magn. Reson. 20, 86. https://doi.org/10.1186/s12968-018-0499-y

Pitson, D.J., Sandell, A., Van Den Hout, R., Stradling, J.R., 1995. Use of pulse transit time as a measure of inspiratory effort in patients with obstructive sleep apnoea. Eur. Respir. J. 8, 1669–1674. https://doi.org/10.1183/09031936.95.08101669

Poels, M.M.F., Zaccai, K., Verwoert, G.C., Vernooij, M.W., Hofman, A., Van Der Lugt, A., Witteman, J.C.M., Breteler, M.M.B., Mattace-Raso, F.U.S., Ikram, M.A., 2012. Arterial stiffness and cerebral small vessel disease: The rotterdam scan study. Stroke 43, 2637–2642. https://doi.org/10.1161/STROKEAHA.111.642264

Pollonini, L., Olds, C., Abaya, H., Bortfeld, H., Beauchamp, M.S., Oghalai, J.S., 2014. Auditory cortex activation to natural speech and simulated cochlear implant speech measured with functional near-infrared spectroscopy. Hear. Res. 309, 84–93. https://doi.org/10.1016/j.heares.2013.11.007

Raz, N., Ghisletta, P., Rodrigue, K.M., Kennedy, K.M., Lindenberger, U., 2010. Trajectories of brain aging in middle-aged and older adults: Regional and individual differences. Neuroimage 51, 501–511. https://doi.org/10.1016/j.neuroimage.2010.03.020

Rey Auditory Verbal Learning Test (RAVLT) [WWW Document], 1964. URL https://www.wpspublish.com/ravlt-rey-auditory-verbal-learning-test (accessed 2.8.20).

Rogers, W.J., Hu, Y.L., Coast, D., Vido, D.A., Kramer, C.M., Pyeritz, R.E., Reichek, N., 2001.

Age-associated changes in regional aortic pulse wave velocity. J. Am. Coll. Cardiol. 38, 1123–1129. https://doi.org/10.1016/S0735-1097(01)01504-2

Salat, D.H., Buckner, R.L., Snyder, A.Z., Greve, D.N., Desikan, R.S.R., Busa, E., Morris, J.C., Dale, A.M., Fischl, B., 2004. Thinning of the cerebral cortex in aging. Cereb. Cortex 14, 721–730. https://doi.org/10.1093/cercor/bhh032

Saritas, T., Greber, R., Venema, B., Puelles, V.G., Ernst, S., Blazek, V., Floege, J., Leonhardt, S., Schlieper, G., 2019. Non-invasive evaluation of coronary heart disease in patients with chronic kidney disease using photoplethysmography. Clin. Kidney J. 12, 538–545. https://doi.org/10.1093/ckj/sfy135

Schubert, T., Pansini, M., Bieri, O., Stippich, C., Wetzel, S., Schaedelin, S., Von Hessling, A., Santini, F., 2015. Attenuation of blood flow pulsatility along the Atlas slope: A physiologic property of the distal vertebral artery? Am. J. Neuroradiol. 36, 562–567. https://doi.org/10.3174/ajnr.A4148

Scuteri, A., Tesauro, M., Appolloni, S., Preziosi, F., Brancati, A.M., Volpe, M., 2007. Arterial stiffness as an independent predictor of longitudinal changes in cognitive function in the older individual. J. Hypertens. 25, 1035–1040. https://doi.org/10.1097/HJH.0b013e3280895b55

Smith, R.P., Argod, J., Pépin, J.L., Lévy, P.A., 1999. Pulse transit time: An appraisal of potential clinical applications. Thorax. https://doi.org/10.1136/thx.54.5.452

Smith, S.M., Jenkinson, M., Woolrich, M.W., Beckmann, C.F., Behrens, T.E.J., Johansen-Berg, H., Bannister, P.R., De Luca, M., Drobnjak, I., Flitney, D.E., Niazy, R.K., Saunders, J., Vickers, J., Zhang, Y., De Stefano, N., Brady, J.M., Matthews, P.M., 2004. Advances in functional and structural MR image analysis and implementation as FSL, in: NeuroImage. https://doi.org/10.1016/j.neuroimage.2004.07.051

Spence, J David, 2019. Blood pressure gradients in the brain: Their importance to understanding pathogenesis of cerebral small vessel disease. Brain Sci. https://doi.org/10.3390/brainsci9020021

Spence, J. David, 2019. The Importance of Blood Pressure Gradients in the Brain: Cerebral Small Vessel Disease. JAMA Neurol. https://doi.org/10.1001/jamaneurol.2018.4627

Stamatakis, E., Hamer, M., O'Donovan, G., Batty, G.D., Kivimaki, M., 2013. A non-exercise testing method for estimating cardiorespiratory fitness: associations with all-cause and cardiovascular mortality in a pooled analysis of eight population-based cohorts. Eur. Heart J.

34, 750–758. https://doi.org/10.1093/eurheartj/ehs097

Stone, J., Johnstone, D.M., Mitrofanis, J., O'Rourke, M., 2015. The mechanical cause of age-related dementia (Alzheimer's Disease): The brain is destroyed by the pulse. J. Alzheimer's Dis. https://doi.org/10.3233/JAD-141884

Stoquart-ElSankari, S., Balédent, O., Gondry-Jouet, C., Makki, M., Godefroy, O., Meyer, M.E., 2007. Aging effects on cerebral blood and cerebrospinal fluid flows. J. Cereb. Blood Flow Metab. 27, 1563–1572. https://doi.org/10.1038/sj.jcbfm.9600462

Storsve, A.B., Fjell, A.M., Tamnes, C.K., Westlye, L.T., Overbye, K., Aasland, H.W., Walhovd, K.B., 2014. Differential longitudinal changes in cortical thickness, surface area and volume across the adult life span: Regions of accelerating and decelerating change. J. Neurosci. 34, 8488–8498. https://doi.org/10.1523/JNEUROSCI.0391-14.2014

Suever, J.D., Oshinski, J., Rojas-Campos, E., Huneycutt, D., Cardarelli, F., Stillman, A.E., Raggi, P., 2012. Reproducibility of pulse wave velocity measurements with phase contrast magnetic resonance and applanation tonometry. Int. J. Cardiovasc. Imaging 28, 1141–1146. https://doi.org/10.1007/s10554-011-9929-8

Tan, C.H., Low, K.A., Chiarelli, A.M., Fletcher, M.A., Navarra, R., Burzynska, A.Z., Kong, T.S., Zimmerman, B., Maclin, E.L., Sutton, B.P., Gratton, G., Fabiani, M., 2019. Optical measures of cerebral arterial stiffness are associated with white matter signal abnormalities and cognitive performance in normal aging. Neurobiol. Aging. https://doi.org/10.1016/j.neurobiolaging.2019.08.004

Tan, C.H., Low, K.A., Kong, T., Fletcher, M.A., Zimmerman, B., MacLin, E.L., Chiarelli, A.M., Gratton, G., Fabiani, M., 2017. Mapping cerebral pulse pressure and arterial compliance over the adult lifespan with optical imaging. PLoS One 12. https://doi.org/10.1371/journal.pone.0171305

Tang, Z., Tamura, T., Sekine, M., Huang, M., Chen, W., Yoshida, M., Sakatani, K., Kobayashi, H., Kanaya, S., 2017. A Chair-Based Unobtrusive Cuffless Blood Pressure Monitoring System Based on Pulse Arrival Time. IEEE J. Biomed. Heal. Informatics 21, 1194–1205. https://doi.org/10.1109/JBHI.2016.2614962

Thambisetty, M., Wan, J., Carass, A., An, Y., Prince, J.L., Resnick, S.M., 2010. Longitudinal changes in cortical thickness associated with normal aging. Neuroimage 52, 1215–1223. https://doi.org/10.1016/j.neuroimage.2010.04.258

Themelis, G., D'Arceuil, H., Diamond, S.G., Thaker, S., Huppert, T.J., Boas, D.A., Franceschini, M.A., 2007. Near-infrared spectroscopy measurement of the pulsatile component of cerebral blood flow and volume from arterial oscillations. J. Biomed. Opt. 12, 014033. https://doi.org/10.1117/1.2710250

Toth, P., Csiszar, A., Tucsek, Z., Sosnowska, D., Gautam, T., Koller, A., Schwartzman, M.L., Sonntag, W.E., Ungvari, Z., 2013. Role of 20-HETE, TRPC channels, and BKCa in dysregulation of pressure-induced Ca2+ signaling and myogenic constriction of cerebral arteries in aged hypertensive mice. Am. J. Physiol. - Hear. Circ. Physiol. 305, H1698–H1708. https://doi.org/10.1152/ajpheart.00377.2013

Tsao, C.W., Seshadri, S., Beiser, A.S., Westwood, A.J., DeCarli, C., Au, R., Himali, J.J., Hamburg, N.M., Vita, J.A., Levy, D., Larson, M.G., Benjamin, E.J., Wolf, P.A., Vasan, R.S., Mitchell, G.F., 2013. Relations of arterial stiffness and endothelial function to brain aging in the community. Neurology 81, 984–991. https://doi.org/10.1212/WNL.0b013e3182a43e1c

Uangpairoj, P., Shibata, M., 2013. Evaluation of vascular wall elasticity of human digital arteries using alternating current-signal photoplethysmography. Vasc. Health Risk Manag. 9, 283–295. https://doi.org/10.2147/vhrm.s43784

Uftring, S.J., Chu, D., Alperin, N., Levin, D.N., 2000. The mechanical state of intracranial tissues in elderly subjects studied by imaging CSF and brain pulsations. Magn. Reson. Imaging 18, 991–6. https://doi.org/10.1016/s0730-725x(00)00195-8

Van Dijk, E.J., Breteler, M.M.B., Schmidt, R., Berger, K., Nilsson, L.G., Oudkerk, M., Pajak, A., Sans, S., De Ridder, M., Dufouil, C., Fuhrer, R., Giampaoli, S., Launer, L.J., Hofman, A., 2004. The association between blood pressure, hypertension, and cerebral white matter lesions: Cardiovascular determinants of dementia study. Hypertension 44, 625–630. https://doi.org/10.1161/01.HYP.0000145857.98904.20

Venema, B., Blanik, N., Blazek, V., Gehring, H., Opp, A., Leonhardt, S., 2012. Advances in reflective oxygen saturation monitoring with a novel in-ear sensor system: Results of a human hypoxia study. IEEE Trans. Biomed. Eng. 59, 2003–2010. https://doi.org/10.1109/TBME.2012.2196276

Vlachopoulos, Charalambos, Michael O'Rourke, and W.W.N., 2011. McDonald's blood flow in arteries: theoretical, experimental and clinical principles. CRC press.

Vuorinen, M., Kåreholt, I., Julkunen, V., Spulber, G., Niskanen, E., Paajanen, T., Soininen, H.,

Kivipelto, M., Solomon, A., 2013. Changes in vascular factors 28 years from midlife and late-life cortical thickness. Neurobiol. Aging 34, 100–109. https://doi.org/10.1016/j.neurobiolaging.2012.07.014

Wagshul, M.E., Eide, P.K., Madsen, J.R., 2011. The pulsating brain: A review of experimental and clinical studies of intracranial pulsatility. Fluids Barriers CNS. https://doi.org/10.1186/2045-8118-8-5

Wåhlin, A., Ambarki, K., Birgander, R., Alperin, N., Malm, J., Eklund, A., 2010. Assessment of craniospinal pressure-volume indices. Am. J. Neuroradiol. 31, 1645–1650. https://doi.org/10.3174/ajnr.A2166

Wåhlin, A., Ambarki, K., Birgander, R., Malm, J., Eklund, A., 2014. Intracranial pulsatility is associated with regional brain volume in elderly individuals. Neurobiol. Aging 35, 365–372. https://doi.org/10.1016/j.neurobiolaging.2013.08.026

Wåhlin, A., Ambarki, K., Hauksson, J., Birgander, R., Malm, J., Eklund, A., 2012. Phase contrast MRI Quantification of pulsatile volumes of brain arteries, veins, and cerebrospinal fluids compartments: Repeatability and physiological interactions. J. Magn. Reson. Imaging 35, 1055–1062. https://doi.org/10.1002/jmri.23527

Waldstein, S.R., Rice, S.C., Thayer, J.F., Najjar, S.S., Scuteri, A., Zonderman, A.B., 2008. Pulse pressure and pulse wave velocity are related to cognitive decline in the Baltimore Longitudinal Study of Aging. Hypertens. (Dallas, Tex. 1979) 51, 99–104. https://doi.org/10.1161/HYPERTENSIONAHA.107.093674

Weber, T., Auer, J., O'Rourke, M.F., Kvas, E., Lassnig, E., Berent, R., Eber, B., 2004. Arterial Stiffness, Wave Reflections, and the Risk of Coronary Artery Disease. Circulation 109, 184–189. https://doi.org/10.1161/01.CIR.0000105767.94169.E3

Weber, T., O'Rourke, M.F., Ammer, M., Kvas, E., Punzengruber, C., Eber, B., 2008. Arterial Stiffness and Arterial Wave Reflections Are Associated With Systolic and Diastolic Function in Patients With Normal Ejection Fraction. Am. J. Hypertens. 21, 1194–1202. https://doi.org/10.1038/ajh.2008.277

Wechsler, D., 1997. Wechsler adult intelligence scale - Third Edition (WAIS-III). San Antonio 1–3.

Wentland, A.L., Grist, T.M., Wieben, O., 2014. Review of MRI-based measurements of pulse wave velocity: a biomarker of arterial stiffness. Cardiovasc. Diagn. Ther. 4, 193–206.

https://doi.org/10.3978/j.issn.2223-3652.2014.03.04

Whedon, J.M., Glassey, D., 2009. Cerebrospinal fluid stasis and its clinical significance. Altern. Ther. Health Med.

Wilson, C.R.E., Gaffan, D., Browning, P.G.F., Baxter, M.G., 2010. Functional localization within the prefrontal cortex: Missing the forest for the trees? Trends Neurosci. 33, 533–540. https://doi.org/10.1016/j.tins.2010.08.001

Wisely, N.A., Cook, L.B., 2001. Arterial flow waveforms from pulse oximetry compared with measured Doppler flow waveforms apparatus. Anaesthesia 56, 556–61. https://doi.org/10.1046/j.1365-2044.2001.01987.x

Yesavage, J.A., Brink, T.L., Rose, T.L., Lum, O., Huang, V., Adey, M., Leirer, V.O., 1982. Development and validation of a geriatric depression screening scale: A preliminary report. J. Psychiatr. Res. 17, 37–49. https://doi.org/10.1016/0022-3956(82)90033-4

Zarrinkoob, L., Ambarki, K., Wahlin, A., Birgander, R., Carlberg, B., Eklund, A., Malm, J., 2016. Aging alters the dampening of pulsatile blood flow in cerebral arteries. J. Cereb. Blood Flow Metab. 36, 1519–1527. https://doi.org/10.1177/0271678X16629486

Zimmerman, B., Sutton, B.P., Low, K.A., Fletcher, M.A., Tan, C.H., Schneider-Garces, N., Li, Y., Ouyang, C., Maclin, E.L., Gratton, G., Fabiani, M., 2014. Cardiorespiratory fitness mediates the effects of aging on cerebral blood flow. Front. Aging Neurosci. 6. https://doi.org/10.3389/fnagi.2014.00059

CHAPTER 5 ARTICLE 2: CORONARY ARTERY DISEASE AND ITS IMPACT ON THE PULSATILE BRAIN: A FUNCTIONAL NIRS STUDY

This article is submitted to Human Brain Mapping.

Hanieh Mohammadi [1,2], Thomas Vincent [2], Ke Peng[3,4], Anil Nigam[5,8], Mathieu Gayda[5,7,8], Sarah Fraser[6], Yves Joanette [2,7], Frédéric Lesage [1,5,7], and Louis Bherer [2,5,8]

[1] Laboratory of Optical and Molecular Imaging, Biomedical Engineering Institute, Polytechnique Montreal, Montreal, Quebec, Canada

[2] Research Center, Institut Universitaire de Geriatrie de Montreal, Montreal, Quebec, Canada

[3] Center for Pain and the Brain, Boston Children's Hospital and Harvard Medical School, Boston, Massachusetts, USA

[4] Research Center, University of Montreal Health Centre, Montreal, Quebec, Canada

[5] Research Center, Montreal Heart Institute, Montreal, Quebec, Canada

[6] Interdisciplinary School of Health Sciences, Faculty of Health Sciences, University of Ottawa, Ottawa, Canada

[7] Faculty of Medicine, University of Montreal, Montreal, Quebec, Canada

[8] Department of Medicine, University of Montreal, Montreal, Quebec, Canada

5.1 Abstract

A chronic higher cerebral pulsatility may abnormally stress cerebral microcirculation, leading to distal macro- and microvascular lesions which contribute to poor brain aging and dementia. Cerebral pulsatility is often translated to a single global index which reflects the elasticity of the arterial wall in the large cerebral arteries. However, the spatial distribution of cerebral pulsatility in the cortex may represent the vulnerability of the underlying vascular network and correlates spatially with damage. This study determined the downstream impact of cardiovascular degradation in participants with low and high cardiovascular risk factors (LCVRF and HCVRF) and coronary artery disease (CAD) on the spatial distribution of cerebral pulsatility across the cortex. Furthermore, low-intensity, short-duration walking was used to study the impact of a brief cardiovascular stress on the dynamics of cerebral pulsatility. A total of 60 elderly participants,

aged 57-79, were enrolled in the study. Participants were grouped according to LCVRF, HCVRF and CAD. Participants were asked to walk freely on a gym track at a self-selected pace while a near-infrared spectroscopy (NIRS) device was recording cerebral pulse simultaneously. Results indicate that in comparison to LCVRF and HCVRF groups, those with CAD showed higher cerebral pulse amplitude at rest. Further, after short-duration walking, there was a significant decrease in cerebral pulse amplitude and diastolic reflection in all groups. Spatially, channel-wise comparisons of cerebral pulse amplitude indicated alterations of cerebral pulse amplitude after short-duration walking in the supplementary motor areas in all groups. This effect was extended to more anterior prefrontal areas for the CAD versus LCVRF and CAD versus HCVRF groups. These findings suggest that cerebral pulse amplitude measured with NIRS may eventually provide complimentary information on cerebrovascular impairments associated with CAD.

Keywords Near-infrared spectroscopy, cerebral pulsatility, cardiovascular risk factors, coronary artery disease, walking, older adults

5.2 Introduction

In a young, healthy individual, the elastic arteries distend optimally during systole (acting as an elastic reservoir) and recoil during diastole. This coordinated action releases the potential energy of the arterial wall and conducts the blood through the artery and reduces the pulsatile fluctuations in blood pressure that are induced in each cardiac cycle. The end sites where damping of the pulsatile flow occurs are the cerebral arterioles, which by vasodilation and vasoconstriction adjust and regulate blood flow as it travels to the cerebral capillaries (Mitchell, 2015; Mitchell et al., 2011). Thereby, despite the pulsatile nature of the flow in the central arteries, there is a mostly steady flow during both systole and diastole in brain capillaries (O'Rourke, 2007; Vlachopoulos, Charalambos, Michael O'Rourke, 2011). Healthy brain metabolism and microvascular integrity is highly dependent on maintaining cerebral blood flow even during diastole (Willie, Tzeng, Fisher, & Ainslie, 2014).

Advancing age is associated with a higher arterial stiffness (Kohn, Lampi, & Reinhart-King, 2015). In an aging artery, the proportion of elastic components decreases (O'Rourke, 2007; Vlachopoulos, Charalambos, Michael O'Rourke, 2011). Consequently, the ability of the artery to act as elastic

reservoir decreases (Hashimoto & Ito, 2009) and a higher pulsatile pressure and flow may travel towards the brain (O'Rourke, 2007; Wåhlin, Ambarki, Birgander, Malm, & Eklund, 2014). Cerebral arterioles respond to this abnormal flow pattern by constricting and remodeling, leading to increased resistance and thus limiting local blood flow to the tissue (Mitchell, 2015). Due to this adaptive mechanism, capillaries are initially protected from higher pulsatile stress. Nevertheless, over time, the reactivity of arterioles can be compromised, and brain capillaries are exposed to the pulsatile flow (Mitchell, 2008, 2015). This microcirculation dysfunction may lead to blood brain barrier (BBB) impairment (Garcia-Polite et al., 2017; Vlachopoulos, Charalambos, Michael O'Rourke, 2011) and microvascular hemorrhage (Stone, Johnstone, Mitrofanis, & O'Rourke, 2015). In conjunction with this effect, cerebral blood flow (CBF) may become uncoupled with the metabolic needs of the underlying tissue (Toth, Tarantini, Csiszar, & Ungvari, 2017). Eventually, a chronic increase in pulsatility is reported to be associated with the presence of hyper-intensities on MRI images (Zwanenburg, 2018), white matter signal abnormalities (Tan et al., 2019) and microstructural white matter changes (Jolly et al., 2013).

Not only aging (Diaz-Otero, Garver, Fink, Jackson, & Dorrance, 2016), but also cardiovascular risk factors such as hypertension (Blanco, Müller, & Spence, 2017) and diabetes mellitus (Kim et al., 2008), are associated with arteriolar disease. Studies have linked hypertension to flow misregulation and BBB modifications (Iadecola & Davisson, 2008). In a study on older adults with classical CVRF the higher pulse wave velocity (PWV) and hypotension were linked to cerebral microvascular damage and lower global cognition (Scuteri et al., 2013). In another research, CVRF were associated with higher pulsatile blood velocities as measured at the middle cerebral arteries (MCA; Pase, Grima, Stough, Scholey, & Pipingas, 2012). Age-related arterial stiffness and CVRF are shared risk factors for CAD (Fukuda et al., 2006). Elevated pulsatility in the central arteries can impair coronary perfusion (Mitchell, 2008) and impose higher load on the heart, especially in the individuals with CVRF (Farasat et al., 2008).

CAD induces alterations in cardiac output and negatively influences vascular homeostasis in the brain (Ng, Turek, & Hakim, 2013). While a large portion of the population is exposed to both CVRF and CAD, little attention has been paid to how CVRF progression and eventually CAD can alter the cerebral pulsatility at the end sites of pulse pressure damping across the cortex. The goal of the

present study is to determine the downstream impact of CVRF and CAD on the distribution of cerebral pulsatility across the cortex.

There are several non-invasive methods for quantitative assessment of cerebral pulsatility. Doppler ultrasound (Figueras et al., 2006) and MRI can index pulsatility in the large arteries, such as carotids and vertebral arteries (Wåhlin et al., 2014), down to the MCA (Zarrinkoob et al., 2016). However, both of these techniques are limited to probing larger vessels. Other indices of pulsatility can be achieved via tonometry (PWV; O'Rourke & Jiang, 2001) which determine velocity by measuring the ratio of pulse transit time in a known vascular path length (often the carotid-femoral arteries). Another simple and inexpensive peripheral index of arterial pulsatility is determined based upon the difference between systole and diastole in the pulse cycle using a pulse plethysmograph (Uangpairoj & Shibata, 2013). However, these techniques introduce a single, global index of pulsatility and do not reveal the spatial distribution of pulsatility across the cortical regions where damage occurs. Cerebral pulsatility is dependent on the distribution of stiffness of the underlying arterial network and thus varies in each segment of the vascular tree across the cortex (Fabiani et al., 2014; Tan et al., 2017).

Near-infrared spectroscopy (NIRS) can assess local cerebral pulsatility across the cortex non-invasively and in a natural setting (Fabiani et al., 2014). The cerebral arterial pulse is a large signal and is identifiable in the functional NIRS data. This signal can be measured in each recording location with and/or without averaging, in each subject with appropriate sensor contact. NIRS signals were recently used to describe the elasticity of local cerebral arterial segments by parameters extracted from the characteristics of the cerebral pulse. Among cerebral pulsatility parameters measured by NIRS that were shown to vary with aging are the cerebral pulse amplitude and the cerebral pulse relaxation function (PRF) (Chiarelli et al., 2017; Tan et al., 2019, 2017; Fabiani et al., 2014). Employing NIRS data to draw maps of cerebral pulsatility parameter values over the adult lifespan, findings demonstrated that optical cerebral pulse parameters are correlated with local cerebrovascular health, and with cognitive load associated with the Sternberg memory task (Chiarelli et al., 2017) as well as cardiorespiratory fitness (Tan et al., 2017).

Several studies reported involvement of the frontal cortex and its subregions in the large spectrum of cognitive functions (Frith & Dolan, 1996; McDonough, Wong, & Gallo, 2013; Rosa, 2016) and motor activities (Bakker et al., 2008; Miller & Cohen, 2001; Vitorio, Stuart, Rochester, Alcock, &

Pantall, 2017). This region of the brain is reported to be particularly vulnerable to the impact of aging (West, 1996) and is linked to poor cognitive function wherein stiffening of the arteries was reported to mediate this association (Singer, Trollor, Baune, Sachdev, & Smith, 2014). While MRI is used as a gold standard for brain imaging, it has limitations in studying hemodynamic changes associated to walking (Vitorio et al., 2017). Walking mimics everyday activity and hence was used to study the impact of a brief cardiovascular stress on the dynamics of cerebral pulsatility.

In the present study, functional NIRS was used to assess pulsatility across the frontal cortex regions in patients with different cardiovascular risk factor loads and those with CAD. The objective of the present study was twofold: (1) To assess the impact of LCVRF, HCVRF and CAD on cerebral pulse across the frontal areas. We hypothesized that cerebral pulse amplitude is higher (and PRF is lower) in the CAD, HCVRF and LCVRF, respectively. (2) To evaluate how short-duration walking could impact cerebral pulsatility across the cortex differently in these clinical groups. It was expected that after walking cerebral pulse amplitude reduces (and PRF increases) compared to before walking.

5.3 Materials and methods

5.3.1 Participants

A total of 60 elderly individuals including both men and women (aged 57-78, right-handed) were recruited for the study and divided into three groups according to their CVRF level and CAD diagnosis. Table 1 summarizes demographic characteristics of the participants.

5.3.2 Screening procedure

Classical cardiovascular risk factors of (1) high total cholesterol (2) diabetes (3) hypertension (4) low high-density lipoprotein (HDL) (5) high low-density lipoprotein (LDL) (6) smoking as well as cardiovascular condition were considered. The cardiologist reviewed the blood test results of participants. The presence or absence of coronary heart disease was determined from the clinical data assessment, the list of participant's medications which enabled the cardiologist to classify the participants in two groups of non-CAD and CAD groups. Patients with CAD had any of the risk

Table 5-1 Baseline characteristics of participants.

Characteristics	LCVRF (n=16)	HCVRF(n=26)	CAD (n=18)
Female/male (n)	11/5	15/11	1/17
Age (years)	66.31 (4.52)	66.96 (5.77)	71.05 (4.06)
Resting SBP (mmHg)	122.68 (7.25)	124.57 (13.55)	125.16 (15.22)
Resting DBP (mmHg)	75.68 (6.38)	76.38 (7.05)	75.27 (7.07)
Pulse pressure (mmHg)	43.24 (2.78)	45.14 (5.98)	57.97 (11.23)
NIRS-estimated heart rate BW (beat/min)	70.49 (7.33)	70.95 (7.75)	73.13 (11.09)
NIRS-estimated heart rate AW (beat/min)	79.10 (10.28)	84.22 (9.06)	92.81 (15.02)
METs	9.34 (2.38)	8.48 (1.99)	8.61 (1.81)
Smoking, n (%)	0	3 (11.54)	1 (0.055)
Blood sample parameters			
Total-cholestrol (mmol. L^{-1})	4.80 (0.74)	4.91 (1.29)	3.65 (0.54)
LDL-cholestrol (mmol. L^{-1})	2.68 (0.65)	2.92 (1.09)	1.80 (0.47)
HDL-cholestrol (mmol. L^{-1})	1.64 (0.29)	1.35 (0.54)	1.27 (0.28)
Medication therapy			
Aspirin, n (%)	1 (5.55)	5 (19.23)	16 (88.89)
Beta-blockers, n (%)	1 (5.55)	4 (15.38)	12 (66.67)
Calcium-antagonist, n (%)	2 (11.11)	4 (15.38)	5 (27.78)
ACE-inhibitor, n (%)	0	3 (11.54)	3 (16.67)
ARA, n (%)	2 (11.11)	8 (30.77)	6 (33.33)
Treatment for CAD			
Coronary angioplasty	0	0	11 (61.11)
CABG	0	0	6 (33.33)
Infarcts	0	0	10 (55.56)

Continuous variables are: mean (standard deviation); n: number of participants, % percent of participants; SBP: systolic blood pressure; DBP: diastolic blood pressure, BW: standing rest before short-duration walking, AW: standing rest after short-duration walking, METs: metabolic equivalents, CABG: coronary artery bypass graft, LDL: low-density lipoprotein, HDL: high-density lipoprotein, ACE: angiotensin converting enzyme, ARA: angiotensin antagonist receptor.

factors (1), (2), (3), (4), (5) in addition to any history of coronary artery disease, coronary artery bypass grafting and myocardial infarction event (that occurred more than a year prior to the experiment). The exclusion criteria for the CAD group were moderate to severe valvular heart disease, congestive heart failure, a recent history of myocardial infarction, overt neuropathy and uncontrolled hypertension.

Non-CAD participants were divided into two groups, which were the LCVRF and the HCVRF groups, based on the Framingham score (Wilson et al., 1998). All participants were screened for any previous head injury, neurological disorder, major psychiatric illness, renal disease, use of central nervous system affecter medication (benzodiazepine or any antidepressants), alcoholism, and a history of migraines. Approval of all aspects of this study was obtained from the ethics committee of the Montreal Heart Institute. Prior to participation, all enrolled participants were provided oral and written explanations of the study and the freedom to drop out. Written consent was obtained from each participant prior to the experiment.

5.3.3 Quantification of cardiovascular risk factors using Framingham scoring

Framingham scoring served as an index that combines scores of gender, age, cholesterol or LDL, HDL, blood pressure, diabetes mellitus and smoking status to estimate 10-year risk of developing coronary heart disease (CHD) events. In the Framingham table published by Wilson et al. (1998), risk factor scoring tables categorize the measure of risk factor to low or very low or moderate, high or very high. The non-CAD participants possessing very low, low or moderate risk factors were assigned to LCVRF group and participants with at least one high or at least one very high risk factor were assigned to the HCVRF group (Bosomworth, 2011). Due to the unavailability of Framingham age-scores for individuals older than 74 years, the age-scores for those five participants older than this age were linearly extrapolated.

5.3.4 Assessment of cardiorespiratory fitness on treadmill

Cardiorespiratory fitness (CRF) was assessed for each participant using a treadmill (T2000, GE Medical Systems, USA) with an individualized ramp protocol following a previously published protocol (Boidin et al., 2015; Gayda, Brun, Juneau, Levesque, & Nigam, 2008). In the time of the

test with the personalized ramp protocol, the speed and slope were gradually raised (each 15 s) to reach a linear load for the total duration of about 10 min (Myers et al., 1992). All participants were instructed to take their medications as they normally would. During the tests, the participant's electrocardiogram (ECG: Marquette case 12, GE Medical Systems, USA) was measured continuously. The participants rate of perceived exhaustion according to Borg's scale (6 to 20) and blood pressure (manual measure: sphygmomanometer, Welsh Allyn, USA) were measured every 2 minutes. Criteria for the symptom-limited maximal exercise test were; rate of perceived exertion ≥18 and/or ≥85% of age-predicted maximal heart rate or patient exhaustion. The exercise discontinued in case of participant fatigue, dyspnea, abnormal blood pressure responses or electrocardiogram abnormalities. Highest level of metabolic equivalent (METs) were estimated from maximal treadmill speed and grade as previously published (Boidin et al., 2015). At the end of the session, each participant had a 5 min passive recovery period.

5.3.5 Blood draw and blood pressure measurement

Blood samples were collected from each of the participants following overnight fasting. Glucose, cholesterol, LDL and HDL levels were measured based on the protocol in Boidin et al., 2015; Gayda et al., 2008. Prior walking, the average blood pressure was determined over 3 minutes of continuous measurement after the participant had rested for 10 minutes in the seated position. The blood pressure was taken on the right upper arm using a digital sphygmomanometer.

5.3.6 Functional NIRS acquisitions

The NIRS system used for acquisitions was an in-house-developed, fully portable system using 16 near-infrared light emitting diode (LED) sources and 16 detectors mounted on a long-lasting, flexible mesh to account for various head contours across the participants (Lareau et al., 2011). The LEDs generated near-infrared light at 735 and 850 nm. The design of the optodes featured a spring that provided stable contact with the scalp. Each source and detector were fixed on sockets using a stretchable band (Figure 5-1A, 1B). An orthogonal orientation is maintained with the skin surface to ensure a good skin-optode contact which boosts light-coupling efficiency and an optimal co-registration with the MRI template. The reflected near-infrared light was recaptured using avalanche photodiodes located on the head. A source-detector separation of 2.5-5.6 cm was used to detect

hemodynamic changes from frontal lobe and motor areas (Figure 5-1A). Pictures of the helmet and the whole system on a participant are shown in Figure 5-1C. One triaxial accelerometer was placed on the helmet. The data from the accelerometer and the 16 detectors were sent in real time by Bluetooth to a computer. A LabView (National Instrument, TX, USA) user interface was used to calibrate the system, start and stop acquisitions, manage tasks triggers and visualize the recorded data. A light weighted black cloth was placed over the helmet to prevent ambient light from being detected by the detectors. The source and detectors were positioned according to the international 10–20 EEG system (Klem, Lüders, Jasper, & Elger, 1999).

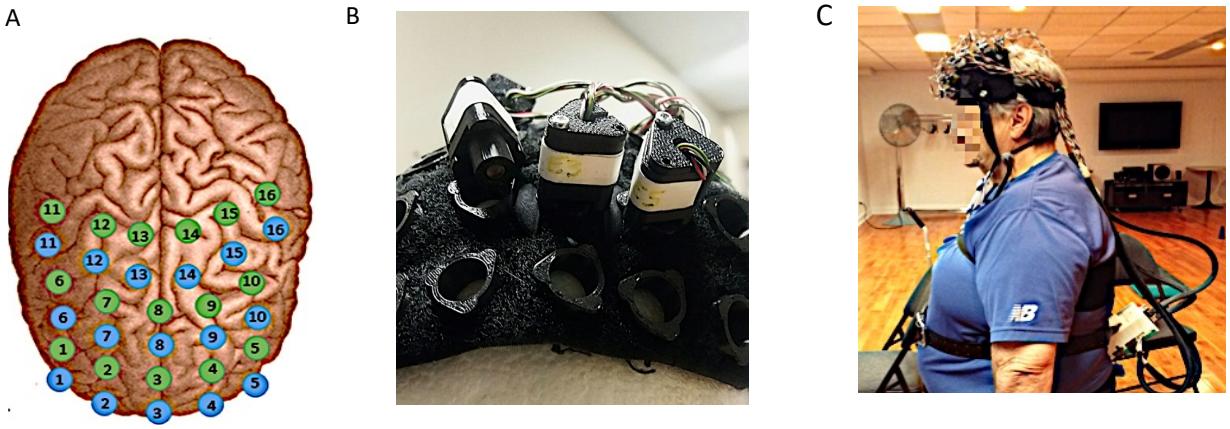

Figure 5-1, Posterior-anterior view of the source and detector placements. Blue dots represent the source and green dots are representing the detector. (B) Helmet and optode sockets. Source and detector housings are identical and are fixed on the helmet's sockets.). 16 sources and 16 detectors were placed on the helmet. (C) Participant equipped with the system. The prototype is attached on the back of the participant and is sending data by Bluetooth to a computer.

5.3.7 Walking paradigm

Participants were asked to walk freely at a self-selected pace (Wert, Brach, Perera, & VanSwearingen, 2013) for two distinct trials identified as blocks 1 and 2. These trials were performed in a quiet room where markings on the ground indicated a 10 meters long trail to follow. Participants were instructed to walk the distance back and forth on a self-selected pace for 30 s. The NIRS helmet was mounted on the participants' foreheads. Care was taken to place the NIRS

optodes on the head of the participant to establish a good coupling between near-infrared optodes and head surface. In each trial, the participants returned to the origin after the end of trial. Participants were accompanied by a trainer ensuring safety in each walking trial. NIRS data were collected continuously during each block.

5.3.8 Windkessel model and cerebral pulsatility parameters

The pulsatile motion of blood expands the elastic arteries and arterioles. It also induces periodic alterations in the concentration of oxy-hemoglobin, which attenuates near-infrared light absorption. Near-infrared source and detector pair can measure this attenuation. A fluid dynamics model has been proposed to explain the association between local alterations of blood volume and detected near-infrared light intensity described by the following equation (Cook, 2001; Wisely & Cook, 2001).

$$\frac{-\delta I}{\delta t} \propto \frac{\partial V}{\partial t} = F \qquad \text{(eq. 1)}$$

Here I is the relative changes of near-infrared light intensity, V is the changes of blood volume, t is the time and $F = F_{in}$-F_{out} is pulsatile flow (the difference between inflow and outflow). F_{in} or inflow is the ejected flow from the left ventricle as estimated from a sine wave (Segers et al., 2008) with assuming amplitude A and frequency 1 Hz[8] or $A.sin(t)$. F_{out} is the out flow or the flow through arterioles with resistance R and pressure drop $P(t)$, and $F_{out} = \frac{P(t)}{R}$. Assuming a linear pressure-volume relationship, the compliance of the artery is defined as $\frac{dV(t)}{dP(t)}$. Thus, the Windkessel equation can be rewritten:

$$\frac{P(t)}{R} + C\frac{dP(t)}{dt} = F_{in}(t) \qquad \text{(eq. 2)}$$

[8] Normal average heart rate is around ω=1 Hz (Segers et al., 2008). Here we assumed 1 Hz as frequency of heartbeat simplify the model. If the frequency is not 1 Hz, then with integrating the *sin* in the eq.4 should be multiplied by 1/ω.

5.3.8.1 Cerebral pulse amplitude

Assuming inflow is predominant during systole, outflow can be neglected ($F_{out}^{systole} = \frac{P(t)}{R} \approx 0$) (Themelis et al., 2007). Therefore, we can rewrite eq. 2 as:

$$C\frac{dP(t)}{dt} = A.sin(t) \qquad \text{(eq. 3)}$$

Integrating both sides of the equation, P can be written:

$$P = -\frac{A}{C}.cos(t) + Const \qquad \text{(eq. 4)}$$

Solving eq.4 for the beginning of the cardiac cycle (t_0=0), and for t_{max} yields: $P \approx -A/C$. It is worth to mention that in this equation, we neglected the negative sign as cerebral pulse amplitude (see Figure 5-2) is a negative number, therefore P yields a positive value. At constant pressure, as the compliance of the arterial wall decreases, the amplitude of the optically detected heartbeat increases. Here, systolic amplitude was calculated as the changes in cerebral pulse amplitude from systolic peak to baseline value of pulse or preceded diastolic peak (Tan et al., 2017, Figure5-2), normalized by the diastolic peak. Therefore, the cerebral pulse amplitude is proportional to the changes of signal intensity with respect to its baseline.

5.3.8.2 Pulse relaxation function

PRF refers to shape of the pulse during diastolic relaxation (Fabiani et al., 2014). At the end of systole, when cardiac ejection ceases, arterial inflow can be neglected ($F_{in} = 0$) and the relaxation of the arterial elastic elements passively flushes the blood into the vascular bed. Solving the Windkessel first degree differential equation for $P(t)$ in the diastolic phase yields:

$$P(t) = P_0 e^{\frac{-t}{RC}} \qquad \text{(eq. 5)}$$

The Windkessel model proposes that during diastole, the relaxation of the artery follows an exponential function with parameters dependent on the compliance of the artery (decay time of RC). This equation assumes that an elastic artery has a delayed recoil (depends on RC) which in

turn allows for an optimal temporal distribution of the pulse. Conversely, the loss of arterial wall elasticity is reflected in a shorter diastolic decay or a quick recoil. Fabiani et al. (2014) simplified the exponential function in eq. 5 to a straight line (Chiarelli et al., 2017) and subtracted the area under the relaxation curve from the area under the diastolic waveform to estimate the reflected wave. Here, PRF was determined by integral of the area under the diastolic phase of the pulse waveform minus the area of the triangle estimating relaxation curve. Next, this value was normalized by systolic amplitude (Fabiani et al., 2014, see Figure 5-2).

Accordingly, the extent of arterial wall elasticity in cerebral arteries and arterioles can be related to the pulse amplitude and the shape of the cerebral heartbeat during diastolic relaxation by the level that arterial wall maintains its expanded volume during diastolic phase (Fabiani et al., 2014; Tan et al., 2017). Since the wavelength of 850 nm is more sensitive to the absorption of oxyhemoglobin concentration (Themelis et al., 2007), data related to this wavelength were used for analysis of pulsatility parameters of the two blocks of the task.

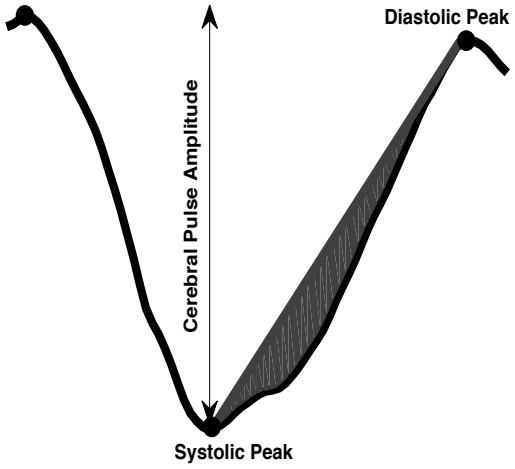

Figure 5-2 Example of single cerebral pulse waveform. The change in intensity between the systolic and the diastolic peak represents cerebral pulse amplitude. The shaded area represents the PRF as estimated by dividing the area from systolic peak to the next diastolic peak, normalized by cerebral pulse amplitude (adapted from Tan et al., 2017). X-axis is time (s) and y-axis is raw NIRS signal intensity.

5.3.9 NIRS data processing

5.3.9.1 Preprocessing

Data analysis was performed using MATLAB 2017a (MathWorks, Natick, MA, USA). In this study, we focused on the pre- and post-walking standing rest periods where data were not contaminated by motion. This distinction between motion and rest periods was made using accelerometer data (Figure 5-3A, B). Saturated channels were removed from the analysis and the raw NIRS data of the remaining channels were normalized to their mean[9] (Fabiani et al., 2014). Intensity data were filtered with a bandpass filter with cut-off frequencies at 0.5-5 Hz (Tan et al., 2017) to preserve brain physiology data while eliminating unwanted high- and low-frequency noises. Motion artefacts were identified using Homer2 toolbox, (motion artifact function, Huppert et al., 2009) and the output vectors were visually checked and often removed from the analysis. We followed the approach in Pollonini et al. (2014), as a quality check for heartbeat epochs in one channel. In short, a good source detector coupling will present a prominent synchronized cardiac oscillation in both wavelengths. Hence, after preserving the cardiac component in both wavelengths, a cross-correlation at the time lag zero shows how well two wavelengths are coupled.

[9] We followed the literature (Fabiani et al., 2014) to normalize the intensity of the acquired NIRS signal to its mean because: (1) we intended to mitigate the influence of all the factors that affect the acquired raw signal strength and (2) to compare the results between subjects. These factors include among other: optode alignment uncertainty, the impact of hair color or skin pigmentation on signal, thickness of skull bone and other trivial parameters which we wish to eliminate.

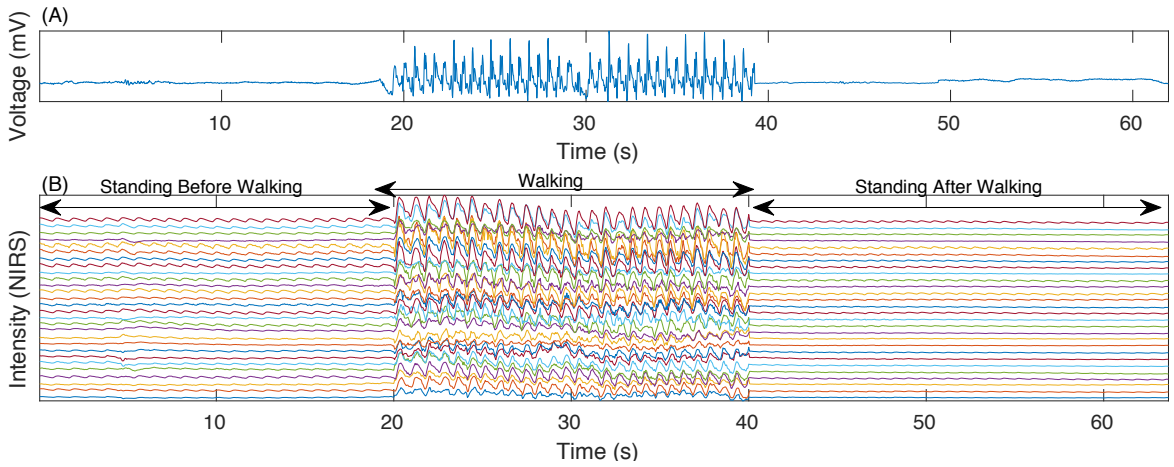

Figure 5-3 (A) Example of accelerometer data averaged over three axes including standing rest before short-duration walking and standing rest after short-duration walking. (B) Example of the NIRS intensity data for wavelength 850 nm. A higher pulse amplitude in the standing rest before short-duration walking in comparison with after short-duration walking is clearly identifiable.

The resulting number is called scalp coupling index (SCI) and serves as a quality check for each channel. In this study, only channels with an SCI≥0.8 were considered for further analysis.

5.3.9.2 Extraction of cerebral pulse amplitude and pulse relaxation function

Heartbeat pulse epochs were analyzed for each resting period, before and after walking separately. Local maxima (peaks) and local minima (nadirs) were determined with a semi-automatic approach using the "FindPeak" function in MATLAB 2018a (MathWorks, Natick, MA, USA). Each heartbeat epoch was tagged based on defining a local extremum. However, if a peak or nadir was flat, the individual heartbeat epoch was discarded from further analysis. Nevertheless, in some channels, we observed heartbeat pulse waveform variability. Therefore, manual and visual inspection were performed on all the channels for each participant to ensure that any misidentification or detection error of the peaks and nadirs were fixed manually. Manual fixes were affected by adjusting the "FindPeak" algorithm parameters or discarding the heartbeat epoch as an artefact from the further analysis. Following identification of peaks and nadirs, each individual heartbeat was separated. The baseline shift of each heartbeat epoch was removed by piecewise cubic spline interpolation.

The waveforms with a peak amplitude with standard deviation twice greater than the mean was considered as motion artifacts and were removed from the analysis. The average waveform of the remaining heartbeats was determined and a correlation between each individual and the average heartbeat epoch was calculated. The heartbeat epochs with a correlation greater than 0.8 were kept. Channel data was divided into four quantiles and the second and third quantiles were averaged. In each heartbeat epoch obtained from the NIRS signal, cerebral pulse amplitude and PRF were calculated separately. Next, the average of pulsatility indices was used to represent the pulsatility index for that channel. In addition, the average across all the channels was used as the global pulsatility index in each participant. Figure 5-4, provides a diagram of NIRS data processing to extract pulsatility indices. For each participant, we averaged the cerebral pulse amplitude across all channels as an indicator of the global cerebral pulse amplitude for the subject. The same procedure was followed for global PRF.

5.3.10 Statistical analysis

A one-way analysis of variance (ANOVA) using group as between subject factor (LCVRF, HCVRF and CAD), was performed on the data. The aim of the analysis was to evaluate whether at rest, cardiovascular degradation from LCVRF to HCVRF and CAD could alter cerebral pulse amplitude and PRF. In this model, dependent variables were cerebral pulse amplitude and PRF. Finally, to explore the impact of walking on alterations of global cerebral pulse amplitude in each group individually, we employed a paired student t-test within each group. All statistical analysis was performed with SPSS (IBM statistics for Macintosh, Version 25.0).

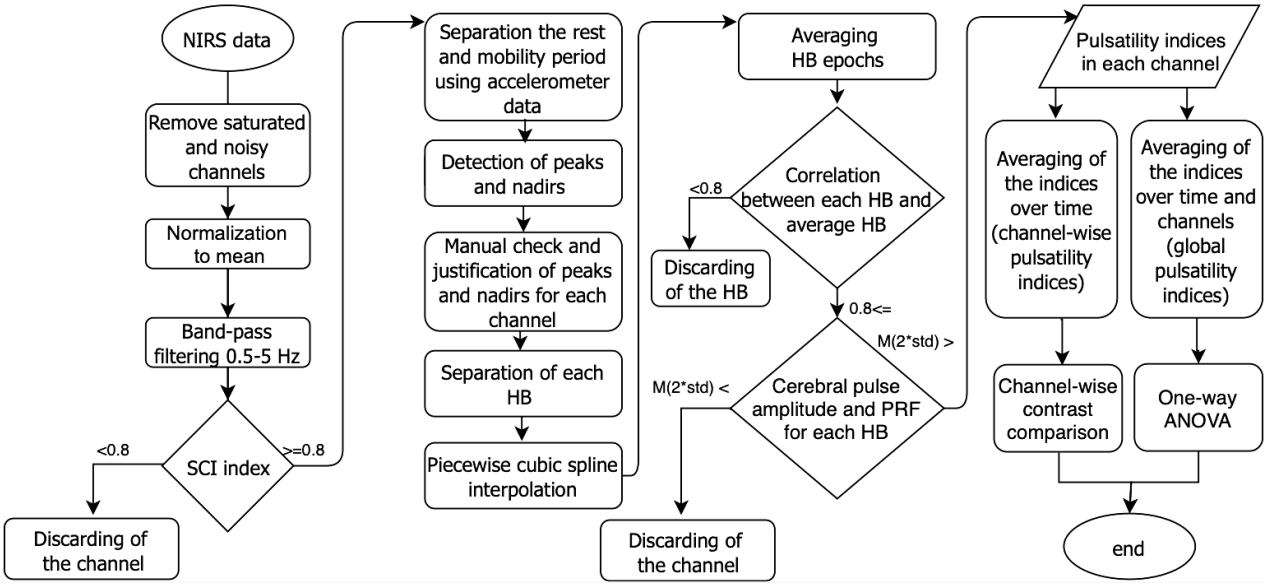

Figure 5-4 Schematic diagram of NIRS data processing to extract pulsatility indices and analysis. HB is a notation for heartbeat epochs. M(std) is a notation for mean±standard deviation.

In addition to the above analysis assessing the global pulsatility index combining all NIRS channels for a single subject, we also conducted channel-wise analysis on pulsatility parameters to explore their spatial properties before and after short-duration walking. A two-sample t-test was then conducted on the pulsatility scores across subject groups, testing the null hypothesis that there was no statistically significant difference in the measured cerebral pulse amplitude or PRF across the three subject groups for this channel. This yielded a total of 38 NIRS channels to be included in the channel-wise analysis (Figure 5-5). The t-values of each comparison were then corrected for multiple comparison with a false discovery rate (FDR) approach (Benjamini & Hochberg, 1995). Along with the raw pulsatility scores, the t-values that survived the FDR correction were then projected on the cortical layer of the Colin27 template based on the anatomical locations of the corresponding channels. This projection was performed using the open source toolbox Atlas Viewer (Aasted et al., 2015). These individual values were then spatially interpolated to generate cortical contrast maps. Channel-wise analysis was performed with Atlas Viewer, HOMER2 (Huppert, Diamond, Franceschini, & Boas, 2009) and some in-house developed scripts.

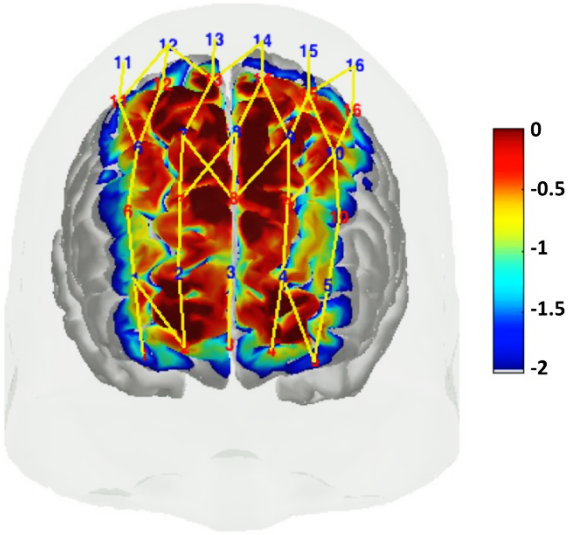

Figure 5-5 Spatial distribution of NIRS channels included in the channel-wise analysis of pulsatility parameters and the corresponding cortical sensitivity matrix, frontal view. Red numbers indicate near-infrared light sources and blue numbers indicate near-infrared light detectors. Yellow lines connecting a source to detectors represent NIRS channels. This figure shows that the 38 channels included in the channels-wise analysis had reasonable sampling sensitivity in most of the prefrontal areas and in bilateral supplementary motor cortices.

5.4 Results

On average, a walking block consisted of a standing rest period (15.20 ± 6.39 s) following by free walking (29 ± 9.2 s) and another standing rest after walking (15.77 ± 7.3 s). Figure 5-6A and Figure 5-8A show the boxplots of *global* pulsatility index (averaged across all the channels) for cerebral pulse amplitude and PRF, respectively, for the three groups, for standing rest before (BW) and after short-duration walking (AW). We controlled for sex in the analysis as our data indicated the sex impact on the cerebral pulse amplitude data (r ($CPA_{\_BW}$, sex) = 0.331, p=0.009). There was no statistically significant association between cerebral pulse amplitude and age (r ($CPA_{\_BW}$, age) =0.174, p=0.185). In addition, data indicated no statistically significant association between PRF data and sex (r ($PRF_{\_BW}$, sex) = 0.0145, p= 0.91) nor with age (r (PRF, age) = -0.11, p= 0.36). r and CPA are notations for correlation and cerebral pulse amplitude respectively.

5.4.1 Impact of cardiovascular status on cerebral pulsatility before walking while standing

5.4.1.1 Cerebral pulse amplitude

For *global* cerebral pulse amplitude BW, after controlling for sex a one-way ANOVA determined a statistically significant difference between groups (F (2,56) = 5.498, p=0.007). A multiple comparison with Bonferroni correction revealed that the global cerebral pulse amplitude was significantly higher in the CAD group (BW: 0.79±0.082) in comparison to HCVRF (BW: 0.69± 0.087, p= 0.037) or LCVRF (BW: 0.66± 0.078, p=0.001) groups. While the global cerebral pulse amplitude was slightly higher in the HCVRF group in comparison with the LCVRF group, the difference did not reach statistical significance (p= *0.708).* Figure 5-6C illustrates input data for channel-wise analysis of cerebral pulse amplitude. Prior to walking, this map reveals a similar trend in the effect of CVRF on cerebral pulse amplitude.

In Figure 5-7(before-walking), after controlling for sex, the difference of cerebral pulse amplitude was shown to be statistically significant in the supplementary motor cortices, especially on the left side (contralateral to the preferred hand) for the three groups. Likewise, HCVRF subjects were seen to have significant higher cerebral pulse amplitude than LCVRF subjects in the supplementary motor cortices, albeit with lower t-values. These regions expanded after walking.

5.4.1.2 Pulse relaxation function

For global PRF, a one-way ANOVA did not indicate a statistically significant difference across the groups (F (2,57) =1.595, p= 0.212). Figure 5-8C illustrates input data for channel-wise analysis of PRF which showed a lower PRF in CAD patients compared to HCVRF and LCVRF groups. As seen in Figure 5-9, before-walking, there was lower PRF in patients with CAD compared with LCVRF participants mostly in the bilateral supplementary motor area. For HCVRF versus HCVRF groups this difference in PRF data was limited to the lateral sensorimotor area, contralateral to preferred hand. We did not observe a statistically significant difference for CAD versus HCVRF groups. PRF results were consistent with the analysis of cerebral pulse amplitude in the previous section, suggesting that cortical regions with higher pulsatile amplitude are also regions with lower PRF.

5.4.2 Impact of short-duration walking on cerebral pulsatility parameters

5.4.2.1 Cerebral pulse amplitude

A paired student t-test indicated a statistically significant difference between rest periods after walking versus before walking. Descriptive statistics showed a reduction of cerebral pulse amplitude within each group: LCVRF group (BW: 0.663± 0.078 to AW: 0.577± 0.098, $p_{\_BWAW}$=0.0104), HCVRF (BW: 0.699± 0.087, AW: 0.645± 0.093, $p_{\_BWAW}$= 0.035 and CAD (BW: 0.793± 0.082 to AW: 0.7409± 0.059, $p_{\_BWAW}$= 0.043). This decrease in cerebral pulse amplitude within each group was accompanied with a higher heart rate estimated from NIRS data (number of detected heartbeats divided by time in one minute, see Table 5-1 and supplementary data. 5-1). Channel-wise comparison of cerebral pulse amplitude *across* the groups after controlling for sex is illustrated in Figure 5-7, after-walking. Results yielded statistically higher cerebral pulse amplitude for the CAD and HCVRF compared to LCVRF groups not only involving the sensorimotor cortices but also extending to other prefrontal areas. A smaller spatial extent of higher cerebral pulse amplitude was observed in the comparisons of CAD versus LCVRF subjects after short duration walking. For the HCVRF versus LCVRF groups, the difference was located in bilateral supplementary motor areas.

5.4.2.2 Pulse relaxation function

For *global* PRF, a *within* group paired t-test also indicated a statistically significant difference between AW and BW in the HCVRF and CAD groups but not for the LCVRF group. Descriptive statistics are as follows: LCVRF group (BW: 0.141± 0.047 to AW= 0.112± 0.053, $p_{\_BWAW}$=0.112), HCVRF (BW: 0.129± 0.057, AW: 0.093± 0.046, $p_{\_BWAW}$=0.0058) and CAD (BW: 0.111± 0.032 to AW: 0.0720± 0.020, p_{BWAW}<0.001). Channel-wise comparison of PRF data AW *across* the groups is illustrated in Figure 5-9. In this figure, the difference of PRF appear to be more significant with lower negative *t*-scores and the larger spatial extents, between CAD and LCVRF groups. Significant results were observed for HCVRF versus LCVRF, albeit with higher *t*-scores.

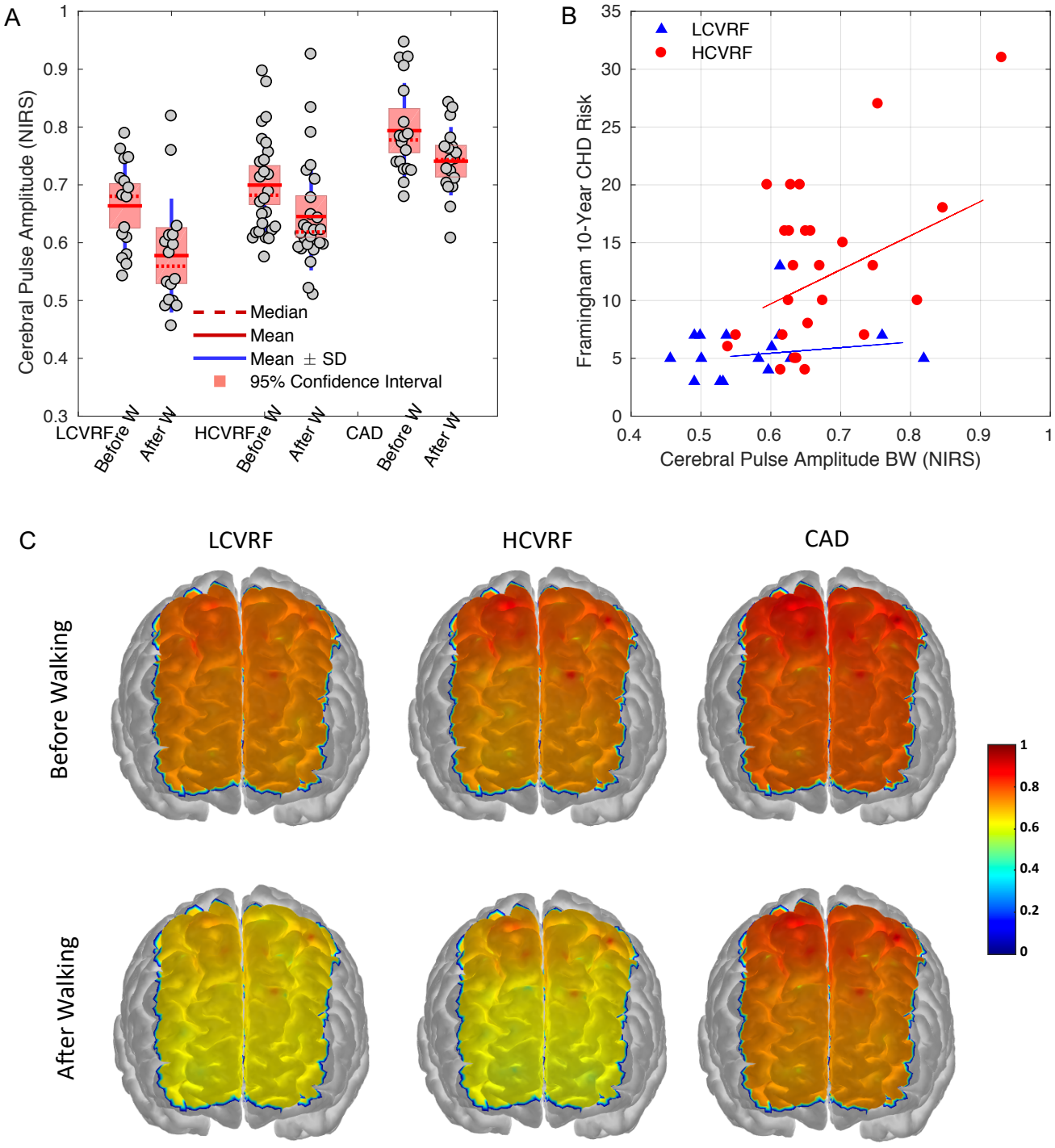
A
Cerebral Pulse Amplitude (NIRS)
1
0.9
0.8
0.7
0.6
0.5
0.4
0.3
Median
Mean
Mean ± SD
95% Confidence Interval
LCVRF
Before W
After W
HCVRF
Before W
After W
CAD
Before W
After W
B
LCVRF
HCVRF
Framingham 10-Year CHD Risk
35
30
25
20
15
10
5
0
0.4
0.5
0.6
0.7
0.8
0.9
1
Cerebral Pulse Amplitude BW (NIRS)
C
LCVRF
HCVRF
CAD
Before Walking
After Walking
1
0.8
0.6
0.4
0.2
0

Figure 5-6 Boxplots of global cerebral pulse amplitude for the three groups, the LCVRF, the HCVRF and CAD, for both BW and AW. (B) Scatter plot for the global cerebral pulse amplitude versus Framingham 10-year CHD risk prediction after controlling for sex (C) Channel-wise spatial distribution of the cerebral pulse amplitude on the Colin27 template. The mean cerebral pulse amplitude in every channel across all the participants is projected onto the brain surface for BW and AW, separately. Red regions indicating higher pulsatile amplitude and yellow regions indicating lower pulsatile amplitude. Figures 6-A, and 6-C are illustrations of the input data for statistical analysis.

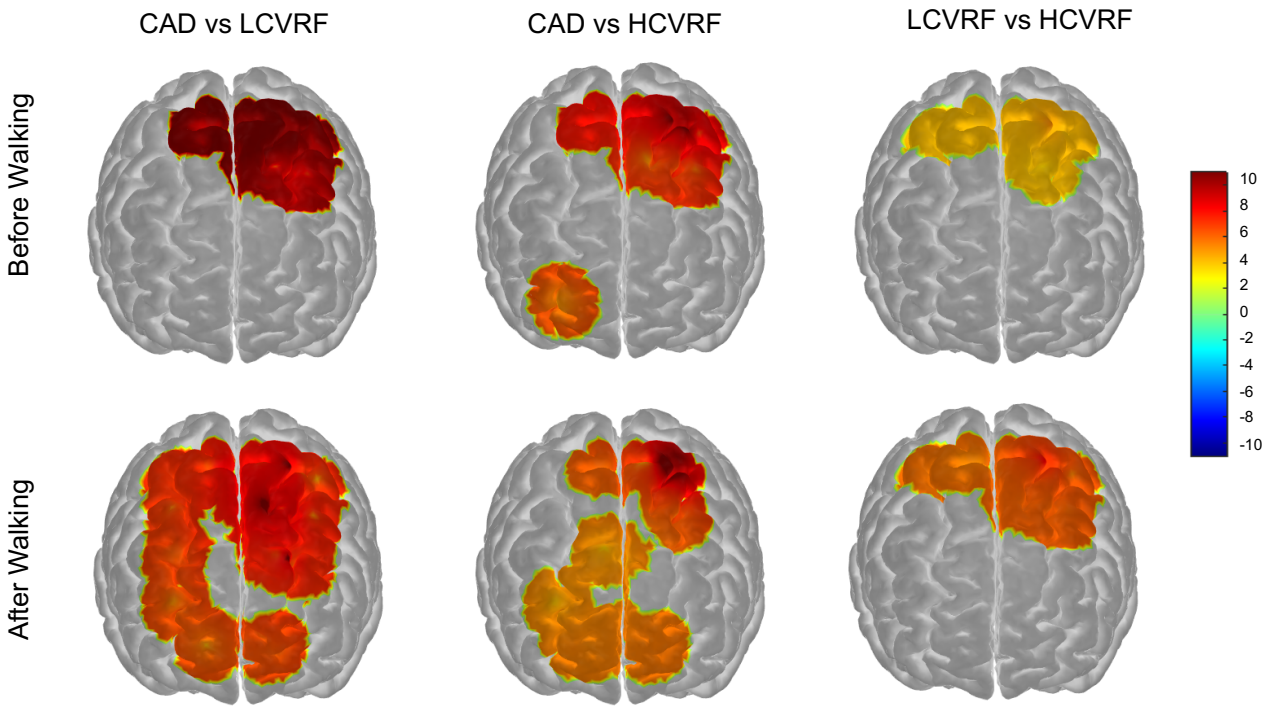

Figure 5-7 t-statistics topographic contrast maps ($p<0.05$) for channel-wise cerebral pulse amplitude contrast after controlling for sex, for BW and AW, respectively. These maps are FDR-corrected for spatial multiple comparisons for CAD versus LCVRF, CAD versus HCVRF and LCVRF versus HCVRF.

It is worth mentioning that although our analysis of global pulsatility metrics revealed the impact of short-duration walking on pulsatility parameters, channel-wise analysis of this parameter within each group generally failed to locate any channel with statistical significance after controlling for multiple comparisons.

5.4.3 Cerebral pulsatility parameters versus METs and blood pressure

Cerebral pulse amplitude was not statistically significantly associated with METs, systolic blood pressure, diastolic blood pressure after controlling for sex (supplementary data, table 5-2). PRF was not statistically significantly associated with METs, systolic blood pressure, diastolic blood pressure (supplementary data, table 5-2).

Cerebral pulse amplitude was significantly associated to pulse pressure in the CAD (r= 0.328, p=0.024) but not for LCVRF and HCVRF.

5.4.4 Correlation between pulsatility parameters and Framingham score

BW data after controlling for sex (Figure 5-6B) indicated that global cerebral pulse amplitude and Framingham 10-year CHD risk prediction are positively correlated and approaching significance for the HCVRF group (r=0.357, p=0.072) but not for LCVRF group. For AW data in the HCVRF group this association was significant (r= 0.518, p=0.006) but not for LCVRF group. PRF did not correlate with Framingham score (Figure 5-8B) for any of the LCVD and HCVD groups neither at BW nor AW (supplementary data.5-3)

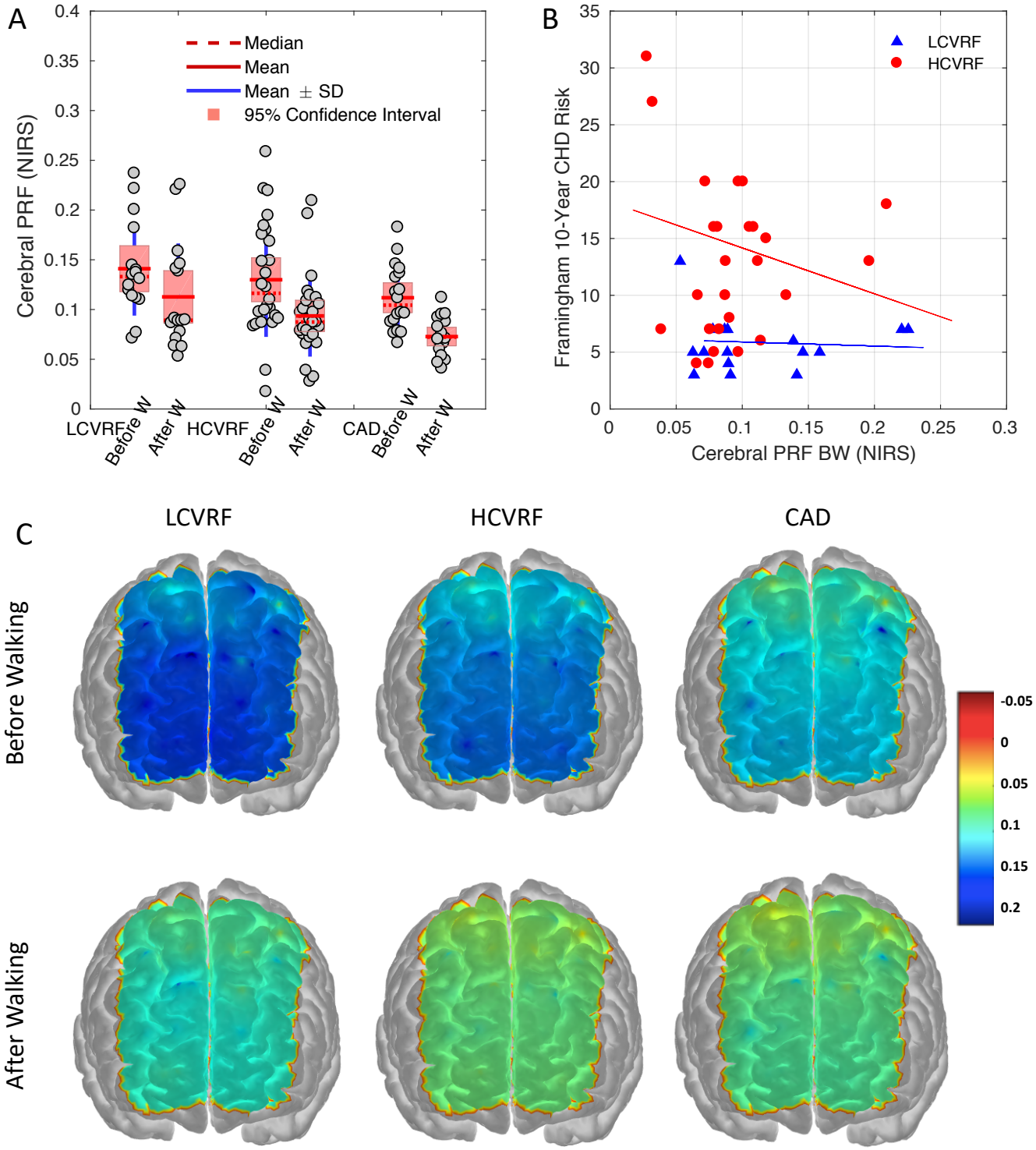

Figure 5-8 Boxplots of global PRF for the three groups BW and AW. (B) Scatter plot for global PRF versus Framingham 10-year CHD risk prediction of LCVRF, HCVRF and CAD. (C) Channel-wise spatial distribution for PRF on the Colin27 template. PRF is projected onto the brain surface BW and AW. Blue areas indicate the higher wave reflection or lower pulsatile stress and green areas are indicate the higher pulsatile stress.

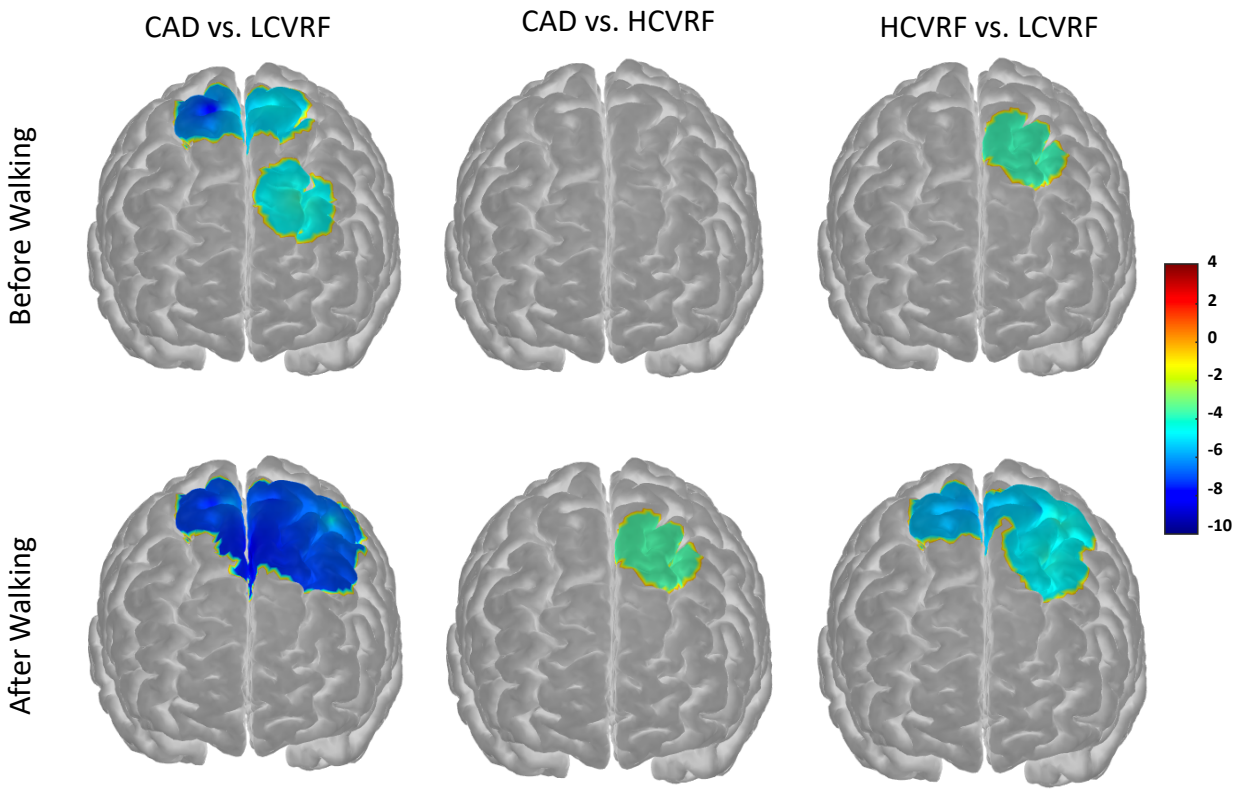

Figure 5-9 t-statistics topographic contrast maps ($p<0.05$) for BW and AW. PRF contrast results are presented across the groups with FDR-corrected for spatial multiple comparisons for CAD versus LCVRF, CAD versus HCVRF, HCVRF versus LCVRF.

5.5 Discussion

This study noninvasively assessed cerebral pulsatility across the cortex using NIRS in three groups of older adults: LCVRF, HCVRF and CAD. Our data indicated that cardiovascular degradation from LCVRF to HCVRF and CAD is associated with increased optically measured cerebral pulse amplitude. In recent years, Tan et al. (2017) reported that the progress of aging from young to middle and old age corresponds with a higher cerebral pulse amplitude measured with NIRS. Their work was based on pulsatility parameters introduced by Fabiani et al. (2014) who discussed that cerebral pulse amplitude measured with NIRS has a close correlation with cerebral pulse pressure and could be used as its indicator.

Results of the present study indicated that CAD patients have higher cerebral pulse amplitude when compared with those with LCVRF or HCVRF. This result agrees with other studies indicating higher PWV in CAD patients (Alarhabi et al., 2009). While it is delicate to distinguish the impact of arterial aging from pathology in the arteries, we deduce that a higher cerebral pulse amplitude in the CAD patients is related to (1) higher central pulse pressure (Khoueiry et al., 2012) (2) premature and/or accelerated vascular pathologies (Song-Tao, Yan-Yan, & Li-Xia, 2010). Aging and the presence of CVRF induce arterial stiffness and degradation of the arterial wall or a decrease in the elasticity of arterial walls (Farasat et al., 2008) and higher velocity of the blood within vessels (Pase et al., 2012). In the stiffer arterial tree with a higher PWV, velocity of transmission increases for both the forward traveling wave (originated from heart left ventricle and the stroke volume) and reflected wave (returning from peripheral circulation). The reflected wave may arrive earlier in the late systole, rather than in early diastole (Mitchell, 2008, 2015). This event could amplify the pressure at the end of systole (O'Rourke, 2007). Therefore, the energy stored in the pulse pressure leads to sharper systolic pulse amplitude (higher cerebral pulse amplitude) and diminished ability to sustain the blood flow during diastole (lower PRF). The negative impact of early wave reflection in the large central arteries is discussed in studies indicating a higher aortic pulse pressure with age, (with PWV approximately twice as high PWV at eighty years old compared to twenty years old (Parikh, Hollingsworth, Kunadian, Blamire, & MacGowan, 2016). The impact of disturbances of this kind on the cerebrovascular system was partially discussed in previous reports linking an increased PWV to cognitive decline (Hazzouri et al., 2013). However, these studies put little attention on the mechanical impact of pulsatile flow on the cerebral tissue. They focused upon a correlation between transmission of a higher central pulsatile flow to the cerebral arteries and cognitive performance (Singer et al., 2013). Bateman et al. (2008), in an MRI study, reported there is a reduction in mean arterial flow while aging and the arterial pulsation augments by about 50%. They also reported a similar pattern of reduction in the baseline arterial blood flow in individuals with Alzheimer's disease, which is accompanied by a higher cerebral blood flow pulsatility compared to healthy controls. In conjunction with this effect, Lennart and colleagues reported that cerebral small vessel disease could be identified by an increased flow pulsation in the perforating arteries of basal ganglia and semioval center (Geurts, Zwanenburg, Klijn, Luijten, & Biessels, 2019). Exposure of the small cerebral vessels such as arterioles and capillaries to a chronic, higher, pulsatile flow and pressure (Mitchell, 2008, 2015) could eventually

damage cerebral microcirculation (Wåhlin et al., 2014; Zarrinkoob et al., 2016) and neuron metabolism (Vlachopoulos, Charalambos, Michael O'Rourke, 2011). This damage could occur via shearing of arterioles endothelia (O'Rourke, 2007) that perhaps, at least partially, explains age-related cerebral pathology.

Statistical analysis of current data did not yield a significant difference between cerebral pulse amplitude for the LCVRF versus the HCVRF group. One possible reason for this observation could be the confounding impact of the vasodilator medications on the arterial wall. These medications are used by the majority of subjects in the HCVRF group (see Table 5-1) and can significantly reduce wave reflection and the building up of the pulse pressure in the central arteries (Akbar & Alorainy, 2014). Thereby, these medications reduce the pulse travelling towards the cerebral arteries. Beta-blockers can reduce heart rate and therefore reduce the number of stress cycles in the arterial walls. Moreover, this medication can impact arterial wall expansion during systole. Some other medications, such as ACE-inhibitors and ARA-inhibitors are reported to delay advancement of arterial stiffness (Guerin et al., 2001) and arterial dilation (Gelb, 2006) respectively. ARA-inhibitors and calcium-antagonists could relax the arterial wall smooth muscle (Williams, Lacy, Thom, et al., 2006) leading to a reduction in the amplitude of the reflected wave coming back to the heart, and in turn reduce the pulse pressure traveling towards the brain. The studies CAFÉ (Williams, Lacy, Thurston, et al., 2006) and REASON (London, Asmar, O'Rourke, & Safar, 2004) also reported that administration of ACE-inhibitors or calcium-antagonists in elderly individuals with hypertension could reduce central systolic aortic pulse pressure and reduce future cardiovascular events. Similar results are reported for ACE-inhibitor, RA-inhibitor and calcium-antagonists, where the impact of the therapy on cerebral microcirculation is evaluated by reduction in dementia severity by approximately 50% (Forette et al., 2002). Linking these pieces of evidence, we infer that in the majority of HCVRF patients, consuming vasoactive medication may attenuate cerebral pulse amplitude as measured with NIRS, in comparison with the LCVRF group. It is important to note that in our results despite use of vasoactive drugs in the group of CAD participants, they still had the highest cerebral pulse amplitude when compared to the HCVRF. This is in line with the results of Cardiovascular Health Study cohort that report that even treated CAD is associated with higher incidence of dementia (Newman et al., 2005). A higher cerebral pulsatility in CAD subjects may mediate the association between small vessel diseases and dementia. Small vessel diseases in turn impair CBF prefusion and regulation and damage BBB

therefore increase the susceptibility of neurovascular unit (Kovacic, Moreno, Nabel, Hachinski, & Fuster, 2011).

In the present study, we employed the Framingham 10-year CHD risk score for the quantification of total cardiovascular risk in an individual. Data indicated that a higher Framingham score predicts a higher cerebral pulse amplitude in older adults, although only marginally significant. This result is in accordance with Pase et al. (2012), who reported that a higher Framingham risk factor score is combined with a lower mean cerebral blood flow and a higher blood flow pulsatility measured in the MCA. A higher Framingham score is a result of higher cumulative effect of classical CVRF and greater damage on the arterial walls. Even treated, risk factors were shown to have a negative impact on arterial stiffness (Amar, Ruidavets, Chamontin, Drouet, & Ferrières, 2001; Mitchell, 2008) indexed by means of a higher PWV. For instance, diabetes mellitus (Climie et al., 2015) and hypertension (Ng et al., 2013) could amplify the functional and structural modifications of the arterial wall and augment the arterial stiffness (Ecobici & Stoicescu, 2017; Hwang et al., 2010; Prenner & Chirinos, 2015).

Our data also indicate a reduction in the cerebral pulse amplitude following short-duration walking in all three groups of participants. This reduction is unlikely to be due to the arterial wall's chronic adaptation in structural characteristics seen alongside regular exercise. Rather, this reduction is more likely due to residual vasodilatory substances in the body, which improve blood flow during movement. The activation of such autoregulation mechanisms regulates tissue blood flow according to changes in metabolic demand. In addition, it was previously shown that CO2-induced vasodilation in arterioles and capillaries occurred as a response to hypercapnia (Battisti-Charbonney, Fisher, & Duffin, 2011; Willie et al., 2014). Therefore, even if the exhaled concentration of CO2 is not measured in this experiment, hypothetically, a lower cerebral pulse amplitude after moderate walking could be due to the effect of increasing CO2 concentration in the blood and relaxation in the small vessel walls. The assumption for increased CO2 is supported by a higher heart rate after short-duration walking (see Table 5-1).

Our data indicated a statistically significant association between cerebral pulse amplitude and pulse pressure for CAD patients. This finding is in agreement with other studies suggested that pulse pressure is an independent and strong predictor of CAD (Winston et al., 2013; Safar & Smulyan, 2004). In a large-scale study on older adults pulse pressure was strongly associated with lesions in cerebral microvascular and reduced cognitive domains (Mitchell et al., 2011).

The results do not indicate a significant and meaningful association between global cerebral pulse amplitude and systolic/diastolic blood pressure. The brain is exposed to both the central pulse pressure and cerebral blood flow autoregulation mechanisms that modify and regulate the CBF via the carotid baroreflex (Purkayastha, Maffuid, Zhu, Zhang, & Raven, 2018) and myogenic tone of the parenchymal arterioles (Faraci & Heistad, 1990). Accordingly, cerebral pulsatility alterations in the cortex are not necessarily evident from the blood pressure measured in the arm. This result is in line with other research indicating no statistically significant association between cerebral pulsatility measured at the level of cervical arteries using phase-contrast MRI with blood pressure measured in the arm (Wåhlin et al., 2014).

Channel-wise spatial comparison of cerebral pulse amplitude reveals that at rest, cerebral pulse amplitude was slightly higher in the collateral supplementary motor cortices in all the three groups of participants. When comparing cerebral pulse amplitude in the CAD group after short-duration walking, a higher cerebral pulse amplitude emerges not only in the sensorimotor cortices but also in the prefrontal areas. This finding is in line with previous research indicating activation of the somatosensory area for maintenance of postural balance premotor regions and supplementary motor areas during human gait (Miyai et al., 2001).

The results of the present study show a significant association between cerebral pulse amplitude and fitness measures. This results was in agreement with Tan et al. (2017). However, our study had difference in type of participant and a difference in method. More precisely, between estimated and measured cardiorespiratory fitness. Tan et al. (2017), employed a non- exercise method to estimate cardiorespiratory fitness (Stamatakis, Hamer, O'Donovan, Batty, & Kivimaki, 2013) in the three groups of healthy young, middle aged and older individuals. Previous research indicated a non-exercise method to assess cardiorespiratory fitness is valid for healthy young (Jurca et al., 2005) and relatively healthy older adults (Mailey et al., 2010) and is even cross-validated in the cohort of hypertensive individuals. In the present study, CRF was assessed for each participant on the treadmill with an individualized ramp protocol, in the three mentioned groups. Further research is needed to explore to what extent a non-exercise method for estimating cardiorespiratory fitness can predict cardiorespiratory fitness measured with exercise in LCVRF, HCVRF and CAD participants.

During the exercise and recovery period, the elevated CO2 concentration in the blood and the relaxation of the arterial wall are expected to promote a longer diastolic period. Heart rate has a

great impact on myocardial oxygen demand. An elevated heart rate is often accompanied by a shorter cardiac cycle and a shorter time for the blood to run out of the arterial bed, which is a premature end of diastole (Boyette et al., 2019). Taken together, an elevated heart rate and shorter diastolic time could reduce PRF. This explanation is in accordance with part of our result indicating a lower PRF after short-duration walking.

Finally, there are several limitations to the present study. We discussed that stiffer arteries lead to an elevated pulsatility at microcirculation in the brain. With this background, a measure of arterial stiffness such as carotid-femoral PWV, transcranial doppler or PC-MRI could help to explore if pulsatility could be predicted with such measure. In our data, there is a large imbalance between female and male participants in the CAD group (1 woman versus 17 men). This imbalance could fail to detect a potential impact of sex on CAD. Further studies are needed to explore whether sex can have a significant impact on changes of cerebral pulsatility parameters in CAD patients. Moreover, in our data, cerebral pulsatility extracted through the skull are projected onto the cortex. However, NIRS signals are known to be contaminated by systemic variation of extracranial vessels. Regional cerebral pulsatility might also be subjected to such variation by extracranial vessels pulsatility. In order to achieve a pulsatility index at the level of cortex, there is a need for inclusion of short channels in the configuration of optodes to regress the heartbeat epochs in the short channels from far channels. Nevertheless, some studies have reported that the arterial pulsations measured by NIRS mostly originate from cerebral arteries and arterioles rather than extracerebral vessels, both in infants (Funane, Homae, Watanabe, Kiguchi, & Taga, 2014) and in younger and older individuals (Fabiani et al., 2014). Despite these reports, these studies lack the short channels and it is still plausible that part of cerebral pulsatility measured with NIRS is originating from external carotid territories and its branches. A more accurate NIRS pulsatility measure including short channels could provide better insight into the impact of extracerebral arteries on cerebral pulsatility. Although NIRS excels in non-invasive in-vivo imaging of the human head in a natural setting with a good time resolution, the technique is limited by path length determination due to variable anatomical head structures and CSF volume across participants. An anatomical MRI (which was not available in this study) could help to refine results. Finally, the clinical profiles of participants containing the actual duration the person has lived with reported health conditions, such as number of years of high blood pressure or high fasting glucose level,

were not available. Further research is needed to determine the impact of duration of exposure of the arterial wall to CVRF and CAD on the cerebral pulsatility.

5.6 Conclusion

Functional NIRS enables optical measure of cerebral pulsatility in the mobility-based experiment. Cerebral pulse amplitude was increased in the presence of CAD compared to LCVRF and HCVRF. After short-duration walking, cerebral pulse amplitude and PRF decreased within all the three groups. Cerebral pulse amplitude was not predicted from blood pressure and the fitness measures of cardiorespiratory fitness. Considering the low cost, non-invasiveness and simplicity of functional NIRS to index pulsatility, further research is needed to explore usefulness of this measure as an early detection tool for individuals who may benefit from selective health management and intervention strategies.

5.7 Acknowledgment

This work was supported by an operating grant (LB, SF, FL, AN, YJ) from the Canadian Institute of Health Research (#120304, MOP-191272 & IOP-271115). FL is supported by the Canadian Research Chair in Optical and Vascular Imaging, LB is supported by the Mirella and Lino Saputo research chair on cardiovascular health and the prevention of cognitive decline. MG is supported by the EPIC foundation and Montreal Heart institute foundation.

5.8 References

Aasted, C. M., Yücel, M. A., Cooper, R. J., Dubb, J., Tsuzuki, D., Becerra, L., … Boas, D. A. (2015). Anatomical guidance for functional near-infrared spectroscopy: AtlasViewer tutorial. *Neurophotonics*, *2*(2), 020801. https://doi.org/10.1117/1.nph.2.2.020801

Akbar, S., & Alorainy, M. S. (2014, November 1). The current status of beta blockers' use in the management of hypertension. *Saudi Medical Journal*, Vol. 35, pp. 1307–1317. Saudi Arabian Armed Forces Hospital.

Alarhabi, A. Y., Mohamed, M. S., Ibrahim, S., Hun, T. M., Musa, K. I., & Yusof, Z. (2009). Pulse wave velocity as a marker of severity of coronary artery disease. *Journal of Clinical Hypertension (Greenwich, Conn.)*, *11*(1), 17–21. https://doi.org/10.1111/j.1751-7176.2008.00061.x

Amar, J., Ruidavets, J. B., Chamontin, B., Drouet, L., & Ferrières, J. (2001). Arterial stiffness and cardiovascular risk factors in a population-based study. *Journal of Hypertension*, *19*(3), 381–387. https://doi.org/10.1097/00004872-200103000-00005

Bakker, M., De Lange, F. P., Helmich, R. C., Scheeringa, R., Bloem, B. R., & Toni, I. (2008). Cerebral correlates of motor imagery of normal and precision gait. *NeuroImage*, *41*(3), 998–1010. https://doi.org/10.1016/j.neuroimage.2008.03.020

Battisti-Charbonney, A., Fisher, J., & Duffin, J. (2011). The cerebrovascular response to carbon dioxide in humans. *Journal of Physiology*, *589*(12), 3039–3048. https://doi.org/10.1113/jphysiol.2011.206052

Benjamini, Y., & Hochberg, Y. (1995). Controlling the False Discovery Rate: A Practical and Powerful Approach to Multiple Testing. *Journal of the Royal Statistical Society: Series B (Methodological)*, *57*(1), 289–300. https://doi.org/10.1111/j.2517-6161.1995.tb02031.x

Blanco, P. J., Müller, L. O., & Spence, J. D. (2017). Blood pressure gradients in cerebral arteries: A clue to pathogenesis of cerebral small vessel disease. *Stroke and Vascular Neurology*, *2*(3), 108–117. https://doi.org/10.1136/svn-2017-000087

Boidin, M., Lapierre, G., Paquette Tanir, L., Nigam, A., Juneau, M., Guilbeault, V., … Gayda, M. (2015). Effect of aquatic interval training with Mediterranean diet counseling in obese patients: Results of a preliminary study. *Annals of Physical and Rehabilitation Medicine*, *58*(5), 269–275. https://doi.org/10.1016/j.rehab.2015.07.002

Bosomworth, N. J. (2011, April). Practical use of the Framingham risk score in primary prevention: Canadian perspective. *Canadian Family Physician*, Vol. 57, pp. 417–423.

Chiarelli, A. M., Fletcher, M. A., Tan, C. H., Low, K. A., Maclin, E. L., Zimmerman, B., … Fabiani, M. (2017). Individual differences in regional cortical volumes across the life span are associated with regional optical measures of arterial elasticity. *NeuroImage*, *162*, 199–213. https://doi.org/10.1016/j.neuroimage.2017.08.064

Climie, R. E. D., Moran, C., Callisaya, M., Blizzard, L., Sharman, J. E., Venn, A., … Srikanth, V. (2015). Abdominal obesity and brain atrophy in type 2 diabetes mellitus. *PLoS ONE*, *10*(11).

https://doi.org/10.1371/journal.pone.0142589

Cook, L. B. (2001). Extracting arterial flow waveforms from pulse oximeter waveforms apparatus. *Anaesthesia*, *56*(6), 551–555. https://doi.org/10.1046/j.1365-2044.2001.01986.x

Diaz-Otero, J. M., Garver, H., Fink, G. D., Jackson, W. F., & Dorrance, A. M. (2016). Aging is associated with changes to the biomechanical properties of the posterior cerebral artery and parenchymal arterioles. *American Journal of Physiology. Heart and Circulatory Physiology*, *310*(3), H365–H375. https://doi.org/10.1152/ajpheart.00562.2015

Ecobici, M., & Stoicescu, C. (2017). Arterial Stiffness and Hypertension - Which Comes First? *Maedica*, *12*(3), 184–190. Retrieved from http://www.ncbi.nlm.nih.gov/pubmed/29218066

Fabiani, M., Low, K. A., Tan, C. H., Zimmerman, B., Fletcher, M. A., Schneider-Garces, N., … Gratton, G. (2014). Taking the pulse of aging: Mapping pulse pressure and elasticity in cerebral arteries with optical methods. *Psychophysiology*, *51*(11), 1072–1088. https://doi.org/10.1111/psyp.12288

Faraci, F. M., & Heistad, D. D. (1990). Regulation of large cerebral arteries and cerebral microvascular pressure. *Circulation Research*, *66*(1), 8–17. https://doi.org/10.1161/01.res.66.1.8

Farasat, S. M., Morrell, C. H., Scuteri, A., Ting, C. T., Yin, F. C., Spurgeon, H. A., … Najjar, S. S. (2008). Pulse pressure is inversely related to aortic root diameter implications for the pathogenesis of systolic hypertension. *Hypertension*, *51*(2), 196–202. https://doi.org/10.1161/HYPERTENSIONAHA.107.099515

Figueras, F., Fernandez, S., Eixarch, E., Gomez, O., Martinez, J. M., Puerto, B., & Gratacos, E. (2006). Middle cerebral artery pulsatility index: Reliability at different sampling sites. *Ultrasound in Obstetrics and Gynecology*, *28*(6), 809–813. https://doi.org/10.1002/uog.2816

Forette, F., Seux, M. L., Staessen, J. A., Thijs, L., Babarskiene, M. R., Babeanu, S., … Birkenhäger, W. H. (2002). The prevention of dementia with antihypertensive treatment: New evidence from the systolic hypertension in Europe (syst-eur) study. *Archives of Internal Medicine*, *162*(18), 2046–2052. https://doi.org/10.1001/archinte.162.18.2046

Frith, C., & Dolan, R. (1996). The role of the prefrontal cortex in higher cognitive functions. *Cognitive Brain Research*, *5*(1–2), 175–181. https://doi.org/10.1016/S0926-6410(96)00054-7

Fukuda, D., Yoshiyama, M., Shimada, K., Yamashita, H., Ehara, S., Nakamura, Y., … Yoshikawa,

J. (2006). Relation between aortic stiffness and coronary flow reserve in patients with coronary artery disease. *Heart*, *92*(6), 759–762. https://doi.org/10.1136/hrt.2005.067934

Funane, T., Homae, F., Watanabe, H., Kiguchi, M., & Taga, G. (2014). Greater contribution of cerebral than extracerebral hemodynamics to near-infrared spectroscopy signals for functional activation and resting-state connectivity in infants. *Neurophotonics*, *1*(2), 025003. https://doi.org/10.1117/1.NPh.1.2.025003

Garcia-Polite, F., Martorell, J., Del Rey-Puech, P., Melgar-Lesmes, P., O'Brien, C. C., Roquer, J., … Balcells, M. (2017). Pulsatility and high shear stress deteriorate barrier phenotype in brain microvascular endothelium. *Journal of Cerebral Blood Flow and Metabolism*, *37*(7), 2614–2625. https://doi.org/10.1177/0271678X16672482

Gayda, M., Brun, C., Juneau, M., Levesque, S., & Nigam, A. (2008). Long-term cardiac rehabilitation and exercise training programs improve metabolic parameters in metabolic syndrome patients with and without coronary heart disease. *Nutrition, Metabolism and Cardiovascular Diseases*, *18*(2), 142–151. https://doi.org/10.1016/j.numecd.2006.07.003

Gelb, B. D. (2006). Marfan's syndrome and related disorders--more tightly connected than we thought. *The New England Journal of Medicine*, *355*(8), 841–844. https://doi.org/10.1056/NEJMe068122

Geurts, L. J., Zwanenburg, J. J. M., Klijn, C. J. M., Luijten, P. R., & Biessels, G. J. (2019). Higher Pulsatility in Cerebral Perforating Arteries in Patients With Small Vessel Disease Related Stroke, a 7T MRI Study. *Stroke*, *50*(1), 62–68. https://doi.org/10.1161/strokeaha.118.022516

Guerin, A. P., Blacher, J., Pannier, B., Marchais, S. J., Safar, M. E., & London, G. M. (2001). Impact of aortic stiffness attenuation on survival of patients in end-stage renal failure. *Circulation*, *103*(7), 987–992. https://doi.org/10.1161/01.CIR.103.7.987

Hashimoto, J., & Ito, S. (2009, October). Some mechanical aspects of arterial aging: Physiological overview based on pulse wave analysis. *Therapeutic Advances in Cardiovascular Disease*, Vol. 3, pp. 367–378. https://doi.org/10.1177/1753944709338942

Hazzouri, A. Z. Al, Newman, A. B., Simonsick, E., Sink, K. M., Tyrrell, K. S., Watson, N., … Yaffe, K. (2013). Pulse wave velocity and cognitive decline in elders: The health, aging, and body composition study. *Stroke*, *44*(2), 388–393. https://doi.org/10.1161/STROKEAHA.112.673533

Huppert, T. J., Diamond, S. G., Franceschini, M. A., & Boas, D. A. (2009). HomER: A review of

time-series analysis methods for near-infrared spectroscopy of the brain. *Applied Optics*, *48*(10). https://doi.org/10.1364/AO.48.00D280

Hwang, S.-J., Vasan, R. S., Larson, M. G., Pencina, M. J., Hamburg, N. M., Levy, D., & Benjamin, E. J. (2010). Arterial stiffness and cardiovascular events: the Framingham Heart Study. *Circulation*, *121*(4), 505–511. https://doi.org/10.1161/CIRCULATIONAHA.109.886655.Arterial

Iadecola, C., & Davisson, R. L. (2008, June 4). Hypertension and Cerebrovascular Dysfunction. *Cell Metabolism*, Vol. 7, pp. 476–484. https://doi.org/10.1016/j.cmet.2008.03.010

Jolly, T. A. D., Bateman, G. A., Levi, C. R., Parsons, M. W., Michie, P. T., & Karayanidis, F. (2013). Early detection of microstructural white matter changes associated with arterial pulsatility. *Frontiers in Human Neuroscience*, (NOV). https://doi.org/10.3389/fnhum.2013.00782

Jurca, R., Jackson, A. S., LaMonte, M. J., Morrow, J. R., Blair, S. N., Wareham, N. J., … Laukkanen, R. (2005). Assessing cardiorespiratory fitness without performing exercise testing. *American Journal of Preventive Medicine*, *29*(3), 185–193. https://doi.org/10.1016/j.amepre.2005.06.004

Khoueiry, G., Azab, B., Torbey, E., Abi Rafeh, N., Atallah, J. P., Ahern, K., … Chemaly, E. R. (2012). Aortic pulse pressure is associated with the localization of coronary artery disease based on coronary flow lateralization. *American Journal of Hypertension*, *25*(10), 1055–1063. https://doi.org/10.1038/ajh.2012.87

Kim, Y. S., Immink, R. V, Stok, W. J., Karemaker, J. M., Secher, N. H., & Van Lieshourt, J. J. (2008). Dynamic cerebral autoregulatory capacity is affected early in Type 2 diabetes. *Clinical Science*, *115*(7–8), 255–262. https://doi.org/10.1042/CS20070458

Klem, G. H., Lüders, H. O., Jasper, H. H., & Elger, C. (1999). The ten-twenty electrode system of the International Federation. The International Federation of Clinical Neurophysiology. *Electroencephalography and Clinical Neurophysiology. Supplement*, *52*, 3–6.

Kohn, J. C., Lampi, M. C., & Reinhart-King, C. A. (2015). Age-related vascular stiffening: Causes and consequences. *Frontiers in Genetics*, Vol. 6, p. 112. https://doi.org/10.3389/fgene.2015.00112

Kovacic, J. C., Moreno, P., Nabel, E. G., Hachinski, V., & Fuster, V. (2011, May 3). Cellular senescence, vascular disease, and aging: Part 2 of a 2-part review: Clinical vascular disease

in the elderly. *Circulation*, Vol. 123, pp. 1900–1910. https://doi.org/10.1161/CIRCULATIONAHA.110.009118

Lareau, E., Lesage, F., Pouliot, P., Nguyen, D., Le Lan, J., & Sawan, M. (2011). Multichannel wearable system dedicated for simultaneous electroencephalography/near-infrared spectroscopy real-time data acquisitions. *Journal of Biomedical Optics*, *16*(9), 096014. https://doi.org/10.1117/1.3625575

London, G. M., Asmar, R. G., O'Rourke, M. F., & Safar, M. E. (2004). Mechanism(s) of Selective Systolic Blood Pressure Reduction after a Low-Dose Combination of Perindopril/Indapamide in Hypertensive Subjects: Comparison with Atenolol. *Journal of the American College of Cardiology*, *43*(1), 92–99. https://doi.org/10.1016/j.jacc.2003.07.039

Mailey, E. L., White, S. M., Wójcicki, T. R., Szabo, A. N., Kramer, A. F., & McAuley, E. (2010). Construct validation of a non-exercise measure of cardiorespiratory fitness in older adults. *BMC Public Health*, *10*. https://doi.org/10.1186/1471-2458-10-59

Mancia, G., Fagard, R., Narkiewicz, K., Redón, J., Zanchetti, A., Böhm, M., … Zannad, F. (2013, October). 2013 Practice guidelines for the management of arterial hypertension of the European Society ofHypertension (ESH) and the European Society of Cardiology (ESC): ESH/ESCTask Force for the Management of Arterial Hypertension. *Journal of Hypertension*, Vol. 31, pp. 1925–1938. https://doi.org/10.1097/HJH.0b013e328364ca4c

McDonald, D. A. (2011). Blood flow in arteries. *EDWARD ARNOLD PUBL.* https://doi.org/10.1146/annurev.fluid.29.1.399

McDonough, I. M., Wong, J. T., & Gallo, D. A. (2013). Age-related differences in prefrontal cortex activity during retrieval monitoring: Testing the compensation and dysfunction accounts. *Cerebral Cortex*, *23*(5), 1049–1060. https://doi.org/10.1093/cercor/bhs064

Miller, E. K., & Cohen, J. D. (2001). An Integrative Theory of Prefrontal Cortex Function. *Annual Review of Neuroscience*, *24*(1), 167–202. https://doi.org/10.1146/annurev.neuro.24.1.167

Mitchell, G. F. (2008, November). Effects of central arterial aging on the structure and function of the peripheral vasculature: Implications for end-organ damage. *Journal of Applied Physiology*, Vol. 105, pp. 1652–1660. https://doi.org/10.1152/japplphysiol.90549.2008

Mitchell, G. F. (2015). Cerebral small vessel disease: Role of aortic stiffness and pulsatile hemodynamics. *Journal of Hypertension*, Vol. 33, pp. 2025–2028. https://doi.org/10.1097/HJH.0000000000000717

Mitchell, G. F., Van Buchem, M. A., Sigurdsson, S., Gotal, J. D., Jonsdottir, M. K., Kjartansson, Ó., … Launer, L. J. (2011). Arterial stiffness, pressure and flow pulsatility and brain structure and function: The Age, Gene/Environment Susceptibility-Reykjavik Study. *Brain*, *134*(11), 3398–3407. https://doi.org/10.1093/brain/awr253

Miyai, I., Tanabe, H. C., Sase, I., Eda, H., Oda, I., Konishi, I., … Kubota, K. (2001). Cortical mapping of gait in humans: a near-infrared spectroscopic topography study. *NeuroImage*, *14*(5), 1186–1192. https://doi.org/10.1006/nimg.2001.0905

Myers, J., Buchanan, N., Smith, D., Neutel, J., Bowes, E., Walsh, D., & Froelicher, V. F. (1992). Individualized ramp treadmill; Observations on a new protocol. *Chest*, *101*(5 SUPPL.), 236S-241S. https://doi.org/10.1378/chest.101.5.236S

Newman, A. B., Fitzpatrick, A. L., Lopez, O., Jackson, S., Lyketsos, C., Jagust, W., … Kuller, L. H. (2005). Dementia and Alzheimer's disease incidence in relationship to cardiovascular disease in the cardiovascular health study cohort. *Journal of the American Geriatrics Society*, *53*(7), 1101–1107. https://doi.org/10.1111/j.1532-5415.2005.53360.x

Ng, J. B., Turek, M., & Hakim, A. M. (2013, April 25). Heart disease as a risk factor for dementia. *Clinical Epidemiology*, Vol. 5, pp. 135–145. https://doi.org/10.2147/CLEP.S30621

O'Rourke, M. F. (2007). Arterial aging: Pathophysiological principles. *Vascular Medicine*, Vol. 12, pp. 329–341. https://doi.org/10.1177/1358863X07083392

O'Rourke, M. F., & Jiang, A. P. X. J. (2001). Pulse wave analysis. *British Journal of Clinical Pharmacology*, Vol. 51, pp. 507–522. https://doi.org/10.1046/j.0306-5251.2001.01400.x

Parikh, J. D., Hollingsworth, K. G., Kunadian, V., Blamire, A., & MacGowan, G. A. (2016). Measurement of pulse wave velocity in normal ageing: comparison of Vicorder and magnetic resonance phase contrast imaging. *BMC Cardiovascular Disorders*, *16*, 50. https://doi.org/10.1186/s12872-016-0224-4

Pase, M. P., Grima, N. A., Stough, C. K., Scholey, A., & Pipingas, A. (2012). Cardiovascular disease risk and cerebral blood flow velocity. *Stroke*, *43*(10), 2803–2805. https://doi.org/10.1161/STROKEAHA.112.666727

Pollonini, L., Olds, C., Abaya, H., Bortfeld, H., Beauchamp, M. S., & Oghalai, J. S. (2014). Auditory cortex activation to natural speech and simulated cochlear implant speech measured with functional near-infrared spectroscopy. *Hearing Research*, *309*, 84–93. https://doi.org/10.1016/j.heares.2013.11.007

Prenner, S. B., & Chirinos, J. A. (2015). Arterial stiffness in diabetes mellitus. *Atherosclerosis*, *238*(2), 370–379. https://doi.org/10.1016/j.atherosclerosis.2014.12.023

Purkayastha, S., Maffuid, K., Zhu, X., Zhang, R., & Raven, P. B. (2018). The influence of the carotid baroreflex on dynamic regulation of cerebral blood flow and cerebral tissue oxygenation in humans at rest and during exercise. *European Journal of Applied Physiology*, *118*(5), 959–969. https://doi.org/10.1007/s00421-018-3831-1

Rosa, J. (2016). From Mock Spanish to Inverted Spanglish: Language ideologies and the racialization of Mexican and Puerto Rican youth in the United States. In *Raciolinguistics: How language shapes our ideas about race* (pp. 65-). https://doi.org/10.1093/acprof:oso

Safar, M. E., & Smulyan, H. (2004). Coronary ischemic disease, arterial stiffness, and pulse pressure. *American Journal of Hypertension*, Vol. 17, pp. 724–726. https://doi.org/10.1016/j.amjhyper.2004.06.004

Scuteri, A., Tesauro, M., Guglini, L., Lauro, D., Fini, M., & Di Daniele, N. (2013). Aortic stiffness and hypotension episodes are associated with impaired cognitive function in older subjects with subjective complaints of memory loss. *International Journal of Cardiology*, *169*(5), 371–377. https://doi.org/10.1016/j.ijcard.2013.09.009

Segers, P., Rietzschel, E. R., De Buyzere, M. L., Stergiopulos, N., Westerhof, N., Van Bortel, L. M., … Verdonck, P. R. (2008). Three-and-four-element Windkessel models: Assessment of their fitting performance in a large cohort of healthy middle-aged individuals. *Proceedings of the Institution of Mechanical Engineers, Part H: Journal of Engineering in Medicine*, *222*(4), 417–428. https://doi.org/10.1243/09544119JEIM287

Song-Tao, A., Yan-Yan, Q., & Li-Xia, W. (2010). The severity of coronary artery disease evaluated by central systolic pressure and fractional diastolic pressure. *North American Journal of Medical Sciences*, *2*(5), 218–21820. https://doi.org/10.4297/najms.2010.2218

Singer, J., Trollor, J. N., Baune, B. T., Sachdev, P. S., & Smith, E. (2014, May). Arterial stiffness, the brain and cognition: A systematic review. *Ageing Research Reviews*, Vol. 15, pp. 16–27. https://doi.org/10.1016/j.arr.2014.02.002

Singer, J., Trollor, J. N., Crawford, J., O'Rourke, M. F., Baune, B. T., Brodaty, H., … Smith, E. (2013). The Association between Pulse Wave Velocity and Cognitive Function: The Sydney Memory and Ageing Study. *PLoS ONE*, *8*(4). https://doi.org/10.1371/journal.pone.0061855

Stamatakis, E., Hamer, M., O'Donovan, G., Batty, G. D., & Kivimaki, M. (2013). A non-exercise

testing method for estimating cardiorespiratory fitness: associations with all-cause and cardiovascular mortality in a pooled analysis of eight population-based cohorts. *European Heart Journal*, *34*(10), 750–758. https://doi.org/10.1093/eurheartj/ehs097

Steppan, J., Barodka, V., Berkowitz, D. E., & Nyhan, D. (2011). Vascular stiffness and increased pulse pressure in the aging cardiovascular system. *Cardiology Research and Practice*, *2011*, 263585. https://doi.org/10.4061/2011/263585

Stone, J., Johnstone, D. M., Mitrofanis, J., & O'Rourke, M. (2015). The mechanical cause of age-related dementia (Alzheimer's Disease): The brain is destroyed by the pulse. *Journal of Alzheimer's Disease*, Vol. 44, pp. 355–373. https://doi.org/10.3233/JAD-141884

Tan, C. H., Low, K. A., Chiarelli, A. M., Fletcher, M. A., Navarra, R., Burzynska, A. Z., … Fabiani, M. (2019). Optical measures of cerebral arterial stiffness are associated with white matter signal abnormalities and cognitive performance in normal aging. *Neurobiology of Aging*. https://doi.org/10.1016/j.neurobiolaging.2019.08.004

Tan, C. H., Low, K. A., Kong, T., Fletcher, M. A., Zimmerman, B., MacLin, E. L., … Fabiani, M. (2017). Mapping cerebral pulse pressure and arterial compliance over the adult lifespan with optical imaging. *PLoS ONE*, *12*(2). https://doi.org/10.1371/journal.pone.0171305

Themelis, G., D'Arceuil, H., Diamond, S. G., Thaker, S., Huppert, T. J., Boas, D. A., & Franceschini, M. A. (2007). Near-infrared spectroscopy measurement of the pulsatile component of cerebral blood flow and volume from arterial oscillations. *Journal of Biomedical Optics*, *12*(1), 014033. https://doi.org/10.1117/1.2710250

Toth, P., Tarantini, S., Csiszar, A., & Ungvari, Z. (2017). Functional vascular contributions to cognitive impairment and dementia: Mechanisms and consequences of cerebral autoregulatory dysfunction, endothelial impairment, and neurovascular uncoupling in aging. *American Journal of Physiology - Heart and Circulatory Physiology*, Vol. 312, pp. H1–H20. https://doi.org/10.1152/ajpheart.00581.2016

Uangpairoj, P., & Shibata, M. (2013). Evaluation of vascular wall elasticity of human digital arteries using alternating current-signal photoplethysmography. *Vascular Health and Risk Management*, *9*, 283–295. https://doi.org/10.2147/vhrm.s43784

Vitorio, R., Stuart, S., Rochester, L., Alcock, L., & Pantall, A. (2017, December 1). fNIRS response during walking — Artefact or cortical activity? A systematic review. *Neuroscience and Biobehavioral Reviews*, Vol. 83, pp. 160–172.

https://doi.org/10.1016/j.neubiorev.2017.10.002

Vlachopoulos, Charalambos, Michael O'Rourke, and W. W. N. (2011). *McDonald's blood flow in arteries: theoretical, experimental and clinical principles*. CRC press.

Wåhlin, A., Ambarki, K., Birgander, R., Malm, J., & Eklund, A. (2014). Intracranial pulsatility is associated with regional brain volume in elderly individuals. *Neurobiology of Aging*, *35*(2), 365–372. https://doi.org/10.1016/j.neurobiolaging.2013.08.026

West, R. L. (1996). An application of prefrontal cortex function theory to cognitive aging. *Psychological Bulletin*, *120*(2), 272–292. https://doi.org/10.1037/0033-2909.120.2.272

Wert, D. M., Brach, J. S., Perera, S., & VanSwearingen, J. (2013). The association between energy cost of walking and physical function in older adults. *Archives of Gerontology and Geriatrics*, *57*(2), 198–203. https://doi.org/10.1016/j.archger.2013.04.007

Williams, B., Lacy, P. S., Thom, S. M., Cruickshank, K., Stanton, A., Collier, D., … O'Rourke, M. (2006). Differential impact of blood pressure-lowering drugs on central aortic pressure and clinical outcomes: Principal results of the Conduit Artery Function Evaluation (CAFE) study. *Circulation*, *113*(9), 1213–1225. https://doi.org/10.1161/CIRCULATIONAHA.105.595496

Williams, B., Lacy, P. S., Thurston, H., Thom, S., Hughes, A., Cruickshank, K., … O'Rourke, M. (2006). Response to letters regarding article, "Differential impact of blood pressure-lowering drugs on central aortic pressure and clinical outcomes: Principal results of the Conduit Artery Function Evaluation (CAFE) Study" [5]. *Circulation*, Vol. 114. https://doi.org/10.1161/CIRCULATIONAHA.106.640870

Willie, C. K., Tzeng, Y. C., Fisher, J. A., & Ainslie, P. N. (2014, March 1). Integrative regulation of human brain blood flow. *Journal of Physiology*, Vol. 592, pp. 841–859. https://doi.org/10.1113/jphysiol.2013.268953

Wilson, P. W. F., D'Agostino, R. B., Levy, D., Belanger, A. M., Silbershatz, H., & Kannel, W. B. (1998). Prediction of coronary heart disease using risk factor categories. *Circulation*, *97*(18), 1837–1847. https://doi.org/10.1161/01.CIR.97.18.1837

Winston, G. J., Palmas, W., Lima, J., Polak, J. F., Bertoni, A. G., Burke, G., … Shea, S. (2013). Pulse pressure and subclinical cardiovascular disease in the multi-ethnic study of atherosclerosis. *American Journal of Hypertension*, *26*(5), 636–642. https://doi.org/10.1093/ajh/hps092

Wisely, N. A., & Cook, L. B. (2001). Arterial flow waveforms from pulse oximetry compared with measured Doppler flow waveforms apparatus. *Anaesthesia*, *56*(6), 556–561. https://doi.org/10.1046/j.1365-2044.2001.01987.x

Zarrinkoob, L., Ambarki, K., Wahlin, A., Birgander, R., Carlberg, B., Eklund, A., & Malm, J. (2016). Aging alters the dampening of pulsatile blood flow in cerebral arteries. *Journal of Cerebral Blood Flow and Metabolism*, *36*(9), 1519–1527. https://doi.org/10.1177/0271678X16629486

Zwanenburg, J. J. M. (2018, January 1). Increased Rather than Decreased Small Vessel Pulsatility in Patients with Progressing Cerebral White Matter Hyperintensities. *Radiology*, Vol. 286, pp. 363–364. https://doi.org/10.1148/radiol.2017172090

5.9 Supplementary data

5.9.1 NIRS-estimated Heart Rate

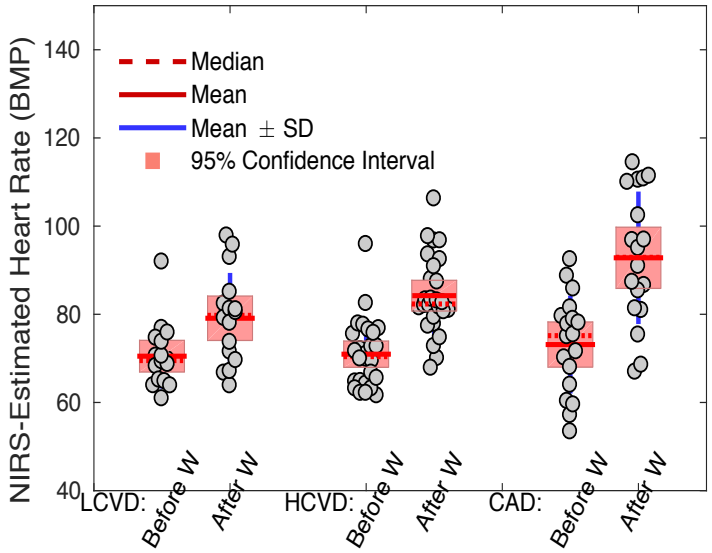

Figure 5-10, NIRS-estimated heart rate. BMP is a notation for beats per minutes

5.9.2 Cerebral pulse amplitude and PRF versus blood pressure and METS

		LCVRF		HCVRF		CAD	
		BW	AW	BW	AW	BW	AW
CPA	METS	0.34, 0.19	-0.02, 0.91	0.19, 0.34	-0.15, 0.43	0.14, 0.57	0.27, 0.26
	Systole BP	-0.14, 0.60	0.31, 0.24	-0.10, 0.61	-0.21, 0.29	0.122, 0.62	0.22, 0.36
	Diastole BP	0.31, 0.24	-0.10, 0.68	-0.21, 0.29	0.33, 0.08	0.22, 0.36	-0.005, 0.98
PRF	METS	0.24, 0.36	-0.27, 0.30	0.22, 0.26	-0.15, 0.45	-0.15, 0.45	0.19, 0.432
	Systole BP	-0.04, 0.86	0.029, 0.91	-0.21, 0.28	0.15, 0.44	-0.44, 0.06	-0.06, 0.80
	Diastole BP	0.54, 0.02	0.41, 0.10	-0.19, 0.33	0.43, 0.02	-0.32, 0.18	0.017, 0.944

Table 5-2 First number indicates correlation (r) and second number indicates p-value. Sex effect is regressed from CPA data before correlation analysis.

5.9.3 Short note on PRF

PRF data (Figure 5-8B) indicated that in the HCVRF group, the global PRF and Framingham 10-year CHD risk prediction are negatively but not significantly correlated (r=-0.33, p= 0.09). This association was not present for the LCVRF group (r= -0.03, p= 0.892). The results was identical for AW.

CHAPTER 6 CEREBRAL PULSATILITY AND COGNITION

6.1 Introduction

Cognitive decline is associated with age-related functional and structural modifications in the brain (Girouard & Munter, 2018). Research on vascular cognitive impairment has linked age-related differences in cognitive performance to cerebrovascular health (Girouard & Munter, 2018; O'Brien et al., 2003).

Higher cerebral pulsatility could lead to cognitive decline because of impairment in the metabolism of neurons (Scuteri et al., 2013). In this regard, several pathways have been suggested to link age-related arterial stiffness (and changes of the pulse pressure) to cerebral microvascular disease and cognitive decline (Farasat et al., 2008; Iadecola & Davisson, 2008; Scuteri et al., 2007). Age-related stiffening of the central elastic arteries is linked to fatigue and fracture of the distensible elements on the walls of the arteries as the result of long-term cyclic circumferential and shearing stress (McDonald, 2011). With stiffening of the arteries their capacity to damp the pulsatile fluctuation of the blood pressure reduces (the impaired Windkessel mechanisms). Over time, such alteration leads to distending of the central pulse pressure (Farasat et al., 2008) and the increased CBF pulsatility (Mitchell, 2018). Primarily, with the higher pulsations, the mechanisms of pressure-dependent myogenic tone lead to constriction of the arterioles to protect the capillaries from higher flow pulsations. The costs of this kind of protection is reduction of the blood flow and impairment in the metabolism of the tissue (Mitchell, 2014)[10]. With long-term constrictions, the arterioles remodel inward and cause even a higher resistance to flow. In conjunction with this effect, the response of the arterioles to vasodilation substances that are essential for flawless neurovascular coupling reduces (Scuteri et al., 2007). Such hemodynamic modification could damage vulnerable cerebral capillaries and impair their function (Maillard et al., 2016; Mitchell, 2014, 2018). Indeed, several studies suggested that higher central arterial stiffness induces cerebral

[10] Recent literature exploring aging-related changes in CMRO2 reported that the CMRO2 rate increases while CBF decreases with age (Peng et al., 2014).

microvascular damage (Chirinos, 2016; Tsao et al., 2016, 2013) concomitantly with altered neurovascular coupling (Toth, Tarantini, Csiszar, & Ungvari, 2017). Impairment of the hemodynamic that contribute to maintaining the metabolic needs of the neuron (Mathiesen, Caesar, Akgören, & Lauritzen, 1998) would support the hypothesis that higher cerebral pulsatility would negatively influence task-evoked responses. Previously, studies linked higher PWV to lower cerebrovascular reserve[11] (DuBose et al., 2018) and altered task reaction time (Jennings & Choi, 1983).

Brain aging does not affect cognitive functions to the same extent. The presence of age-related functional reorganization mechanisms promotes some degree of cognitive preservation in older adults (Martins, Joanette, & Monchi, 2015). In the general sense, our current understanding of age-related functional reorganization is limited to the knowledge that in the older adults, in addition to typically recruited regions, the brain recruits other networks to respond to tasks. It does so because age-related structural changes and metabolic modifications could impair the typically recruited regions. Despite this finding, the link between regional vascular function and functional reorganization remains to be elucidated. It is not entirely clear why the brain recruits these networks. A hypothesized reason is lower pulsatility and this is explored here. Here, it has been hypothesized that spatial regions of the brain with age-related functional reorganization are correlated with regions with lower pulsatile stress. In other words, the brain may recruit the regions with better potential for neurovascular coupling to preserve performance in older adults. We used Stroop color-word interference to test our hypothesis. In the literature, the Stroop test is used to study inhibition and cortical functions in the frontal lobe (MacLeod, 1991). The same participants in article 1 (chapter 4) performed this task following the resting state measures. Functional NIRS data were synchronized with ECG and PPG and were used to index cerebral pulsatility and to capture hemodynamic activity during the Stroop color-word interference task in the block design

[11] DuBose *et al.* (2018), explored the association between carotid-femoral PWV and cerebrovascular reserve (change in global cerebral blood flow following intravenous infusion of acetazolamide) and reported that there is a negative association between these petameters. They concluded that that higher age-related aortic stiffness may at least partially contribute to impaired ability of cerebrovascular to dilate maximally to augment blood flow in response to a stimulus with aging in humans.

fashion. PC-MRI data were used to measure arterial pulsatility in the cervical subarachnoid space. The aims of this study were twofold: (1) To assess the relationship between cerebral pulsatility in the frontal regions and reaction time for the color-word interference Stroop test. We hypothesize that higher pulsatility (measured with functional NIRS) in the frontal lobe is associated with greater reaction time. (2) To assess the spatial relationship between cerebral pulsatility and functional reorganization in the Stroop test. It was expected task-evoked functional reorganization is correlated with regions with lower pulsatile stress. The second aim of this study that is mapping the task-evoked activations from functional NIRS data is underway[12].

6.2 Material and methods

The participants were the same individuals as in article 1 (chapter 4) who performed Stroop color-word interference task right after resting state functional NIRS. The materials and methods are identical to those explained in chapter 3 (experiment I.I) and article 1 (chapter 4). The general steps of the data analysis are as follows. (1) Use the pulsatility parameter extracted from resting state NIRS data and compare it between younger and older adults (statistics contrast map). (2) Draw the map of evoked activations for the Stroop-color word interference test. (3) Explore whether brain regions involved in functional reorganization are spatially correlated to regions that had lower *t*-score in the statistics contrast map in (1). (4) To assess the contrast between the pulsatility parameter during the activation block versus the rest block.
In this chapter, we only addressed part (1) due to time limitations. For now, part (2) is discussed based on our expectations and prior art.

6.2.1 The pulsatile versus the steady component of the blood flow

The total cerebral blood flow waveform extracted from PC-MRI data (C2-C3) was used to calculate the steady (mean CBF) and the pulsatile component of CBF. The latter was calculated from the cumulative integral of the total CBF waveform after subtraction of the mean CBF. The pulsatile component of blood flow was then calculated by subtracting peak and nadir in this curve

[12] Task-evoked activations for Stroop color-word interference for 5 older adults showed activations on left and right inferior frontal lobe. The analysis was performed using HOMER2 (Huppert et al., 2009).

(Wåhlin, Ambarki, Birgander, Malm, & Eklund, 2014). Linear regression was used to adjust for the eTIV for the steady and pulsatile components. Both of these variables were then normalized to the [0, 1] range.

6.3 Results

6.3.1 Cerebral pulsatility and Stroop test reaction time

Reaction time for correct responses of the Stroop color-word interference across the blocks of the task was averaged and used for analysis. Our data indicated that there is a statistically significant association between years of education and response time to the task (r=-0.29, p=0.047). After controlling for years of education, correlation analysis indicated a statistically significant association between $NIRS_{PTTp}$ and reaction time in older (r=-0.452, p=0.003) and younger (r= -0.334, p=0.023) adults. It is to be noted that the $NIRS_{PTTp}$ was averaged for superior, middle and inferior frontal areas and linear regression was used to control for the effect of sex and height in this variable.

Our data indicated that in the older adults, the number of incorrect answers to the Stroop color-word interference test (average across all the blocks of task) was associated to $NIRS_{PTTp}$ (r=-30.13, p=0.041) but not for younger adults (p>0.1).

6.3.2 The pulsatile versus the steady component of the blood flow measured with PC-MRI and its association to task response time

There was a statistically significant difference (t-test, p<0.001) for the pulsatile component of blood flow (0.67± 0.14) for older adults compared to younger adults (0.31±0.07). The steady component blood flow was statistically significantly associated to the pulsatile component of blood flow in older (r=-0.59, p<0.001) and younger adults (r=-0.41, p=0.032).

Correlation analysis showed a statistically significant association between reaction time for correct responses to the Stroop color-word interference test and the pulsatile component of CBF. The correlations were (r=0.511, p=0.006) for older and (r=0.239, p=0.022) for younger adults. For the steady component, this association was (r=-0.34, p=0.031) for older and (r=-0.27, p=0.043) for younger adults.

6.3.3 Cerebral pulsatility statistical contrast map between younger and older adults

Resting state-data was used to perform region-wise comparison of $NIRS_{PTTp}$ for younger and older participants is illustrated in Figure 6-1. The regions are those mentioned in chapter 4 (article 1). The effect of sex and height was removed from the data using linear regression prior to multiple comparisons. The results yielded statistically higher *t*-values for left middle and superior temporal compared to other regions. Left frontal cortex subregions had higher *t*-value compared to the right frontal subregions.

Within left frontal region, left inferior frontal region had higher *t*-score compared to other frontal subregions in the left hemisphere. For the right hemisphere, right inferior frontal region had lowest *t*-score compared to other frontal subregions in the right hemisphere.

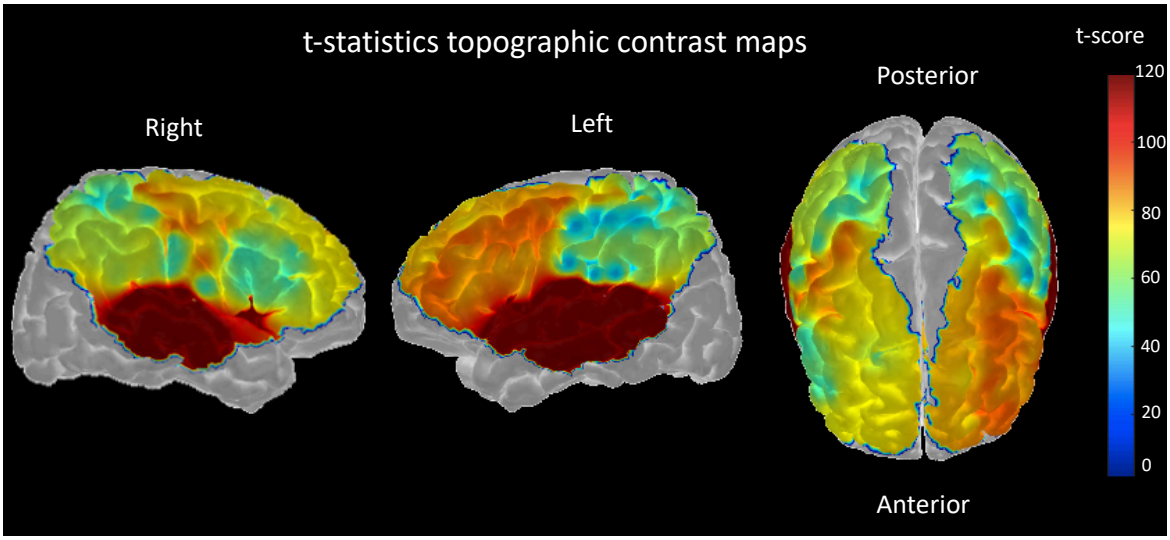

Figure 6-1 *t*-statistics topographic contrast maps ($p<0.05$) for region-wise PTTp for younger 30 and 30 older health participants extracted from resting state data. Prior to analysis, linear regression was used to control for the impact of sex and height. Higher *t*-scores represent regions affected the most by aging when younger adults are compared to older adults for PTTp parameters. The p-values are Bonferroni corrected ($p<0.05$).

6.4 Executive discussion

The present chapter assesses the association between cerebral pulsatility and reaction time to the correct responses in the color-word interference Stroop test. Our results indicated that a higher pulsatility measured with NIRS (lower PTTp) is associated with slower reaction time. Our finding agrees with several studies that reported a strong correlation between age-related arterial stiffness and lower cognitive performance (Mitchell et al., 2011; Poels et al., 2007; Waldstein et al., 2010). The dense network of the arteries is highly involved in the regulation of the local CBF and providing the metabolism needs of the neurons (McDonald, 2011). With aging, central pulse pressure increases and the pulse of blood with higher energy travel to the brain (McDonald, 2011). Brain aging is linked to alterations to cerebral hemodynamics and contributes to diminished neurovascular coupling (Fabiani et al., 2014) and emerging neurodegenerative conditions (Hughes et al., 2018). A manifestation of such age-related changes is cognitive decline (Iadecola, 2010). Studies indicated a link between pulse pressure and abnormal flow patterns that is associated with Alzheimer's disease (Qiu, Winblad, & Fratiglioni, 2005). Studies with PWV reported that higher pulse pressure was strongly linked with lesions in the cerebral microvessels and reduced scores in multiple cognitive domains (Ashley, E. A., & Niebauer, 2004). Not only higher pulse pressure measured in the central arteries but also higher pulsatility assessed with blood pressure variability (measured on the arm) is linked to lower cognitive performance (Scuteri et al., 2013). Consequently, the interpretation we provide to account for our results is compatible with many of the previously proposed dynamic effect of vascular stiffness on cognitive performance.

Our results indicated that the pulsatile component and steady component of blood flow measured with PC-MRI are associated with reaction time to the Stroop color-word interference task (steady and pulsatile components are correlated and are not independent phenomena). However, it is to be noted that compared to the association of the steady component, the pulsatile component had 1.6 times greater association to the reaction time of the task. This finding is in agreement with Pase et al. (2012) who reported that compared to the mean blood flow velocity, the pulsatile component of velocity in MCA is a stronger predictor of aging (Pase, Herbert, Grima, Pipingas, & O'Rourke, 2012). Previously, Ündar et al. (2002) reported that flow pulsatility is associated with the energy gradient of the pulse that is getting delivered to the brain. In a simulation where the mean pressure was kept constant, Shepard et al (1966) reported that under pulsatile flow, about 2.4 times more

energy was delivered to the tissue than under steady flow. Therefore, our finding agrees with studies reporting that mean and pulsatile component of blood velocity could promote cerebral pathology and cognitive decline.

Our statistical contrast map for cerebral pulsatility between old and younger adults indicated that the left inferior frontal gyrus had a higher *t*-score (more affected by the impact of aging when younger are compared to older) compared to other frontal subregions. This result is in agreement with the previous studies that reported a greater task-evoked activation for Stroop color-word interference in the left inferior frontal gyrus in older adults compared to younger adults (Langenecker, Nielson, & Rao, 2004; Zysset, Schroeter, Neumann, & Yves von Cramon, 2007). We hypothesize that higher pulsatility (higher circumferential and shear stress) in the left inferior frontal gyrus contributes to the impaired regional metabolic needs of the neuron as they demand a higher level of activation to respond to the task. In addition, the statistical map showed that there is lower *t*-score (less affected by the impact of aging as compared between young and older) in the right inferior frontal gyrus compared to the other frontal subregions in the right hemisphere. Interestingly, previous studies suggested that there is functional reorganization in the brain of the older adults in the right inferior frontal gyrus (Langenecker et al., 2004; MacLeod, 1991; Zysset et al., 2007). As the work continues, we may test our hypothesize that the brain is recruiting the regions with lower pulsatility to make use of a better neurovascular coupling. This discussion can be amended when the analysis is complete.

CHAPTER 7 GENERAL DISCUSSION

This thesis explored brain aging with a focus on cerebrovascular aging and its impact on the hemodynamic and anatomical alterations in the brain, making use of two complementary imaging techniques, functional NIRS and MRI. Two scientific articles were included, followed by a chapter with results which may appear in a future article. These chapters present the results of three studies conducted on humans. These results were addressed the impact of healthy aging on brain pulsatility and its association with structural changes in the brain. They also addressed the impact of CVRF continuum and CAD and its downstream impact on brain pulsatility. In this chapter, the objectives of this thesis are recalled for a general overview and critique of the results and their analysis.

7.1 First objective

The first study addresses the first objective by reporting that regional cerebral pulsatility is correlated with regional cortical thickness in 30 healthy and non-demented older adults. Our initial hypothesis was that regional cortical thickness is associated with regional cerebral pulsatility. However, our results did not show this association in the 30 healthy younger adults who participated this study. This may be because of higher elasticity in the arteries of younger adults (Chiarelli et al., 2017), their lower accumulated oxidative stress and vascular damage (Toth, Tarantini, Csiszar, & Ungvari, 2017), and their more effective vascular repair mechanisms (Assar et al., 2012; Hoenig, Bianchi, Rosenzweig, & Sellke, 2008). Chiarelli et al. (2017) had similar results and reported that the association between cortical atrophy and reducing arterial elasticity was seen after the age of 48 (our younger participants were between 19 and 31 years old).

The association between cerebral pulsatility and atrophy was strong and significant across our older participants (65 to 75 years old). One may infer that it is not pulsatility itself, but rather higher pulsatility in the aged arteries of the older adults that is associated with cortical thinning.

Literature reported that higher PWV is an index of higher central arterial stiffness (Nichols et al., 2008). PWV is determined by measuring the ratio of pulse transit time to a known vascular path length, often in the carotid-femoral arteries. It is for this reason that we also measured PTTp using NIRS in order to link our observations to the literature. However, we did not have the exact length of the arteries from the heart to the location of measurement in the brain to calculate this parameter

for the cerebral arteries. The length of the large arteries in the brain could be measured from 3D-TOF-MRA. With a measure of the pulse in the neck and the other of pulse measure in the brain, the pulse transit time could be measured and PWV calculation for the brain could be achieved. This could be tested in a future study; however, in the present data with the heart as the reference point, NIRS sources and detectors were positioned at multiple sites on the cortex and hence the length of the arterial travel path behaves as a confounding factor associated with the time that it takes for the blood to travel from the heart to the measurement location. To control for the differences in the arterial travel paths to each cortical region, the association between cortical thickness and cerebral pulsatility was evaluated for each cortical region individually, contrasting older and younger adults. The pulsatility parameter was correlated with arterial flow pulsatility as measured with PC-MRI. The flow pulsatility measured with PC-MRI is related to arterial stiffness (Peper et al., 2018) and is correlated with cortical thinning (Wåhlin et al., 2014). It is to be noted that flow pulsatility as measured with PC-MRI represents arterial pulsatility as it is directly measured in the arteries entering the intracranial compartment. However, for NIRS, we employ the term "cerebral pulsatility" rather than arterial pulsatility. In the young healthy individuals, arterial pulsatility is absent from capillaries and veins (Themelis et al., 2007) and therefore pulsatility measured with NIRS is related to arterial pulsatility. However, in an older adult, as the result of compromised Windkessel mechanisms, higher pulse pressure may penetrate to capillaries and transmit to venules, leading to pulsatile capillary and venule flow (Thorin-Trescases et al., 2018). Therefore, the pulse measured with NIRS is a superimposed impact of arteries, arterioles, capillaries and venules, the largest contribution of which is still arterial pulsatility (as it originates from heart pulsation, which is the main driving force). Therefore, interpreting the NIRS pulsatility results between young and older adults should be done with caution. Hence, further mathematical modeling and simulation of capillary and venule behavior are needed to determine how much pulsatility is transmitted to capillaries and to what extent the transmission confounds the arterial pulsatility results in the older adults.

It was mentioned before that since the human brain is encased in a rigid cranium, optimal intracranial pressure depends on mechanical coupling between blood, CSF and brain volumes where systolic distention in the intracranial compartment accommodates the increased systolic blood volume (Stoquart-ElSankari et al., 2007; Wagshul, Eide, & Madsen, 2011; Wåhlin, Ambarki, Birgander, Malm, & Eklund, 2014). Blood and CSF are incompressible fluids and the augmented

volume thus increases CSF pressure (Wagshul et al., 2011). The incoming blood thereby induces a pressure gradient that is then partially compensated by pushing the CSF to the spinal canal (Alperin, Lee, Loth, Raksin, & Lichtor, 2000; Balédent, Henry-Feugeas, & Idy-Peretti, 2001; Wåhlin et al., 2010). This increased pressure propagates through all the intracranial compartments, including brain tissue and CSF (Wagshul et al., 2011). This higher intracranial pressure also pushes the brain in the direction of the foramen magnum (Uftring, Chu, Alperin, & Levin, 2000), which also tends to compress the cerebral vasculature (Bragin, Bush, & Nemoto, 2013) and in a feedback loop amplifies the resistance of cerebral vasculature to blood flow (Chiarelli et al., 2017). Hence, the cerebral pulsatility measured with functional NIRS may be affected by the increased arterial resistance to flow that is induced by augmented CSF pressure in addition to the resistance to flow induced by arterial stiffening.

Despite having statistically significant results addressing objective 1, the experiment was cross-sectional and hence was influenced by the limitations inherent to cohorts as well as several recruitment biases across the groups. Our younger participants (19-31 years old) were on average more educated compared to the older adults (65-75 years old), which may confound the comparison in cortical thickness between these groups (Jung et al., 2018). Because of the age range of the younger group, they were often students and thus actively involved in their courses and part time jobs, some of them in academic research. By contrast, the older participants who were educated (even master level) were often retired long ago. Some of the older participants were unemployed for more than 8 years and some of them had part time jobs of varying mental stimulation. Two of our participants played piano, which reportedly has a positive impact on brain elasticity (Jäncke, 2009). Some play memory-demanding games such as bridge (3 participants) (Clarkson-Smith & Hartley, 1990). All these factors could in some way bias our results.

Another limitation that was noted at the end of recruitment was that despite our intention to have a sample of participants representing the healthy older adult population, the older adults who were confident about themselves and their cognitive abilities volunteered to come for the study. About 35 percent of the participants claimed that they considered themselves to be superior-functioning older individuals compared to their friends. Designing longitudinal studies in with follow-ups on individuals would track changes in participants with reference to their own baselines, thereby providing a safer approach when it comes to interpretation of results.

7.2 Second objective

The second article responded to the second objective by reporting that cerebral pulsatility as quantified from the functional NIRS data is higher in the CAD patients compared to the LCVRF and HCVRF groups (60 older adults altogether). In the literature, the lower damping of the pulsatility in the central arteries has been linked to altered composition and thickening of the vessel walls, to enhanced stiffness and to evolving geometry (Farasat et al., 2008; Izzo & Mitchell, 2007; Vlachopoulos, Charalambos, Michael O'Rourke, 2011). The literature reports that these modifications cause extending of the central pulse pressure (Franklin, 2006), which causes higher CBF pulsatility that eventually damages the vulnerable cerebral vasculature (Mitchell et al., 2011). Therefore, our initial hypothesis was that the cerebral pulse amplitude is higher in the CAD, HCVRF and then LCVRF groups, respectively. However, our data showed that there is no statistically significant difference between HCVRF and LCVRF. This is likely because several participants in the HCVRF group were using a combination of medicinal treatments including, among others: beta-blockers and calcium-antagonists that reduce heartrate or lower the tension from vessel walls (Akbar & Alorainy, 2014; Guerin et al., 2001); and ACE-inhibitors which decreases the central pulse pressure (Mahmud & Feely, 2000). The downstream effect of such treatment is discussed in the studies reporting improved cognitive functions in the individuals who had three months treatment with ACE-inhibitors although this treatment did not cause a significant improvement in vessels geometry metrics (Csikai et al., 2019). In the literature, the central arteries are reported to damp more than fifty percent of the pulse pressure originating from the heart (Stergiopulos, Segers, & Westerhof, 1999) and so it is reasonable that targeted treatment on the central arteries could influence the cerebral pulse amplitude and PRF. Although the CAD group was using several treatments (Table 5-1 in article 2) that could influence the heart function and vessel walls, the CAD group still had significantly higher cerebral pulse amplitude compared to the other two groups.

One may inquire whether functional NIRS is insufficiently sensitive for the detection of the contrast in damage in the vasculature between LCVRF and HCVRF, as the distinction between these is much less than with the CAD group. To answer this question, we attempted to find functional NIRS data sets from individuals with untreated risk factors (such as untreated hypertension) to compare them with our NIRS pulsatility data; however, such cohorts are not easily available in Canada with

this country's easy access to treatment. To address this limitation, an arterial stiffness measure such as PWV, transcranial doppler ultrasound or PC-MRI could support exploring the association between indices of cerebral pulsatility and indices of arterial stiffness. Is the sensitivity of NIRS to blame for the subtle difference between LCVRF and HCVRF because of using the medication? If the index of arterial stiffness can detect the differences between LCVRF and HCVRF, especially in the MCA, which is spatially closer to cortical microcirculation, but the pulsatility measured with functional NIRS cannot (even with functional NIRS measurement with higher sampling rates), then we may question the sensitivity of functional NIRS. We have planned to continue the pulsatility experiment on the CAD patients, in parallel with sessions for functional NIRS, MRI (including structural MRI and PC-MRI) and PPG.

As part of the second objective, the changes in PRF were explored. Our data do not indicate a statistically significant association between PRF and cardiovascular status. There could be several reasons for this result. Fabiani et al. (2014) and Tan et al. (2017) reported that the PRF measurement could be improved with a denser optical array (about 750 oxyhemoglobin channels in their more recent study versus 190 oxyhemoglobin channels in their older study and a longer recording time (from 72 s to 360 s). This improvement brought the correlation of the PRF measure between two task blocks from $\{0.56, p<0.001\}$ to $\{0.75, p<0.001\}$. Our study leveraged a medium-sized montage (128 oxyhemoglobin channels) with a short recording time (on average 15 sec for BW or AW). These intermediate attributes may explain why we failed to detect an appreciable difference between the three groups.

Nevertheless, in the data that we acquired for the first objective (article 1), the correlation of PRF across the eight blocks of resting state for the total of 640 s was $\{0.71, p<0.001\}$ across older adults. In the data acquired for the first objective, we did not have a dense optical array but the laser power was 20 mW (compared to Fabiani et al., that laser power was 10 mW). Therefore, it is possible that with a higher laser power and a longer recording time even with medium-sized arrays we could achieve higher PRF reliability across the blocks.

To close with objective 2, the author suggests an improvement to the PRF nomenclature. "PRF" has referred to "pulse relaxation function" perhaps ought to mean "pulse reflection function." In the literature, a diastolic waveform is customarily modeled as the superposition of a relaxation waveform and a reflection waveform (Liao, Cheng, Sung, Yu, & Chen, 2011; Nichols et al., 2008). Fabiani et al. (2014) approximated the exponential function of the arterial relaxation waveform as

a straight line. The area under this line was then subtracted from the area of the diastolic waveform. They named this parameter "pulse relaxation function (PRF)." In the article in which the second objective was addressed, we followed the literature (Chiarelli et al., 2017; Tan et al., 2019, 2016) and called this parameter "PRF." However, the term "pulse reflection function" is a better choice to describe this parameter as the estimation of relaxation is subtracted from the diastolic waveform and the remaining number is estimation of reflection.

7.3 Third objective

Objective 3 could not be completed due to time constraints, though the analysis is ongoing and the results are promising. Here some parts of the results that are completed are briefly discussed. Cerebral pulsatility resting state data were used to delineate a statistical contrast map for the young and older participants. This map for the frontal subregions showed that the left inferior frontal region has a higher PTTp *t*-score when compared between young and older to the right inferior frontal region. The literature suggests that the task-evoked activations from the word-color interference Stroop test for young individuals are located in the left inferior frontal region. For the older individuals, the right inferior frontal is also activated (functional reorganization). We hypothesize that the brain recruits spatial regions with lower pulsatile stress on the underlying vasculature for functional reorganization. For objective 3, we will complete the analysis of task-evoked responses for the color-word interference Stroop test spatially to compare task-evoked regions with our pulsatility results. The promising part is that the fMRI studies on the same subsection of the Stroop test reported that in the younger adults, the left inferior frontal gyrus is a task-activated region and for older adults both the left inferior frontal gyrus and the right inferior frontal gyrus are recruited. The literature relates the activation in the right inferior frontal gyrus to age-related functional reorganization (Zysset, Schroeter, Neumann, & Yves von Cramon, 2007).
On average, we observed higher pulsatility in most subregions of the left hemisphere compared to the right hemisphere. This asymmetry in the pulsatility could be the consequence of anatomical arterial asymmetry. The left ICA is a branch of the left common carotid artery which directly originates from the aortic arch. However, the right ICA is a branch of the right common carotid artery, which is a branch of the right brachiocephalic artery. Therefore, a higher pulsatility in the central aorta may impact the tissues supplied by the left ICA more than the right ICA. Our results showed a higher pulsatility in the left hemisphere compared to right hemisphere (Figure 6-1). This

finding is in agreement with cohort that report left hemisphere stroke is more common (Hedna et al., 2013). Our PC-MRI revealed that more than 75% of the older participants had the highest blood flow pulsatility in the left ICA compared to the VAs and right ICA. One may hypothesize that lower pulsatility in the right hemisphere helps to maintain the right hemisphere cortical thickness and at least partially compensates for the thinning in the left hemisphere.

7.4 Area of agreement and controversy

The results of this thesis showed that in the older adults the greatest association between cerebral pulsatility and cortical thickness was in the superior and middle temporal, superior, middle and inferior frontal regions (which are spatially closer to ICAs). We hypothesized that the regions of the brain upstream of the ICAs that are served first are most vulnerable to the higher pulsatility induced by age-related arterial stiffness. Our results agree with the bulk of the literature which reports preferential vulnerability in the prefrontal cortex (Lemaitre et al., 2012; Salat et al., 2004; Storsve et al., 2014; Thambisetty et al., 2010) and some temporal subregions (Fjell et al., 2009; McGinnis, Brickhouse, Pascual, & Dickerson, 2011; Salat et al., 2004). If this hypothesis is accurate, then the temporal areas should be more vulnerable than the prefrontal region, yet only some of the literature reports temporal areas vulnerability (Fjell et al., 2009; McGinnis, Brickhouse, Pascual, & Dickerson, 2011; Salat et al., 2004). Further research on cerebral blood flow and pressure especially in the watershed areas of cerebral arteries is needed to clarify on this.

7.5 General conclusion

Taken together, the results and observations of the three studies suggest a new hypothesis on brain aging and pulsatility. Our results showed that healthy aging, CVRF and CAD increase pulsatility. Additionally, the cerebral pulsatility in the CVRF and CAD patients reduced after short duration walking. The new hypothesis is that regular physical exercise can reduce functional-NIRS-measured cerebral pulsatility. This hypothesis could be approached with a longitudinal study on the effects of exercise on the cerebral pulsatility parameters.

In addition, our results indicated that in the older adults there is greater delay between arterial inflow and CSF outflow systolic peak. Other studies reported that increased resistance of the spinal canal delays the shift of CSF, which temporarily amplifies the pressure in the cranium (Uftring et

al., 2000), causing compression of the capillaries and a contribution to cortical thinning. It would therefore be informative to index the CSF flow resistance similarly to the technique introduced by Mardal, et al. (2013) to test whether higher CSF resistance to flow is associated with greater delay between systolic inflow and CSF outflow systolic peak. If this hypothesis is confirmed, then the subsequent hypothesis could be: medication that attenuates spinal canal resistance could likewise lower intracranial pressure. There is controversy (Tully et al., 2016) on the long-term effects of antihypertensive medications on the brain, some studies having reported that such medications were associated with increased risk of stroke incidents. New strategies for lowering intracranial pressure by lowering the resistance of spinal canal might be beneficial. However, this approach as same as antihypertensive medications may push the autoregulation limit to higher pressure. Further pre-clinical and clinical research are needed to explore the feasibility of such experiments.

7.6 Clinical aspects of cerebral pulsatility

The scope of our study was to determine the age-related changes in cerebral pulsatility and their association to structural and functional changes in the brain. However, in the larger picture, cerebral pulsatility research might be expanded and detailed for clinical applications. Longitudinal studies tracking the evolution of pulsatility indices would refine our knowledge of this parameter. Evolution may include changes in the pulsatility indices and corresponding changes in the broader sense of cerebrovascular health. Such studies may thereby strengthen the body of knowledge to the point that pulsatility measurement may have practical predictive value. Intracranial hypertension and some strokes may be prevented with the help of such non-invasive, inexpensive monitoring tools. Persons at risk of dementia might similarly be identified. Markers for such conditions may support preventive and early intervention outcomes that may help public health.

CHAPTER 8 CONCLUSION AND RECOMMENDATIONS

The experiments in this thesis highlight the potential use of functional NIRS data to quantify indices associated with cerebrovascular health. In the experiment on healthy individuals, the multimodal brain imaging techniques of NIRS and MRI were used to explore the impact of healthy aging on cerebral pulsatility and its association with anatomical, morphological measures and cognitive decline. The main finding of this work relates higher cerebral pulsatility to cortical thinning in healthy older adults. The index of cerebral pulsatility measured with functional NIRS is a novel measure and may challenge our interpretation of the results. Thereby, the use of PC-MRI to assess blood flow pulsatility in cervical arteries, which is reported to reflect arterial stiffness and its association to cerebral pulsatility measured with NIRS, was invaluable for evaluating and interpreting the results. A higher delay between arterial systolic inflow and diastolic CSF systolic outflow was associated with lower global cortical thickness in the older adults. As the brain is contained in the cranium, an interplay between intracranial compartments such as arterial flow and CSF were also seen to influence intracranial pulsatility. Intracranial pressure is therefore hypothesized to contribute to the temporal uncoupling between the arteries and the CSF. Although blood pressure was similar and within the healthy range for the younger and older participants, cerebral pulsatility parameters measured with functional NIRS varied across the groups and between participants.

Older participants with higher cerebral pulsatility measured with NIRS had lower performance in the MoCA task. We also found lower pulsatility in subregions of the frontal lobe in the right hemisphere and in the literature these regions are associated with age-related functional reorganization. This finding could lead to a hypothesis that for functional reorganization the brain is recruiting the brain regions with lower pulsatile stress and thus better neurovascular coupling.

Two different participants with similar blood pressure could have different cerebral pulsatility, cortical thickness and reaction time to the Stroop color-word interference test. Moreover, peripheral measures of pulsatility such as PPG could not predict cerebral pulsatility in the experiments conducted. Taken together, our finding highlights the importance of measuring pulsatility in the brain rather than its peripheral measurement.

In the second study, cerebral pulsatility increased in the CAD patients compared to LCVRF and HCVRF, likely because of accumulated damage on the vessel walls and impaired heart-brain

interaction. In the CAD patients cerebral pulsatility had significant association with pulse pressure. A measure of arterial stiffness such as PC-MRI is needed to respond effectively to such a hypothesis. Short-duration walking of as little as 15 s, lowered the cerebral pulsatility measured with NIRS, likely in a transient manner. It is likely that CO_2, as a strong vasodilator and biproduct of metabolism resulting from physical activity, reduces pulsatility. The measurement of the end-tidal CO_2 could improve such interpretation. Longitudinal studies and richer data are needed to track changes in cerebral pulsatility as the result of regular exercise intervention.

8.1 FUTURE WORK

On a first level, the third study, which addresses cerebral pulsatility versus cognition, is pending completion. The statistical map contrasting the activation block and the rest block needs to be delineated. Then, we can explore if functional reorganization is spatially correlated with regions with lower pulsatility.

At a second level, given the findings of this thesis, several research questions and new hypotheses could be made from our data set. It would be interesting to explore the association of regional cerebral blood flow and cerebral pulsatility. This could be by arterial spin labeling (ASL) measured with MRI and cerebral pulsatility measured with functional NIRS. It is expected that regions of the brain with higher cerebral pulsatility are correlated with lower regional CBF. Arterial, CSF and vein pulsatility measured with PC-MRI can provide the full picture of total cerebrovascular compliance and its association with CBF, cortical thickness and volume.

At a third level we can add a sequence of MRI to our data and explore a new hypothesis. In article 1, it was discussed that it is likely that as pulse travels along the cerebral arteries further away from the ICAs, the autoregulation mechanism further damps and regulates the pulse (Spence, 2019; Zarrinkoob et al., 2016) and this may be the reason why some regions of the brain are more or less susceptible to the impact of the pulse. To test this hypothesis, we need to simulate blood flow and pressure dynamics in the cerebral arteries using the geometry of cerebral arteries (Figure 8-1) that could be obtained by 3D TOF-MRA (Valencia & Solis, 2006). Hence, the association between both regional blood flow and pressure parameters with the surrounding tissue characteristics such as cortical thickness and volume could be explored.

Figure 8-1 3D-TOF-MRA. The geometry of the vessels are clearly identifiable. Image source: http://imaging-mri.blogspot.com/2012/12/an-mra-of-brain-will-evaluate.html

REFERENCES

Abdelkarim, D., Zhao, Y., Turner, M. P., Sivakolundu, D. K., Lu, H., & Rypma, B. (2019, December 1). A neural-vascular complex of age-related changes in the human brain: Anatomy, physiology, and implications for neurocognitive aging. *Neuroscience and Biobehavioral Reviews*, Vol. 107, pp. 927. https://doi.org/10.1016/j.neubiorev.2019.09.005

Ashley, E. A., & Niebauer, J. (2004). *Cardiology explained*. Reemedica.

Amiri, M., Pouliot, P., Bonnéry, C., Leclerc, P. O., Desjardins, M., Lesage, F., & Joanette, Y. (2014). An exploration of the effect of hemodynamic changes due to normal aging on aging on the fNIRS response to semantic processing of words. *Frontiers in Neurology*, *5*(NOV). https://doi.org/10.3389/fneur.2014.00249

Alperin, N. J., Lee, S. H., Loth, F., Raksin, P. B., & Lichtor, T. (2000). MR-intracranial pressure (ICP): A method to measure intracranial elastance and pressure noninvasively by means of MR imaging: Baboon and human study. *Radiology*, *217*(3), 877–885.

Akbar, S., & Alorainy, M. S. (2014, November 1). The current status of beta blockers' use in the management of hypertension. *Saudi Medical Journal*, Vol. 35, pp. 1307–1317. Saudi Arabian Armed Forces Hospital.

Amar, J., Ruidavets, J. B., Chamontin, B., Drouet, L., & Ferrières, J. (2001). Arterial stiffness and cardiovascular risk factors in a population-based study. *Journal of Hypertension*, *19*(3), 381–387. https://doi.org/10.1097/00004872-200103000-00005

Attwell, D., Buchan, A. M., Charpak, S., Lauritzen, M., MacVicar, B. A., & Newman, E. A. (2010, November 11). Glial and neuronal control of brain blood flow. *Nature*, Vol. 468, pp. 232–243. https://doi.org/10.1038/nature09613

Alperin, N. J., Lee, S. H., Loth, F., Raksin, P. B., & Lichtor, T. (2000). MR-intracranial pressure (ICP): A method to measure intracranial elastance and pressure noninvasively by means of MR imaging: Baboon and human study. *Radiology*, *217*(3), 877–885. https://doi.org/10.1148/radiology.217.3.r00dc42877

Baker, G. F., Tortora, G. J., & Nostakos, N. P. A. (1976). Principles of Anatomy and Physiology. *The American Journal of Nursing*, *76*(3), 477. https://doi.org/10.2307/3423898

Baldo, M. P., Cunha, R. S., Molina, M. del C. B., Chór, D., Griep, R. H., Duncan, B. B., … Mill, J. G. (2018). Carotid-femoral pulse wave velocity in a healthy adult sample: The ELSA-Brasil

study. *International Journal of Cardiology*, *251*, 90–95. https://doi.org/10.1016/j.ijcard.2017.10.075

Baraghis, E., Bolduc, V., Lefebvre, J., Srinivasan, V. J., Boudoux, C., Thorin, E., & Lesage, F. (2011). Measurement of cerebral microvascular compliance in a model of atherosclerosis with optical coherence tomography. *Biomedical Optics Express*, *2*(11), 3079. https://doi.org/10.1364/boe.2.003079

Bateman, G. A., Levi, C. R., Schofield, P., Wang, Y., & Lovett, E. C. (2008). The venous manifestations of pulse wave encephalopathy: Windkessel dysfunction in normal aging and senile dementia. *Neuroradiology*, *50*(6), 491–497. https://doi.org/10.1007/s00234-008-0374-x

Benetos, A., Adamopoulos, C., Bureau, J. M., Temmar, M., Labat, C., Bean, K., … Guize, L. (2002). Determinants of accelerated progression of arterial stiffness in normotensive subjects and in treated hypertensive subjects over a 6-year period. *Circulation*, *105*(10), 1202–1207. https://doi.org/10.1161/hc1002.105135

Benetos, A., Watfa, G., Hanon, O., Salvi, P., Fantin, F., Toulza, O., … Gautier, S. (2012). Pulse Wave Velocity is Associated With 1-Year Cognitive Decline in the Elderly Older than 80 Years: The PARTAGE Study. *Journal of the American Medical Directors Association*, *13*(3), 239–243. https://doi.org/10.1016/j.jamda.2010.08.014

Blanco, P. J., Müller, L. O., & Spence, J. D. (2017). Blood pressure gradients in cerebral arteries: A clue to pathogenesis of cerebral small vessel disease. *Stroke and Vascular Neurology*, *2*(3), 108–117. https://doi.org/10.1136/svn-2017-000087

Balédent, O., Henry-Feugeas, M. C. C., & Idy-Peretti, I. (2001). Cerebrospinal fluid dynamics and relation with blood flow: A magnetic resonance study with semiautomated cerebrospinal fluid segmentation. *Investigative Radiology*, *36*(7), 368–377. https://doi.org/10.1097/00004424-200107000-00003

Bragin, D. E., Bush, R. C., & Nemoto, E. M. (2013). Effect of cerebral perfusion pressure on cerebral cortical microvascular shunting at high intracranial pressure in rats. *Stroke*, *44*(1), 177–181. https://doi.org/10.1161/STROKEAHA.112.668293

Caisberger, F., & Vališ, M. (2018). Vascular dementia. *Interni Medicina pro Praxi*, *20*(3), 159–162. https://doi.org/10.4068/cmj.2011.47.2.66

Canada, S. (2015). *Statistics Canada, Population Projections for Canada (2013-2063), Provience*

Territories (2013-2038). https://doi.org/91-520-X

Casey, D. A., Antimisiaris, D., & O'Brien, J. (2010). Drugs for Alzheimer's disease: Are they effective? *P and T*, Vol. 35, pp. 208–211. Medi Media USA Inc.

Cecelja, M., & Chowienczyk, P. (2012). Role of arterial stiffness in cardiovascular disease. *JRSM Cardiovascular Disease*, *1*(4), 1–10. https://doi.org/10.1258/cvd.2012.012016

Day, G. S. (2019). Reversible dementias. *CONTINUUM Lifelong Learning in Neurology*, Vol. 25, pp. 234–253. https://doi.org/10.1212/CON.0000000000000688

Deary, I. J., Corley, J., Gow, A. J., Harris, S. E., Houlihan, L. M., Marioni, R. E., … Starr, J. M. (2009). Age-associated cognitive decline. *British Medical Bulletin*, Vol. 92, pp. 135–152. https://doi.org/10.1093/bmb/ldp033

Cecelja, M., & Chowienczyk, P. (2012). Role of arterial stiffness in cardiovascular disease. *JRSM Cardiovascular Disease*, *1*(4), 1–10. https://doi.org/10.1258/cvd.2012.012016

Chantler, P. D., Lakatta, E. G., & Najjar, S. S. (2008). Arterial-ventricular coupling: Mechanistic insights into cardiovascular performance at rest and during exercise. *Journal of Applied Physiology*, Vol. 105, pp. 1342–1351. https://doi.org/10.1152/japplphysiol.90600.2008

Chiarelli, A. M., Fletcher, M. A., Tan, C. H., Low, K. A., Maclin, E. L., Zimmerman, B., … Fabiani, M. (2017). Individual differences in regional cortical volumes across the life span are associated with regional optical measures of arterial elasticity. *NeuroImage*, *162*, 199–213. https://doi.org/10.1016/j.neuroimage.2017.08.064

Chirinos, J. A. (2016, December 1). Large artery stiffness, microvascular function, and cardiovascular risk. *Circulation: Cardiovascular Imaging*, Vol. 9. https://doi.org/10.1161/CIRCIMAGING.116.005903

Clark, D. J., Christou, E. A., Ring, S. A., Williamson, J. B., & Doty, L. (2014). Enhanced somatosensory feedback reduces prefrontal cortical activity during walking in older adults. *Journals of Gerontology - Series A Biological Sciences and Medical Sciences*, *69*(11), 1422–1428. https://doi.org/10.1093/gerona/glu125

Clark, D. J. (2015). Automaticity of walking: Functional significance, mechanisms, measurement and rehabilitation strategies. *Frontiers in Human Neuroscience*, Vol. 9. https://doi.org/10.3389/fnhum.2015.00246

Clarkson-Smith, L., & Hartley, A. A. (1990). The game of bridge as an exercise in working

memory and reasoning. *Journals of Gerontology*, *45*(6), P233–P238. https://doi.org/10.1093/geronj/45.6.p233

Csikai, E., Andrejkovics, M., Balajthy-Hidegh, B., Hofgárt, G., Kardos, L., Diószegi, Á., … Csiba, L. (2019). Influence of angiotensin-converting enzyme inhibition on reversibility of alterations in arterial wall and cognitive performance associated with early hypertension: A follow-up study. *Medicine*, *98*(34), e16966. https://doi.org/10.1097/MD.0000000000016966

Darne, B., Girerd, X., Safar, M., Cambien, F., & Guize, L. (1989). Pulsatile versus steady component of blood pressure: A cross-sectional analysis and a prospective analysis on cardiovascular mortality. *Hypertension*, *13*(4), 392–400. https://doi.org/10.1161/01.HYP.13.4.392

De La Torre, J. C. (2012). Cardiovascular risk factors promote brain hypoperfusion leading to cognitive decline and dementia. *Cardiovascular Psychiatry and Neurology*. https://doi.org/10.1155/2012/367516

Del Zoppo, G. J., & Mabuchi, T. (2003). Cerebral microvessel responses to focal ischemia. *Journal of Cerebral Blood Flow and Metabolism*, Vol. 23, pp. 879–894. https://doi.org/10.1097/01.WCB.0000078322.96027.78

De Montgolfier, O., Thorin-Trescases, N., & Thorin, E. (2020). Pathological continuum from the rise in pulse pressure to impared neurovascular coupling. *American Journal of Hypertension*. https://doi.org/10.1093/ajh/hpaa001

Deckers, K., Schievink, S. H. J., Rodriquez, M. M. F., Van Oostenbrugge, R. J., Van Boxtel, M. P. J., Verhey, F. R. J., & Köhler, S. (2017). Coronary heart disease and risk for cognitive impairment or dementia: Systematic review and meta-analysis. *PLoS ONE*, *12*(9). https://doi.org/10.1371/journal.pone.0184244

Desai, A. S., Mitchell, G. F., Fang, J. C., & Creager, M. A. (2009). Central Aortic Stiffness is Increased in Patients With Heart Failure and Preserved Ejection Fraction. *Journal of Cardiac Failure*, *15*(8), 658–664. https://doi.org/10.1016/j.cardfail.2009.03.006

De Riva, N., Budohoski, K. P., Smielewski, P., Kasprowicz, M., Zweifel, C., Steiner, L. A., … Czosnyka, M. (2012). Transcranial doppler pulsatility index: What it is and what it isn't. *Neurocritical Care*, *17*(1), 58–66. https://doi.org/10.1007/s12028-012-9672-6

Diaz-Otero, J. M., Garver, H., Fink, G. D., Jackson, W. F., & Dorrance, A. M. (2016). Aging is associated with changes to the biomechanical properties of the posterior cerebral artery and

parenchymal arterioles. *American Journal of Physiology. Heart and Circulatory Physiology*, *310*(3), H365–H375. https://doi.org/10.1152/ajpheart.00562.2015

Donato, A. J., Machin, D. R., & Lesniewski, L. A. (2018). Mechanisms of dysfunction in the aging vasculature and role in age-related disease. *Circulation Research*, *123*(7), 825–848. https://doi.org/10.1161/CIRCRESAHA.118.312563

DuBose, L. E., Boles Ponto, L. L., Moser, D. J., Harlynn, E., Reierson, L., & Pierce, G. L. (2018). Higher aortic stiffness is associated with lower global cerebrovascular reserve among older humans. *Hypertension*, *72*(2), 476–482. https://doi.org/10.1161/HYPERTENSIONAHA.118.11143

Eggenberger, P., Wolf, M., Schumann, M., & de Bruin, E. D. (2016). Exergame and balance training modulate prefrontal brain activity during walking and enhance executive function in older adults. *Frontiers in Aging Neuroscience*, *8*(APR). https://doi.org/10.3389/fnagi.2016.00066

Elias, P. K., Elias, M. F., D'Agostino, R. B., Cupples, L. A., Wilson, P. W., Silbershatz, H., & Wolf, P. A. (1997). NIDDM and blood pressure as risk factors for poor cognitive performance: The Framingham Study. *Diabetes Care*, *20*(9), 1388–1395. https://doi.org/10.2337/diacare.20.9.1388

El Assar, M., Angulo, J., Vallejo, S., Peiró, C., Sánchez-Ferrer, C. F., & Rodríguez-Mañas, L. (2012). Mechanisms involved in the aging-induced vascular dysfunction. *Frontiers in Physiology*, *3 MAY*. https://doi.org/10.3389/fphys.2012.00132

Enzmann, D. R., Pelc, N. J., & McComb, J. G. (1993). Cerebrospinal fluid flow measured by phase-contrast cine MR. *American Journal of Neuroradiology*, *14*(6), 1301-1307+1309.

Fabiani, M., Low, K. A., Tan, C. H., Zimmerman, B., Fletcher, M. A., Schneider-Garces, N., … Gratton, G. (2014). Taking the pulse of aging: Mapping pulse pressure and elasticity in cerebral arteries with optical methods. *Psychophysiology*, *51*(11), 1072–1088. https://doi.org/10.1111/psyp.12288

Farasat, S. M., Morrell, C. H., Scuteri, A., Ting, C. T., Yin, F. C., Spurgeon, H. A., … Najjar, S. S. (2008). Pulse pressure is inversely related to aortic root diameter implications for the pathogenesis of systolic hypertension. *Hypertension*, *51*(2), 196–202. https://doi.org/10.1161/HYPERTENSIONAHA.107.099515

Faury, G. (2001). Function-structure relationship of elastic arteries in evolution: From microfibrils

to elastin and elastic fibres. *Pathologie Biologie*, Vol. 49, pp. 310–325. https://doi.org/10.1016/S0369-8114(01)00147-X

Finn, A. V, Kolodgie, F. D., & Virmani, R. (2010). Correlation between carotid intimal/medial thickness and atherosclerosis: A point of view from pathology. *Arteriosclerosis, Thrombosis, and Vascular Biology*, Vol. 30, pp. 177–181. https://doi.org/10.1161/ATVBAHA.108.173609

Fraser, S. A., Dupuy, O., Pouliot, P., Lesage, F., & Bherer, L. (2016). Comparable cerebral oxygenation patterns in younger and older adults during dual-task walking with increasing load. *Frontiers in Aging Neuroscience*, *8*(OCT). https://doi.org/10.3389/fnagi.2016.00240

Figueras, F., Fernandez, S., Eixarch, E., Gomez, O., Martinez, J. M., Puerto, B., & Gratacos, E. (2006). Middle cerebral artery pulsatility index: Reliability at different sampling sites. *Ultrasound in Obstetrics and Gynecology*, *28*(6), 809–813. https://doi.org/10.1002/uog.2816

Fjell, A. M., Westlye, L. T., Amlien, I., Espeseth, T., Reinvang, I., Raz, N., … Walhovd, K. B. (2009). High consistency of regional cortical thinning in aging across multiple samples. *Cerebral Cortex*, *19*(9), 2001–2012. https://doi.org/10.1093/cercor/bhn232

Franklin, S. S. (2006). Hypertension in older people: part 1. *Journal of Clinical Hypertension (Greenwich, Conn.)*, Vol. 8, pp. 444–449. https://doi.org/10.1111/j.1524-6175.2006.05113.x

Fujiwara, Y., Chaves, P. H. M., Takahashi, R., Amano, H., Yoshida, H., Kumagai, S., … Shinkai, S. (2005). Arterial pulse wave velocity as a marker of poor cognitive function in an elderly community-dwelling population. *Journals of Gerontology - Series A Biological Sciences and Medical Sciences*, *60*(5), 607–612. https://doi.org/10.1093/gerona/60.5.607

Garcia-Polite, F., Martorell, J., Del Rey-Puech, P., Melgar-Lesmes, P., O'Brien, C. C., Roquer, J., … Balcells, M. (2017). Pulsatility and high shear stress deteriorate barrier phenotype in brain microvascular endothelium. *Journal of Cerebral Blood Flow and Metabolism*, *37*(7), 2614–2625. https://doi.org/10.1177/0271678X16672482

Girouard, H., & Munter, L. M. (2018). The many faces of vascular cognitive impairment. *Journal of Neurochemistry*, Vol. 144, pp. 509–512. https://doi.org/10.1111/jnc.14287

Guerin, A. P., Blacher, J., Pannier, B., Marchais, S. J., Safar, M. E., & London, G. M. (2001). Impact of aortic stiffness attenuation on survival of patients in end-stage renal failure. *Circulation*, *103*(7), 987–992. https://doi.org/10.1161/01.CIR.103.7.987

Haeusler, K. G., Laufs, U., & Endres, M. (2011). Chronic heart failure and ischemic stroke. *Stroke*, Vol. 42, pp. 2977–2982. https://doi.org/10.1161/STROKEAHA.111.628479

Harris, S., Reyhan, T., Ramli, Y., Prihartono, J., & Kurniawan, M. (2018). Middle cerebral artery pulsatility index as predictor of cognitive impairment in hypertensive patients. *Frontiers in Neurology*, *9*(JUL), 538. https://doi.org/10.3389/fneur.2018.00538

Hashimoto, J., & Ito, S. (2009). Some mechanical aspects of arterial aging: Physiological overview based on pulse wave analysis. *Therapeutic Advances in Cardiovascular Disease*, Vol. 3, pp. 367–378. https://doi.org/10.1177/1753944709338942

Henry Feugeas, M. C., De Marco, G., Peretti, I. I., Godon-Hardy, S., Fredy, D., & Claeys, E. S. (2005). Age-related cerebral white matter changes and pulse-wave encephalopathy: Observations with three-dimensional MRI. *Magnetic Resonance Imaging*, *23*(9), 929–937. https://doi.org/10.1016/j.mri.2005.09.002

Hazzouri, A. Z. Al, Newman, A. B., Simonsick, E., Sink, K. M., Tyrrell, K. S., Watson, N., … Yaffe, K. (2013). Pulse wave velocity and cognitive decline in elders: The health, aging, and body composition study. *Stroke*, *44*(2), 388–393. https://doi.org/10.1161/STROKEAHA.112.673533

Hedna, V. S., Bodhit, A. N., Ansari, S., Falchook, A. D., Stead, L., Heilman, K. M., & Waters, M. F. (2013). Hemispheric differences in ischemic stroke: Is left-hemisphere stroke more common? *Journal of Clinical Neurology (Korea)*, *9*(2), 97–102. https://doi.org/10.3988/jcn.2013.9.2.97

Huneau, C., Benali, H., & Chabriat, H. (2015). Investigating human neurovascular coupling using functional neuroimaging: A critical review of dynamic models. *Frontiers in Neuroscience*, *9*(DEC), 467. https://doi.org/10.3389/fnins.2015.00467

Hill, D.K and Kynes, R.D . (1949). Opacity changes in simulated nerve. *Physiol*. https://doi.org/108;278-281

Hirata, K., Yaginuma, T., O'Rourke, M. F., & Kawakami, M. (2006). Age-related changes in carotid artery flow and pressure pulses: Possible implications for cerebral microvascular disease. *Stroke*, *37*(10), 2552–2556. https://doi.org/10.1161/01.STR.0000242289.20381.f4

Hodis, S., & Zamir, M. (2009). Mechanical events within the arterial wall: The dynamic context for elastin fatigue. *Journal of Biomechanics*, *42*(8), 1010–1016. https://doi.org/10.1016/j.jbiomech.2009.02.010

Holmgren, M., Wåhlin, A., Dunås, T., Malm, J., & Eklund, A. (2019). Assessment of Cerebral Blood Flow Pulsatility and Cerebral Arterial Compliance With 4D Flow MRI. *Journal of*

Magnetic Resonance Imaging. https://doi.org/10.1002/jmri.26978

Hoenig, M., Bianchi, C., Rosenzweig, A., & Sellke, F. (2008). Decreased Vascular Repair and Neovascularization with Ageing: Mechanisms and Clinical Relevance with an Emphasis on Hypoxia- Inducible Factor-1. *Current Molecular Medicine*, *8*(8), 754–767. https://doi.org/10.2174/156652408786733685

Holtzer, R., Schoen, C., Demetriou, E., Mahoney, J. R., Izzetoglu, M., Wang, C., & Verghese, J. (2017). Stress and gender effects on prefrontal cortex oxygenation levels assessed during single and dual-task walking conditions. *European Journal of Neuroscience*, *45*(5), 660–670. https://doi.org/10.1111/ejn.13518

Hughes, T. M., Kuller, L. H., Barinas-Mitchell, E. J. M., Mackey, R. H., McDade, E. M., Klunk, W. E., … Lopez, O. L. (2013). Pulse wave velocity is associated with β-amyloid deposition in the brains of very elderly adults. *Neurology*, *81*(19), 1711–1718. https://doi.org/10.1212/01.wnl.0000435301.64776.37

Hughes, T. M., Wagenknecht, L. E., Craft, S., Mintz, A., Heiss, G., Palta, P., … Gottesman, R. F. (2018). Arterial stiffness and dementia pathology: Atherosclerosis risk in communities (ARIC)-PET study. *Neurology*, *90*(14), E1248–E1256. https://doi.org/10.1212/WNL.0000000000005259

Hughes, A. D., & Parker, K. H. (2009). Forward and backward waves in the arterial system: Impedance or wave intensity analysis? *Medical and Biological Engineering and Computing*, *47*(2), 207–210. https://doi.org/10.1007/s11517-009-0444-1

Huppert, T.J., Diamond, S.G., Franceschini, M.A., Boas, D.A., 2009. HomER: A review of time-series analysis methods for near-infrared spectroscopy of the brain. Appl. Opt. 48. https://doi.org/10.1364/AO.48.00D280

Iadecola, C., & Davisson, R. L. (2008). Hypertension and Cerebrovascular Dysfunction. *Cell Metabolism*, Vol. 7, pp. 476–484. https://doi.org/10.1016/j.cmet.2008.03.010

Iadecola, C. (2010). The overlap between neurodegenerative and vascular factors in the pathogenesis of dementia. *Acta Neuropathologica*, Vol. 120, pp. 287–296. https://doi.org/10.1007/s00401-010-0718-6

Institut de la Statistique du Québec. (2015). Institut de la statistique du Québec. In *Rapport québécois du Programme pour l'évaluation internationale des compétences des adultes (PEICA)*. Retrieved from www.stat.gouv.qc.ca/droits_auteur.htm

Itoh, Y., Suzuki, N., 2012. Control of brain capillary blood flow. J. Cereb. Blood Flow Metab. https://doi.org/10.1038/jcbfm.2012.5

Izzetoglu, M., Bunce, S., Izzetoglu, K., Onaral, B., & Pourrezaei, A. (2007). Functional brain imaging using near-infrared technology. *IEEE Engineering in Medicine and Biology Magazine*, *26*(4), 38–46. https://doi.org/10.1109/MEMB.2007.384094

Izzo, J. L., & Mitchell, G. F. (2007). Aging and arterial structure-function relations. *Advances in Cardiology*, Vol. 44, pp. 19–34. https://doi.org/10.1159/000096701

Jäncke, L. (2009). Music drives brain plasticity. *F1000 Biology Reports*, *1*. https://doi.org/10.3410/b1-78

Jefferson, A. L., Cambronero, F. E., Liu, D., Moore, E. E., Neal, J. E., Terry, J. G., … Carr, J. J. (2018). Higher aortic stiffness is related to lower cerebral blood flow and preserved cerebrovascular reactivity in older adults. *Circulation*, *138*(2018), 1951–1962. https://doi.org/10.1161/CIRCULATIONAHA.118.032410

Jennings, J. R., & Choi, S. (1983). An Arterial to Peripheral Pulse Wave Velocity Measure. *Psychophysiology*, *20*(4), 410–417. https://doi.org/10.1111/j.1469-8986.1983.tb00922.x

Jobsis, F. (1977). Noninvasive, infrared monitoring of cerebral and myocardial oxygen sufficiency and circulatory parameters. *Science*, *198*(4323), 1264–1267. https://doi.org/10.1126/science.929199

Jue, T., & Masuda, K. (2013). Application of near infrared spectroscopy in biomedicine. In *Application of Near Infrared Spectroscopy in Biomedicine*. https://doi.org/10.1007/978-1-4614-6252-1

Jung, N. Y., Cho, H., Kim, Y. J., Kim, H. J., Lee, J. M., Park, S., … Seo, S. W. (2018). The impact of education on cortical thickness in amyloid-negative subcortical vascular dementia: Cognitive reserve hypothesis. *Alzheimer's Research and Therapy*, *10*(1). https://doi.org/10.1186/s13195-018-0432-5

Kaffashian, S., Dugravot, A., Nabi, H., Batty, G. D., Brunner, E., Kivimki, M., & Singh-Manoux, A. (2011). Predictive utility of the Framingham general cardiovascular disease risk profile for cognitive function: Evidence from the Whitehall II study. *European Heart Journal*, *32*(18), 2326–2332. https://doi.org/10.1093/eurheartj/ehr133

Jellinger, K. A. (2008). The pathology of "vascular dementia": A critical update. *Journal of Alzheimer's Disease*, Vol. 14, pp. 107–123. https://doi.org/10.3233/JAD-2008-14110

Kalaria, R. N. (2016). Neuropathological diagnosis of vascular cognitive impairment and vascular dementia with implications for Alzheimer's disease. *Acta Neuropathologica*, Vol. 131, pp. 659–685. https://doi.org/10.1007/s00401-016-1571-z

Kalaria, R. N. (2018). The pathology and pathophysiology of vascular dementia. *Neuropharmacology*, Vol. 134, pp. 226–239. https://doi.org/10.1016/j.neuropharm.2017.12.030

Kidwell, C. S., El-Saden, S., Livshits, Z., Martin, N. A., Glenn, T. C., & Saver, J. L. (2001). Transcranial doppler pulsatility indices as a measure of diffuse small-vessel disease. *Journal of Neuroimaging*, *11*(3), 229–235. https://doi.org/10.1111/j.1552-6569.2001.tb00039.x

Knopman, D., Boland, L. L., Mosley, T., Howard, G., Liao, D., Szklo, M., … Folsom, A. R. (2001). Cardiovascular risk factors and cognitive decline in middle-aged adults. *Neurology*, *56*(1), 42–48. https://doi.org/10.1212/WNL.56.1.42

Kohn, J. C., Lampi, M. C., & Reinhart-King, C. A. (2015). Age-related vascular stiffening: Causes and consequences. *Frontiers in Genetics*, Vol. 6, p. 112. https://doi.org/10.3389/fgene.2015.00112

Kirlilna, E., Yu, N., Jelzow, A., Wabnitz, H., Jacobs, A. M., & Tachtsidis, L. (2013). Identifying and quantifying main components of physiological noise in functional near infrared spectroscopy on the prefrontal cortex. *Frontiers in Human Neuroscience*, *7*(DEC).

Lane, R. J. (1991). "Cardiogenic dementia" revisited. *Journal of the Royal Society of Medicine*, *84*(10), 577–579. Retrieved from http://www.ncbi.nlm.nih.gov/pubmed/1744834

Langenecker, S. A., Nielson, K. A., & Rao, S. M. (2004). fMRI of healthy older adults during Stroop interference. *NeuroImage*, *21*(1), 192–200. https://doi.org/10.1016/j.neuroimage.2003.08.027

Lee, J. G., & Joo, S. J. (2019, May 1). Arterial stiffness and cardiovascular risk. *Korean Journal of Internal Medicine*, Vol. 34, pp. 504–506. https://doi.org/10.3904/kjim.2019.110

Lemaitre, H., Goldman, A. L., Sambataro, F., Verchinski, B. A., Meyer-Lindenberg, A., Weinberger, D. R., & Mattay, V. S. (2012). Normal age-related brain morphometric changes: Nonuniformity across cortical thickness, surface area and gray matter volume? *Neurobiology of Aging*, *33*(3), 617.e1-617.e9. https://doi.org/10.1016/j.neurobiolaging.2010.07.013

Li, X., Lyu, P., Ren, Y., An, J., & Dong, Y. (2017). Arterial stiffness and cognitive impairment. *Journal of the Neurological Sciences*, Vol. 380, pp. 1–10.

https://doi.org/10.1016/j.jns.2017.06.018

Liao, C. F., Cheng, H. M., Sung, S. H., Yu, W. C., & Chen, C. H. (2011). Determinants of pressure wave reflection: Characterization by the transit time-independent reflected wave amplitude. *Journal of Human Hypertension*, *25*(11), 665–671. https://doi.org/10.1038/jhh.2010.106

Likitlersuang, S., Teachavorasinskun, S., Surarak, C., Oh, E., & Balasubramaniam, A. (2013). Small strain stiffness and stiffness degradation curve of Bangkok Clays. *Soils and Foundations*, *53*(4), 498–509. https://doi.org/10.1016/j.sandf.2013.06.003

Lutz, W., & Kc, S. (2010). Dimensions of global population projections: What do we know about future population trends and structures? *Philosophical Transactions of the Royal Society B: Biological Sciences*, Vol. 365, pp. 2779–2791. https://doi.org/10.1098/rstb.2010.0133

Leritz, E. C., Salat, D. H., Williams, V. J., Schnyer, D. M., Rudolph, J. L., Lipsitz, L., … Milberg, W. P. (2011). Thickness of the human cerebral cortex is associated with metrics of cerebrovascular health in a normative sample of community dwelling older adults. *NeuroImage*, *54*(4), 2659–2671. https://doi.org/10.1016/j.neuroimage.2010.10.050

Mardal, K. A., Rutkowska, G., Linge, S., & Haughton, V. (2013). Estimation of CSF flow resistance in the upper cervical spine. *Neuroradiology Journal*, *26*(1), 106–110. https://doi.org/10.1177/197140091302600118

Marmarou, A., Shulman, K., & LaMorgese, J. (1975). Compartmental analysis of compliance and outflow resistance of the cerebrospinal fluid system. *Journal of Neurosurgery*, *43*(5), 523–534. https://doi.org/10.3171/jns.1975.43.5.0523

Martins, R., Joanette, Y., & Monchi, O. (2015). The implications of age-related neurofunctional compensatory mechanisms in executive function and language processing including the new temporal Hypothesis for Compensation. *Frontiers in Human Neuroscience*, *9*(APR). https://doi.org/10.3389/fnhum.2015.00221

Matas, A., Sowa, M. G., Taylor, G., & Mantsch, H. H. (2002). Melanin as a confounding factor in near infrared spectroscopy of skin. *Vibrational Spectroscopy*, *28*(1), 45–52. https://doi.org/10.1016/S0924-2031(01)00144-8

Maillard, P., Mitchell, G. F., Himali, J. J., Beiser, A., Tsao, C. W., Pase, M. P., … De Carli, C. (2016). Effects of arterial stiffness on brain integrity in young adults from the framingham heart study. *Stroke*, *47*(4), 1030–1036. https://doi.org/10.1161/STROKEAHA.116.012949

Matsumae, M., Kikinis, R., Mórocz, I. A., Lorenzo, A. V., Sándor, T., Albert, M. S., … Jolesz, F.

A. (1996). Age-related changes in intracranial compartment volumes in normal adults assessed by magnetic resonance imaging. *Journal of Neurosurgery*, *84*(6), 982–991. https://doi.org/10.3171/jns.1996.84.6.0982

Mathiesen, C., Caesar, K., Akgören, N., & Lauritzen, M. (1998). Modification of activity-dependent increases of cerebral blood flow by excitatory synaptic activity and spikes in rat cerebellar cortex. *Journal of Physiology*, *512*(2), 555–566. https://doi.org/10.1111/j.1469-7793.1998.555be.x

MacLeod, C. M. (1991). Half a century of reseach on the stroop effect: An integrative review. *Psychological Bulletin*, *109*(2), 163–203. https://doi.org/10.1037/0033-2909.109.2.163

Miescher, F. (1866). Ueber die chemische Zusammensetzung der Eiterzellen IN: Hoppe-Seyler ed Medicinsich-chemische Untersuchungen, Heft 4, 441-60 | Miescher. Retrieved October 7, 2019, from https://www.jnorman.com/pages/books/42605/miescher/ueber-die-chemische-zusammensetzung-der-eiterzellen-in-hoppe-seyler-ed-medicinsich-chemische

Mahmud, A., & Feely, J. (2000). Favourable effects on arterial wave reflection and pulse pressure amplification of adding angiotensin II receptor blockade in resistant hypertension. *Journal of Human Hypertension*, *14*(9), 541–546. https://doi.org/10.1038/sj.jhh.1001053

McGinnis, S. M., Brickhouse, M., Pascual, B., & Dickerson, B. C. (2011). Age-Related changes in the thickness of cortical zones in humans. *Brain Topography*, *24*(3–4), 279–291. https://doi.org/10.1007/s10548-011-0198-6

McLellan, T. M., Caldwell, J. A., & Lieberman, H. R. (2016). A review of caffeine's effects on cognitive, physical and occupational performance. *Neuroscience and Biobehavioral Reviews*, Vol. 71, pp. 294–312. https://doi.org/10.1016/j.neubiorev.2016.09.001

McDonald, D. A. (1974). Blood flow in arteries. *EDWARD ARNOLD PUBL.*, *£12.*-(1), 399–434. https://doi.org/10.1146/annurev.fluid.29.1.399

McDonald, D. A. (2011). Blood flow in arteries. *EDWARD ARNOLD PUBL.* https://doi.org/10.1146/annurev.fluid.29.1.399

Metzger, F. G., Ehlis, A. C., Haeussinger, F. B., Schneeweiss, P., Hudak, J., Fallgatter, A. J., & Schneider, S. (2017). Functional brain imaging of walking while talking – An fNIRS study. *Neuroscience*, *343*, 85–93. https://doi.org/10.1016/j.neuroscience.2016.11.032

Mirelman, A., Maidan, I., Bernad-Elazari, H., Nieuwhof, F., Reelick, M., Giladi, N., & Hausdorff, J. M. (2014). Increased frontal brain activation during walking while dual tasking: An fNIRS

study in healthy young adults. *Journal of NeuroEngineering and Rehabilitation*, *11*(1), 85. https://doi.org/10.1186/1743-0003-11-85

Mitchell, G. F. (2008). Effects of central arterial aging on the structure and function of the peripheral vasculature: Implications for end-organ damage. *Journal of Applied Physiology*, Vol. 105, pp. 1652–1660. https://doi.org/10.1152/japplphysiol.90549.2008

Mitchell, G. F. (2014). Arterial stiffness and hypertension: Chicken or egg? *Hypertension*, Vol. 64, pp. 210–214. https://doi.org/10.1161/HYPERTENSIONAHA.114.03449

Mitchell, G. F. (2015). Cerebral small vessel disease: Role of aortic stiffness and pulsatile hemodynamics. *Journal of Hypertension*, Vol. 33, pp. 2025–2028. https://doi.org/10.1097/HJH.0000000000000717

Mitchell, G. F. (2018). Aortic stiffness, pressure and flow pulsatility, and target organ damage. *Journal of Applied Physiology*, Vol. 125, pp. 1871–1880. https://doi.org/10.1152/japplphysiol.00108.2018

Mitchell, G. F., Parise, H., Benjamin, E. J., Larson, M. G., Keyes, M. J., Vita, J. A., … Levy, D. (2004). Changes in arterial stiffness and wave reflection with advancing age in healthy men and women: The Framingham Heart Study. *Hypertension*, *43*(6), 1239–1245. https://doi.org/10.1161/01.HYP.0000128420.01881.aa

Mitchell, G. F., Van Buchem, M. A., Sigurdsson, S., Gotal, J. D., Jonsdottir, M. K., Kjartansson, Ó., … Launer, L. J. (2011). Arterial stiffness, pressure and flow pulsatility and brain structure and function: The Age, Gene/Environment Susceptibility-Reykjavik Study. *Brain*, *134*(11), 3398–3407. https://doi.org/10.1093/brain/awr253

Mok, V., Ding, D., Fu, J., Xiong, Y., Chu, W. W. C., Wang, D., … Wong, K. S. (2012). Transcranial Doppler ultrasound for screening cerebral small vessel disease: a community study. *Stroke*, *43*(10), 2791–2793. https://doi.org/10.1161/STROKEAHA.112.665711

Nakamura, N., & Muraoka, I. (2018). Resistance Training Augments Cerebral Blood Flow Pulsatility: Cross-Sectional Study. *American Journal of Hypertension*, *31*(7), 811–817. https://doi.org/10.1093/ajh/hpy034

Nation, D. A., Preis, S. R., Beiser, A., Bangen, K. J., Delano-Wood, L., Lamar, M., … Au, R. (2016). Pulse pressure is associated with early brain atrophy and cognitive decline: Modifying effects of APOE-ϵ4. *Alzheimer Disease and Associated Disorders*, *30*(3), 210–215. https://doi.org/10.1097/WAD.0000000000000127

Ng, J. B., Turek, M., & Hakim, A. M. (2013, April 25). Heart disease as a risk factor for dementia. *Clinical Epidemiology*, Vol. 5, pp. 135–145.

Nguyen, Q., Dominguez, J., Nguyen, L., & Gullapalli, N. (2010). Hypertension management: An update. *American Health and Drug Benefits*, *3*(1), 47–55.

Nichols, W. W., Denardo, S. J., Wilkinson, I. B., McEniery, C. M., Cockcroft, J., & O'Rourke, M. F. (2008). Effects of arterial stiffness, pulse wave velocity, and wave reflections on the central aortic pressure waveform. *Journal of Clinical Hypertension*, Vol. 10, pp. 295–303. https://doi.org/10.1111/j.1751-7176.2008.04746.x

Nishtala, A., Preis, S. R., Beiser, A., Devine, S., Hankee, L., Seshadri, S., … Au, R. (2014). Midlife cardiovascular risk impacts executive function: Framingham offspring study. *Alzheimer Disease and Associated Disorders*, *28*(1), 16–22. https://doi.org/10.1097/WAD.0b013e3182a715bc

O'Brien, J. T., Erkinjuntti, T., Reisberg, B., Roman, G., Sawada, T., Pantoni, L., … DeKosky, S. T. (2003). Vascular cognitive impairment. *Lancet Neurology*, Vol. 2, pp. 89–98. https://doi.org/10.1016/S1474-4422(03)00305-3

O'connell, J. E. A. (1943). The vascular factor tn intracranial pressure and the maintenance of the cerebrospinal fluid circulation. *Brain*, *66*(3), 204–228. https://doi.org/10.1093/brain/66.3.204

de Montgolfier, O., Thorin-Trescases, N., & Thorin, E. (2020). Pathological Continuum From the Rise in Pulse Pressure to Impaired Neurovascular Coupling and Cognitive Decline. *American Journal of Hypertension*, *33*(5), 375-390.

Osofundiya, O., Benden, M. E., Dowdy, D., & Mehta, R. K. (2016). Obesity-specific neural cost of maintaining gait performance under complex conditions in community-dwelling older adults. *Clinical Biomechanics*, *35*, 42–48. https://doi.org/10.1016/j.clinbiomech.2016.03.011

O'Rourke, M. F. (1987). *Hemodynamic basis for the concept of resistance and impedance in hypertension*. https://doi.org/10.1007/978-94-009-3303-3_1

O'Rourke, M. F. (2007). Arterial aging: Pathophysiological principles. *Vascular Medicine*, Vol. 12, pp. 329–341. https://doi.org/10.1177/1358863X07083392

O'Rourke, M. F., & Hashimoto, J. (2007). Mechanical factors in arterial aging: a clinical perspective. *Journal of the American College of Cardiology*, *50*(1), 1–13. https://doi.org/10.1016/j.jacc.2006.12.050

O'Rourke, M. F., & Safar, M. E. (2005). Relationship between aortic stiffening and microvascular

disease in brain and kidney: Cause and logic of therapy. *Hypertension*, *46*(1), 200–204. https://doi.org/10.1161/01.HYP.0000168052.00426.65

O'Rourke, M. F., Safar, M. E., & Dzau, V. (2010). The Cardiovascular Continuum extended: Aging effects on the aorta and microvasculature. *Vascular Medicine*, *15*(6), 461–468. https://doi.org/10.1177/1358863X10382946

Obisesan, T. O., Obisesan, O. A., Martins, S., Alamgir, L., Bond, V., Maxwell, C., & Gillum, R. F. (2008). High blood pressure, hypertension, and high pulse pressure are associated with poorer cognitive function in persons aged 60 and older: The Third National Health and Nutrition Examination Survey. *Journal of the American Geriatrics Society*, *56*(3), 501–509. https://doi.org/10.1111/j.1532-5415.2007.01592.x

Pase, M. P., Herbert, A., Grima, N. A., Pipingas, A., & O'Rourke, M. F. (2012). Arterial stiffness as a cause of cognitive decline and dementia: A systematic review and meta-analysis. *Internal Medicine Journal*, *42*(7), 808–815. https://doi.org/10.1111/j.1445-5994.2011.02645.x

Pase, Matthew P, Grima, N. A., Stough, C. K., Scholey, A., & Pipingas, A. (2012). Cardiovascular disease risk and cerebral blood flow velocity. *Stroke*, *43*(10), 2803–2805. https://doi.org/10.1161/STROKEAHA.112.666727

Pase, Matthew P, Pipingas, A., Kras, M., Nolidin, K., Gibbs, A. L., Wesnes, K. A., … Stough, C. (2010). Healthy middle-aged individuals are vulnerable to cognitive deficits as a result of increased arterial stiffness. *Journal of Hypertension*, *28*(8), 1724–1729. https://doi.org/10.1097/HJH.0b013e32833b1ee7

Palta, P., Sharrett, A. R., Wei, J., Meyer, M. L., Kucharska-Newton, A., Power, M. C., … Heiss, G. (2019). Central arterial stiffness is associated with structural brain damage and poorer cognitive performance: The ARIC study. *Journal of the American Heart Association*, *8*(2), e011045. https://doi.org/10.1161/JAHA.118.011045

Pasha, E. P., Kaur, S. S., Gonzales, M. M., Machin, D. R., Kasischke, K., Tanaka, H., & Haley, A. P. (2015). Vascular function, cerebral cortical thickness, and cognitive performance in middle-aged hispanic and non-hispanic caucasian adults. *Journal of Clinical Hypertension*, *17*(4), 306–312. https://doi.org/10.1111/jch.12512

Paulson, O. B., Strandgaard, S., & Edvinsson, L. (1990). Cerebral autoregulation. *Cerebrovascular and Brain Metabolism Reviews*, Vol. 2, pp. 161–192. https://doi.org/10.1161/01.str.15.3.413

Pelicioni, P. H. S., Tijsma, M., Lord, S. R., & Menant, J. (2019). Prefrontal cortical activation

measured by fNIRS during walking: effects of age, disease and secondary task. *PeerJ*, *7*, e6833. https://doi.org/10.7717/peerj.6833

Poels, M. M. F., Zaccai, K., Verwoert, G. C., Vernooij, M. W., Hofman, A., Van Der Lugt, A., … Ikram, M. A. (2012). Arterial stiffness and cerebral small vessel disease: The rotterdam scan study. *Stroke*, *43*(10), 2637–2642. https://doi.org/10.1161/STROKEAHA.111.642264

Poels, M. M. F., Van Oijen, M., Mattace-Raso, F. U. S., Hofman, A., Koudstaal, P. J., Witteman, J. C. M., & Breteler, M. M. B. (2007). Arterial stiffness, cognitive decline, and risk of dementia: The Rotterdam study. *Stroke*, *38*(3), 888–892. https://doi.org/10.1161/01.STR.0000257998.33768.87

Priyanka A. Abhang. (2016). Temporal Lobe - an overview | ScienceDirect Topics. Retrieved January 17, 2020, from https://www.sciencedirect.com/topics/medicine-and-dentistry/temporal-lobe

Peters, R. (2006). Ageing and the brain. *Postgraduate Medical Journal*, Vol. 82, pp. 84–88. https://doi.org/10.1136/pgmj.2005.036665

Peper, E. S., Strijkers, G. J., Gazzola, K., Potters, W. V., Motaal, A. G., Luirink, I. K., … Coolen, B. F. (2018). Regional assessment of carotid artery pulse wave velocity using compressed sensing accelerated high temporal resolution 2D CINE phase contrast cardiovascular magnetic resonance. *Journal of Cardiovascular Magnetic Resonance*, *20*(1), 86. https://doi.org/10.1186/s12968-018-0499-y

Peng, S. L., Dumas, J. A., Park, D. C., Liu, P., Filbey, F. M., McAdams, C. J., … Lu, H. (2014). Age-related increase of resting metabolic rate in the human brain. *NeuroImage*, *98*, 176–183. https://doi.org/10.1016/j.neuroimage.2014.04.078

Qiu, C., Winblad, B., & Fratiglioni, L. (2005). The age-dependent relation of blood pressure to cognitive function and dementia. *Lancet Neurology*, Vol. 4, pp. 487–499. https://doi.org/10.1016/S1474-4422(05)70141-1

Qiu, C., Kivipelto, M., & Von Strauss, E. (2009). Epidemiology of Alzheimer's disease: Occurrence, determinants, and strategies toward intervention. *Dialogues in Clinical Neuroscience*, Vol. 11, pp. 111–128. Les Laboratoires Servier.

Quebec, I. de la statistique du. (2014). *Institut de la statistique du Que´bec. Perspectives de´mographiques du Que´bec et des re´gions, 2011– 2061.*

Quaresima, V., & Ferrari, M. (2019). A mini-review on functional near-infrared spectroscopy

(fNIRS): Where do we stand, and where should we go? *Photonics*, Vol. 6, p. 87. https://doi.org/10.3390/photonics6030087

Rabkin, S. W. (2012). Arterial stiffness: Detection and consequences in cognitive impairment and dementia of the elderly. *Journal of Alzheimer's Disease*, Vol. 32, pp. 541–549. https://doi.org/10.3233/JAD-2012-120757

Rakesh, G., Szabo, S. T., Alexopoulos, G. S., & Zannas, A. S. (2017). Strategies for dementia prevention: latest evidence and implications. *Therapeutic Advances in Chronic Disease*, Vol. 8, pp. 121–136. https://doi.org/10.1177/2040622317712442

Raz, N., Ghisletta, P., Rodrigue, K. M., Kennedy, K. M., & Lindenberger, U. (2010). Trajectories of brain aging in middle-aged and older adults: Regional and individual differences. *NeuroImage*, *51*(2), 501–511. https://doi.org/10.1016/j.neuroimage.2010.03.020

Raz, N., Lindenberger, U., Rodrigue, K. M., Kennedy, K. M., Head, D., Williamson, A., … Acker, J. D. (2005). Regional brain changes in aging healthy adults: General trends, individual differences and modifiers. *Cerebral Cortex*, *15*(11), 1676–1689. https://doi.org/10.1093/cercor/bhi044

Raz, N., & Rodrigue, K. M. (2006). Differential aging of the brain: Patterns, cognitive correlates and modifiers. *Neuroscience and Biobehavioral Reviews*, Vol. 30, pp. 730–748. https://doi.org/10.1016/j.neubiorev.2006.07.001

Raignault, A., Bolduc, V., Lesage, F., & Thorin, E. (2017). Pulse pressure-dependent cerebrovascular eNOS regulation in mice. *Journal of Cerebral Blood Flow and Metabolism*, *37*(2), 413–424. https://doi.org/10.1177/0271678X16629155

Rodrigue, K. M., Kennedy, K. M., Devous, M. D., Rieck, J. R., Hebrank, A. C., Diaz-Arrastia, R., … Park, D. C. (2012). β-amyloid burden in healthy aging: Regional distribution and cognitive consequences. *Neurology*, *78*(6), 387–395. https://doi.org/10.1212/WNL.0b013e318245d295

Ruesch, A., Yang, J., Schmitt, S., Acharya, D., Smith, M. A., & Kainerstorfer, J. M. (2020). Estimating intracranial pressure using pulsatile cerebral blood flow measured with diffuse correlation spectroscopy. *Biomedical Optics Express*, *11*(3), 1462. https://doi.org/10.1364/BOE.386612

Salat, D. H., Buckner, R. L., Snyder, A. Z., Greve, D. N., Desikan, R. S. R., Busa, E., … Fischl, B. (2004). Thinning of the cerebral cortex in aging. *Cerebral Cortex*, *14*(7), 721–730. https://doi.org/10.1093/cercor/bhh032

Sadekova, N., Iulita, M. F., Vallerand, D., Muhire, G., Bourmoum, M., Claing, A., & Girouard, H. (2018). Arterial stiffness induced by carotid calcification leads to cerebral gliosis mediated by oxidative stress. *Journal of hypertension*, *36*(2), 286-298.

Salthouse, T. A. (2010). Selective review of cognitive aging. *Journal of the International Neuropsychological Society*, Vol. 16, pp. 754–760. https://doi.org/10.1017/S1355617710000706

Shabir, O., Berwick, J., & Francis, S. E. (2018). Neurovascular dysfunction in vascular dementia, Alzheimer's and atherosclerosis. *BMC Neuroscience*, Vol. 19. https://doi.org/10.1186/s12868-018-0465-5

Stoquart-ElSankari, S., Balédent, O., Gondry-Jouet, C., Makki, M., Godefroy, O., & Meyer, M. E. (2007). Aging effects on cerebral blood and cerebrospinal fluid flows. *Journal of Cerebral Blood Flow and Metabolism*, *27*(9), 1563–1572. https://doi.org/10.1038/sj.jcbfm.9600462

Schubert, T., Pansini, M., Bieri, O., Stippich, C., Wetzel, S., Schaedelin, S., … Santini, F. (2015). Attenuation of blood flow pulsatility along the Atlas slope: A physiologic property of the distal vertebral artery? *American Journal of Neuroradiology*, *36*(3), 562–567. https://doi.org/10.3174/ajnr.A4148

Scuteri, A., Tesauro, M., Appolloni, S., Preziosi, F., Brancati, A. M., & Volpe, M. (2007). Arterial stiffness as an independent predictor of longitudinal changes in cognitive function in the older individual. *Journal of Hypertension*, *25*(5), 1035–1040. https://doi.org/10.1097/HJH.0b013e3280895b55

Scuteri, A., Tesauro, M., Guglini, L., Lauro, D., Fini, M., & Di Daniele, N. (2013). Aortic stiffness and hypotension episodes are associated with impaired cognitive function in older subjects with subjective complaints of memory loss. *International Journal of Cardiology*, *169*(5), 371–377. https://doi.org/10.1016/j.ijcard.2013.09.009

Scioli, M. G., Bielli, A., Arcuri, G., Ferlosio, A., & Orlandi, A. (2014, September 16). Ageing and microvasculature. *Vascular Cell*, Vol. 6. https://doi.org/10.1186/2045-824X-6-19

Shepard, R. B., Simpson, D. C., & Sharp, J. F. (1966). Energy Equivalent Pressure. *Archives of Surgery*, *93*(5), 730–740. https://doi.org/10.1001/archsurg.1966.01330050034005

Shi, Y., Thrippleton, M. J., Blair, G. W., Dickie, D. A., Marshall, I., Hamilton, I., … Wardlaw, J. M. (2020). Small vessel disease is associated with altered cerebrovascular pulsatility but not resting cerebral blood flow. *Journal of Cerebral Blood Flow and Metabolism*, *40*(1), 85–99.

https://doi.org/10.1177/0271678X18803956

Shi, L., Sordillo, L. A., Rodríguez-Contreras, A., & Alfano, R. (2016, January 1). Transmission in near-infrared optical windows for deep brain imaging. *Journal of Biophotonics*, Vol. 9, pp. 38–43. https://doi.org/10.1002/jbio.201500192

Schaller, B. (2004, November). Physiology of cerebral venous blood flow: From experimental data in animals to normal function in humans. *Brain Research Reviews*, Vol. 46, pp. 243–260. https://doi.org/10.1016/j.brainresrev.2004.04.005

Singer, J., Trollor, J. N., Crawford, J., O'Rourke, M. F., Baune, B. T., Brodaty, H., … Smith, E. (2013). The Association between Pulse Wave Velocity and Cognitive Function: The Sydney Memory and Ageing Study. *PLoS ONE*, *8*(4), e61855. https://doi.org/10.1371/journal.pone.0061855

Springo, Z., Toth, P., Tarantini, S., Ashpole, N. M., Tucsek, Z., Sonntag, W. E., … Ungvari, Z. I. (2015). Aging impairs myogenic adaptation to pulsatile pressure in mouse cerebral arteries. *Journal of Cerebral Blood Flow and Metabolism*, *35*, 527–530. https://doi.org/10.1038/jcbfm.2014.256

Smith, R. P., Argod, J., Pépin, J. L., & Lévy, P. A. (1999, May 1). Pulse transit time: An appraisal of potential clinical applications. *Thorax*, Vol. 54, pp. 452–457. https://doi.org/10.1136/thx.54.5.452

Smith, A. M., Mancini, M. C., & Nie, S. (2009). Bioimaging: Second window for in vivo imaging. *Nature Nanotechnology*, Vol. 4, pp. 710–711. https://doi.org/10.1038/nnano.2009.326

Small, B. J., Dixon, R. A., & McArdle, J. J. (2011). Tracking cognition-health changes from 55 to 95 years of age. *The Journals of Gerontology. Series B, Psychological Sciences and Social Sciences*, *66 Suppl 1*(Suppl 1), i153. https://doi.org/10.1093/geronb/gbq093

Stone, J., Johnstone, D. M., Mitrofanis, J., & O'Rourke, M. (2015). The mechanical cause of age-related dementia (Alzheimer's Disease): The brain is destroyed by the pulse. *Journal of Alzheimer's Disease*, Vol. 44, pp. 355–373. https://doi.org/10.3233/JAD-141884

Storsve, A. B., Fjell, A. M., Tamnes, C. K., Westlye, L. T., Overbye, K., Aasland, H. W., & Walhovd, K. B. (2014). Differential longitudinal changes in cortical thickness, surface area and volume across the adult life span: Regions of accelerating and decelerating change. *Journal of Neuroscience*, *34*(25), 8488–8498. https://doi.org/10.1523/JNEUROSCI.0391-14.2014

Stergiopulos, N., Segers, P., & Westerhof, N. (1999). Use of pulse pressure method for estimating total arterial compliance in vivo. *American Journal of Physiology - Heart and Circulatory Physiology*, *276*(2 45-2). https://doi.org/10.1152/ajpheart.1999.276.2.h424

Takahashi, T., Takikawa, Y., Kawagoe, R., Shibuya, S., Iwano, T., & Kitazawa, S. (2011). Influence of skin blood flow on near-infrared spectroscopy signals measured on the forehead during a verbal fluency task. *NeuroImage*, *57*(3), 991–1002. https://doi.org/10.1016/j.neuroimage.2011.05.012

Tan, C. H., Low, K. A., Chiarelli, A. M., Fletcher, M. A., Navarra, R., Burzynska, A. Z., … Fabiani, M. (2019). Optical measures of cerebral arterial stiffness are associated with white matter signal abnormalities and cognitive performance in normal aging. *Neurobiology of Aging*. https://doi.org/10.1016/j.neurobiolaging.2019.08.004

Thambisetty, M., Wan, J., Carass, A., An, Y., Prince, J. L., & Resnick, S. M. (2010). Longitudinal changes in cortical thickness associated with normal aging. *NeuroImage*, *52*(4), 1215–1223. https://doi.org/10.1016/j.neuroimage.2010.04.258

Tan, C. H., Low, K. A., Kong, T., Fletcher, M. A., Zimmerman, B., MacLin, E. L., … Fabiani, M. (2017). Mapping cerebral pulse pressure and arterial compliance over the adult lifespan with optical imaging. *PLoS ONE*, *12*(2). https://doi.org/10.1371/journal.pone.0171305

Tan, C. H., Low, K. A., Schneider-Garces, N., Zimmerman, B., Fletcher, M. A., Maclin, E. L., … Fabiani, M. (2016). Optical measures of changes in cerebral vascular tone during voluntary breath holding and a Sternberg memory task. *Biological Psychology*, *118*, 184–194. https://doi.org/10.1016/j.biopsycho.2016.05.008

Taquet, A., Bonithon-Kopp, C., Simon, A., Levenson, J., Scarabin, Y., Malmejac, A., … Guize, L. (1993). Relations of cardiovascular risk factors to aortic pulse wave velocity in asymptomatic middle-aged women. *European Journal of Epidemiology*, *9*(3), 298–306. https://doi.org/10.1007/BF00146267

Tarumi, T., Ayaz Khan, M., Liu, J., Tseng, B. M., Parker, R., Riley, J., … Zhang, R. (2014). Cerebral hemodynamics in normal aging: Central artery stiffness, wave reflection, and pressure pulsatility. *Journal of Cerebral Blood Flow and Metabolism*, *34*(6), 971–978. https://doi.org/10.1038/jcbfm.2014.44

Themelis, G., D'Arceuil, H., Diamond, S. G., Thaker, S., Huppert, T. J., Boas, D. A., & Franceschini, M. A. (2007). Near-infrared spectroscopy measurement of the pulsatile

component of cerebral blood flow and volume from arterial oscillations. *Journal of Biomedical Optics*, *12*(1), 014033. https://doi.org/10.1117/1.2710250

Terzi, S., Arslanoğlu, S., Demiray, U., Eren, E., & Cancuri, O. (2014). Carotid Doppler Ultrasound Evaluation in Patients with Pulsatile Tinnitus. *Indian Journal of Otolaryngology and Head and Neck Surgery*, *67*(1), 43–47. https://doi.org/10.1007/s12070-014-0756-9

Tsao, C. W., Seshadri, S., Beiser, A. S., Westwood, A. J., DeCarli, C., Au, R., … Mitchell, G. F. (2013). Relations of arterial stiffness and endothelial function to brain aging in the community. *Neurology*, *81*(11), 984–991. https://doi.org/10.1212/WNL.0b013e3182a43e1c

Toth, P., Tarantini, S., Csiszar, A., & Ungvari, Z. (2017). Functional vascular contributions to cognitive impairment and dementia: Mechanisms and consequences of cerebral autoregulatory dysfunction, endothelial impairment, and neurovascular uncoupling in aging. *American Journal of Physiology - Heart and Circulatory Physiology*, Vol. 312, pp. H1–H20. https://doi.org/10.1152/ajpheart.00581.2016

Tong, Y., & Frederick, B. de B. (2010). Time lag dependent multimodal processing of concurrent fMRI and near-infrared spectroscopy (NIRS) data suggests a global circulatory origin for low-frequency oscillation signals in human brain. *NeuroImage*, *53*(2), 553–564. https://doi.org/10.1016/j.neuroimage.2010.06.049

Thorin-Trescases, N., de Montgolfier, O., Pinçon, A., Raignault, A., Caland, L., Labbé, P., & Thorin, X. E. (2018, June 18). Impact of pulse pressure on cerebrovascular events leading to age-related cognitive decline. *American Journal of Physiology - Heart and Circulatory Physiology*, Vol. 314, pp. H1214–H1224. https://doi.org/10.1152/ajpheart.00637.2017

Tully, P. J., Debette, S., Dartigues, J. F., Helmer, C., Artero, S., & Tzourio, C. (2016). Antihypertensive Drug Use, Blood Pressure Variability, and Incident Stroke Risk in Older Adults: Three-City Cohort Study. *Stroke*, *47*(5), 1194–1200. https://doi.org/10.1161/STROKEAHA.115.012321

Uftring, S. J., Chu, D., Alperin, N., & Levin, D. N. (2000). The mechanical state of intracranial tissues in elderly subjects studied by imaging CSF and brain pulsations. *Magnetic Resonance Imaging*, *18*(8), 991–996. https://doi.org/10.1016/s0730-725x(00)00195-8

Uangpairoj, P., & Shibata, M. (2013). Evaluation of vascular wall elasticity of human digital arteries using alternating current-signal photoplethysmography. *Vascular Health and Risk*

Management, *9*, 283–295. https://doi.org/10.2147/vhrm.s43

Ündar, A., Fraser, C. D., Nishinaka, T., Tatsumi, E., Taenaka, Y., & Takano, H. (2002, September 28). The alphabet of research on pulsatile and nonpulsatile (continuous flow) perfusion during chronic support [1] (multiple letters). *Artificial Organs*, Vol. 26, pp. 812–813. https://doi.org/10.1046/j.1525-1594.2002.00919.x

Unnerbäck, M., Bloomfield, E. L., Söderström, S., & Reinstrup, P. (2019). The intracranial pressure curve correlates to the pulsatile component of cerebral blood flow. *Journal of Clinical Monitoring and Computing*, *33*(1), 77–83. https://doi.org/10.1007/s10877-018-0129-0

Vlachopoulos, Charalambos, Michael O'Rourke, and W. W. N. (2011). *McDonald's blood flow in arteries: theoretical, experimental and clinical principles*. CRC press

van Vliet, P., van de Water, W., de Craen, A. J. M., & Westendorp, R. G. J. (2009). The influence of age on the association between cholesterol and cognitive function. *Experimental Gerontology*, *44*(1–2), 112–122. https://doi.org/10.1016/j.exger.2008.05.004

Veraar, C. M., Rinösl, H., Kühn, K., Skhirtladze-Dworschak, K., Felli, A., Mouhieddine, M., … Dworschak, M. (2019). Non-pulsatile blood flow is associated with enhanced cerebrovascular carbon dioxide reactivity and an attenuated relationship between cerebral blood flow and regional brain oxygenation. *Critical Care*, *23*(1), 426. https://doi.org/10.1186/s13054-019-2671-7

Verghese, J., Wang, C., Ayers, E., Izzetoglu, M., & Holtzer, R. (2017). Brain activation in high-functioning older adults and falls: Prospective cohort study. *Neurology*, *88*(2), 191–197. https://doi.org/10.1212/WNL.0000000000003421

Vikner, T., Nyberg, L., Holmgren, M., Malm, J., Eklund, A., & Wåhlin, A. (2019). Characterizing pulsatility in distal cerebral arteries using 4D flow MRI. *Journal of Cerebral Blood Flow and Metabolism*, 0271678X1988666. https://doi.org/10.1177/0271678X19886667

Viola, S., Viola, P., Buongarzone, M. P., Fiorelli, L., & Litterio, P. (2013). Tissue oxygen saturation and pulsatility index as markers for amnestic mild cognitive impairment: NIRS and TCD study. *Clinical Neurophysiology*, *124*(5), 851–856. https://doi.org/10.1016/j.clinph.2012.11.013

Vlachopoulos, Charalambos, Michael O'Rourke, and W. W. N. (2011). *McDonald's blood flow in arteries: theoretical, experimental and clinical principles*. CRC press.

Vrselja, Z., Brkic, H., Mrdenovic, S., Radic, R., & Curic, G. (2014). Function of circle of Willis. *Journal of Cerebral Blood Flow and Metabolism*, Vol. 34, pp. 578–584. https://doi.org/10.1038/jcbfm.2014.7

Wagshul, M. E., Eide, P. K., & Madsen, J. R. (2011). The pulsating brain: A review of experimental and clinical studies of intracranial pulsatility. *Fluids and Barriers of the CNS*, Vol. 8. https://doi.org/10.1186/2045-8118-8-5

Waldstein, S., Rice, S., Thayer, J., Najjar, S., Scuteri, A., & Zonderman, A. (2008). Pulse pressure and pulse wave velocity are related to cognitive decline in the Baltimore Longitudinal Study of Aging. *Hypertension*, *51*(1).

Wåhlin, A., Ambarki, K., Birgander, R., Alperin, N., Malm, J., & Eklund, A. (2010). Assessment of craniospinal pressure-volume indices. *American Journal of Neuroradiology*, *31*(9), 1645–1650. https://doi.org/10.3174/ajnr.A2166

Wåhlin, A., Ambarki, K., Birgander, R., Malm, J., & Eklund, A. (2014). Intracranial pulsatility is associated with regional brain volume in elderly individuals. *Neurobiology of Aging*, *35*(2), 365–372. https://doi.org/10.1016/j.neurobiolaging.2013.08.026

Wang, H., Kim, M., Normoyle, K. P., & Llano, D. (2016). Thermal regulation of the brain-an anatomical and physiological review for clinical neuroscientists. *Frontiers in Neuroscience*, Vol. 9. https://doi.org/10.3389/fnins.2015.00528

Wardlaw, J. M., Allerhand, M., Eadie, E., Thomas, A., Corley, J., Pattie, A., … Deary, I. J. (2017). Carotid disease at age 73 and cognitive change from age 70 to 76 years: A longitudinal cohort study. *Journal of Cerebral Blood Flow and Metabolism*, *37*(8), 3042–3052. https://doi.org/10.1177/0271678X16683693

Watanabe, E., Mavanagi, Y., Ito, Y., & Koizumi, H. (1995). Spatial and Temporal Analysis of Human Motor Activity Using Noninvasive NIR Topography. *Medical Physics*, *22*(12), 1997–2005. https://doi.org/10.1118/1.597496

Watson, N. L., Sutton-Tyrrell, K., Youk, A. O., Boudreau, R. M., MacKey, R. H., Simonsick, E. M., … Nemwan, A. B. (2011). Arterial stiffness and gait speed in older adults with and without peripheral arterial disease. *American Journal of Hypertension*, *24*(1), 90–95. https://doi.org/10.1038/ajh.2010.193

Whedon, J.M., Glassey, D., 2009. Cerebrospinal fluid stasis and its clinical significance. Altern. Ther. Health Med.

Wert, D. M., Brach, J. S., Perera, S., & VanSwearingen, J. (2013). The association between energy cost of walking and physical function in older adults. *Archives of Gerontology and Geriatrics*, *57*(2), 198–203. https://doi.org/10.1016/j.archger.2013.04.007

Willie, C. K., Tzeng, Y. C., Fisher, J. A., & Ainslie, P. N. (2014). Integrative regulation of human brain blood flow. *Journal of Physiology*, Vol. 592, pp. 841–859. https://doi.org/10.1113/jphysiol.2013.268953

Wilson, P. W. F., D'Agostino, R. B., Levy, D., Belanger, A. M., Silbershatz, H., & Kannel, W. B. (1998). Prediction of coronary heart disease using risk factor categories. *Circulation*, *97*(18), 1837–1847. https://doi.org/10.1161/01.CIR.97.18.1837

Wymer, D. T., Patel, K. P., Burke, W. F., & Bhatia, V. K. (2020). Phase-contrast MRI: Physics, techniques, and clinical applications. *Radiographics*, *40*(1), 122–140. https://doi.org/10.1148/rg.2020190039

Xi, G., Keep, R. F., & Hoff, J. T. (2006, January). Mechanisms of brain injury after intracerebral haemorrhage. *Lancet Neurology*, Vol. 5, pp. 53–63. https://doi.org/10.1016/S1474-4422(05)70283-0

Yang, G. Y., Betz, A. L., Chenevert, T. L., Brunberg, J. A., & Hoff, J. T. (1994). Experimental intracerebral hemorrhage: Relationship between brain edema, blood flow, and blood-brain barrier permeability in rats. *Journal of Neurosurgery*, *81*(1), 93–102. https://doi.org/10.3171/jns.1994.81.1.0093
https://doi.org/10.1148/rg.2020190039

Yang, M., Yang, Z., Yuan, T., Feng, W., & Wang, P. (2019, February 5). A systemic review of functional near-infrared spectroscopy for stroke: Current application and future directions. *Frontiers in Neurology*, Vol. 10, p. 58. https://doi.org/10.3389/fneur.2019.00058

Zarrinkoob, L., Ambarki, K., Wahlin, A., Birgander, R., Carlberg, B., Eklund, A., & Malm, J. (2016). Aging alters the dampening of pulsatile blood flow in cerebral arteries. *Journal of Cerebral Blood Flow and Metabolism*, *36*(9), 1519–1527. https://doi.org/10.1177/0271678X16629486

Zhai, F. F., Ye, Y. C., Chen, S. Y., Ding, F. M., Han, F., Yang, X. L., … Zhu, Y. C. (2018). Arterial stiffness and cerebral small vessel disease. *Frontiers in Neurology*, https://doi.org/10.3389/fneur.2018.00723

Zysset, S., Schroeter, M. L., Neumann, J., & Yves von Cramon, D. (2007). Stroop interference,

hemodynamic response and aging: An event-related fMRI study. *Neurobiology of Aging*, *28*(6), 937–946. https://doi.org/10.1016/j.neurobiolaging.2006.05.008